PHYTOCHEMISTRY AND ANTI-TYROSINASE ACTIVITY OF *ANAXAGOREA LUZONENSIS* A. GRAY

WIYADA NOORING

**A THESIS SUBMITTED IN PARTIAL FULFILLMENT
OF THE REQUIREMENTS FOR
THE DEGREE OF MASTER OF SCIENCE
(PHARMACEUTICAL CHEMISTRY AND PHYTOCHEMISTRY)
FACULTY OF GRADUATE STUDIES
MAHIDOL UNIVERSITY
2010**

Thesis
entitled

PHYTOCHEMISTRY AND ANTI-TYROSINASE ACTIVITY OF *ANAXAGOREA LUZONENSIS* A. GRAY

……...
Miss Wiyada Nooring
Candidate

…….....
Assist. Prof. Aimon Somanabandhu,
Ph.D.
Major advisor

……...
Assoc. Prof. Weena Jiratchariyakul,
Dr.rer.nat.
Co-advisor

……
Prof. Banchong Mahaisavariya,
M.D., Dip Thai Board of Orthopedics
Dean
Faculty of Graduate Studies
Mahidol University

……...
Assoc. Prof. Opa Vajragupta
Ph.D.
Program Director
Master of Science Program
in Pharmaceutical Chemistry and
Phytochemistry
Faculty of Pharmacy,
Mahidol University

Thesis
entitled

PHYTOCHEMISTRY AND ANTI-TYROSINASE ACTIVITY OF *ANAXAGOREA LUZONENSIS* A. GRAY

was submitted to the Faculty of Graduate Studies, Mahidol University
for the degree of Master of Science (Pharmaceutical Chemistry and Phytochemistry)
on
30 April, 2010

……..
Miss Wiyada Nooring
Candidate

……...
Assoc. Prof. Nijsiri Ruangrungsi,
Ph.D.
Chair

…….
Assist. Prof. Weena Jiratchariyakul,
Dr.rer.nat.
Member

……..
Assoc. Prof. Aimon Somanabandhu,
Ph.D.
Member

……
Prof. Banchong Mahaisavariya,
M.D., Dip Thai Board of Orthopedics
Dean
Faculty of Graduate Studies
Mahidol University

……...
Assoc. Prof. Chuthamanee Suthisisang,
Ph.D.
Dean
Faculty of Pharmacy
Mahidol University

ACKNOWLEDGEMENTS

I would like to express my sincere gratitude and appreciation to my advisor, Associate Professor Dr. Aimon Somanabandhu, for her guidance, invaluable advice, continuous supervision and kind attention throughout my study. I also wish to express my deepest gratitude to my co-advisor, Associate Professor Dr. Weena Jiratchariyakul for her valuable advice on structural elucidation and Associate Professor Dr.Nijsiri Ruangrungsi for the helpful suggestion.

I am deeply grateful to Mrs. Patcharin Poochaiwatananon, NMR technician of the department of chemistry, Faculty of Science, Mahidol University for her kind assistance in my training on structural elucidation, the master degree and Ph.D students at the Faculty of Pharmacy, Mahidol University especially the department of Pharmaceutical chemistry and Pharmacognosy and the staffs of both department for their kindness, helpful suggestions, understanding and continuous encouragement.

Finally, I would like to express my deepest gratitude and appreciation to, my dear parents, my sister and my friends for their love, care, support and endless encouragement throughout my life.

Wiyada Nooring

PHYTOCHEMISTRY AND ANTI-TYROSINASE ACTIVITY OF *ANAXAGOREA LUZONENSIS* A. GRAY

WIYADA NOORING 4837858 PYPP/M

M.Sc. (PHARMACEUTICAL CHEMISTRY AND PHYTOCHEMISTRY)

THESIS ADVISORY COMMITEE: AIMON SOMANABANDHU, Ph.D., WEENA JIRATCHARIYAKUL, Dr.rer.nat.

ABSTRACT

Phytochemical and anti-tyrosinase studies were performed on the stems of *Anaxagorea luzonensis* A. Gray, collected from a forest area in Petchaburee Province, Thailand. The hexane, dichloromethane and ethyl acetate extracts were found to be active against mushroom tyrosinase with percent inhibition at 0.909 mg/ml of 28.56 %, 58.27 % and 86.76 %, respectively. Results also confirmed the antioxidant activities of these extracts as shown by the IC_{50} values of 162.7, 10.60 and 3.33 µg/ml, respectively. Bioassay-guided fractionation of these extracts was carried out by chromatographic methods. Phytochemical investigation of these extracts resulted in the isolation and identification of five compounds; the three xanthones were found to be 1,6-dihydroxy-5-methoxy-4′,5′-dihydro-4′,4′,5′-trimethyl-furano-(2′,3′:3,4)-xanthone (**A**), 2-deprenyl-rheediaxanthone B (**B**) and 1,3,6-trihydroxy-5-methoxyxanthone(**C**) and the two flavonols were identified as kaempferol (**D**) and quercetin (**E**). Their structures were established by spectroscopic methods (UV, IR, MS, ^{1}H-NMR and ^{13}C-NMR). This is the first report on the anti-tyrosinase activity of the *A. luzonensis*, compounds **A** (IC_{50} 1.18 mM) and **B** (IC_{50} 1.35 mM), while compound **D** (kaempferol) and **E** (quercetin), are known anti-tyrosinase agents. These compounds exhibited scavenging activity toward DPPH radical with IC_{50} values of 5.56 (**A**), 7.62 (**B**), 6.94 (**D**) and 5.30 (**E**) µM. However, compound **C** was found to be inactive against mushroom tyrosinase and to have little free radical scavenging activity.

The results of this study demonstrated the potential of *A.luzonensis* as tyrosinase inhibitory and antioxidant agents for applications in the pharmaceutical and cosmeceutical fields.

KEY WORD ANAXAGOREA LUZONENSIS A. GRAY, XANTHONES, FLAVONOIDS, ANTITYROSINASE, FREE RADICAL SCAVENGING ACTIVITY

174 pages

พฤกษเคมี และฤทธิ์ต้านเอ็นไซม์ไทโรซิเนสของต้นกำลังวัวเถลิง

PHYTOCHEMISTRY AND ANTI-TYROSINASE ACTIVITY OF *ANAXAGOREA LUZONENSIS* A. GRAY

วิยะดา หนูริง 4837858 PYPP/M

วท.ม. (เภสัชเคมีและพฤกษเคมี)

คณะกรรมการที่ปรึกษาวิทยานิพนธ์ : เอมอร โสมนะพันธุ์, Ph.D., วีณา จิรัจฉริยากูล, Dr.rer.nat.

บทคัดย่อ

ศึกษาองค์ประกอบทางเคมีและฤทธิ์ต้านเอ็นไซม์ไทโรซิเนส จากต้นกำลังวัวเถลิง (*Anaxagorea luzonensis* A. Gray) โดยเก็บตัวอย่างพืชจากบริเวณป่าในจังหวัดเพชรบุรี พบว่าสารสกัดชั้น เฮกเซน ไดคลอโรมีเทน และ เอททิวอะซีเตท มีฤทธิ์ต้านเอนไซม์ไทโรซิเนสจากเห็ด มีค่า IC_{50} เท่ากับ 28.56%, 58.27% และ 86.76 % ตามลำดับ ที่ความเข้มข้น 0.909 mg/ml ผลการศึกษายืนยันถึงฤทธิ์ต้านอนุมูลอิสระของสารสกัดทั้งสามมีค่า IC_{50} เท่ากับ 162.7, 10.60 และ 3.33 μg/ml ตามลำดับ เมื่อทำการแยกสารจากสารสกัดเหล่านี้ ควบคู่กับการทดสอบฤทธิ์ต้านการทำงานของเอนไซม์ไทโรซิเนสด้วยวิธีทางโครมาโตกราฟี สามารถทำการแยกและวิเคราะห์โครงสร้างของสารได้ 5 ชนิด พบสารกลุ่มแซนโทน 3 ชนิด คือ 1,6-dihydroxy-5-methoxy-4′,5′-dihydro-4′,4′,5′-trimethyl-furano-(2′,3′:3,4)-xanthone (**A**), 2-deprenylrheedia-xanthone B (**B**) และ 1,3,6-trihydroxy-5-methoxy-xanthone(**C**) และฟลาโวนอยด์ 2 ชนิด คือ kaempferol (**D**) และ quercetin (**E**) โครงสร้างของสารเหล่านี้ยืนยันด้วยวิธีทางวีธีทางสเปกโตรสโคปี (UV, IR, MS, ^{1}H-NMR และ ^{13}C-NMR). การศึกษานี้เป็นการรายงานครั้งแรก ถึงฤทธิ์ต้านเอนไซม์ไทโรซิเนสของต้นกำลังวัวเถลิง ของสาร A และ B โดยสาร A , B, D และ E มีค่า IC_{50} เท่ากับ 1.18, 1.35, 2.49 และ1.56 mM ตามลำดับ ซึ่งสาร D และ E เคยมีการรายงานถึงฤทธิ์นี้มาแล้ว ขณะที่ kojic acid มีค่า IC_{50} เท่ากับ 0.197 mM ซึ่งเป็นสารที่มีฤทธิ์ต้านเอ็นไซม์ไทโรซิเนส และสารเหล่านี้ยังแสดงฤทธิ์การต้านอนุมูลอิสระที่สูงซึ่งมีค่า IC_{50} เท่ากับ 5.56 (A), 7.62(B), 6.94 (D) และ 5.30 (E) μM ส่วนสาร C พบว่าไม่มีฤทธิ์ยับยั้งการทำงานของเอ็นไซม์ไทโรซิเนส และมีฤทธิ์เพียงเล็กน้อยต่อการต้านอนุมูลอิสระ

ผลการศึกษานี้แสดงให้เห็นถึงศักยภาพของต้นกำลังวัวเถลิง ในการเป็นสารต้านเอ็นไซม์ไทโรซิเนส และต้านอนุมูลอิสระสำหรับการนำไปประยุกต์ใช้ในด้าน เภสัชกรรมและเครื่องสำอาง

174 หน้า

CONTENTS

CONTENTS (cont.)

CONTENTS (cont.)

CONTENTS (cont.)

CONTENTS (cont.)

LIST OF TABLES

LIST OF TABLES (cont.)

LIST OF FIGURES

LIST OF FIGURES (cont.)

LIST OF FIGURES (cont.)

LIST OF ABBREVIATIONS

^{1}H-NMR	=	Proton nuclear magnetic resonance
^{13}C-NMR	=	Carbon 13 nuclear magnetic resonance
$CDCl_3$	=	Deuterated chloroform
EtOAc	=	Ethyl acetate
CH_2Cl_2	=	Dichloromethane, methylene chloride
$CHCl_3$	=	Chloroform
MeOH	=	Methanol
EtOH	=	Ethanol
CD_3OD	=	deuteromethanol
DMSO	=	dimethylsulfoxide
d	=	Doublet (for NMR spectra)
dd	=	Doublet of doublets (for NMR spectra)
DEPT	=	Distortionless Enhancement by Polarization Transfer
DMSO-d_4	=	Deuterated dimethylsulfoxide
DPPH	=	2,2-diphenyl-1-1-(2,4,6-trinitrophenyl) hydrazyl
EI-MS	=	Electron Impact Mass Spectrometry
ESI-MS	=	Electrospray Ionization Mass Spectrometry
HMBC	=	^{1}H-detected Heteronuclear Multiple Bond Coherence
HMQC	=	^{1}H-detected Heteronuclear Multiple Quantum Coherence
IC_{50}	=	Fifty percent Inhibitory Concentration
i.d.	=	internal diameter
i.e.	=	id est. (that is)
IR	=	Infrared Spectrum
J	=	Coupling constant
KBr	=	Potassium bromide
L	=	Liter

LIST OF ABBREVIATIONS (cont.)

L-DOPA	=	levo 3,4-Didroxyphenyl alanine
µg	=	Microgram
µl	=	Microliter
m	=	Multiplet (for NMR spectra)
MW	=	Molecular weight
m/z	=	Mass to charge ratio
M^+	=	Molecular ion
$[M+H]^+$	=	Protonated molecular ion
MHz	=	Megahertz
mg	=	Milligram
ml	=	Milliliter
mM	=	Millimolar
µM	=	Micromolar
NaH_2PO_4	=	Sodium dihydrogen phosphate
o	=	Ortho
p	=	Para
ppm	=	Part per million
q	=	Quartet (for NMR spectra)
ROS	=	Reactive oxygen species
R_f	=	Retention factor
conc.	=	concentration
cont.	=	continued
s	=	Singlet (for NMR spectra)
SD	=	Standard deviation
t	=	Triplet (for NMR spectra)
TLC	=	Thin Layer Chromatography
ed.	=	editor
e.g.	=	example gratia (Latin), such as

LIST OF ABBREVIATIONS (cont.)

et al	=	et.alii (Latin), and other
g	=	gram
δ	=	Chemical shift
UV	=	Ultraviolet
UV-VIS	=	Ultraviolet and Visible Spectrophotometry
ν_{max}	=	Wave number at maximal absorption
λ_{max}	=	Wave length at maximal absorption
ºC	=	degree Celsius
min	=	minute
Ref.	=	reference
Na_2HPO_4	=	Disodium hydrogen phosphate
NP	=	Natural Products (diphenylborinic acid aminoethylester)
PEG	=	Polyehtylene glycol
nm	=	Nanometer
i.e.	=	id est (Latin), that is
cm	=	centimeter

CHAPTER I
INTRODUCTION

Tyrosinase is known to be a key enzyme in melanin biosynthesis, involved in determining the color of mammalian skin and hair. The enzyme is responsible for melanization in animals and browning in plants and fungi. The color of mammalian skin and hair is determined by a number of factors, the most important of which is the degree and distribution of melanin pigmentation. Melanin is the main component for the darkening of the skin (1). It is secreted by melanocyte cells distributed in the basal layer of the epidermis. The role of melanin is to protect the skin from ultraviolet (UV) damage by absorbing UV sunlight and removing reactive oxygen species (ROS). Various dermatological disorders result in the accumulation of an excessive level of epidermal pigmentation. These hyperpigmented lentigenes include melasma, age spots and sites of actinic damage (2). Skin is an important component of body image and has immense psychological importance for both women and men, so skin pigmentation can be a source of significant emotional distress in individuals (3). Most of the women in some specific countries, especially in Asia, want to have white skin. To satisfy this desire many cosmetics have been developed for melanogenesis inhibition. Tyrosinase is the key enzyme in the synthesis of melanin and intervenes in several intermediate stages of pigment formation (4, 5). Tyrosinase inhibition is the most common approach to achieve skin hypopigmentation as this enzyme catalyses the rate-limiting step of pigmentation (7, 10). Tyrosinase catalyses both the hydroxylation reaction that converts tyrosine into 3-(3,4-dihydroxyphenyl)-l-alanine (DOPA) and the oxidation reaction that converts DOPA into dopaquinone, which further led to the polymerization of brown pigments (8). Therefore, the use of tyrosinase inhibitors such as kojic acid and hydroquinone has become increasingly important in the cosmetic industry because of their anti-pigmenting effects. Despite the extensive research on lightening agents, the existing agents have several limitations in terms of high toxicity,

low stability, poor skin-penetration and insufficient activity (9). So alternatives to them are being sought, including naturally occurring compounds.

A random screening of various plant extracts for anti-tyrosinase activity revealed that the ethanolic extract of the *Anaxagorea luzonensis* A. Gray (Annonaceae) inhibited more than 80% of activity of mushroom tyrosinase. A literature survey of the phytochemistry of this plant indicates the presence of several xanthones and flavonoids with antioxidant activity. Flavonoids are reported to possess a wide range of biological activities. So far, there has been no report on the anti-tyrosinase activity of *A.luzonensis* (SciFinder, Accessed since November, 2007). Therefore, it is of interest to study *A.luzonensis* as a model for anti-tyrosinase agent.

The present study was designed to search for anti-tyrosinase compounds and to confirm the anti-oxidant activity of this plant. Crude extracts were separated by chromatographic means and thin layer chromatographic technique was developed for rapid tyrosinase inhibitor detection. The anti-tyrosinase and free radical scavenging activities were calculated in terms of % inhibition and comparison was made between different fractions. The structure identification of isolated chemical constituents was performed using spectroscopic techniques.

OBJECTIVES

1. To study the chemical profile and the anti-tyrosinase and free radical scavenging activities of *Anaxagorea luzonensis*.
2. To isolate compounds from active fraction (s) of *A. luzonensis*.
3. To identify chemical structures of the isolated compounds.
4. To study their anti-tyrosinase and free radical scavenging activities.

CHAPTER II
LITERATURE REVIEW

2.1 Melanogenesis in humans

2.1.1 Melanin-formation and distribution in the skin (9)

Melanogenesis is the process of human skin pigment formation. The differences that can be seen in skin coloration depends greatly on the skin pigment. Synthesis and distribution of melanin in the skin and hair bulbs are cause of visible pigmentation in mammals. The site of formation and distribution of pigmentation in the epidermis is demonstrated in Figure 1. Melanin is secreted by melanocyte cells distributed in the basal layer of the dermis. Melanins play an important role in the absorption of free radicals generated within the cytoplasm and in shielding the host cells from various types of ionizing radiations, including UV light. Melanins are categorized into two basic types: eumelanins, which are brown or black, and pheomelanins, which are red or yellow. In mammals, mixtures of both types are typically found. Interestingly, pheomelanin has the ability to produce free radicals in response to UV radiation. Since free radicals can inflict cell injury, pheomelanin may actually contribute to intensifying UV-induced skin damage rather than protecting the skin.

After the completion of melanogenesis, melanin pigments formed are stored within the melanosomes located in the cytoplasm of melanocytes. There melanosomes are transferred upward to the keratinocytes through the dendrites of melanocytes. The distribution of the amounts and types of melanin in the keratinocytes determines the various shades of skin and hair colors (Figure 1).

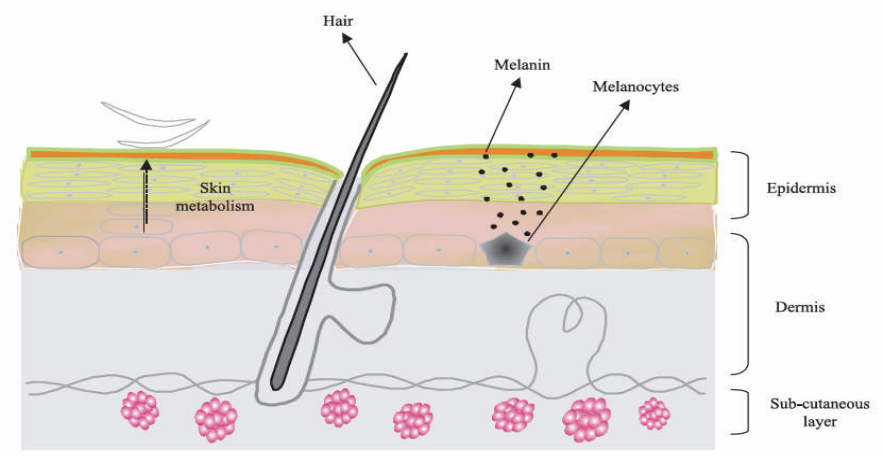

Figure 1 Outline of mammalian skin indicating three main layers epidermis, dermis and sub-cutaneous, visible pigmentation results from the synthesis and distribution of melanin in the melanocytes in the epidermal layer of the skin (9)

2.1.2 Tyrosinase

Tyrosinase (EC 1.14.18.1) is a copper-containing enzyme that catalyzes two distinct reactions of melanin synthesis, which is widely distributed in plants and animals, and is involved in the formation of melanin pigments (10-12). Of catalyzes the hydroxylation of tyrosine by monophenolase action and the oxidation of 3,4-dihydroxyphenylalanine (L-DOPA) to *o*-dopaquinone by diphenolase action. However, if L-DOPA is an active cofactor, its formation as an intermediate during *o*-dopaquinone production is still controversial. *o*-dopaquinone is unstable in aqueous solution and rapidly suffers a non-enzymatic cyclization to leukodopachrome, which is further oxidized non enzymatically by another molecule of *o*-dopaquinone to yield dopachrome and one molecule of regenerated L-DOPA (13-15).

In the food industry, tyrosinase is a very important enzyme in controlling the quality and economics of fruits and vegetables (16-18). Tyrosinase catalyzes the oxidation of phenolic compounds to the corresponding quinones and is responsible for the enzymatic browning of fruits and vegetables. In addition to the undesirable color and flavor, the quinone compounds produced in the browning reaction may irreversibly react with the amino and sulfhydryl groups of proteins. The quinone-

protein reaction decreases the digestibility of the protein and the bioavailability of essential amino acids, including lysine and cysteine. Therefore, development of high-performance tyrosinase inhibitors is much needed in the agricultural and food fields.

2.1.2.1 Biochemical characteristics and reaction mechanism of tyrosinase

In higher plants and fungi, tyrosinases exist in immature, mature latent and active isoforms (19, 20). However, bio-chemical characterization of the kinetics and relationship between the isoforms is not yet complete. The active site of tyrosinase consists of two copper atoms and three states. Structural models for the active site of these three forms of tyrosinase have been proposed (19–22).

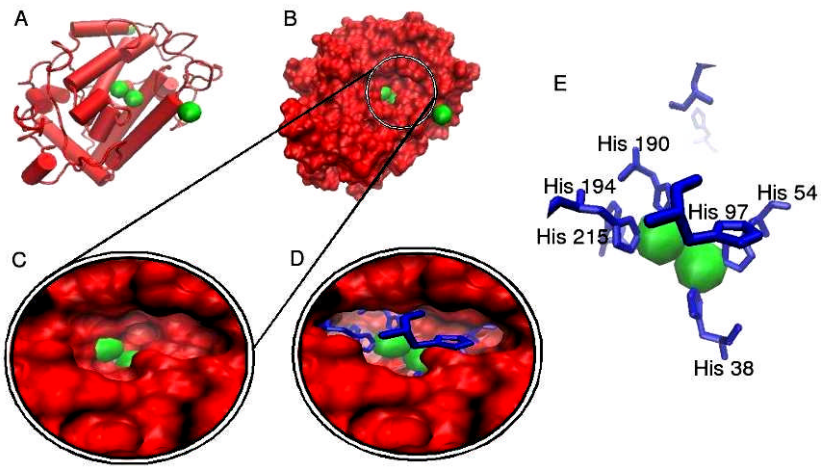

Figure 2 A model of the structure of tyrosinase enzyme, crystallographic structure (23) of a *Streptomyces* derived tyrosinase in complex with a so called "caddie protein". (from http//en.wikipedia.org/wiki/Tyrosinase)

The two copper atoms within the active site of tyrosinase enzymes interact with dioxygen to form a highly reactive chemical intermediate that then oxidizes the substrate (24-25). In all models only the tyrosinase molecule is shown (Figure 2), copper atoms are shown in green and the molecular surface is

shown in red. In models D and E, the amino acid histidine is shown as a blue line representation. From model E it can be clearly seen that each copper atom within the active site is indeed complexed with three histidine residues, forming a type 3 copper center. It can also be seen from models C and D that the active site for this protein sits within a pillus formed on the molecular surface of the molecule.

Classification and properties of tyrosinase

The most well studied multi-copper oxygenase is tyrosinase, which contains a coupled binuclear copper active site. Tyrosinase catalyzes both the *o*-hydroxylation of monophenols and the two-electron oxidation of *o*-diphenols to *o*-quinones. The second reaction is much faster than the first; thus, the hydroxylation of tyrosine to L-DOPA is considered to be the rate-determining step. Labelling studies demonstrated that the oxygen incorporated into the phenolic substrate derives from molecular O_2 (26). The two electrons required to reduce the second oxygen atom to H_2O are supplied by the substrate.

The best-characterized tyrosinases are derived from *Streptomyces glausescens*, the fungi *Neurospora crassa* and *Agaricus bisporus*. The first two are monomeric proteins, while the last is a tetramer with two different subunits, heavy and light. Tyrosinases have been isolated and at least partially purified from numerous plant and animal sources, but few of them have been well characterized. Unlike the fungal tyrosinase, human tyrosinase is a membrane-bound glycoprotein (13% carbohydrate) (27). Many of these enzymes have been sequenced, including ones from *N. crassa* and humans (28–30). A variety of mutations in the human tyrosinase gene has been correlated with the pigment deficiency of oculocutaneous albinism (31). This nearly ubiquitous enzyme has been adapted to serve diverse physiological roles in different organisms (32-33). In fungi and vertebrates, tyrosinase catalyzes the initial step in the formation of the pigment melanin from tyrosine. In plants, the physiological substrates are a variety of phenolics. Tyrosinase oxidizes them in the browning pathway observed when tissues are injured; however, the function of this reaction is not clear. One possible role is the protection of wounds from pathogens or insects. In the latter, tyrosinase is thought to be involved in wound healing and possibly sclerotization of the cuticle.

Structure of the active center of tyrosinase

Chemical and spectroscopic studies of tyrosinase have demonstrated that the geometric and electronic structures of the binuclear copper active site of this enzyme are extremely similar to those found in hemocyanins (34-36). While it is unfortunate that there is no crystal structure presently available for any tyrosinases, much insight into their active site and contribution of the active site to reactivity can be obtained from correlations to hemocyanins, of which crystal structures exist for both the deoxy and oxy forms of the active sites (21, 37, 38).

In the formation of melanin pigments, three types of tyrosinase (met, oxy and deoxytyrosinases) with different binuclear copper structures of the active site are involved (39-41).

Mettyrosinase, the resting form of tyrosinase, contains two tetragonal Cu (II) ions antiferromagnetically coupled through an endogenous bridge, although hydroxide exogenous ligands other than peroxide are bound to the copper site. The antiferromagnetic coupling between the Cu (II) ions of mettyrosinase triggers the lack of an electron paramagnetic resonance (EPR) signal, which requires a superexchange pathway associated with a bridging ligand (42). This species can be converted by addition of peroxide to oxytyrosinase, which in turn decays back to mettyrosinase when the peroxide is lost. The resting form of tyrosinase is found to be a mixture of 85% met and 15% oxy forms.

Oxytyrosinase also can be produced by the two-electron reduction of deoxytyrosinase, followed by the reversible binding of dioxygen (21, 43) which reacts with monophenol as well as *o*-diphenol substrate. The exogenous oxygen molecule is bound as peroxide and bridges the two copper centers. Peroxide bound in this mode confers a distinct $O^{2-}_2 \rightarrow$ Cu (II) charge transfer spectrum which can be correlated to the optical features of the oxy form of tyrosinase and includes an extremely intense absorption band at 350 nm and CD band at 325 nm (40, 44).

Deoxytyrosinase, an analogue of deoxyhemocyanin, has a bicuprous structure [(Cu (I)–Cu (I)]. These three copper states in the active site of tyrosinase led to a structural model being proposed for the reaction mechanism involved in the *o*-hydroxylation of monophenols and oxidation of the resulting *o*-diphenols, which is based on an associative ligand substitution at the active site of

tyrosinase. Figure 3 shows the interrelationship between these three froms of tyrosinase.

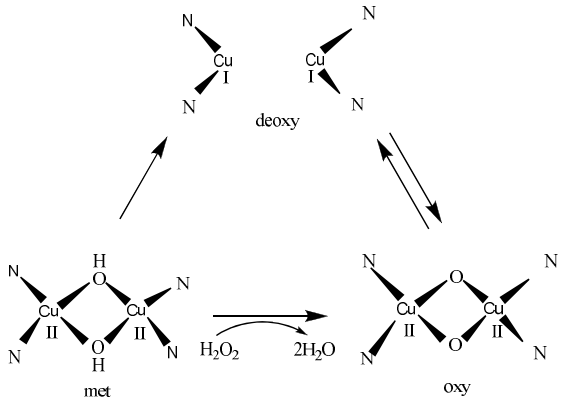

Figure 3 Interrelation of the three function states of tyrosinase

Mechanism of tyrosinase action

The above considerations have led to the molecular mechanism for the monophenolase and diphenolase activity of tyrosinase. The mechanism for the monophenolase activity of tyrosinase has been widely studied (40, 48, 49) based on three forms of the enzyme. In the monophenolase cycle, the monophenol can react only with the oxy form and binds to the axial position of one of the coppers of this oxy form. Rearrangement through a trigonal bipyramidal intermediate leads to *o*-hydroxylation of monophenol by the bound peroxide (Figure 4). This generates a coordinated *o*-diphenol, which is oxidized to the *o*-quinone, resulting in a deoxy form ready for further dioxygen binding.

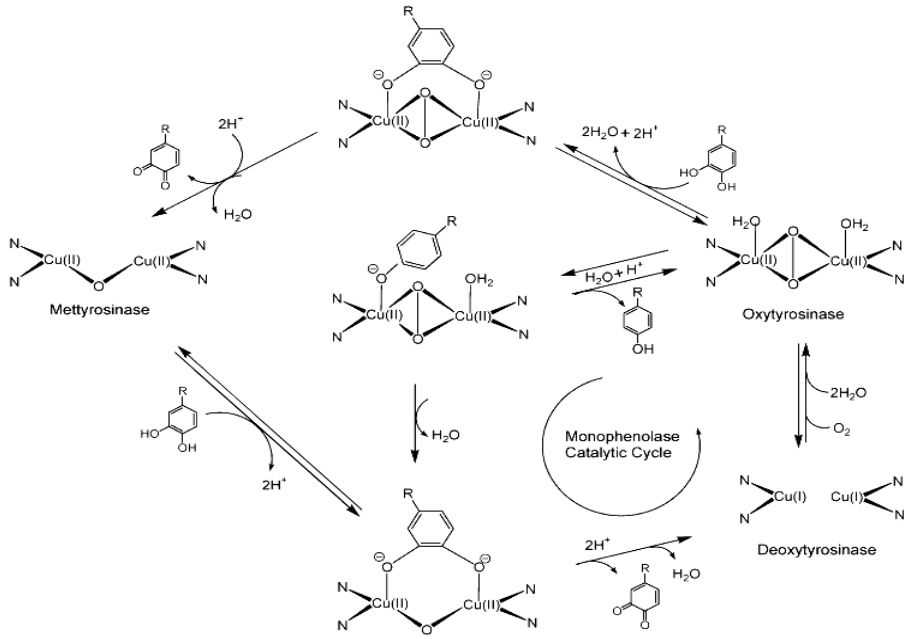

Figure 4 Catalytic cycles of the hydroxylation of monophenol and oxidation of *o*-diphenol to *o*-quinone by tyrosinase (43).

The *o*-diphenol can react with the met form present to give the coordinated o-diphenol in the monophenolase cycle.

In the diphenolase cycle, both the oxy and met forms react with *o*-diphenol, oxidizing it to the *o*-quinone. However, monophenol can compete with *o*-diphenol for binding to the met form site, inhibiting its reduction. Comparing the kinetic constants for monophenolic versus *o*-diphenolic substrates, bulky substituents on the ring dramatically reduce monophenolase activity but not diphenolase activity (40). This suggests that while monophenolic substrates require the axial to equatorial arrangement for *o*-hydroxylation, *o*-diphenolic substrates need not undergo rearrangement at the copper site for simple electron transfer.

Kinetic studies of the steady state of the pathway show the lower catalytic efficiency of tyrosinase on monophenols than on *o*-diphenols (41, 50, 51). Monophenolase activity is typically characterized by a lag time (48, 49, 52, 53) which is dependent on factors such as substrate and enzyme concentrations, and presence of a hydrogen donor (15). In the kinetic studies, lag time is the time required

for the resting met form to be drawn into the active deoxy form by the reducing agent, arising via action of the small amounts of the oxy form that usually accompany the met form. In the presence of reducing agents known as cofactors, especially *o*-diphenol derivatives such as L-DOPA and (+)-catechin, tyrosinase is activated and the lag time is shortened or abolished as shown in Figure 5 (44,52,53). L-DOPA at a very low concentration is the most effective reducing agent for eliminating lag time.

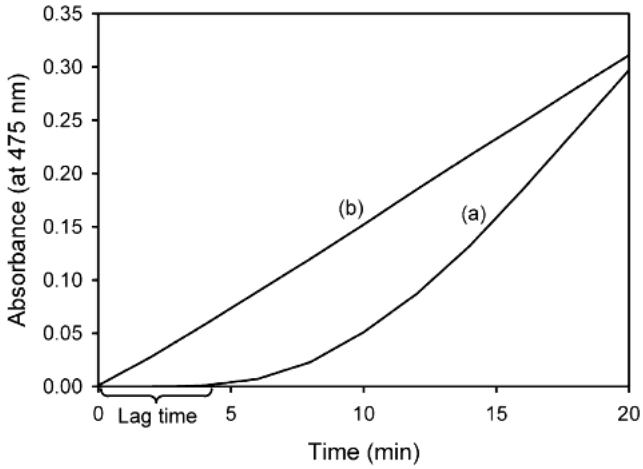

Figure 5 Hydroxylation of tyrosine by monophenolase action of mushroom tyrosinase in the absence (a) and presence (b) of L-DOPA (44). The increase of the absorbance at 475 nm is due to the formation of dopachrome by the hydroxylation of tyrosine.

2.1.2.2 Pathway of melanin biosynthesis in mammalians

Mammalian melanocytes can produce two types of melanin: eumelanin, which is black or brown and pheomelanin which is red or yellow in color (54, 55). Switching between these two types of melanins in follicular melanocytes elicits a temporary shift from eumelanogenesis to pheomelanogenesis, which is responsible for the wild-type agouti pigment of murine hair color (56). For many decades, melanosomal proteins that regulate melanin biosynthesis have been studied and characterized, especially those required for eumelanogenesis (57).

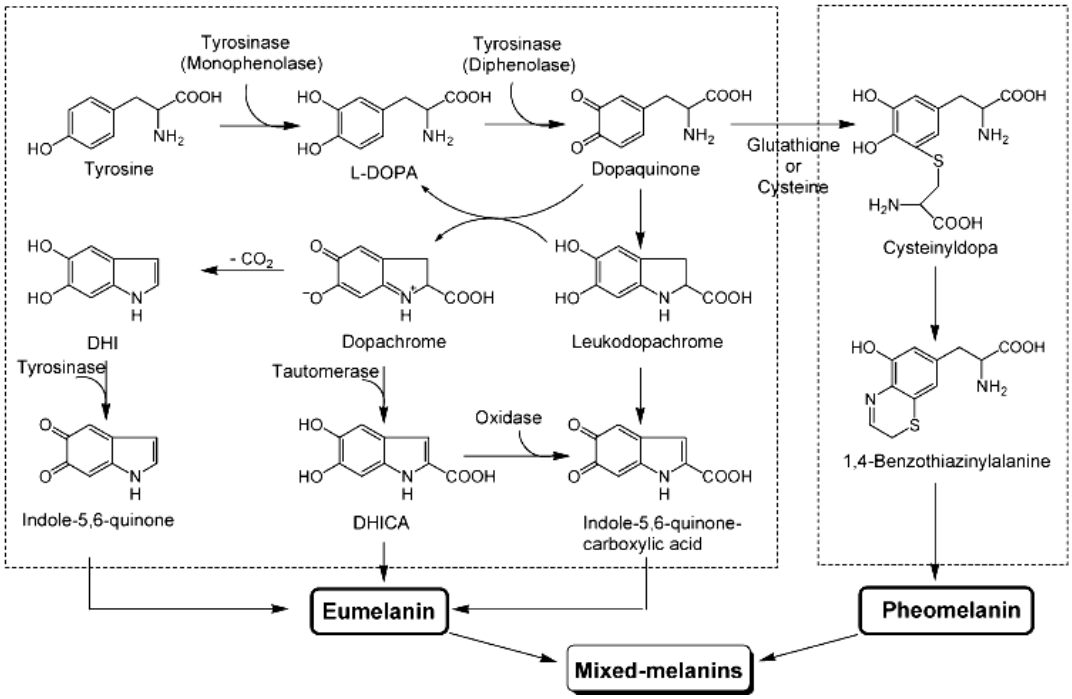

Figure 6 Biosynthetic pathway of melanin (46, 58).

The pathway of eumelanogenesis may be divided into two phases, one proximal and the other distal (Figure 6) (46, 58). The proximal phase consists of the enzymatic oxidation of tyrosine or L-DOPA to its corresponding *o*-dopaquinone catalyzed by tyrosinase. This nascent *o*-dopaquinone can undergo two different types of reactions: intramolecular 1, 4-addition to the benzene ring or a water addition reaction. The amino group of an *o*-dopaquinone side chain first undergoes an intramolecular 1, 4-addition to the benzene ring, which causes its cyclization into leukodopachrome, as shown in the above Figure. This intermediate is quickly oxidized to dopachrome by another *o*-dopaquinone, which is reduced back L-DOPA (43, 46, 47).

The second reaction occurs with cyclizable and noncyclizable quinones and consists of a water addition to the benzene ring, which leads to the formation of a three-hydroxylated phenol, 2,4,5-trihydroxyphenylalanine (TOPA), which is chemically oxidized to *p*-topaquinone by another *o*-dopaquinone (43, 59).

This *p*-topaquinone evolves through a series of slow reactions to dopachrome, which is the final product of the proximal phase.

The distal phase is represented by chemical and enzymatic reactions which occur after dopachrome formation and lead to the synthesis of eumelanins (Figure 6) This phase starts with the slow chemical decarboxylation of dopachrome to 5,6-dihydroxyindole (DHI) and its subsequent oxidation to indole-5,6-quinone. As an alternative to this chemical evolution in the distal phase, dopachrome may be enzymatically transformed into 5,6-dihydroxyindole- 2-carboxylic acid (DHICA) by dopachrome tautomerase (60, 61). DHICA is further oxidized by a redox reaction with *o*-dopaquinone to form indole-5,6- quinone carboxylic acid, which can exist in three tautomeric forms, including the quinone-imine and the corresponding highly reactive quinone-methide (62, 63). Properties of DHI-derived and DHICA-derived melanins differ from each other in that the former are black and flocculent, while the latter are yellowish-brown and finely dispersed (60).

During pheomelanogenesis, the thiol group of sulfhydryl compounds such as glutathione and cysteine nucleophilically attacks *o*-dopaquinone made enzymatically by tyrosinase to produce cysteinyldopa or glutathionyldopa. This thiol group can be added to different ring positions, although the 5-position is the favored position. Subsequent cyclization and polymerization of cysteinyldopa or glutathionyldopa in an uncharacterized series of reactions result in the production of pheomelanins and trichochromes (55, 57). The interaction between the eumelanin and pheomelanin compounds gives rise to a heterogeneous pool of mixed-type melanins.

2.1.3 Machanisms of skin depigmentation and their inhibitors

The processes of depigmentation involved in the production and the transfer of pigment granules can be interfered with at various steps. The possible modes of action of compounds which are considered as depigmenting agents have been summarized (64). These compounds may:

- selectively destroy the melanocytes
- inhibit the formation of melanosomes and alter their structures

- inhibit the biosynthesis of tyrosinase enzyme
- inhibit tyrosinase activity
- interfere with the transfer of melanosomes from melanocyte cells to keratinocyte cells

2.1.3.1 Skin depigmenting agents

Hydroquinone is one of the most effective depigmenting agents. Its mode of action is trought to include the inhibition of the conversion of tyrosine to melanin, degradation of melanocytes and inhibition of the DNA and RNA synthesis of melanocyte.

Mercury Compounds as depigmenting agents was in a form of mercury salts such as mercuric oxide and mercurous chloride. The disadvantage of mercuric chloride usually in liquid form is the release of hydrochloric acid which can damage the epidermis. The inhibition mechanism of ammoniated mercury is to replace the copper ions of the tyrosinase. This prevents the enzyme from functioning properly in skin pigmentation.

Catechol and its derivatives are effective skin color reducing compound but they are also cytotoxic to pigmented cell, their inhibition mechanism being in the process of dopa oxidation.

Kojic acid is inhibition mechanism involves chelation of the copper ions in the active sites of the enzyme tyrosinase.

Vitamin C Derivatives are changed to γ-ascorbic acid which is the active form by the enzyme in the skin, ascorbic acid (5-10%) is a copper chelator, anti-oxidant, and inhibits melanocyte proliferation (7, 71).

Niacinamide (5%), which is also known as vitamin B-3, reduces the transfer of melanosomes from melanocytes to keratinocytes or melanin transfer (serine protease inhibitors)

Alpha hydroxy acids: Glycolic acids (6-12%) are a group of organic carboxylic acids that have been popularized since they are considered to be natural substances. The mechanism of action of AHAs is thought to be as an exfloliating agent and thereby, removes epidermal keratinocytes (desquamation), shortens the cell cycle and facilitates rapid pigment loss (71).

Table 1 Some Skin depigmenting agents and their possible modes of action of compounds

Melanin synthetic pathway & related processes		Inhibitors	References
Before melanin synthesis	Tyrosinase transcription via MITF	- Tretinoin	Briganti,2003
		- Dihydrolipoic acid - Lipoic acid	Lin *et al.*,2002
		- Resveratrol	
		- *Ephedra sinica*	Kim *et al*.,2006
		- *Lepidium apetalum*	Choi *et al*.,2005
		- *Nardostachys chinensis*	Lee S *et al*.,2006
		- *Angelica gigantia* (ethanolic extract)	Na Ly *et al*.,2007
		- Betulin from Birch bark	Muceniece *et al*, 2007
	Tyrosinase maturation & stimulation via α-MSH	- *Cnidium officinale* extract	Lee K *et al*.,2006
		- Crocusatin K from *Crocus sativus* petals	Li *et al*.,2004
		- Piperlonguminine from *Piper longum* fruits	Kyeong-Soo *et al*., 2006
		- *Rumex* spp.(TyrostatTM)	Fytokem Products
		- Senkyunolide A from *Ligusticum chuanxiong*	Lee K *et a*l.,2006
		- *Sophora angustifolia* root extract	Tomonori,2000
After melanin synthesis	Inhibition of melanosome transfer	- Serine protease inhibitors	Seiberg *et al*, 2000 a,b
		- Lectins & neoglycoproteins	Minwalla *et al*.,2001
		- Soybean/milk extracts	Briganti,2003
		- Niacinamide	Hakozaki *et al*., 2002
		- Mandresy extract (*Buddleja auxillaris* leaf Extract)	Bayer's Serdex Division
	Acceleration of tyrosinase degradation	- 25-hydroxycholesterol - Linoleic acid - α-Linolenic acid	Ando *et al*., 2006
	Skin turnover accelerators	- Glycolic acid - Lactic acid - Malic acid - Salicylic acid	Solano *et al*.,2006
		- Linoleic acid	Ando *et al*., 2006
		- Liquiritin - Retinoic acid - *Helix aspera* Muller - 4-S-Cystaminylphenol	Briganti, 2003

2.1.4 Commonly used skin depigmentation agents

2.1.4.1 Hydroquinone

Hydroquinone has a variety of uses principally associated with its action as a reducing agent which is soluble in water, it is a ubiquitous chemical readily available in cosmetic and nonprescription forms for skin lightening. It is considered one of the most effective inhibitors of melanogenesis *in vitro* and *in vivo*, and is widely used for the treatment of melanosis and other hyperpigmentary disorders. This phenolic compound has been successfully used as a skin-lightening agent for the treatment of melasma, post-inflammatory hyperpigmentation and other disorders of hyperpigmentation. Hydroquinone decreases tyrosinase activity by 90% at the concentrate of 4% and causes reversible inhibition of cellular metabolism by affecting both DNA and RNA synthesis.

Hydroquinone occurs naturally in many plants as well as in coffee, tea, beer and wine. The cytotoxic effects of HQ are not limited to melanocytes, although the dose required to inhibit cellular metabolism is much higher for nonmelanotic cells than for melanocytes. Thus, HQ can be considered a potent melanocyte cytotoxic agent with relatively high melanocyte specific cytotoxicity.

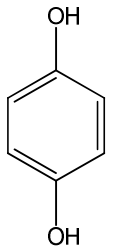

Hydroquinone

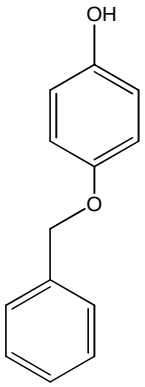

Monobenzyl hydroquinone (Benoquin; PBP)

The side effects of HQ include both acute and chronic effects. Acute side effects are allergic and irritant contact dermatitis, nail discoloration, and post inflammatory hyper-pigmentation. In 2006, the United States Food and Drug

Administration (FAD) revoked its previous approval of hydroquinone and proposed a ban on all over-the-counter preparations (65). The FDA stated that hydroquinone cannot be ruled out as a potential carcinogen. This conclusion was reached based on the extent of absorption in humans and the incidence of neoplasms in rats in several studies where adult rats were found to have increased rates of tumours, including thyroid follicular cell hyperplasias, anisokaryosis, mononuclear cell leukemia, hepatocellular adenomas and renal tubule cell ademonas .

2.1.4.2 Monobenzyl ether of hydroquinone

Like HQ, monobenzyl ether of hydroquinone (MBEH) belongs to the phenol/catechol class of chemical agents. However, unlike HQ, MBEH almost always causes a nearly irreversible depigmentation of skin. Traces of MBEH have been found in disinfectants, germicides, rubber covered dish trays, adhesive tape, powdered rubber condoms and rubber aprons (66). MBEH should be used only to eliminate residual areas of normally pigmented skin in patients with refractory and generalized vitiligo. It has been suggested that the mechanism of depigmentation by MBEH involves selective melanocytic destruction through free radical formation and competitive inhibition of the tyrosinase enzyme system (67).

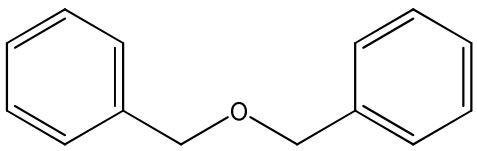

Monobenzyl ether

The phenomenon of repigmentation occurred within a few weeks of discontinuing successful depigmentation therapy with monobenzyl ether of hydroquinone in a patient with extensive vitiligo. Patients undertaking depigmentation therapy should be warned that this may occur, although the mechanism by which this occurs is unknown (68).

2.1.4.3 Hydroxyanisole

Many of the well-known depigmenting agents such as hydroquinone and 4-hydroxyanisole are, in fact, melanocytotoxic chemicals which are oxidized in melanocytes to produce highly toxic compounds such as quinines (69). These cytotoxic compounds are responsible for the destruction of pigment cells, resulting in skin depigmentation. However, cells are capable of protecting themselves against cytotoxic agents by intracellular glutathione (GSH). This protection takes place under the enzymatic action of the detoxification enzyme glutathione S-transferase (GST), which is responsible for the conjugation of toxic species to GSH. The depigmenting effect of hydroquinone is shown to be potentiated by buthionine sulfoximine (BSO) and cystamine as a result of their reducing intracellular GSH levels. Additionally, BSO and cystamine are shown to inhibit the activity of GST. The combination of all-trans-retinoic acid (tretinoin, TRA) with hydroquinone or 4-hydroxyanisole is also known to produce synergistic skin depigmentation. This agent was also shown to reduce the level of intracellular GSH in certain cells (69).

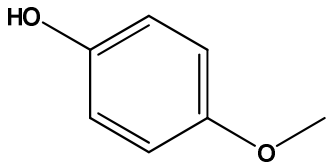

4-hydroxyanisole

2.1.4.4 Arbutin

Arbutin is both an ether and a glycoside; a glycosylated hydroquinone. It inhibits tyrosinase and thus prevents the formation of melanin. Arbutin is therefore used as a skin-lightening agent. Arbutin is also found in wheat, and is concentrated in pear skins. Arbutin (hydroquinone-O-beta-D-glucopyranoside) is a natural product which was first isolated from the fresh fruit of the California buckeye, *Aesculus californica* (70). At was later isolated from several the plant sources, especially bearberry plant in the genus *Arctostaphylos*, i.e. *Arctostaphylor urva-ur*si. Arbutin can inhibit the oxidation of L-DOPA catalysed by mushroom tyrosinase, and is effective in the topical treatment of various cutaneous

hyperpigmentations characterized by hyperactive melanocyte function. It can inhibit melanin synthesis by inhibiting the tyrosinase activity. This appears to be due to the inhibition of melanosomal tyrosinase activity rather than the suppression of this enzyme's synthesis and expression. Arbutin inhibits the oxidation of L-tyrosine (monophenolase activity) catalysed by mushroom tyrosinase (71) and it competes for active binding sites in the enzyme tyrosinase without being oxidized. However, arbutin itself was oxidized as a monophenol substrate at an extremely slow rate, and the oxidation was accelerated as soon as catalytic amounts (0.01 mM) of l-3,4-dihydroxyphenylalanine (L-DOPA) became available as a cofactor (70).

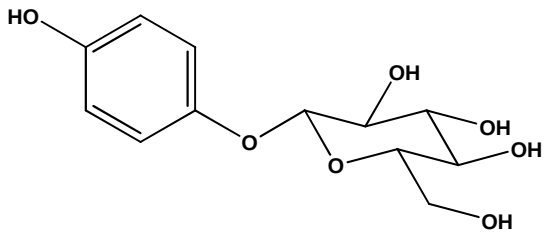

Arbutin (4-Hydroxyphenyl-β-D-glucopyranoside)

2.2 Enzymatic browning of plant-derived foods

The enzymatic browning of plant-derived foods and beverages takes place in the presence of oxygen when tyrosinase and their polyphenolic substrates are mixed after brushing, peeling and crushing operations, which lead to rupture of cell structure (72). The fundamental step in enzymatic browning is the transformation of an *o*-diphenol such as L-DOPA to the corresponding *o*-quinone, which can undergo further oxidation to brown melanin pigment (73, 74). *O*-Quinones are powerful electrophiles which can suffer nucleophilic attack by water, other polyphenols, amino acids, peptides and proteins, leading to Michael-type addition products (75-77). This enzymatic browning can be prevented by trapping the *o*-dopaquinone intermediate with cysteine or ascorbic acid (Figure 7) (7, 78).

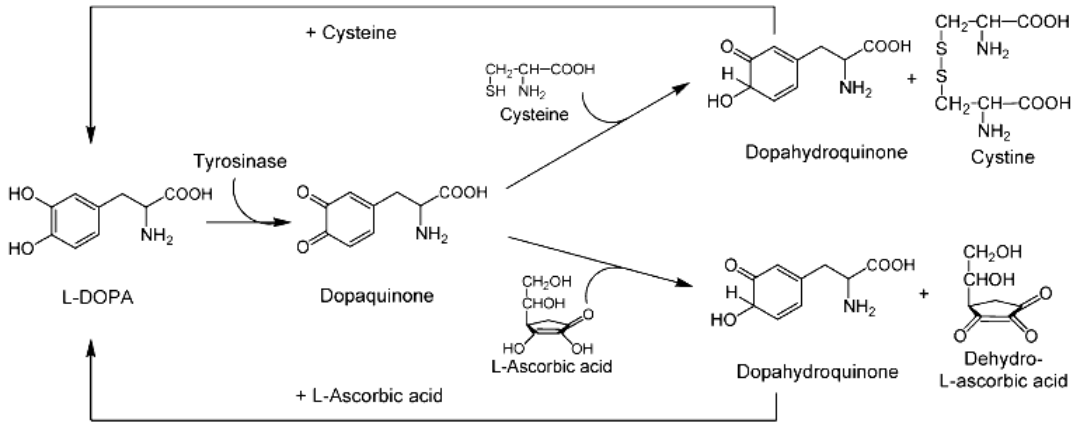

Figure 7. Inhibition of tyrosinase-catalyzed enzymatic browning by trapping the dopaquinone intermediate with cysteine or ascorbic acid (10, 78)

Chlorogenic acid, the major phenolic compound of plant derived foods, is also oxidized by tyrosinase to a highly reactive *o*-quinone intermediate which then could interact with NH_2 groups of lysine, SCH_3 groups of methionines and indole rings of tryptophan in nucleophilic addition and in polymerization reactions, the so-called browning and greening reactions. These transformations destroy essential amino acids, impair digestibility and nutritional quality, and may also result in the formation of toxic compounds (79, 80).

2.3 Natural inhibitors of tyrosinase

Numerous plant derived compounds with anti-tyrosinase activity have been isolated and characterized. These include phenylpropanoids, flavonoide, stilbenoide, etc.

2.3.1 Plant polyphenols as inhibitors (81)

Plant polyphenols are usually referred to as a diverse group of compounds containing multiple phenolic functionalities. These compounds are produced as secondary metabolites by most higher plants, in which they have numerous biological activities.

2.3.1.1 Flavonoids

Flavonoids are one of the most numerous and best-studied groups of plant polyphenols, that is benzo-γ-pyrone derivatives consisting of phenolic and pyrane rings. Widely distributed in the leaves, seeds, bark and flowers of plants, over 4000 flavonoids have been identified to date. In plants, these compounds afford protection against UV radiation, pathogens and herbivores. They are also responsible for the characteristic red and blue colors of flowers berries, and certain vegetables.

Flavonoids may be subdivided into six major groups (flavanols, flavones, flavonols, flavanones, isoflavones and anthocyanidins), which differ in the arrangements of the hydroxyl, methoxy and glycosidic side groups, and in the conjugation between the A- and B-rings.

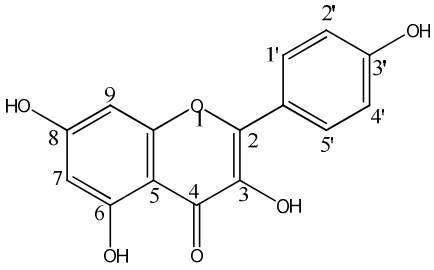

Flavonols

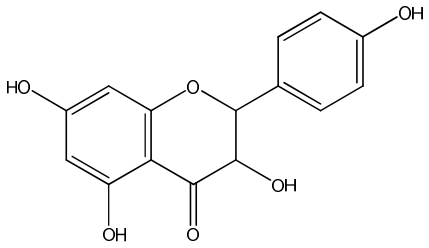

Flavanols

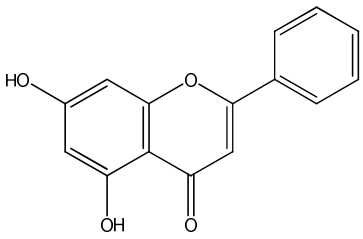

Flavones

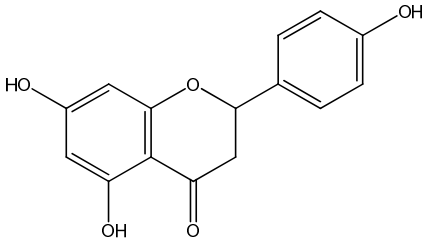

Flavanone

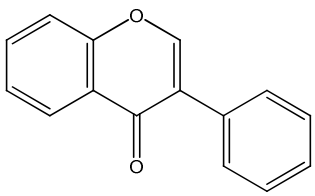

Isoflavones

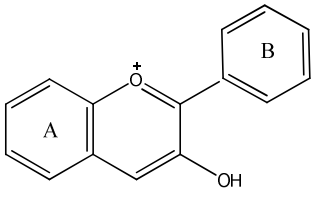

Anthocyanidins

Figure 8 Structures of different classes of flavonoids

Some flavonoids, such as kaempferol, quercetin and morin, show the inhibitory activity on tyrosinase, while others, e.g. catechin and rhamnetin, act as cofactors or substrates of tyrosinase. A number of studies have been carried out to identify and characterize inhibitors from natural sources and to establish the relationship between their inhibitory activity and their structures (Table 3). It was found that flavonoids containing an α-keto group show potent tyrosinase inhibitory activity (82). This inhibition ability may be explained in terms of similarity between the dihydroxyphenyl group in L-DOPA and the α-keto group in flavonoids.

Some flavonols possessing a 3-hydroxy-4-keto moiety, such as kaempferol and quercetin, competitively inhibit tyrosinase activity by their ability to chelate the copper atoms in the active site, leading to irreversible inactivation of tyrosinase. After chelation to tyrosinase, kaempferol and quercetin in the resulting complex theoretically should lose their planar structure and should be somehow twisted. This chelation behavior was verified by UV-visible measurement; the characteristic bathochromic shifts in the spectra of kaempferol and quercetin were observed by adding excess copper ions. This copper chelation mechanism is further supported by observation of a noticeable spectral shift when kaempferol and quercetin are incubated with tyrosinase. Interestingly, quercetin and kaempferol can chelate copper in the met form of tyrosinase. This behavior differs from that of kojic acid, which chelates via the oxy form (83).

Table 2. Summary of tyrosinase inhibitory activity of compounds from natural sources (81).

Compounds	Type of inhibition	IC_{50}(mM)
Flavanols		
(–)-Epigallocatechin	competitive[a]	0.035
(–)-Epicatechin gallate	competitive[a]	0.017
(–)-Epigallocatechin gallate	competitive[a]	0.034
Flavonols		
Quercetin	competitive[b]	0.070
Kaempferol	competitive[b]	0.230
Morin	competitive[b]	2.320
Flavones		
Luteolin	noncompetitive[b]	0.190
Luteoilin 7-O-glucoside	noncompetitive[b]	0.500
Isoflavans		
Glabridin	noncompetitive[b]	0.004
Glabrene	mixed-type[b]	7.600
Isoliquiritigenin	mixed-type[b]	0.047
Other compounds		
Kojic acid	mixed-type[b]	0.014
Anisaldehyde	noncompetitive[b]	0.320
Cuminaldehyde	noncompetitive[b]	0.050
Cinnamaldehyde	noncompetitive[b]	0.980

[a] Inhibition of monophenolase activity.

[b] Inhibition of diphenolase activity.

IC_{50}, concentration causing 50% inhibition of the enzyme activity

In contrast to kaempferol and quercetin, 3-*O*-glycoside derivatives (kaempferol 3-*O*-glucoside, kaempferol 3-*O*-sophoroside, quercetin 3-*O*-glucoside and quercetin 3-*O*-rutinoside) did not exhibit inhibitory activity even at high concentrations. This means that the free hydroxyl group at the C-3 position seems to play an important role in eliciting the activity. As far as flavonols are concerned, it seems that aglycones exhibit tyrosinase inhibitory activity but not their 3-glycoside derivatives. However, although this hydroxyl group somehow relates to the activity, it may not be essential because several flavones, such as luteolin and luteolin 7-*O*-glucoside, which lack this 3-hydroxyl group still showed tyrosinase inhibitory activity (83). Generally, most competitive inhibitors closely resemble, at least in part if not all, the structure of the substrate tyrosine and / or L-DOPA. Conclusions, based on this concern, seem to imply that the molecule of kaempferol or quercetin fits loosely into the active site of tyrosinase and prevents entry of L-DOPA. On the other hand, a bulky sugar moiety attached to the 3-hydroxyl group in the flavonols may hinder their approach to the active site of tyrosinase. In contrast, the sugar moiety of flavone glycosides such as luteolin 7-*O*-glucoside and buddlenoids did not disturb their nearness to the active site for inhibition. The additional hydroxyl group at the 3'-position also somewhat affected the activity since quercetin exhibited slightly more potent activity than the more lipophilic kaempferol.

Gallates, gallic acid and its esters, are widely used as additives in food industries. Gallic acid, the parent compound of gallates, inhibits the oxidation of L-DOPA catalyzed by tyrosinase. In addition, gallic acid itself seems to act as a substrate, being oxidized prior to L-DOPA, which accelerates the oxidation of gallic acid. The resulting *o*-quinones of gallic acid may condense with one another through a Michael-type addition, yielding a relatively stable quinol-quinone intermediate. It appears that *o*-dopaquinone could act as a redox cycler, oxidizing gallic acid to the corresponding *o*-quinone and being reduced back to L-DOPA. Various gallic acid derivatives have been isolated from green tea and *Galla rhois*. Some of them showed a potent inhibitory effect against tyrosinase, indicating that the flavan-3-ol skeleton with a galloyl moiety at the 3-position is an important structural requirement for optimum inhibition of tyrosinase activity. It has been reported that the tyrosinase inhibitory activity of aromatic carboxylic acids decreases through esterification, hydroxylation or

methylation of the benzene ring. However, 1,2,3,4,6-penta-Ogalloyl-b-D-glucose isolated from Galla rhois exhibited high tyrosinase inhibitory activity.

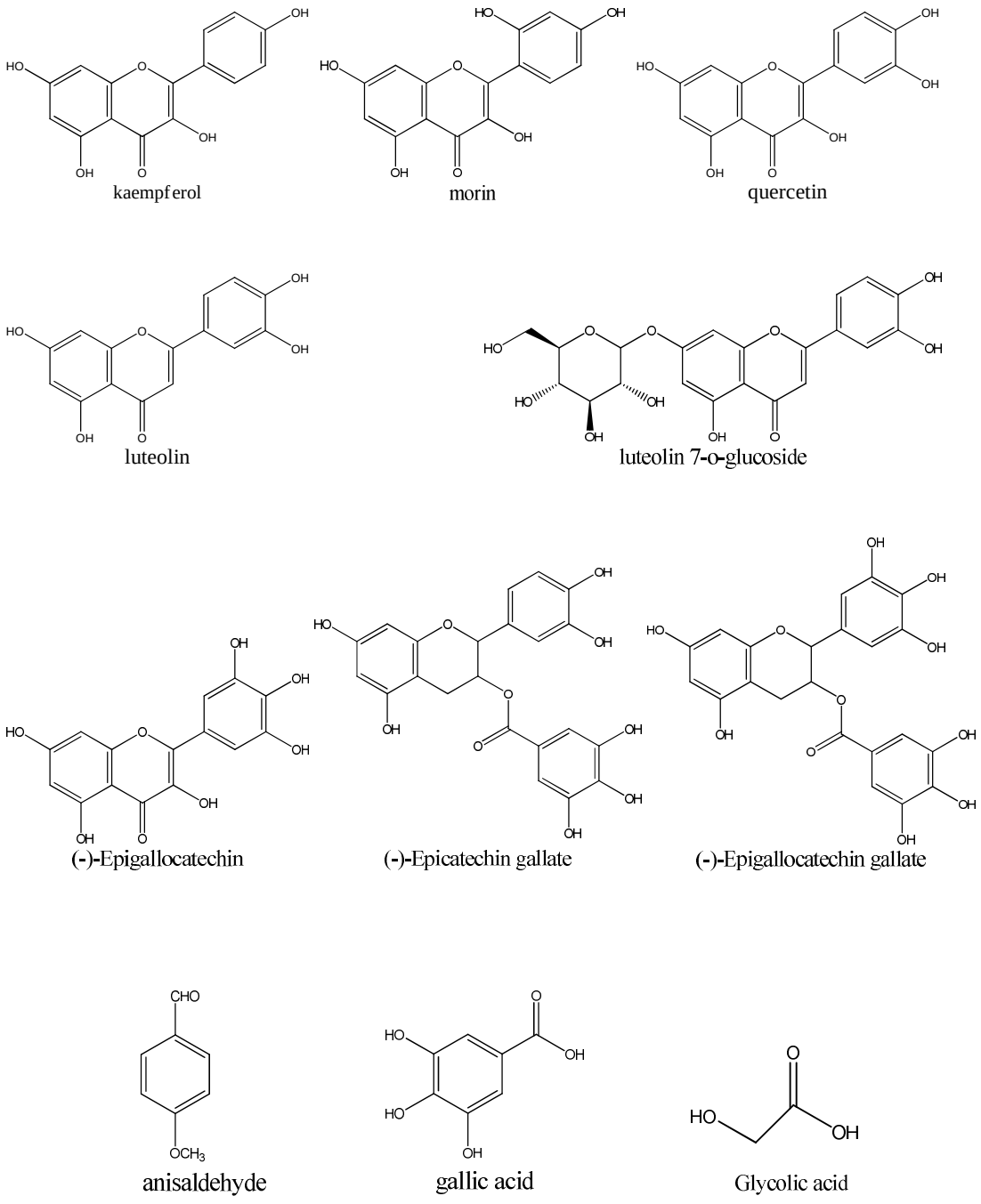

Figure 9 Structures of some of tyrosinase inhibitors from natural sources.

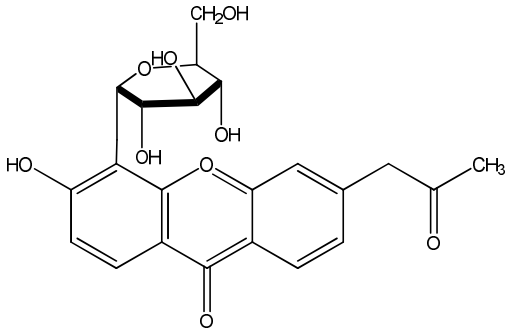

Aloesin

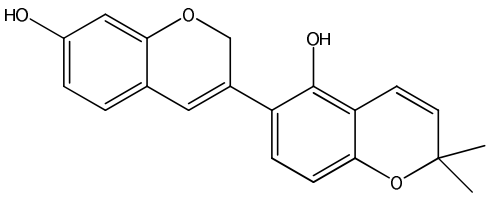

Glabrene

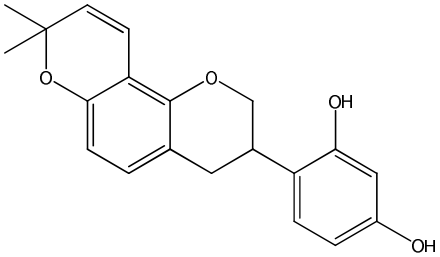

Glabridin

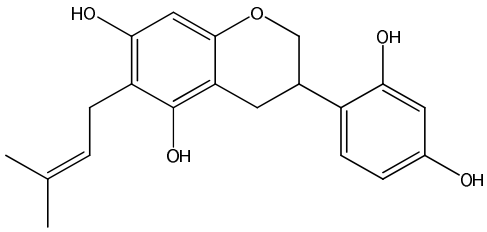

Glyasperin C

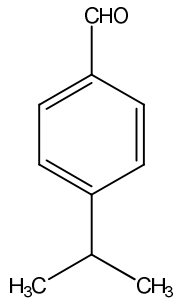

Cuminaldehyde

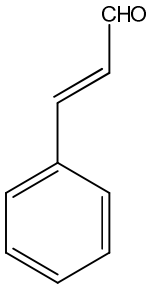

Cinnamaldehyde

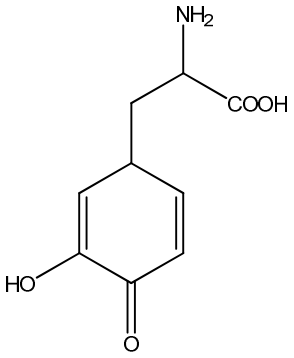

L-Mimosine

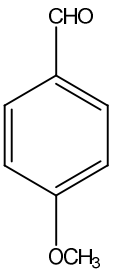

Anisaldehyde

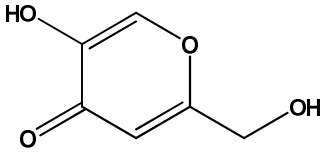

Kojic acid

Figure 9 Structures of some of tyrosinase inhibitors from natural sources (cont.)

2.3.1.2 Xanthones (91)

Xanthones are natural constituents of plants in the familie Bounetiaceae and Clusiaceae. Current reseach on xanthones they are beneficial in many conditions including: allergies, infections (bacterial, fungus, viral), inflammation, and skin disorder. Most xanthones also exhibit strong antioxidant activity. Cudraxanthones (Figure 11) isolated from root bark of *Cudrania tricuspidata,* which has been used as traditional medicine in Korea and China, especially cudraxanthone M (furano prenylxanthone) showed potent anti-tyrosinase activity with IC_{50} value of 16.5 μM, and appeared to inhibit the polyphenol oxidase activity of tyrosinase in an noncompetitive mode (K_i = 1.6 μM) when L-tyrosine was used as a substrate and kojic acid (IC_{50} value 14.6 μM) as a positive control. In an investigation on constituent from root bark of *Cudrania tricuspidata*, it was found that xanthones showed potent tyrosinase inhibitory and antioxidant activities. In this paper (Sang Seok, 2007) three xanthones were isolated; these were cudraxanthone L, cudraxanthone D and cudraxanthone M. Only Cudraxanthone M showed potent tyrosinase inhibitory activity.

Table 3. The inhibibtory effects of copounds 1-3 (1, cudraxanthone L, 2, cudraxanthone D and 3, cudraxanthone M) on tyrosinase activities (91)

Compound	IC_{50} (μM)	Inhibition type
1	>100	NT*
2	>100	NT*
3	16.5	uncompetitive
Kojic acid	14.6	NT*

NT* : not tested

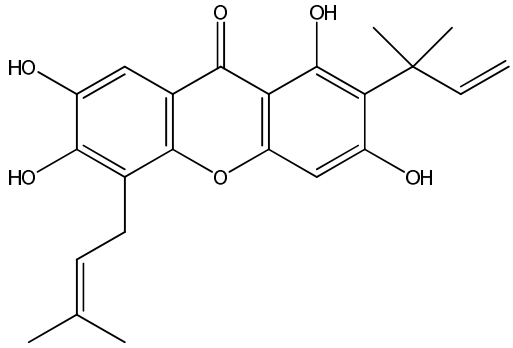

Cudraxanthone L

(1)

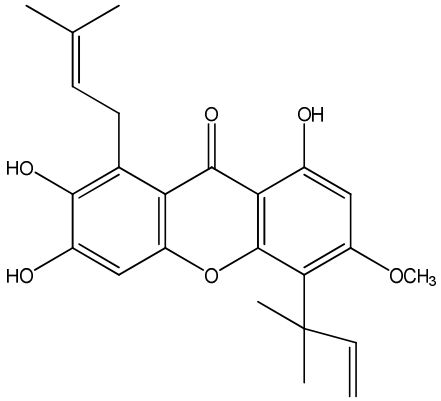

Cudraxanthone D

(2)

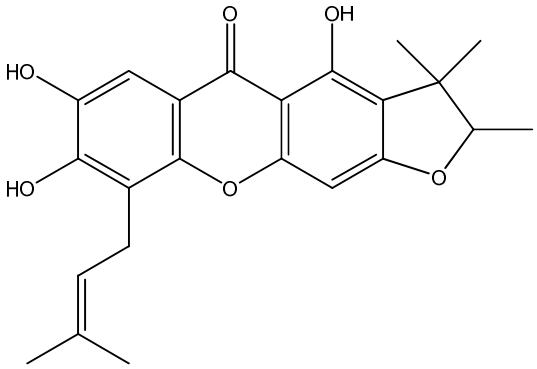

Cudraxanthone M

(3)

Figure 10 Chemical structures of xanthones with anti-tyrosinase activity

2.3.2 Aldehydes and other compounds from higher plants (81)

A large number of aldehydes and other compounds were also isolated and characterized as tyrosinase inhibitors, such as cinnaldehyde, (2E)-alkenals, 2-hydroxy-4-methoxybenzaldehyde, anisaldehyde, cuminaldehyde and cumic acid. The aldehyde group is known to react with biologically important nucleophilic groups, e.g. sulfhydryl, amino and hydroxyl groups. Their tyrosinase inhibitory mechanism

presumably comes from their ability to form a Schiff base with a primary amino group in the enzyme. Interestingly, the addition of an electron-donating group at the para position of benzaldehyde increases inhibitory activity, probably stabilizing the Schiff base. For example, the inhibitory activity of anisaldehyde and cuminaldehyde was about 2.5- and 16-fold more potent than that of benzaldehyde, respectively. In addition to stabilizing the binding site, the binding affinity of the hydrophobic electron-donating groups such as methoxy and isopropyl to the enzyme also may be related to the inhibitory effect.

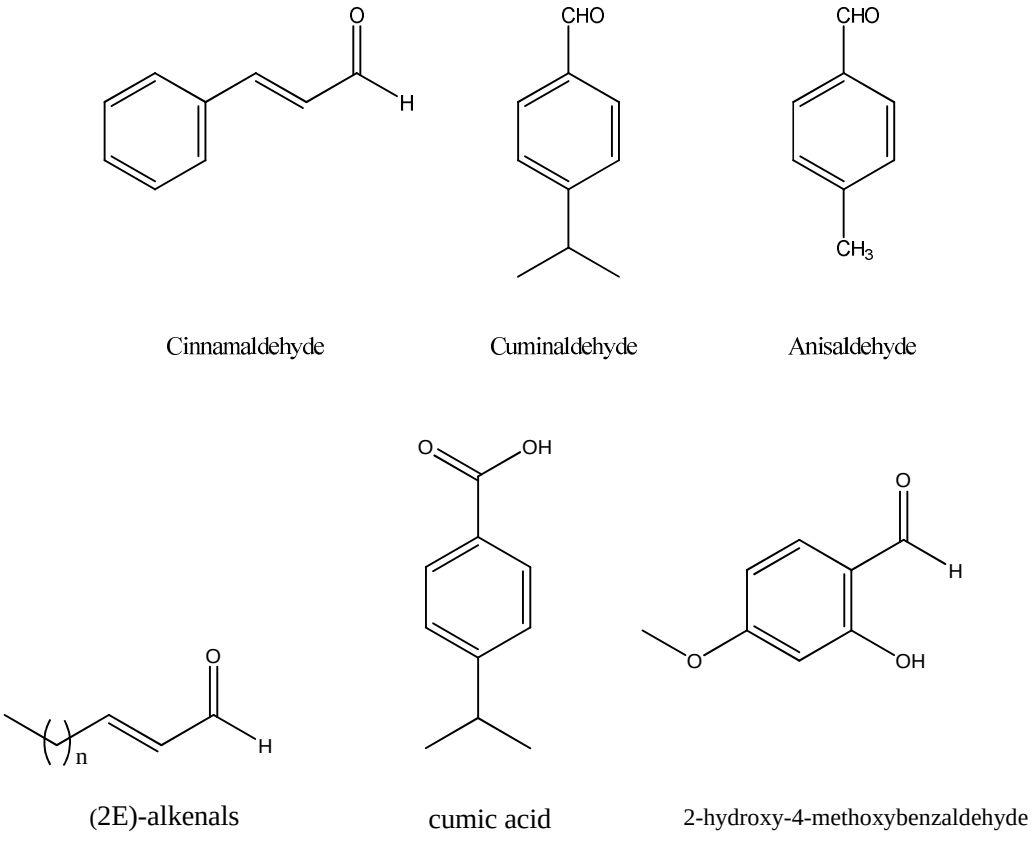

Figure 11 Structures of aldehydes exhibiting anti-tyrosinase activity

Interestingly, (2E)-alkenals did not inhibit monophenolase activity but inhibited the oxidation of L-DOPA by tyrosinase in a noncompetitive manner. (2E)-Alkenals with a longer alkyl group may better associate with the

hydrophobic protein pocket close to the binuclear active site. However, a cyclic α,β-unsaturated aldehyde sesquiterpene, polygodial, did not inhibit the oxidation of L-DOPA by tyrosinase. This compound is known to form a Schiff base, but its hydrophobic decaline moiety may not associate well with the protein pocket in the enzyme.

2.3.3 Fungal metabolites as inhibitors (81)

Besides higher plants, some compounds from fungal sources have also been identified and reported for their inhibitory activity on tyrosinase. Azelaic acid (1,7-heptanedicarboxylic acid) is a naturally occurring straight-chain, saturated dicarboxylic acid which is produced by lipoperoxidation of free and esterified cis-polyunsaturated fatty acids by a yeast, *Pityrosporum ovale*. This dicarboxylic acid has a definite cytotoxic effect on malignant melanocytes of primary cutaneous melanoma, though normal melanocytes appeared not to be affected. Azelaic acid acts as a rather weak competitive inhibitor of tyrosinase *in vitro*, which may be a major cause of its melanocytotoxicity.

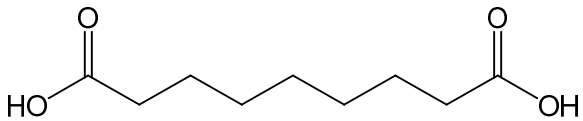

1,7-heptanedicarboxylic acid

2.3.3.1 Kojic acid

Kojic acid (5-hydoxy-4-pyran-4-one-2-methyl) is a by-product in the fermentation process of malting rice for use in the manufacturing of rice wine. It is a tyrosinase inhibitor derived from various fungal species such as *Aspergillus Penicillium* (84). It is a good chelator of transition metal ions and a good scavenger of free radicals (85, 86). It inhibited the tyrosinases of various *Aspergillus* species, *N. crassa* and mushrooms, as well as those of some plants and crustaceans by chelating

copper at the active site (87-90). It also acts as an antioxidant and prevents the conversion of the o-quinone to DL-DOPA and dopamine to its corresponding melanin. Melanocytes that are treated with kojic acid become nondendritic and have decreased melanin content. Kojic acid also acts as a free radical scavenger. It is used widely in Asia both topically as a skin-lightening agent and was reported to have a high-sensitizing potential and to potentially cause irritant contact dermatitis. However, it is useful in patients who cannot tolerate hydroquinone and it may be combined with a topical corticosteroid to reduce irritation. Kojic acid also inhibits the catecholase activity of tyrosinase, which is the rate-limiting step in melanogenesis, Moreover, kojic acid effectively inhibits the formation of pigmented products and oxygen uptake when catecholamines such as DL-DOPA, norepinephrine and dopamine are oxidized by tyrosinase, This means that kojic acid is able to reduce *o*-quinone to *o*-diphenol to prevent the final pigment forming and be oxidized to a yellow product by chemical interaction with *o*-quinone (91).

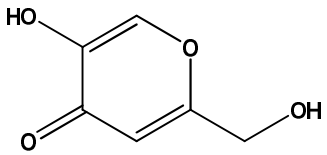

kojic acid

2.3.3.2 Yeast

Yeasts are eukaryotic micro-organisms classified in the kingdom Fungi, with about 1,500 species currently described (92). The yeast metallothioneins are ubiquitous cytosolic proteins, usually characterized by selective binding of a large amount of heavy metal ions (Zn^{2+} , Cu^{2+} and Cd^{2+}) and high cysteine content (93, 94). *Neurospora crassa* copper-metallothionein is a metal donor for apotyrosinase. Metallothionein from *Aspergillus niger* is also found to be an inhibitor for a commercially purified mushroom tyrosinase, and exhibited a higher inhibitory effect on the oxidation of catechin compared with that of chlorogenic acid (95).

Other fungal extracts such as agaritine and inhibitors (Ia and Ib) from Agaricus species is also isolated, purified and characterized (96, 97). Agaritine, β-N-(γ-L(+)-glutamyl)-4-hydroxymethylphenyl-hydrazine, showed a depigmenting effect that prevented melanin formation. The inhibition was uncompetitive when L-DOPA was used as the substrate and partially competitive when tyrosine was used as the substrate (97). Taking into account that agaritine is very abundant in *Agaricus bisporus* mushrooms, it might be suggested that agaritine could play a role in vivo as endogenous regulator of mushroom tyrosinase activity and the extent of o-quinone concentration formed.

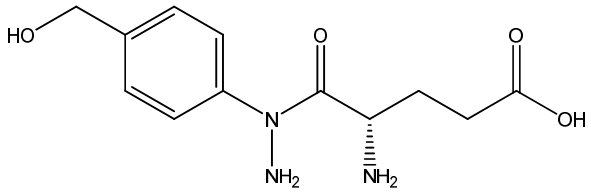

N-(-L(+)-glutamyl)-4-hydroxymethylphenyl-hydrazine

2.3.4 Plant Extracts

2.3.4.1 Licorice extract – glabridin (9)

Licorice extract is obtained from the roots of *Glycyrrhiza glabra* Linn. The depigmenting efficacy of glabridin has been shown by various researchers to be greater than that of hydroquinone and the inhibitory effect of licorice extract on tyrosinase activity has been noted to be higher than that of purified glabridin.

Five different flavonoids were isolated from licorice and characterized as new tyrosinase inhibitors for depigmenting agents. The isolated flavonoids were identified as liquiritin, licuraside, isoliquiritin, liquiritigenin (from *Glycyrrhiza uralensis* Fisch) and licochalcone A (from *Glycyrrhiza inflate* Bat) and all were found to be competitive inhibitors. In contrast to the above flavonoids, no inhibitory activity was observed for liquiritin, whereas liquiritigenin activated the monophenolase activity as a cofactor. The inhibitory effect of licuraside, isoliquiritin

and licochalcone A on diphenolase activity with L-DOPA as the substrate was much lower than that with L-tyrosine and have great potential for use as depigmenting agents.

Glabrene and isoliquiritigenin (2',4',4-trihydroxychalcone) in the licorice extract can inhibit both mono- and diphenolase tyrosinase activities, and these effects on tyrosinase activity were dose-dependent and correlated to their ability to inhibit melanin formation in melanocytes.

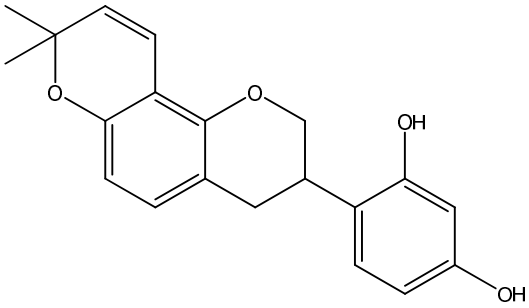

Glabridin

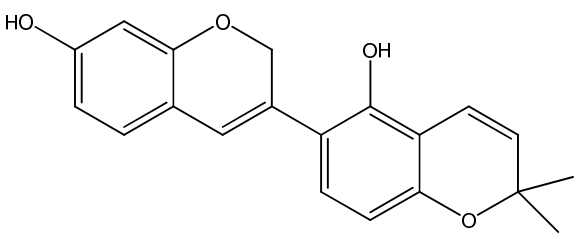

Glabrene

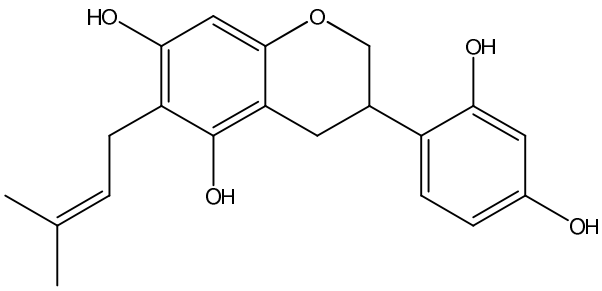

GlyasperinC

Glycyrrhiza uralensis extract was examined by measuring the inhibitory activity on tyrosinase and melanin synthesis and was shown to have no detectable effect on their DNA synthesis. Glycyrrhisoflavone and glyasperin C were identified as tyrosinase inhibitors for the first time. Glyasperin C showed a stronger tyrosinase inhibitory activity than glabridin and a moderate inhibition of melanin production, making it a promising candidate in the design of skin-whitening agents.

2.3.4.2 **Green tea** (9)

Epidemiologically, it is well known that the consumption of green tea may help to prevent cancers in humans and also to reduce several free radicals including peroxynitrite. Yang (1999) studied to assess the efficacy of the inhibition of mushroom tyrosinase, ten kinds of traditional Korean teas were screened for their tyrosinase inhibitory activity. Green tea is the strongest inhibitor, and its major active constituents are (-)-epicatechin 3-O-gallate (ECG), (-)-gallocatechin 3-O-gallate (GCG) and (-)- epigallocatechin 3-O-gallate (EGCG). All are catechins with a gallic acid group as an active moiety. The kinetic analysis of the inhibition of tyrosinase revealed a competitive nature of GCG against L-tyrosine for the binding at the active site the enzyme.

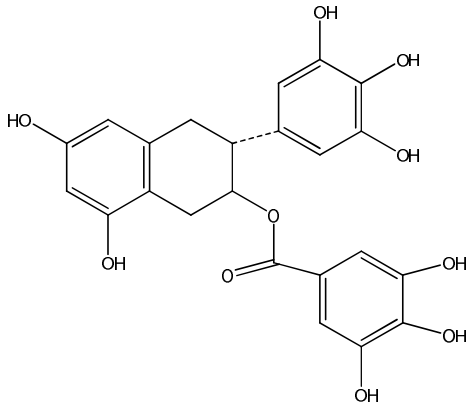

(+)-Gallocatechin-3-*O*-gallate (GCG)

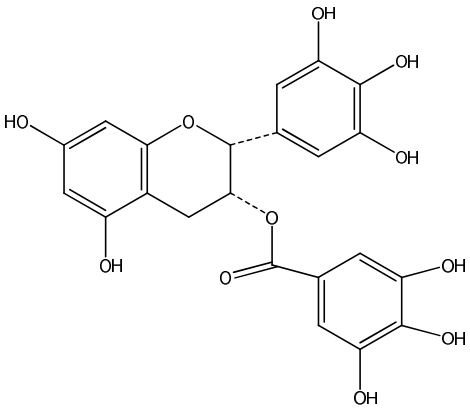

(-)-Epigallocatechin-3-*O*-gallate (EGCG)

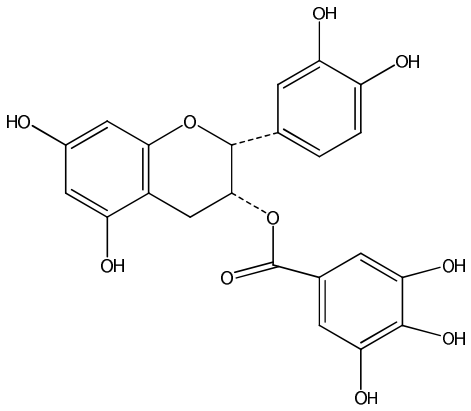

(-)-Epicatechin-3-*O*-gallate (ECG)

2.3.4.3 Soy (9)

Natural soybeans contain small proteins, such as Bowman Birk inhibitor (BBI) and soybean trypsin inhibitor (STI). These serine protease inhibitors inhibit the protease-activated receptor-2 (PAR-2) pathway expressed on keratinocytes. Interference with the PAR-2 pathway has been shown to induce depigmentation by reducing the phagocytosis of melanosomes by keratinocytes, thus reducing melanin transfer. This mechanism of action is different to that of hydroquinone, kojic acid or glabridin. It is important to note that this depigmenting effect is available only with fresh soymilk and not with pasteurized soymilk.

A number of attempts have been made by various researchers, and total soy is now being incorporated into skin care products to improve mottled hyperpigmentation and solar lentigines that frequently result from photodamage. In addition, soy has been shown to lighten and slow the regrowth of unwanted facial hair.There are many studies showing that fermented soy products containing the isoflavones, daidzein and genistein, may function as weak phytoestrogens. A known biotransformed compound, 6,7,4'-trihydroxyisoflavone, was identified as a potent tyrosinase inhibitor, which has six times the anti-tyrosinase activity of kojic acid. Currently, several manufacturers are producing facial and body care products that contain total soy to even the skin tone.

2.3.4.4 Mangosteen pericarp extract (47)

Mangosteen (*Garcinia mangostana* Linn, Guttiferae) is a plant mostly found in Asia, especially in Thailand. The pericarp of the fruits of this plant has been used as a medicinal agent in Southeast Asia for the treatment of skin infections and wounds, inflammation, and diarrhea. Its pericarp contains a variety of xanthones, such as α-, β-, γ-mangostins which have remarkable biological activities. The biological activities of xanthones isolated from mangosteen include antioxidant, antitumoral, antibacterial, antiviral, antifungal, antiallergic, and anti-inflammatory properties. The result of the MPC inhibit the tyrosinase enzyme at IC50 = 134 ng/ml. The MPC consisted of 1:1 mangosteen pericarp extract and PVP K30, thus, the mangosteen pericarp extract itself inhibited the tyrosinase enzyme at IC50 = 67 ng/ml.

Owing to its the excellent antityrosinase activity, the mangosteen pericarp extract might be used as anti-melasma agent. However, a large amount of α-mangostin was found in the mangosteen pericarp extract, so, it is very possible that the antityrosinase activity of the mangosteen pericarp extract might be from the α-mangostin.

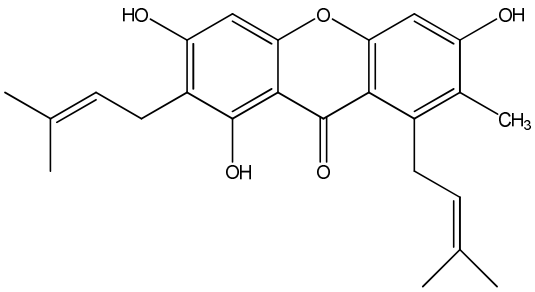

alpha-mangostins

In recent years, the popularity of skin whitening products is on the rise, especially in Asia and other parts of the world. With the ban imposed on the use of hydroquinone and kojic acid in cosmetics by many countries, the search is on for new natural depigmentation agents.

Therefore, it is interesting to investigate new plant-based compounds for use in the management of the production of skin pigments. There are many plants that have been found to have anti-tyrosinase activity. Some of these plants are listed in the following Table.

Table 4 Plants with Tyrosinase Inhibiting Activity

Plant Name	References
Morus alba	124, 130
Glycyrrhyza glabra	129
Rheum officinale Baillon	125
Artocarpus incisus	123
Artocarpus gomezianus	114
Aloe vera	127
Olea europaea L.	115
Crocus sativus L.	121
Mondia whitei (Hook), *Rhus vulgaris* Meikle, *Sclerocarya caffra* Sond	115
Anacardium occidentale L., *Buddleia coriacea* Remy, *Gnaphalium cheiranthifolinm* Lam, *Scheekea princes* (Mart.), *Heterotheca inuloides* Cass	113, 122, 126, 128

Several groups of plant-derived compounds have been found to inhibit the tryrosinase enzyme and examples of these are shown in Table 5

Table 5 Anti-tyrosinase compounds from plants

1. Phenylpropanoids

Compounds	IC_{50}(mM)	Sources	References
Ferulic acid	0.045	Authentic sample	57
4-Hydroxy-3-methoxycinnamaldehyde	0.077	Authentic sample	57
Curcumin	0.047	Authentic sample	115
Yakuchinone A	0.514	*Alpinia oxyphylla*	115
Yakuchinone B	0.057	Synthetic compound	115
Eugenol	0.923	*Syzygium aromaticum*	115
Capsaicin	0.087	Authentic sample	115

2. Flavonoids

Compounds	IC_{50}(mM)	Sources	References
Kaemferol	0.230	*Crocus sativus* L.	129, 115
Quercetin	0.070	*Heterotheca inuloides, Myrica rubra*	120, 128
Dihydromorin	0.025	*Artocarpus incisus*	123
Norartocarpanone	0.0018	*Artocarpus incisus*	123
Norartocarpitin	0.0144	*Artocarpus gomezianus*	106, 114
Kurarinone	0.0105	*Sophora flavescens*	132
(+)-Gallocatechin-3-O-gallate	0.0173	*Thea sinensis L.*	131
Mulberanol	0.0011	*Morus alba*	130

3. Stilbenoids

Compounds	IC_{50}(mM)	Sources	References
Chlorophorin	0.26	*Artocarpus incisus*	123
4-Prenyloxyl-resveratrol	0.66	*Artocarpus incisus*	123
Artocarbene	2.45	*Artocarpus incisus*	123
Oxyresveratrol	1.50 1.00	*Artocarpus gomezianus* *A. lakoocha* *Morus alba*	123 114 124 130
Resveratrol	14.4	*Artocarpus gomezianus*	106, 114
Resveratrol 4'-O-β-D-(2"-O-galloyl)-glucopyranoside	6.71	*Rheum officinale*	125

4. Phenolic compounds

Compounds	IC_{50}(mM)	Sources	References
2-Hydroxy-4-methoxybenzaldehyde	0.03	*Mondia whitei,* *Rhus vulgaris* *Sclerocarya caffra*	115
5-[8(z),11(z),14-Penta-decatrienyl] resorcinol	0.04	*Anacardium occidentale*	129
5-[8(z),11(z)-pentade-catrienyl] resorcinol	0.05	*Anacardium occidentale*	129
5-[8(z)-pentadecatrienyl] resorcinol	0.08	*Anacardium occidentale*	129
Agrimoniin	0.061	*Buddleia coriacea*	129
L-Mimosine	0.001	*Leucaena spp.* *Mimosa spp.*	51

5. Cyclic peptides

Compounds	IC_{50}(mM)	Sources	References
Pseudostellarin A	0.131	*Pseudostellaria heterophylla*	133
Pseudostellarin B	0.187	*Pseudostellaria heterophylla*	133
Pseudostellarin C	0.063	*Pseudostellaria heterophylla*	133

6. Aldehydes

Compounds	IC_{50}(mM)	Sources	References
Cuminaldehyde	0.05	*Cuminum cymonum*	134
Anisaldehyde	0.32	*Pimpinella anisum*	134

7. Terpenoids

Compounds	IC_{50}(mM)	Source	References
Cucurbitacin 1	0.18	*Trichosanthes kirilowii*	135
Cucurbitacin 2	6.7	*Trichosanthes kirilowii*	135

8. Coumarin

Compound	IC_{50}(mM)	Source	References
Esculetin	43	*Euphorbia lathyris* L.	136

9. Chromones

Compounds	%Inhibition (at 50 ppm)	Source	References
8-C-glucosyl-7-O-methyl-(s)-aloesol	-	*Aloe barbadensis* Miller	127
Isoaloeresin D	22%	*Aloe barbadensis* Miller	127
Aloeresin E	44%	*Aloe barbadensis* Miller	127

2.4 Antioxidant (98)

Antioxidants are a group of substances which, when present in low concentration, in relation to oxidizable substrates, significantly inhibit or delay oxidative processes, while often being oxidized themselves. The main characteristic of an antioxidant is its ability to trap free radicals. Highly reactive free radicals and oxygen species are present in biological system from a wide variety of sources. These free radicals may oxidize nucleic acids, proteins, lipids or DNA and can initiate degenerative diseases. Antioxidant compounds like phenolic acids, polyphenols and flavonoids scavenge free radicals such as peroxide, hydroperoxide or lipid peroxyl and thus inhibit the oxidative mechanisms that lead to degenerative diseases.

The function of antioxidants consists of scavenging active radicals ($R^{\bullet}$) generated in different ways in higher organisms. Thus they prevent undesired chemical decays in cells and the development of diseases like cancer, atherosclerosis, inflammations, etc. The scavenging reaction of phenolic antioxidants can be illustrated by Scheme 1.

$$Ar–OH + R^{\bullet} \rightarrow Ar–O^{\bullet} + R–H$$

Scheme 1 Reaction between phenolic antioxidants and active radicals

The parent antioxidant molecule transforms into a radical which has no capacity for initiating unwanted chain radical processes. Consequently, this radical takes part in trapping active radicals called “second radical scavenging” (Scheme 2).

$$Ar–O^{\bullet} + R^{\bullet} \rightarrow Ar–O–R$$

Scheme 2 Second radical scavenging reaction

The reaction mechanism of the first step is arguable; hence, various alternatives are discussed in the literature: direct H-atom transfer, electron transfer followed by proton transfer, sequential proton loss and electron transfer, etc.

In fact, the antioxidant efficiency is determined by the rate and the conversion degree of these reactions and all experimentally determinable and

theoretically computable descriptors of antioxidant/scavenging activity originate from kinetics and conversion data. They can be divided into the following groups: (I) indices estimating O–H bond strength–bond dissociation enthalpy (BDE) or structural parameters–bond length, charge distributions etc.; (II) indices presenting molecular electron-donation capacity–ionization potential or its theoretical analogue–HOMO energy and (III) indices showing the stability of the obtained phenoxyl radicals (Ar–O$^{\bullet}$)–spin distribution, C–O bond length in the radicals, etc.

Correlations between antioxidant activity and theoretically or experimentally derived descriptors belonging to the types mentioned above are usually obscured by the dependence of the antioxidant activity on additional factors such as their permeability into the cells (lipophilicity), coordination ability, and resistance to enzymatic degradation. Therefore, a preceeding analysis of correlation between the main descriptors and scavenging activity is more meaningful.

The establishment of relations between basic descriptors and antioxidant/ scavenging activity is also hindered due to the different reaction mechanisms in operation. In polar solvents, a more probable reaction mechanism is the two-step electron–proton transfer rather than one-step hydrogen atom abstraction. In such a case the proper descriptor is not the O–H BDE but the ionization potential (or HOMO energy) of the molecule.

2.4.1 **Antioxidant activity of xanthones** (102)

The catecholic xanthones with antioxidant activity was activity isolated from *Cudrania tricuspidata*. Catecholic xanthones possessed potent free radical scavenging activities. The catecholic xanthone, 1,3,7-trihydroxy-4-(1,1-dimethyl-2-propenyl)-5,6-(2,2-dimethylchromeno)-xanthone (1), among the range of catecholic xanthones, 6,7-dihydroxyl xanthones (3–8), exhibited a strong scavenging effect on the DPPH radical. When one of the catecholic hydroxyl groups was protected as in compounds 1 and 2, DPPH radical scavenging activity was markedly decreased (IC_{50} > 200 μM). DPPH activities were consistent with electrochemical response by cyclic voltammetry, compounds (1, 2) which had the weak activities on DPPH, exhibited both potent superoxide and hydroxyl radical scavenging activities. The strong activity on the hydroxyl radical of compounds (1, 2) could be rationalized by

their chelating effect with iron (Fe^{2+}) due to a redshift of their complex (structure shown in Figure12).

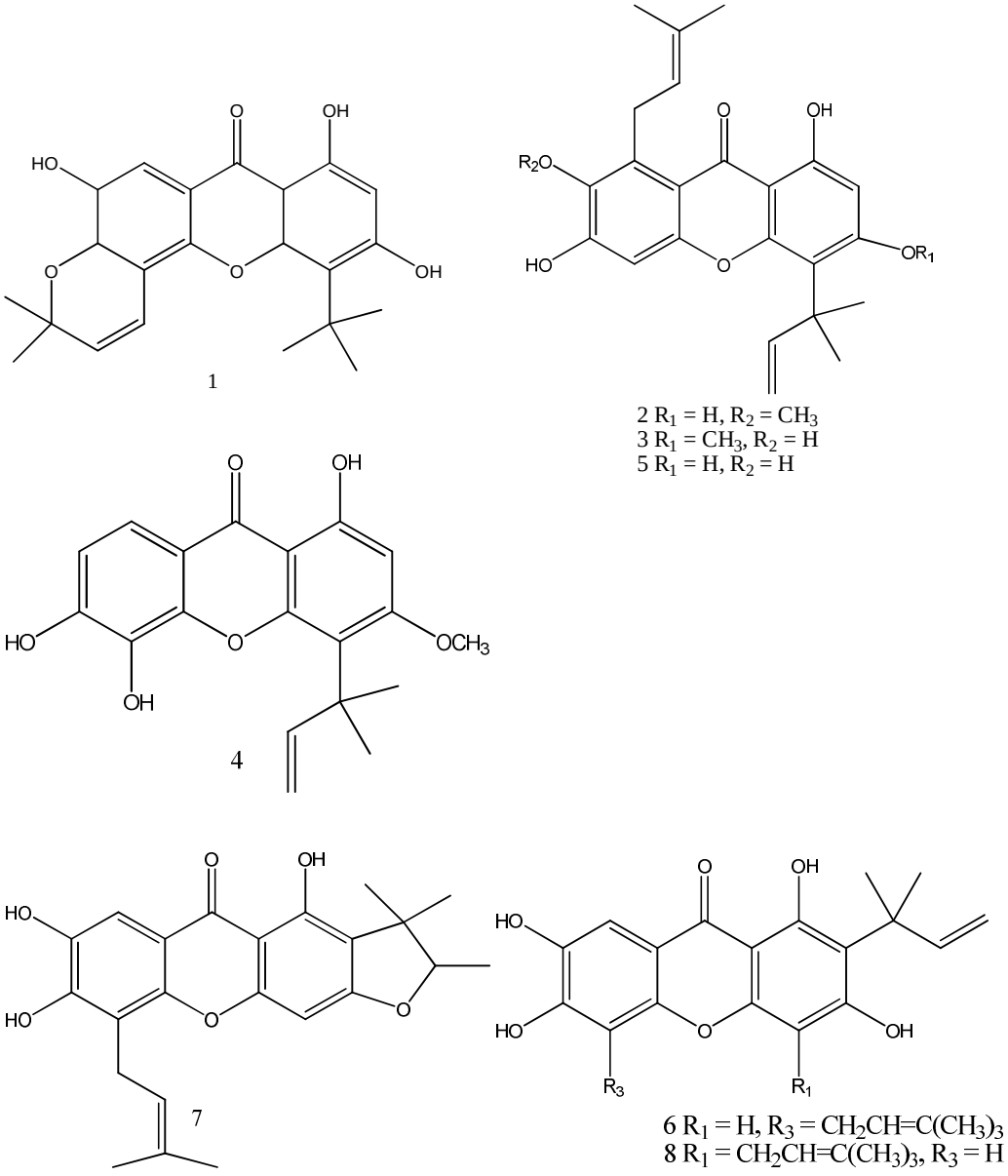

Figure 12 Structures of xanthones shown to have antioxidant activity

2.5 Annonaceous Plants (99)

The family Annonaceae is a large family comprising 130 genera and more than 2,300 species (6). They occur in tropical and subtropical regions. They are woody trees, shubs and vines. The leaves are entire, extipulate and pinnately veined. Flowers can be numerous or solitary. The flowers are bisexual and astinomorphic, possessing 3 whorls of peranth with 3 segments in each whorl. The elongated floral axis also bears many elliptically disposed stamens and several to many simple pistils. All of floral parts are distinct. Sectioned seed reveal channels or partitions in the ruminate endosperm. The pistils generally remain distinct and develop into berry-like fruits but sometimes they coalesce into aggregate fruits.

Annonaceous plants became important in pharmaceutic research because of the antifungal, bacteriostatic, and especially cytostatic capability of some chemical constituents of the leaves and bark.

The genus *Anaxagorea*

The genus *Anaxagorea* comprises approximately forty-three species widely distributed mostly in Central and South America, a few in Asia, i.e. Sri Lanka, Myanmar, Thailand, Indo-China, Borneo, Java, Sumatra and the Philippines. A typical example of the plants in this genus is *A. javanica*.

2.5.1 ***Anaxagorea javanica* Blume.** (จำปูน) (100)

Shrub or small tree 4-6 m hight. Leaves thinly coriaceous, elliptic or elliptic-oblong, apex acute or acuminate, base slightly acute, glabrous, width 4-10 cm., length 10-26 cm., petiole length 5-22 mm. Flower(s) 1-4, terminal and extraaxillary, fragrant; pedicels 1 cm; sepals 3, oblong, glabrous, petals 3, elliptic, glabrous; apex acute, width 12-14 mm., length 14-16 mm, inner apex acute, greenish outside, white inside. Fruits follicle, gradually narrowed into a stalk, carpels 4-8 clavate. Seed(s) 2, black, shining (Sinclair, 1995).

Anaxagorea javanica Blume var. *tripetala*

Anaxagorea javanica Blume

Figure 13 *Anaxagorea javanica* Blume (Thai Journal of Phytopharmacy Vol.12 (1) June.2005)

2.6 *Anaxagorea luzonensis* A. Gray

Thai Name : Kam – lang – wua - talerng (กำลังวัวเถลิง)

Family : Annonaceae

Description

Glabrous shrub. Leaves membranous oblong-elliptic-oblong acuminate, base cuneate; nerves 7 to 8 cm pairs; 5 to 7 cm in long, wide; petioles 25 to 35 mm long. Flowers 5 mm long; pedicles 25 mm long. Bracts amplexicaul. Sepals round obtuse. Petals 6, elliptic-optuse white. Carpels cuneate clavate apiculate, 9 mm long, follicular portion 4 mm long (101).

Figure 14 *Anaxagorea luzonensis* A.Gray from Flora of Thailand

Figure 15 *Anaxagotrea luzonensis* A. Gray

Kam-lang-wua-talerng has the botanical name of *Anaxagorea luzonensis* A.Gray, in the family Annonaceae, and is a tree indigenous to Thailand. Its heartwood is available in pieces of varying size, consisting of reddish-brown heartwood to which a little of the whitish bark still adheres. The wood is hard but easily splits (103).

Distribution

A. luzonensis A.Gray occurs in Burma, Ceylon to Malay Archipelago, Cambodia, India, Selangor, Indonesia, Laos, Philippines, Viet Nam**.** In Thailand *A. luzonensis* is found mainly in the northern to soutuern regions of dry to moist deciduous forests (101).

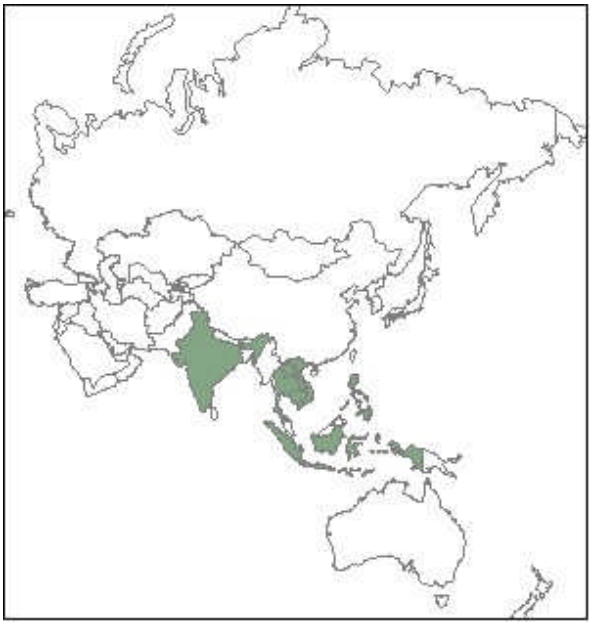

Figure 16 Distribution of *A.luzonensis* A. Gray in Southeast Asia

Medicinal uses

The plant is used in traditional medicine as a blood tonic, stomachic, antipyretic and for the treatment of muscular pain (103).

Chemical Constituents (103)

Literature survey of chemical constituents of *A.luzonensis* A.Gray revealed the presence of the following compounds; 1,3,6-trihydroxy-5-methoxy-4-prenylxanthone, 1,3,5-trihydroxy-6-methoxy-2-prenylxanthone, 1,3,5-trihydroxy-4-(3-hydroxy-3-methylbutyl) xanthone, 1,3,6-trihydroxy-4-prenylxanthone,3,6-dihydroxy. 1,5-dimethoxyxanthone. 3,5,7,4'-tetrahydroxy-2'-methoxyflavone. 1,3,6-trihydroxy-5-methoxy-4-prenylxanthone . 1,3,5-trihydroxy-6-methoxy-2-prenylxan-thone, 1,3,5-trihydroxy-4-(3-hydroxy-3-methylbutyl) xanthone , 1,3,6-trihydroxy-4-prenylxanthone, 3,6-dihydroxy-1,5-dimethoxyxanthone , 3,7-dihydroxy-1-methoxy-6-O-β.-D-glucopyranosyl xanthone, 5,6-dihydroxy-1-methoxy-3-O-.β.-D-glucopyranosylxanthone, Flavonoids such as 3,5,7,4'-tetrahydroxy-2'-methoxy-flavone, biochanin A, chrysin , 3'-methylorobol, orobol, taxifolin, kaempferol and quercetin

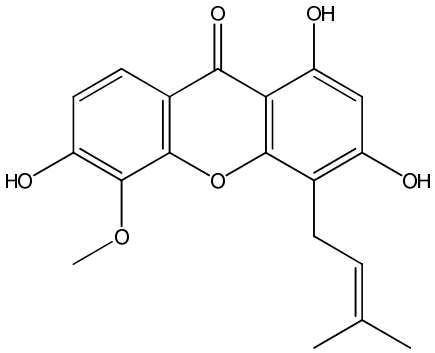

1,3,6-trihydroxy-5-methoxy-4-prenylxanthone

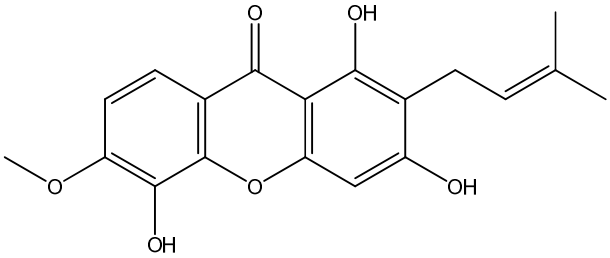

1,3,5-trihydroxy-6-methoxy-2-prenylxanthone

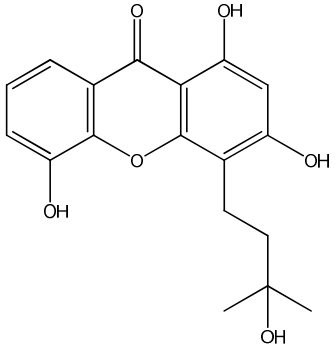

1,3,5-trihydroxy-4-(3-hydroxy-3-methylbutyl) xanthone

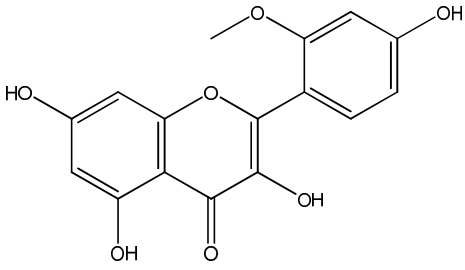

3,5,7,4'-tetrahydroxy-2'-methoxyflavone

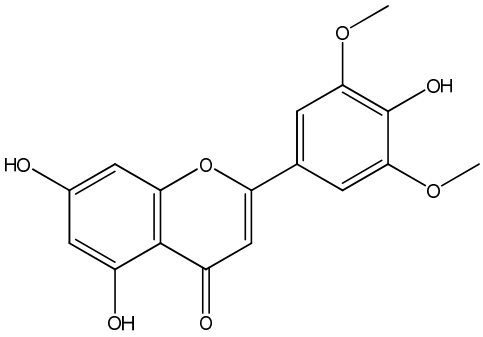

chrysin

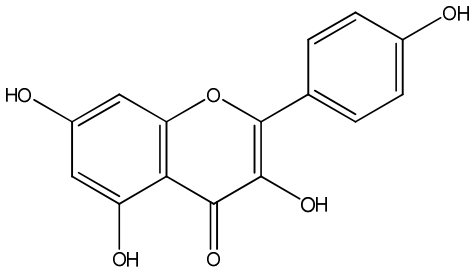

kaempferol

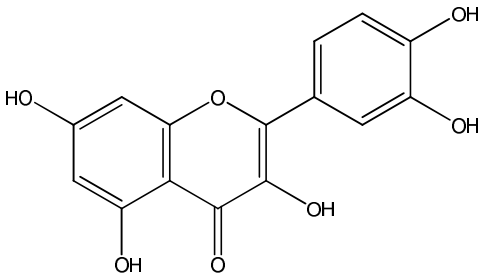

quercetin

Figure 17 Structures of some compounds present in *A.luzonensis* A.Gray

A random screening of various plant extracts for anti-tyrosinase activity revealed that the ethanol extract of the stem *A.luzonensis* A.Gray (Annonaceae) inhibited more than 80% of mushroom tyrosinase activity at the concentration of 0.909 mg/ml. A literature survey of the phytochemistry of this plant indicated the presence of several xanthones and flavonoids. Flavonoids are reported to possess a wide range of biological activities.

So far, there has been no report on the anti-tyrosinase activity of *A.luzonensis* A.Gray (SciFinder, Accessed since November, 2007). Therefore, it is of interest to study *A.luzonensis* A.Gray as a model for anti-tyrosinase agent.

CHAPTER III
MATERIALS AND METHODS

Part I Phytochemistry

A. Materials

3.1 Plant materials

The stems of *Anaxagorea luzonensis* were collected from Khanjanaburee, province, Thailand, in July 2006

3.2 Chemicals used in this study were as follows:

3.2.1 Solvents

95% Ethanol, commercial grade	(The Excise Department, Thailand)
Hexane, AR grade	(Fisher, Apex chemicals Co, LTD)
Dichloromethane, AR grade	(Fisher, Apex chemicals Co, LTD)
Ethyl acetate, AR grade	(Fisher, Apex chemicals Co, LTD)
Methanol, AR grade	(Fisher, Apex chemicals Co, LTD)
Formic acid	(Labscan Asia co, LTD)

3.2.2 Chemicals

Qurecetin	(Fluka, Switzerland)
Isoquercitrin	(Sigma, Germany)
Rutin	(Sigma, Germany)
chlorogenic acid	(Sigma, Germany)
kojic acid	(Riedel-de Haën, Germany)
Ascorbic acid	(Fluka, Switzerland)
DPPH	(Fluka, Switzerland)

3.2.3 Spraying reagents

NP-PEG (Natural products – Polyethylene glycol) (Fluka, Switzerland)

Anisaldehyde-sulfuric acid (Fluka, Switzerland)

3.3 Chromatography

3.3.1 Packing materials

Silica gel 60 for column chromatography (particle size 0.063-0.200 mm.), (Merck, Germany)

Silica gel 60 for column chromatography (particle size 0.040-0.063 mm.), (Merck, Germany)

Sephadex LH20 (Fluka, Switzerland)

3.3.2 Chromatogrphic columns

Sintered glass with inner diameter of 10 cm and 13 cm long (for quick column, silica gel 400 g.)

Glass column with diameter of 4.5 cm and 45 cm long

Glass column with diameter of 2.5 cm and 45 cm long

Glass column with diameter of 1.5 cm and 35 cm long

3.3.3 Solvent systems

Hexane : ethyl acetate	(0-100%, gradient system)
Dichloromethane : methanol	(0-100%, gradient system)
Dichloromethane : ethyl acetate	(0-100%, gradient system)

3.4 Identification

Melting point apparatus,	(Electrothermal 9100, Eng. Ltd.)
UV spectrophotometer,	(Perkin-Elmer, Lambda 35^{TM} , USA)
FT-IR spectrometer	(FTIR spectrum GX, Perkin elmer), Department of Chemistry, Faculty of Science, Mahidol University)

NMR spectrometer,	(Bruker DRX 500), National Science and Technology Development Agency (NSTDA), Thailand Science Park. (Bruker DRX 300), Department of Chemistry, Faculty of Science, Mahidol University)
Mass spectrometer,	(EI-MS, TOF-MS) Faculty of Science, Mahidol University

3.5 Others

Water bath	(Optima WB-710M, Japan)
Rotary evaporator	(Rotaevaporator R-200, BUCHI, Switzerland)
Ultrasonic bath	(Elma Transsonic 460/H, Germany)
TLC Tank designed for TLC plate size 10 x 10 cm. and 15 x15 cm.	(CAMAG, Germany)
pH meter	(Precisa pH900, Switzerland)
Hot air oven	(Mammert, Germany)
Soxhlet apparatus	(VN Supply, Thailand)

B. Methods

The collected plant materials were cleaned, separated, chopped and dried in a forced draught oven at a temperature of 60 °C. After that they were pulverized with a Thomas WILEY laboratory mill to a moderately coarse powder.

3.1. Extraction of *Anaxagorea luzonensis* for biological screening

Ten grams of the dried powdered drug were sonicated for 30 min three times with 95% ethanol. The ethanol extracts were combined and filtered before being evaporated on a water bath and the dried extracts were weighed and stored in tightly closed containers at 10 °C.

3.1.1 Preparation of test solutions

The dried extracts were dissolved in methanol to a final concentration of 10,000 μg/ml. This solution was again diluted to 5000, 2000, 1000, 500 and 100 μg/ml. The diluted samples were then subjected to the assay for anti-tyrosinase and free radical scavenging activities.

3.2 Extraction and isolation of compounds from the *Anaxagorea luzonensis*

The powdered drug (700 g.) was extracted consecutively with solvents of increasing polarity, namely, hexane, dichloromethane, ethyl-acetate, and 95% ethanol in a soxhlet apparatus (Figure 18). After the evaporation of solvents, each extract was subjected to tyrosinase inhibitory test. The hexane, dichloromethane and ethyl acetate extracts were further fractionated by chromatographic technique and each fraction was assessed for its anti-tyrosinase activity.

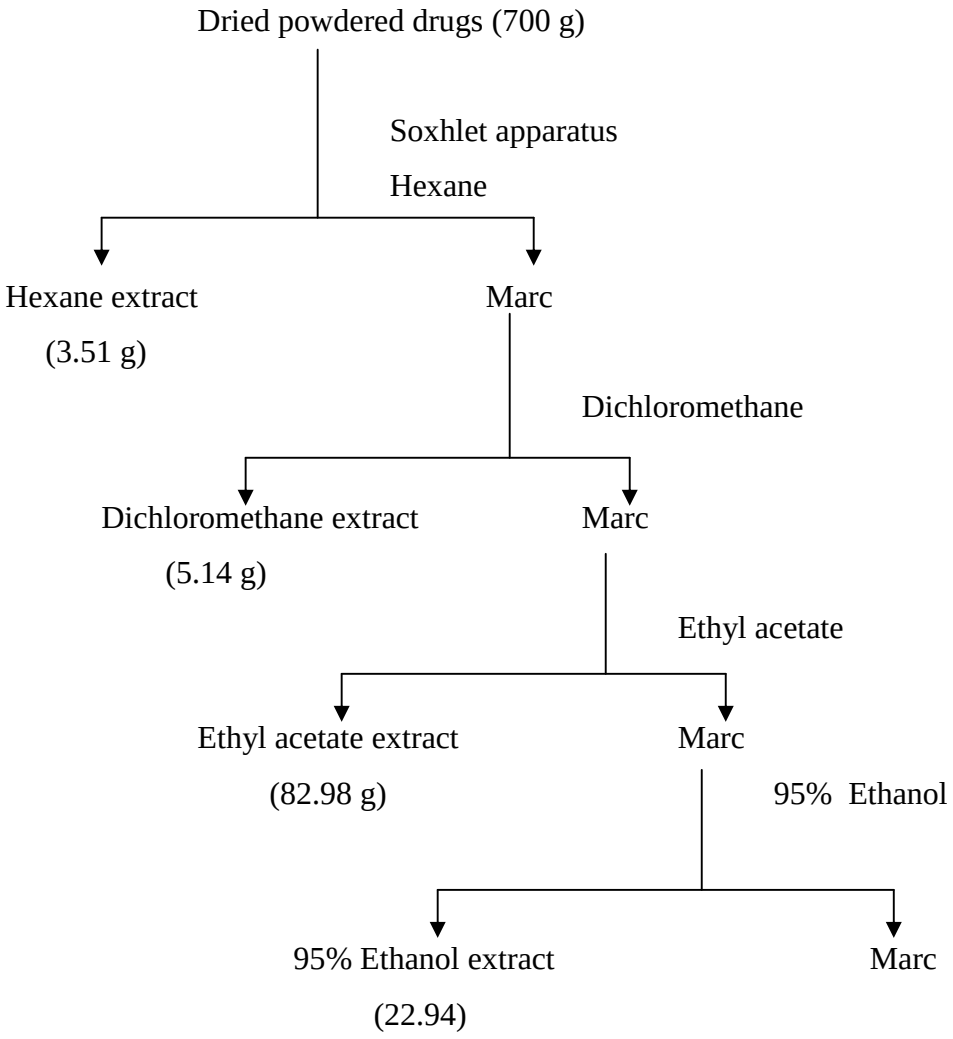

Figure 18 Extraction of *A. luzonensis* with solvents of increasing polarity in a soxhlet apparatus.

3.2.1 The isolation of compound from the hexane extract of *A.luzonensis*

The hexane extracts were combined and reduced to dryness under reduced pressure to yield a yellow residue (3.5068 g). Part of the hexane extract (3.12 g) was chromatographed over a silica gel column (silica gel No. 7729 10 g upper; No.7734 180 g lower; 4 cm diameter x 32 cm long) using mixtures of hexane/ethyl-acetate of increasing polarity (3% ethyl-acetate 3000 ml ,4% ethyl acetate 500 ml, 5% ethyl acetate 1500 ml and 10% ethyl acetate 3500 ml). Fractions were monitored by TLC

on silica gel GF_{254} plates, developed with hexane-ethyl acetate- formic acid (30-10-1.5), detected with NP-PEG and anisaldehyde spray reagent. Similar fractions were combined to afford fractions H1 (200-600 ml, 683.3 mg), H2 (600-3500 ml, 315.9 mg), H3 (600 - 4250 ml, 50.8 mg), H4 (4250 - 4650 ml, 368.6 mg), H5 (4650 - 4850 ml, 4.1 mg), H6 (4850 - 4950 ml, 15.8 mg), H7 (4950-6510 ml, 32.1 mg), H8 (6510 - 7010 ml, 24.3 mg), H9 (7010 - 8500 ml, 30.1 mg). Each fraction was tested by TLC technique for tyrosinase inhibitory activity. Further purification was carried out on fraction H6.

Compound **A** (10.8 mg) was obtained from fraction H6, after washing with cold hexane and further purified by recrystallization from hot hexane. The procedure of isolation of compound A was shown in Figure 19.

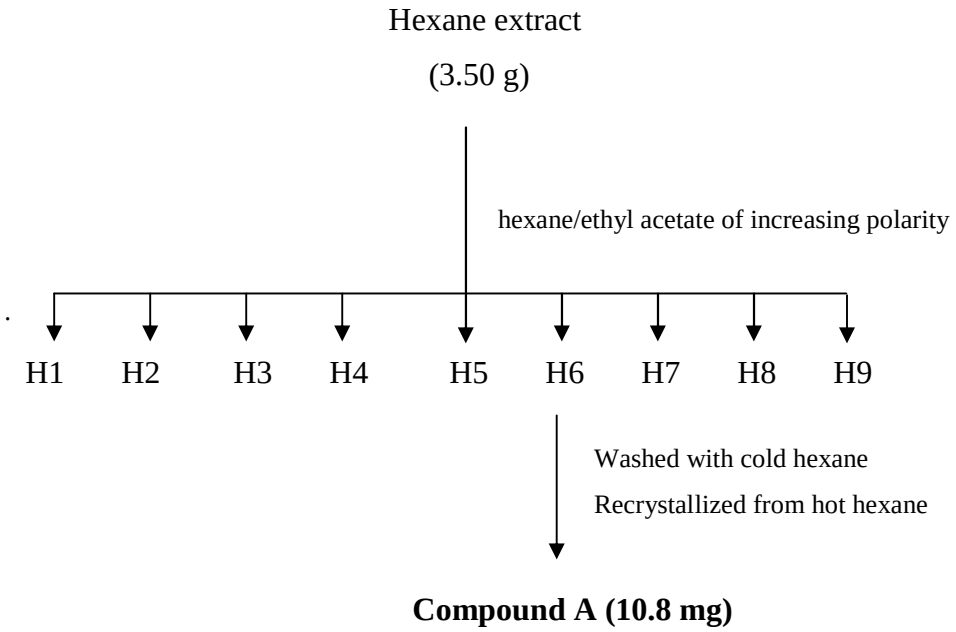

Figure 19 Isolation of compound A from the hexane extract of *A. luzonensis*

3.2.2 The isolation of compounds from dichloromethane extract of *A. luzoneusis*

The dichloromethane extract which exhibited moderate antityrosinase activity against mushroom tyrosinase was selected for further investigation. A portion of the extract (2 g) was dissolved in a small amount of methanol: dichloromethane and

mixed with silica gel 60 (0.063 - 0.200 mm.). The mixture was evaporated on a Rotary evaporator until the extract appeared as dry granules. The granules were placed on top of a silica gel column (2.5 cm diameter x 10 cm long, silica gel 42.28 g). The column was eluted with bi-gradient of increasing amounts of CH_2Cl_2 (30-100%) in n-hexane and ethyl acetate (0 - 100%) in CH_2Cl_2.

Fractions of 20 ml each were collected and were profiled by thin-layer chromatography (TLC) on silica gel GF_{254}, developed with dichloromethane – methanol-formic acid (9:0.5:0.5). The TLC plates, were detected under UV 254, UV 366 and with NP-PEG spray reagent under UV 366 nm.

Fractions with similar profiles were combined and concentrated. This resulted in a total of 13 fractions. Fractions 7 and 8 were selected for further separation. Fraction **f7** (413.2 mg) was dissolved in MeOH, filtered and then rechromatographed on Sephadex LH-20 (2.0 cm diameter x 20 cm long). The column was eluted with MeOH. The composition of each collecting fraction was examined by TLC on silica gel GF_{254} plates, developed with dichloromethane - methanol - formic acid (9:0.5:0.5) and detected under UV 254, UV 366 and with NP-PEG spray reagent under UV 366 nm . Similar fractions were combined to give fractions sep71-sep73, and on standing fraction **sep72** yielded yellow crystals, which upon cleaning with ethyl-acetate-methanol and recrystallization gave compound B (39.7 mg).

The combined fraction $\mathbf{f_8}$ (239.7 mg.) was further fractionated on another Sephadex LH-20 column (2.0 cm diameter x 20 cm long) and eluted with methanol. The composition of each collected fraction was examined by TLC and combined to give three fractions. The combined fraction **Sep 82** (138.7 mg) was further fractionated on another silica gel column (silica gel No 9385 12g; 1.5 cm diameter x 20 cm long) and successively eluted with a stepwise bi-gradient of chloroform (30-100%) in hexane and ethyl-acetate (0-50%) in chloroform. The eluent was collected and examined by TLC and similar fractions were combined to give 4 fractions. The combined fraction **sf4** yielded yellowish precipitate, which upon recrystallization in $CHCl_3$: hexane (1:1) gave needle crystals of compound C (14.1 mg).

The procedure for the extraction and isolation of compounds **B** and **C** was shown in Figure 20.

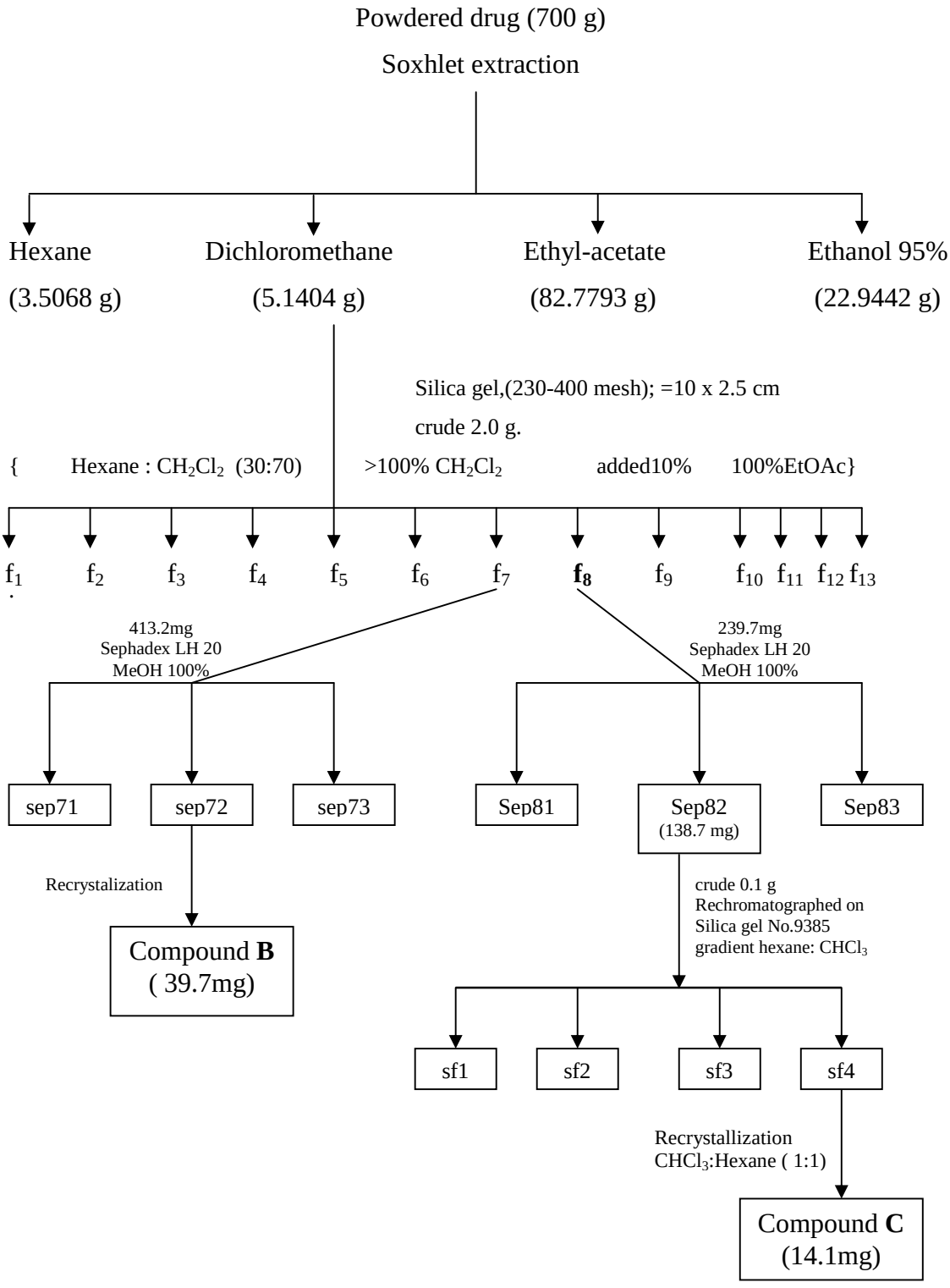

Figure 20 The procedure of extraction and isolation of compounds **B** and **C** from the dichloromethane extract of *A. luzonensis*.

3.2.3 The isolation of compounds from ethyl acetate extract of *A. luzonensis*

The ethyl acetate extract was further fractionated by chromatographic technique and each fraction was assessed for its tyrosinase inhibitory activity. The ethyl acetate extract (20.0 g.) was dissolved in a small amount of dichloromethane - methanol and continuously mixed with silica gel 60 (230-400 mesh) on a water bath until the extract appeared as dry granules. The granules were placed on top of a silica gel quick column (20 cm diameter x 20 cm long; silica gel 200 g.) and eluted with hexane - dichloromethane - ethyl acetate - methanol with increasing polarity (0 - 100 %), 100 ml fractions were collected and monitored by thin-layer chromatography (TLC) on silica gel GF_{254} plates, developed with dichloromethane - ethyl acetate - methanol - formic acid (25-1.5-1.5-1.5), detected under UV 254, UV 366 and with NP-PEG spray reagent under UV 366 nm. Similar fractions were then combined to give seven crude fractions A, B, C, D, E, F and G. Each fraction was tested for *in vitro* anti-tyrosinase activity. Further purification was carried out on fraction D.

Fraction D (4.0 g) was rechromatographed on silica gel (No.7729) quick column (10 cm diameter x 10 cm long; silica gel 50 g.). The column was eluted with a stepwise gradient of dichloromethane - ethyl acetate (8:2, 7:3, 6:4, 5:5, 2:8 and 0:10). Fifty milliliter fractions were collected and monitored by thin-layer chromatography (TLC) on silica gel GF_{254} plates, developed with dichloromethane - ethyl acetate - methanol - formic acid (25-1.5-1.5-1.5), detected under UV 254, UV 366 and with NP-PEG spray reagent under UV 366 nm. Similar fractions were combined to give crude fractions Qf1 (106.4 mg), Qf2 (259.1mg), Qf3 (607.8 mg), Qf4 (1.6615 g) and Qf5 (403.2 mg).

Fraction **Qf2** (0.2591 g), after washing with methanol to remove the orange color, gave a white precipitate which after washing with cold methanol and further purified by recrytallizing with hot methanol, gave yellowish needles of **compound C** (25.6 mg).

The **orange residue** was rechromatographed on Sephadex LH-20 (2.0 cm diameter x 20 cm long). The column was eluted with MeOH. Ten milliliter fractions were collected and analysed by TLC on silica gel GF_{254} plates, developed with dichloromethane–methanol-formic acid (9:0.5:0.5) and detected under UV 254, UV

366 and with NP-PEG spray reagent under UV 366 nm and similar fractions were combined to give fractions f_2s1-f_2s10. Fraction **f_2s9** yielded yellow precipitate, which upon cleansing with dichloromethane-methanol to remove color contaminants and recrystallizing gave **compound D** (2.5 mg).

Fraction **Qf4** (1.6615 g) was rechromatographed on silica gel (silica gel No.7729) quick column (10 cm diameter x 10 cm long; silica gel 50 g.). The column was eluted with hexane - ethyl acetate (75-25) in an isocratic manner. Fifty milliliter fractions were collected and monitored by thin-layer chromatography (TLC) on silica gel GF_{254} plates, developed with dichloromethane - ethyl acetate – methanol - formic acid (25-1.5-1.5-1.5), detected under UV 254, UV 366 and with NP-PEG spray reagent under UV 366 nm. Similar fractions were combined to give three crude fractions, Qf4a, Qf4b and Qf4c.

Fraction **Qf4b** was dissolved in MeOH, filtered and then rechromatographed on Sephadex LH-20 (2.0 cm diameter x 20 cm long). The column was eluted with MeOH. The composition of each collected fraction was examined by TLC on silica gel GF_{254} plates, developed with dichloromethane – methanol – formic acid (9:0.5:0.5) and detected under UV 254, UV 366 and with NP-PEG spray reagent under UV 366 nm and similar fractions were combined to give two fractions S-1 and S-2. Fraction S-2 (412.7mg) yielded yellow precipitate, which upon cleansing with dichloromethane – water – methanol to remove color contaminants and recrystallizing in dichloromethane : methanol (8:2) gave **Compound E** (71.9 mg).

The procedure for the isolation of compounds **C**, **D** and **E** were shown in Figure 21.

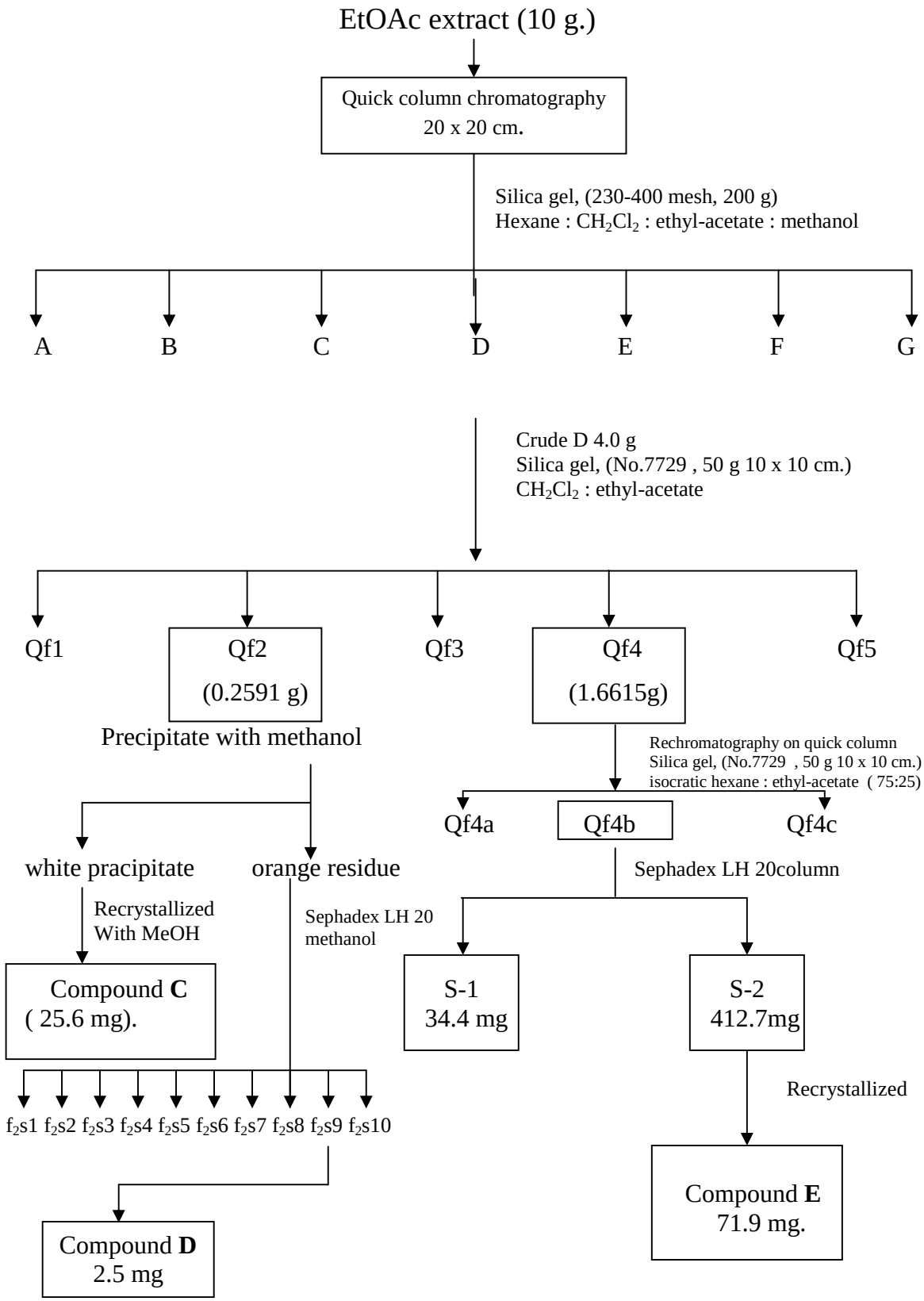

Figure 21 Isolation of compounds **C**, **D** and **E** from the ethyl acetate extract of *A. luzonensis*

3.3 Structure Elucidation of Chemical Constituents

3.3.1 Melting point

The melting points were determined on an Electrothermal melting point apparatus (Electrothermal 9100).

3.3.2 Ultraviolet spectra (UV)

Ultraviolet spectra were recorded in methanol by UV spectrophotometry, Perkin-Elmer, Lambda 35™, USA at Faculty of Pharmacy, Mahidol University.

3.3.3 Fourier Transform Infrared spectra (FT-IR)

Fourier Transform Infrared (FT-IR, Magna-IR™ spectrometer 550 Nicolet) spectra were recorded at Faculty of Pharmacy and Science, Mahidol University.

3.3.4 Nuclear Magnetic Resonance (NMR)

^{1}H-NMR, ^{13}C-NMR spectra were recorded on a Bruker DRX 300 (300 MH_Z) for compounds A, C, D and E. ^{1}H-NMR and ^{13}C-NMR spectra were recorded at Faculty of Science, Mahidol University. Bruker DRX 500 (500 MH_Z), National Science and Technology Development Agency (NSTDA), Thailand Science Park of compound B.

3.3.5 Electron Impact Mass Spectra (EI-MS)

Electron impact mass spectra were recorded at Faculty of Science, Mahidol University.

3.3.6 TOF Mass Spectra (TOF-MS)

Time-of-flight mass spectrometry were recorded at Faculty of Science, Mahidol University.

PART II Assessment of *in vitro* tyrosinase inhibitory activity and free radical scavenging activity

The assessment of *in vitro* tyrosinase inhibitory (Kubo and Kinst-Hori. 1998.) and free radical scavenging activity (Miliauskas, G, Venskutonis, 2004) of crude extracts, fractions and pure compounds in this study was conducted at the Central Laboratory, Faculty of Pharmacy, Mahidol University.

3.1 Material for *in vitro* tyrosinase inhibitory activity

3.1.1 Reagents

Disodium hydrogen orthophosphate dihydrate, AR grade ($Na_2HPO_4.2H_2O$) (APS Chemicals, Australia)

Sodium dihydrogen orthophosphate dihydrate, AR grade ($NaH_2PO_4.2H_2O$) (APS Chemicals, Australia)

Mushroom Tyrosinase (Sigma, USA)

L-Tyrosine (Sigma, USA)

3-(3,4-Dihydroxyphenyl)-L-alanine (Fluka, Switzerland)

Kojic acid (Riedel-de Haën, Germany)

Water,distilled (Central Laboratory Unit, Faculty of Pharmacy, Mahidol University)

Tween 20, 80 (Namsiang, Thailand)

3.1.2 Equipments

96-well plates (Brand, Germany)

Autopipettes

- 10-100 µl (Boeco, Germany)
- 100-1000 µl (Brand, Germany)
- 8 channels 20-200 µl (Slamed, Germany)

Microplate reader (Molecular Devices Thermomax Microplate Reader, USA)

UV spectrophotometer, (Perkin-Elmer, Lambda 35^{TM}, USA)

3.1.3 Methods for the assessment of tyrosinase inhibitory activity

3.1.3.1 Preparation of the test solutions of isolated compounds (104)

The stock solutions containing each of the isolated compounds as well as kojic acid were first prepared by dissolving each compound in the 1:3 volume ratio mixture of Tween 20 and phosphate buffered saline solution pH 6.8. The stock solution was diluted with phosphate buffer to give the optimum concentration for the evaluation the IC_{50} (mg/ml) of the compounds.

3.1.3.2 Preparation of the reaction mixture

50 mM Phosphate buffer pH 6.8

Fifty millimolar $Na_2HPO_4.2H_2O$ and 50 mM $NaH_2PO_4.2H_2O$ solutions were prepared in distilled water. Both solutions were then mixed until a pH 6.8 was reached.

Tween 80

Ten milliter of Tween 80 was diluted with distilled water and made up to 100 ml to a give 10% (v/v) solution.

Sample solutions

Samples of plant extracts and kojic acid were prepared in methanol to different concentrations.

Tyrosinase stock solution

The 2500 mg of mushroom tyrosinase were dissolved in 50 mM phosphate buffer pH 6.8, to make 500 U/ml solution.

5 mM Tyrosine solution

The solution was prepared by dissolving tyrosine powder with 50 mM Phosphate buffer pH 6.8 to the concentration of 5 mM.

3.1.4 TLC screening assay for tyrosinase inhibitory detection (105)

Tyrosinase stock solution of 500 U/ml was diluted to 250 U/ml using the same phosphate buffer. L-tyrosine was dissolved in 50 mM phosphate buffer, pH 6.8 to give final concentration of 2 mM (9.8 mg in 25 ml, MW 181.19 g/mol). An exact amount of each sample (2.0-5.0 µl) was spotted onto a stationary phase (silica gel 60 F_{254} plates) using an analytical syringe and the plate was developed with 25:2:2:1.5 (v/v) CH_2Cl_2 : EtOAc : Methanol : formic acid as a mobile phase. After allowing the plate to dry at room temperature, the enzyme solution was sprayed over the entire surface of the stationary phase. Immediately after that, L-tyrosine solution was sprayed over the same area. After appropriate time intervals (5, 10, 15 and 20 min), active components appeared as white spots against dark grey background.

3.1.5 Measurement of anti-tyrosinase activity (106)

Phosphate buffer pH 6.8 was added to each well in a 96-well plates, followed by diluted Tween 80 solution, methanol with or without test sample, and tyrosinase solution respectively. After pre-incubation of the reaction mixture at the temperature of 37 $^{\circ}$C for 10 minutes, L-tyrosine solution was added. Then the reaction mixture was measured for its absorbance (A, B) at the wavelength of 490 nm. An incubation at the temperature of 37°C was required for another 20 minutes. After incubation, the reaction mixture was again measured for its absorbance (C, D) at the same wavelength. The inhibition level was calculated as the percentage of tyrosinase inhibition.

The summary of the composition of reaction mixture in well plate were as follow.

3.1.5.1 Samples of plant extracts

A (Control)

50 mM Phosphate buffer (pH 6.8)	120	µl
Tween 80	20	µl
Solvent (methanol)	40	µl

Mushroom tyrosinase	20	µl
L-tyrosine	20	µl

B (Blank A)

50 mM Phosphate buffer (pH 6.8)	140	µl
Tween 80	20	µl
Solvent (methanol)	40	µl
L-tyrosine	20	µl

C (Sample)

50 mM Phosphate buffer (pH 6.8)	120	µl
Tween 80	20	µl
Sample	40	µl
Mushroom tyrosinase	20	µl
L-tyrosine	20	µl

D (Blank C)

50 mM Phosphate buffer (pH 6.8)	140	µl
Tween 80	20	µl
Sample	40	µl
L-tyrosine	20	µl

3.1.5.2 Isolated compounds from *A.luzonensis*

A (Control)

50 mM Phosphate buffer (pH 6.8)	140	µl
Solvent (methanol)	40	µl
Mushroom tyrosinase	20	µl
L-tyrosine	20	µl

B (Blank A)

50 mM Phosphate buffer (pH 6.8)	160	µl
Solvent (methanol)	40	µl
L-tyrosine	20	µl

C (Sample)

50 mM Phosphate buffer (pH 6.8)	100	µl
Sample	40	µl
Solvent (methanol)	40	µl
Mushroom tyrosinase	20	µl
L-tyrosine	20	µl

D (Blank C)

50 mM Phosphate buffer (pH 6.8)	120	µl
Solvent (methanol)	40	µl
Sample	40	µl
L-tyrosine	20	µl

3.1.6 Evaluation of % tyrosinase inhibition

The inhibition level was calculated using the following equation. Kojic acid was used as a positive control.

$$\% \text{ Inhibition} = \frac{[(A-B) - (C-D)]}{(A-B)} \times 100 \ldots\ldots\ldots (1)$$

Where; A-B = The difference between the absorbance of test solution without test sample after and before incubation

C-D = The difference between the absorbance of test solution with test sample after and before incubation

Percent inhibition of each sample was calculated using equation (1). For the isolated compounds, the percent inhibition was plotted versus the concentrations and the concentrations that inhibited tyrosinase activity by 50% were determined as IC_{50}.

3.1.7 Statistical analysis

All the experiments were carried out in triplicate (n=3) and the data expressed as mean of the three measurements ± SD

3.2 Determination of free radical scavenging activity

3.2.1 TLC screening assay for antioxidant activity (107)

The test samples were applied on a TLC plate and developed with suitable developing solvents. After drying, the TLC plate was sprayed with 0.1% solution of 2, 2-Diphenyl-1-Picrylhydrazyl (DPPH) in methanol. After 30 min, active components appeared as yellow spots against purple background.

3.2.2 DPPH Free Radical Scavenging activity assay (108)

3.2.2.1 Preparation of 0.1 mM DPPH solution

The DPPH solution was freshly prepared by dissolving 3 mg of DPPH in 50 ml of methanol. The solution was then sonicated for 10 min. The final concentration was 1.52×10^{-4} M.

3.2.2.2 Preparation of the test sample solutions

The test sample solutions were prepared as methanolic solution with initial concentration of 200 µg /ml. Each stock solution was further diluted with methanol until a suitable range of concentrations (µg/ml) was obtained including 100, 40, 20, 15, 10, 5, 2 and 1 µg/ml. The DPPH solution (1.0 ml) was added to each of the test samples solution (1.0 ml) to make the total volume of 2.0 ml. The final concentration was calculated as shown below.

Where,

$$C_1V_1 = C_2V_2$$

C_1 = Beginning concentration (µg/ml)
V_1 = Beginning volume (ml)
C_2 = Final concentration (µg/ml)
V_2 = Final volume (ml)

3.2.2.3 Measurement of free radical scavenging activity

The assay mixture contained 1 ml of 1.52 x 10^{-4} M of DPPH radical solution and 1 ml of test sample solution. The mixture was shaken vigorously and allowed to stand for 30 min at room temperature in the dark, the absorbent of the mixture was measured at 517 nm using UV-vis spectrophotometer. Methanol was used as the control. The mixture of each concentration was prepared and measured in triplicate.

In addition to the crude *A.luzonensis* methanol extracts, other extracts and isolated compounds were also tested for DPPH scavenging activity, with ascorbic acid as the positive control. The decrease in absorbance of the DPPH radical (deep purple) after the addition of an antioxidant was used to determine the antioxidant activity.

3.2.2.4 Calculation for the percentage of antioxidant activity

The percentage of antioxidant activity (%inhibition) was calculated as follow

$$\% \text{ Inhibition} = \frac{(A_{control} - A_{sample})}{A_{control}} \times 100 \quad \ldots\ldots\ldots\ldots\ldots (2)$$

Where,

$A_{control}$ = The absorbance of the mixture containing 1ml of 0.1mM DPPH radical solution and 1ml of methanol without the test sample solution.

A_{sample} = The absorbance of the mixture containing 1ml of 0.1mM DPPH radical solution and 1ml of the test sample solution.

Percent inhibition of each sample was calculated using equation (2). The graph between the percentage of inhibitions and the concentrations were plotted using Microsoft Excel. Each data point was a mean of three measurements (n=3). The IC_{50} of each sample was then obtained from the linear equation. A lower IC_{50} value indicates greater antioxidant activity.

CHAPTER IV
RESULTS AND DISCUSSION

4.1 A Preliminary Phytochemical Investigation of *A.luzonensis* extracts

A random screening of various plant extracts for the anti-tyrosinase activity revealed that the ethanol extract of the *Anaxagorea luzonensis* inhibited more than 80% of mushroom tyrosinase activity. A literature survey of the phytochemistry of this plant indicated the presence of several xanthones and flavonoids with antioxidant activity (100, 109). Flavonoids are reported to possess a wide range of biological activities. TLC chromatograms of extracts from *A.luzonensis* were shown to have several colored bands when detected with NP/PEG reagent (under UV 366) reagent as shown in Figure 22, indicating the presence of flavonoid-type compounds.

So far, there has been no report on the anti-tyrosinase activity of *A. luzonensis* (SciFinder, Accessed since November, 2007). Therefore, it is of interest to study *A.luzonensis* as a model for anti-tyrosinase and antioxidant activities.

4.2 Biological screening of *A.luzonensis* extracts

4.2.1 Biological screening of *A.luzonensis* extracts

The stems of *Anaxagorea luzonensis* were collected from Phetchabure Province and extracted in a Soxhlet apparatus with the following solvents of increasing polarity, i.e. hexane, dichloromethane, ethyl acetate and ethanol.

(S1)

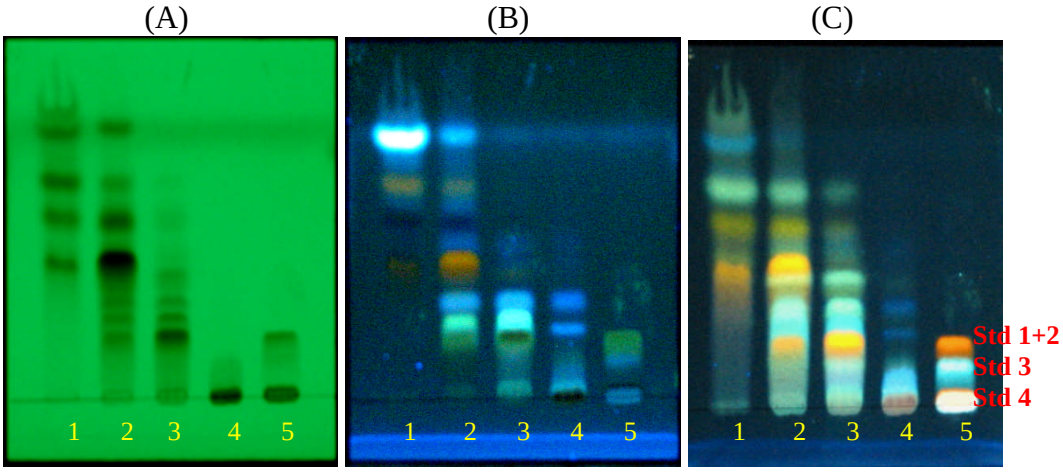

(S2)

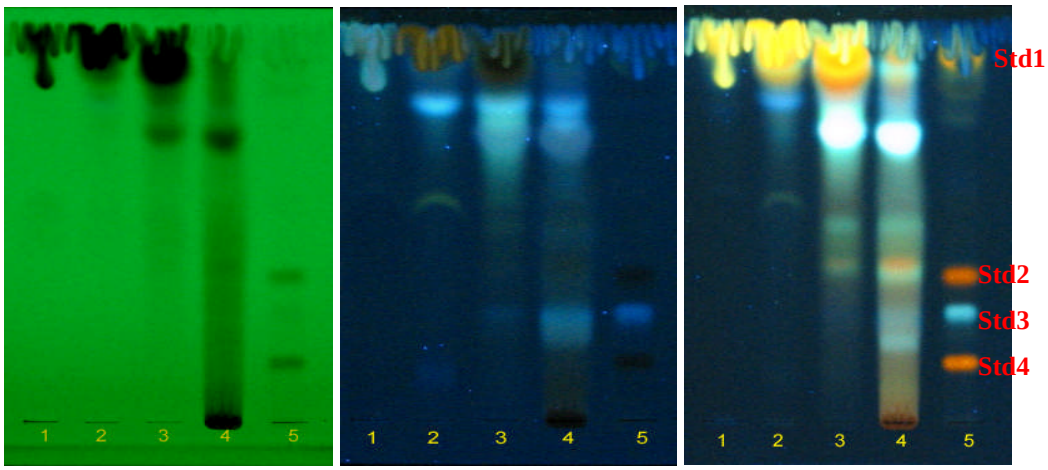

Figure 22 Thin-layer chromatogram of the crude extracts from *A. luzonensis*

(A) under UV short wavelength (254 nm.), **(B)** under UV long wavelength (366 nm.), **(C)** NP/PEG under UV long wavelength (366 nm.) , by solvent system 1 (non-polar) and 2 (polar).

Track 1 = Hexane extract Track 3 = Ethyl acetate extract

Track 2 = Dichloromethane extract Track 4 = ethanol extract

Track 5 = Reference compound ; Std 1, quercetin; Std 2, isoquercitrin, Std 3, chlorogenic acid, Std 4, rutin

Absorbent : Silica gel GF_{254}

Solvent system : (S1) $CHCl_3$ – EtOAc –MeOH- Formic acid (9-0.5-0.5-0.5)

(S2) EtOAc- H_2O- Formic acid (8 -1 -1)

Detection : (A) UV 254, (B) UV 366, (C) NP/PEG (under UV 366)

The assessment of *in vitro* anti-tyrosinase and antioxidant activities of various extracts of *A.luzonensis* was shown in Table 6. The dichloromethane, ethyl acetate and ethanol extracts exhibited an anti-tyrosinase activity with the percent inhibition of 58.27%, 86.76% and 80.83 %, respectively, while the hexane extract exhibited the lowest anti-tyrosinase activity of 28.56% at the same concentration tested (0.909 mg/ml). However, these inhibitory activities were lower compared to the standard whitening agent, kojic acid, and the ethanol extract of *Artocarpus lakoocha* Roxb., which were used as positive controls (99.87 and 98.79 % inhibition, respectively (Table 6)). The result also confirmed the presence of free radical scavenging activity of each extract as shown by the IC_{50} values of 10.60, 3.33, 5.51 µg/ml for dichloromethane, ethyl acetate and ethanol extracts, respectively, while the hexane extract had low antioxidant activity with an IC_{50} value of 162.70 µg/ml (Table 6).

Table 6 Results of anti-tyrosinase and free radical scavenging activities of different extracts from *A.luzonensis* with different solvents

A. luzonensis Extracts	% Inhibition of tyrosinase (0.909 mg/ml)	IC_{50} DPPH inhibition (µg/ml)
Hexane	28.56 ± 0.45	162.70 ± 5.37
Dichloromethane	58.27 ± 0.38	10.60 ± 1.44
Ethy acetate	86.76 ± 0.55	3.33 ± 0.35
Ethanol	80.83 ± 0.74	5.51 ± 0.35
Artocarpus lakoocha Roxb. extract	98.79 ± 0.69	-
Kojic acid	99.87 ± 0.65	-
Ascorbic acid	-	5.20 ± 0.36

Results are means of three measurements ± SD (n =3×3). The Ethanol extract of *Artocarpus lakoocha* Roxb, kojic acid and ascorbic acid were used as positive controls for anti-tyrosinase and antioxidant activities, respectively.

4.2.2 Biological screening of *A.luzonensis* extracts using TLC techniques

4.2.2.1 Free radical scavenging activity

The free radical scavenging activity test using TLC techniques was adapted from Hostettman et al, 1997 (107) were detected using DPPH spraying reagent. The DPPH free radical scavenging activity of each extract from *A.luzonensis* using silica gel 60 F_{254} plates as an absorbent and $CHCl_3$–EtOAc–MeOH–Formic acid (9-0.5-0.5-0.5) as a developing solvent system was shown in Figure 23. When detected by spraying with DPPH, after 30 min, active components appeared as yellowish white spots against purple background. Quercetin was used as a reference compound. The hexane, dichloromethane and ethyl-acetate extracts showed potent antiradical effect towards the stable radical DPPH as shown in Figure 23.

4.2.2.2 Anti-tyrosinase activity

For the TLC screening of tyrosinase inhibiting activity of crude extracts of *A.luzonensis,* the method involved spraying the TLC plate containing sample spots with tyrosinase and L-tyrosine solutions, successively. A positive result could be visualized directly as white spots against a brownish-purple background (105), using kojic acid as positive control. This method can be used as a quick screening for tyrosinase inhibitor detection and a guiding procedure for the isolation of tyrosinase inhibitors from natural products. The TLC (silica gel 60 F_{254} plates as an absorbent) was developed using 25:2:2:1.5 (v/v) CH_2Cl_2 : EtOAc : methanol : formic acid as a mobile phase and this plate was then sprayed with tyrosinase and L-tyrosine and visualized under white light. The hexane extract showed one positive white spot with an Rf of 0.79 against the darker background, while the dichloromethane and ethyl acetate extracts showed several positive white spots (Figure 24).

(A) (B) (C)

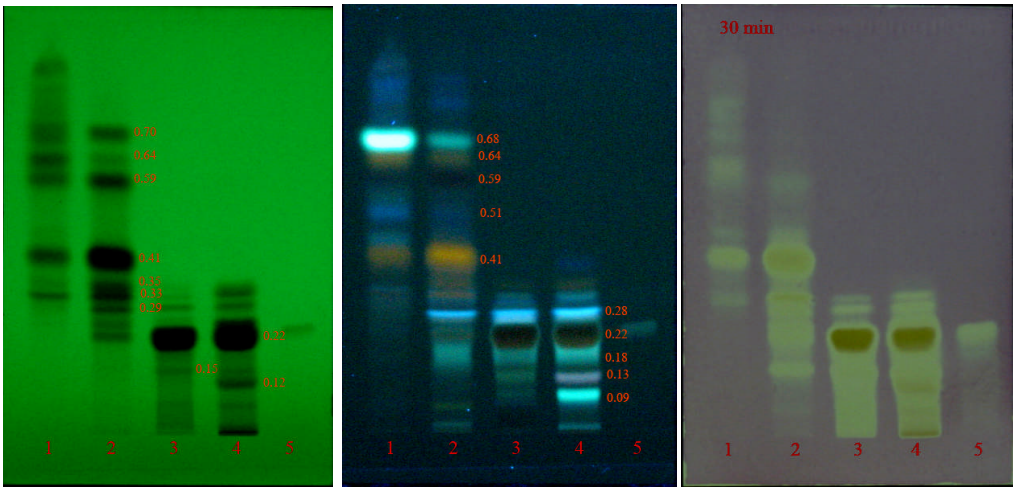

(D)

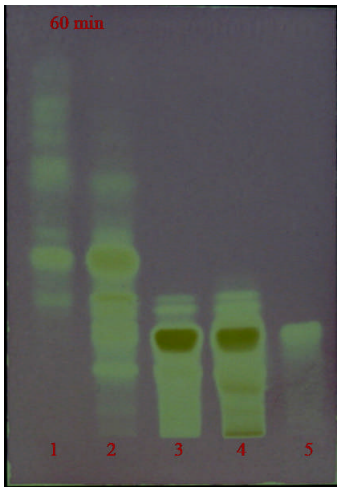

Track 1 = Hexane extract
Track 2 = Dichloromethane extract
Track 3 = Ethyl acetate extract
Track 4 = Ethanol extract
Track 5 = Std1, quercetin

Figure 23 Thin-layer chromatogram of the crude extracts from *A.luzonensis*, showing spots with DPPH scavenging activity

Absorbent	Silica gel GF_{254}
Solvent system	$CHCl_3$–EtOAc–MeOH- formic acid (9-0.5-0.5-0.5)
Detection	(A) UV 254, (B) UV 366, (C) DPPH reagent at 30 min.
	(D) DPPH 0.1% after 60 min

(S1)

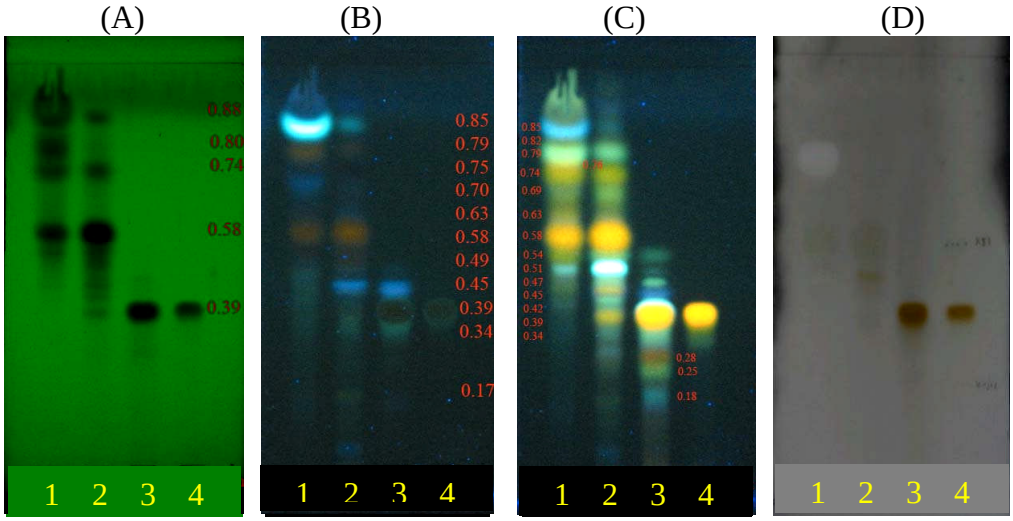

254 nm 366 nm NP/PEG (366 nm) enzyme tyrosinase/ L-tyrosine

(S2)

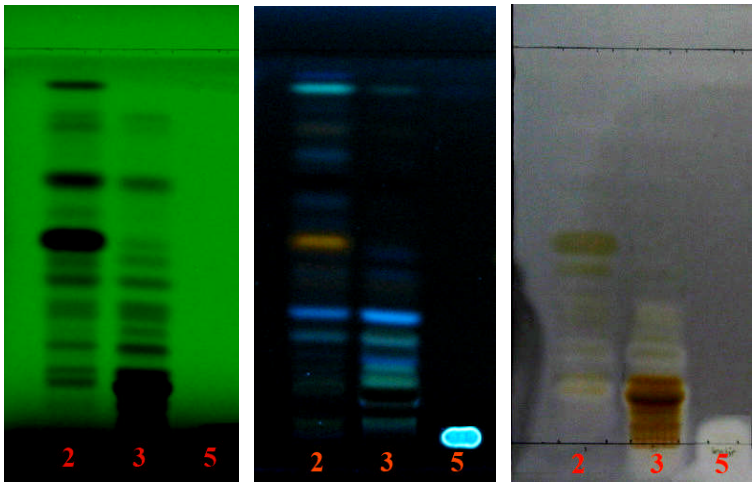

254 nm 366 nm enzyme tyrosinase/ L-tyrosine

Figure 24 Thin-layer chromatogram of the crude extracts from *A. luzonensis* sprayed with enzyme tyrosinase and L-tyrosine

Solvent system : (S1) CH_2Cl_2 : EtOAc : Methanol : formic acid (25-2-2-1.5)

(S2) $CHCl_3$: MeOH : Formic acid (9 : 0.5 :0.5)

Detection : NP/PEG, tyrosinase enzyme and L-tyrosine (white spots)

Track 1 = Hexane extract, Track 2 = Dichloromethane extract,
Track 3 = Ethyl acetate extract, Track 4 = quercetin, Track 5 = kojic acid
(A) under UV short wavelength (254 nm.), (B) under UV long wavelength (366 nm.), (C) NP/PEG under UV long wavelength (366 nm.), (D) detected with enzyme tyrosinase and L-tyrosine spraying reagents after 30 min.

Table 7 Biological TLC screening for the DPPH scavenging t and anti-tyrosinase activities of each extract from *A. luzonensis*.

***A. luzonensis* A. Gray Extracts**	**DPPH scavenging activity***	**Anti-tyrosinase activity***
Hexane	++	+
Dichloromethane	+++	++
Ethyl acetate	+++	++
Ethanol	+++	-
Quercetin	+++	+
Kojic acid	-	+++

* by observation

+++	Strong activity	++	Moderate activity
+	Weak activity	-	not tested

4.3 Isolation of chemical constituents from *A.luzonensis*

A sample of the powdered stems (700 g) was extracted consecutively with solvents of increasing polarity, namely hexane, dichloromethane, ethyl acetate and ethanol in a soxhlet apparatus. The extracts were dried under reduced pressure to yield the dried residues as shown in Table 8. The TLC patterns of these extracts were shown in Figure 22.

Table 8 Results of the extraction of *A.luzonensis* with different solvents

Plant	Extraction solvent	Weight (g)	% Yield
A.luzonensis	Hexane	3.5068	0.500
	Dichloromethane	5.1405	0.734
	Ethyl acetate	82.9773	11.854
	Ethanol	22.9442	3.278

The crude hexane, dichloromethane and ethyl acetate extracts were subjected to test for their antityrosinase and antioxidant activities. The results of assessment the antityrosinase and antioxidant activities of each extracts were shown in Table 6. The hexane, dichloromethane, and ethyl-acetate extracts exhibited an anti-tyrosinase activity with the percent inhibition of 28.56, 58.27, and 86.76%, respectively and the antioxidant activity with the IC_{50} values of 162.74, 10.60 and 3.33 µg/ ml, respectively. Although the hexane extract had low antioxidant and anti-tyrosinase activities, the result of the antityrosinase activity of the hexane extract using TLC method showed one positive white spot against the darker background, while dichloromethane and ethyl acetate extracts showed several positive white spots (Figure 24). The hexane, dichloromethane and ethyl acetate extracts showed potent antiradical effect towards the stable radical DPPH as shown in Figure 23. Hence, these crude extracts were selected for further chemical investigation.

4.3.1 Separation and isolation of the active compounds from the hexane, dichloromethane and ethyl acetate extracts of *A. luzonensis*.

The hexane extract (3.12 g) was chromatographed on silica gel 60 column using mixtures of hexane/ ethyl acetate of increasing polarity. Fractions were monitored by TLC on silica gel GF_{254} plates, developed with hexane-ethyl acetate - formic acid (30-10-1.5), detected with NP-PEG and anisal-dehyde spray reagents. Similar fractions were combined to afford fractions H1-H6. Each fraction was tested for TLC technique for tyrosinase inhibitory detection. Compound A (10.8 mg) was obtained from fraction H6 (15.8 mg), after washing with cold hexane and further purified by recrystallization from hot hexane. The procedure of isolation of compound **A** from the hexane extract was shown in Figure 19.

The dichloromethane extract (2 g) was further fractionated by chromatographic technique, the column being eluted with bi-gradient of increasing CH_2Cl_2 (30-100%) in n-hexane and ethyl-acetate (0-100%) in CH_2Cl_2. Fractions were collected and profiled by thin-layer chromatography (TLC) on silica gel GF_{254}, developed with dichloromethane –methanol-formic acid (9:0.5:0.5). The TLC plates, were detected under UV 254, UV 366 and with NP-PEG spray reagent under UV 366 nm. This resulted in a total of 13 fractions (f7-f13). Fraction f7 (413.2 mg) showed the major component on TLC with high yield. It was further rechromatographed on Sephadex LH-20 column which was eluted with MeOH. Similar fractions were combined to give fractions sep71-sep73, and on standing fraction sep72 yielded yellow crystals, which upon cleaning with ethyl-acetate-methanol and recrystallization with methanol gave compound **B**.

Fraction f_8 (239.7 mg) was further fractionated on another Sephadex LH-20 and eluted with methanol. The composition of each collected fraction was examined by TLC and combined to give three fractions (Sep81-83). The combined fraction Sep 82 (138.7 mg) was further fractionated on another silica gel column and successively eluted with a stepwise bi-gradient of chloroform in hexane and ethyl acetate in chloroform. The eluent was collected and examined by TLC and similar fractions were combined to give 4 fractions. The combined fraction sf4 yielded yellowish precipitate, which upon recrystallization in $CHCl_3$: hexane (1:1) gave needle crystals of compound

C. The procedure for the isolation of compounds **B** and **C** from dichloromethane extract were shown in Figure 20.

The ethyl acetate extract (20 g) was first separated by quick column chromatography and eluted with hexane – dichloromethane – ethyl-acetate – methanol with increasing polarity, the eluent being collected and monitored by thin-layer chromatography (TLC) on silica gel GF_{254} plates, developed with dichloromethane – ethyl-acetate – methanol - formic acid (25-1.5-1.5-1.5), detected under UV 254, UV 366 and with NP-PEG spray reagent under UV 366 nm. Similar fractions were then combined to give seven fractions A, B, C, D, E, F and G. Fraction D (4.0 g) was rechromatographed on silica gel 60 column and eluted with a stepwise gradient of dichloromethane–ethyl acetate. Similar fractions were combined to give crude fractions Qf1 –Qf5

Fraction Qf2 (259.1mg), after washing with methanol to remove the orange color, gave a white precipitate which was further purified by recrytallizing with methanol, to gave yellowish needles of compound **C**

The orange residue from fraction Qf2 was rechromatographed on Sephadex LH-20 and eluted with MeOH. Similar fractions were combined to give fractions f_2s1-f_2s10. Fraction f_2s9 yielded yellow precipitate, which upon cleansing with dichloromethane-methanol to remove color and recrystallization gave compound **D**.

Fraction Qf4 (1.6615 g) was rechromatographed on silica gel quick column and eluted with hexane–ethyl acetate (75-25) in an isocratic manner. Similar fractions were combined to give three fractions, Qf4a, Qf4b and Qf4c. Fraction Qf4b was rechromatographed on Sephadex LH-20 eluted with MeOH. Similar fractions were combined to give two fractions S-1 and S-2. Fraction S-2 yielded yellow precipitate, which upon cleansing with dichloromethane -water-methanol to remove the color contaminants and recrystallizing in dichloromethane : methanol (8:2) gave compound **E**.

The procedure for the isolation of compounds C, D and E from the ethyl acetate extract were shown in Figure 21.

The thin-layer chromatograms of the isolated compounds A, B, C, D and E from *A.lusonensis* extracts were shown in Figures 25 and 26. Compounds A, B, C, D and E were then subjected to further study on its structure elucidation using UV, IR,

MS and NMR and the compounds were tested for their anti-tyrosinase and antioxidant capabilities.

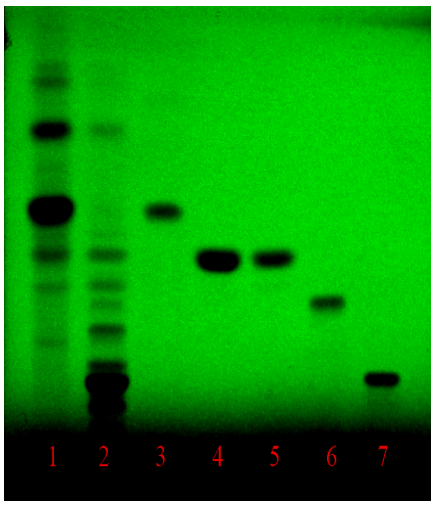

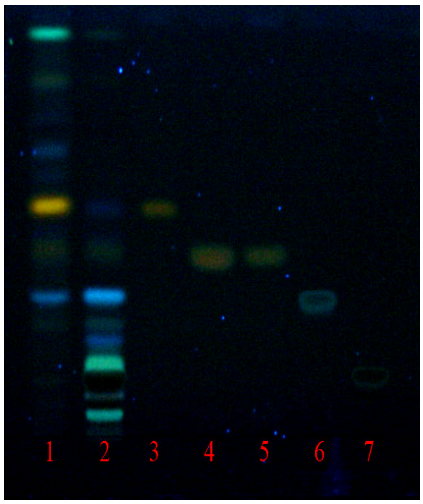

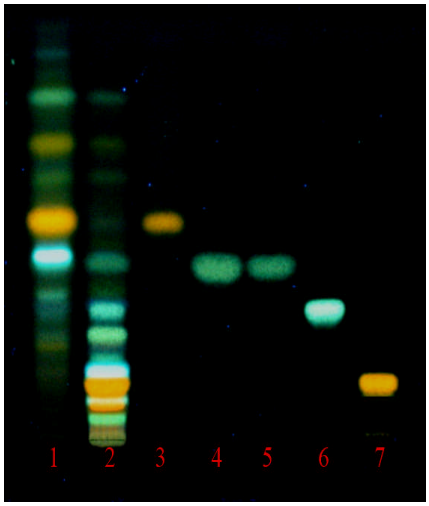

Track 1 = Dichloromethane extract
Track 2 = Ethyl acetate extract
Track 3 = Compound B from CH_2Cl_2 extract
Track 4 = Compound C from CH_2Cl_2 extract
Track 5 = Compound C from EtOAc extract
Track 6 = Compound D from EtOAc extract
Track 7 = Compound E from EtOAc extract

Figure 25 Thin–layer chromatograms of isolated compounds from the dichloromethane and ethyl acetate extracts of *A. luzonensis*.

Adsorbent :	Silica gel GF_{254}
Solvent system :	Chlorofrom : ethyl acetate : methanol : formic acid (9-0.5-0.5-0.5)
Detector :	UV 254, UV 366, NP-PEG (under UV 366)

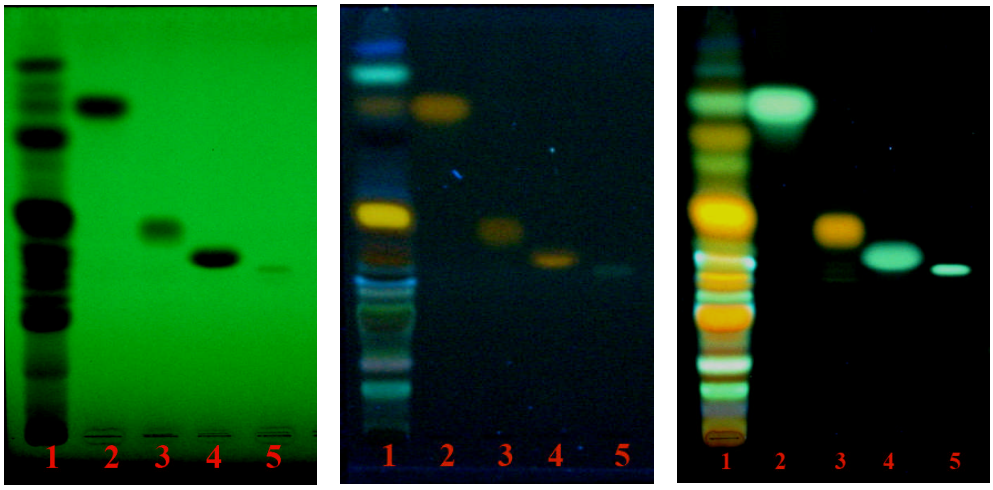

254 nm 366 nm NP/PEG (under 366 nm)

Figure 26 Thin–layer chromatograms of isolated compounds from the hexane dichloromethane and ethyl acetate extracts of *A.luzonensis*.

Track 1 = *A.luzonensis* extract
Track 2 = Compound A from hexane extract
Track 3 = Compound B from CH_2Cl_2 extract
Track 4 = Compound C from CH_2Cl_2 extract
Track 5 = Compound D from EtOAc extract

Adsorbent :	Silica gel GF_{254} plate
Solvent system :	Chlorofrom : ethyl acetate : methanol : formic acid (9-0.5-0.5-0.5)
Detector :	UV 254, UV 366, NP-PEG (under UV 366)

4.4 Structure elucidation

4.4.1 Compound A

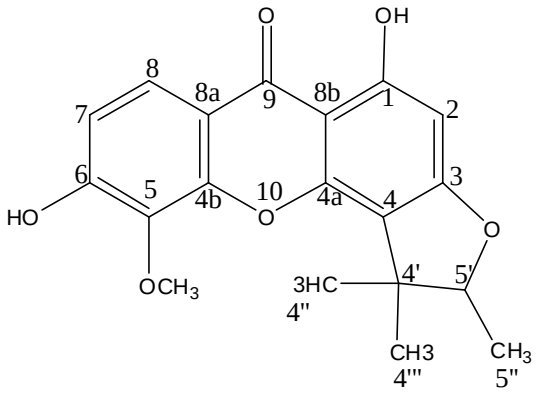

1,6-dihydroxy-5-methoxy-4',4',5'-trimethylfurano-(2',3' :3,4)–xanthone

Compound A. Yellow crystals with the melting point of 221-223 ^{o}C. The UV spectrum (Figure 27) in methanol of compound A exhibited absorptions at 242 and 318 nm. The FTIR spectrum in $CHCl_3$ (Figure 28) indicated the vibrations of the hydroxyl stretching (ν_{OH}) at 3517.82 cm^{-1}, carbonyl stretching ($\nu_{C=O}$) at 1650.54 cm^{-1}, double bond of aromatic rings ($\nu_{C=C}$) 1603.67 cm^{-1}, 1584.68 cm^{-1}. The molecular formula of compound A was deduced as $C_{19}H_{18}0_6$ (m/z =342) from the TOF-MS (Figure 40), which showed the molecular ion [M- Na]$^{+}$ at 365.1072, and ^{13}C NMR data.

The ^{1}H NMR spectra (Figures 29-31) revealed the presence of a chelated hydroxyl (δ 13.35), two aromatic protons (δ 7.02 and 7.98 ,each, *d*, *J* 8.8 Hz, H-7, H-8), methine protons (δ 6.30 *s*, H-2; δ 4.56, *dd*, *J* 6.56, 13.1 Hz, H-5'); methyl protons (δ 1.45, *d*, *J* 6.6 Hz, H_3-5"; δ 1.65, 1.35, H_3-4", H_3-4''') and a methoxyl protons (δ 4.10, s). The methoxy group was proved to be ortho-substituted by the chemical shift of C-5 (61.8 ppm).

The ^{13}C-NMR spectrum data of compound A afforded 18 lines as shown in Figure 32, indicating a number of carbon atoms in the molecule. The resonance at δ 179.73 (C-9) indicated a carbonyl group (C=O), while the resonances at δ 166.08 (C-1), 154.45 (C-6) were assigned to the quaternary carbons near hydroxyl groups. The

resonances at δ 112.23 and δ 122.25 were assigned to the methine carbons at C-7, C-8 positions, respectively. The resonance at δ 61.8 (5-OCH_3) indicated the presence methoxy group. Other carbon signals were assigned as presented in **Table 9.** The carbon type was indicate by DEPT spectrum (Figure 34). The normal HMQC (Figure 34) assisted the proton assignment **(Table 10).**

The heteronuclear multiple bond correlation (HMBC) spectra of compound A revealed the presence of C-H long-range correlations (Figures 35-39). The data of HMBC were shown in **Table 11**.

The ^{1}H and ^{13}C chemical shifts of the compound A were assigned by comparing with literature (109) as showed in **Table 9**. From the above data, it could be concluded that the structure of **compound A** was 1,6 - dihydroxy - 5 - methoxy - 4',4',5' - trimethylfurano - (2',3' :3,4) – xanthone (109).

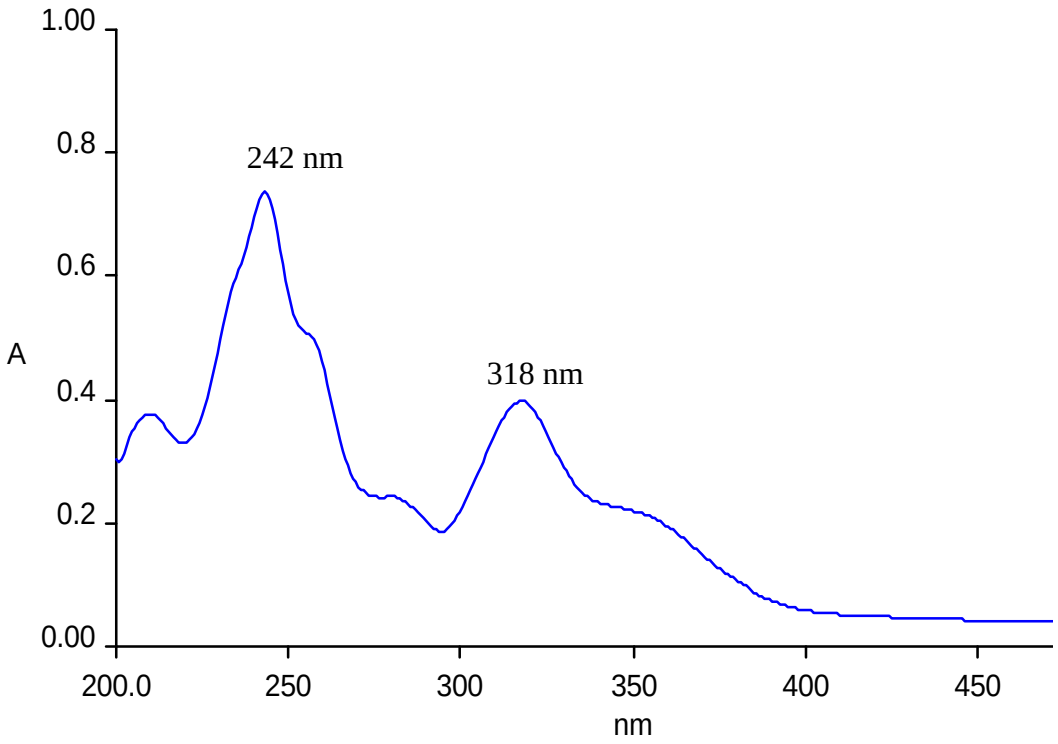

Figure 27 UV spectrum of compound **A** in methanol

Table 9 Comparison of ^{1}H, ^{13}C-NMR data of compound A with literature values (109)

Proton Position	Chemical shift(δ) 75 MHz ^{-13}C-NMR		Chemical shift(δ) 300 MHz ^{1}H-NMR	
	Lit. (acetone-d_6)	Compound A ($CDCl_3$)	Lit (acetone-d_6)	Compound A ($CDCl_3$)
1	166.9	166.1		
2	92.8	94.1	6.18, *s*, H-2	6.30, *s* , H-2
3	165.2	164.5		
4	113.8	112.7		
5	135.7	133.8		
6	157.5	154.5		
7	114.5	112.2	7.03, *d*, *J* 8.6 Hz	7.02, *d*, *J* 8.8 Hz
8	122.3	122.3	7.85, *d*, *J* 8.6 Hz	7.98, *d*, *J* 8.8 Hz
9	180.7	179.7		
4a	153.6	152.4		
4b	151.4	149.4		
8a	114.9	115.1		
8b	103.6	103.3		
4′	44.5	43.6		
5′	91.6	90.6	4.60, *q*, *J* 6.6 Hz	4.56, *dd*, *J* 6.6, 13.1 Hz
5"-CH_3	14.4	14.0	1.43, *d*, *J*6.6 Hz, 5"-H_3	1.45, *d*, *J* 6.6 Hz, 5"-H_3
4"-CH_3	25.8	25.6	1.65, *s*, 4"-H_3	1.65, *s*, 4"-H_3
4'"-CH_3	21.7	21.4	1.35, *s*, 4'"-H_3	1.35, *s* ,4'"-H_3
5-OCH_3	61.8	61.8	4.02, *s*, 5-OCH_3	4.10, *s*, 5-OCH_3

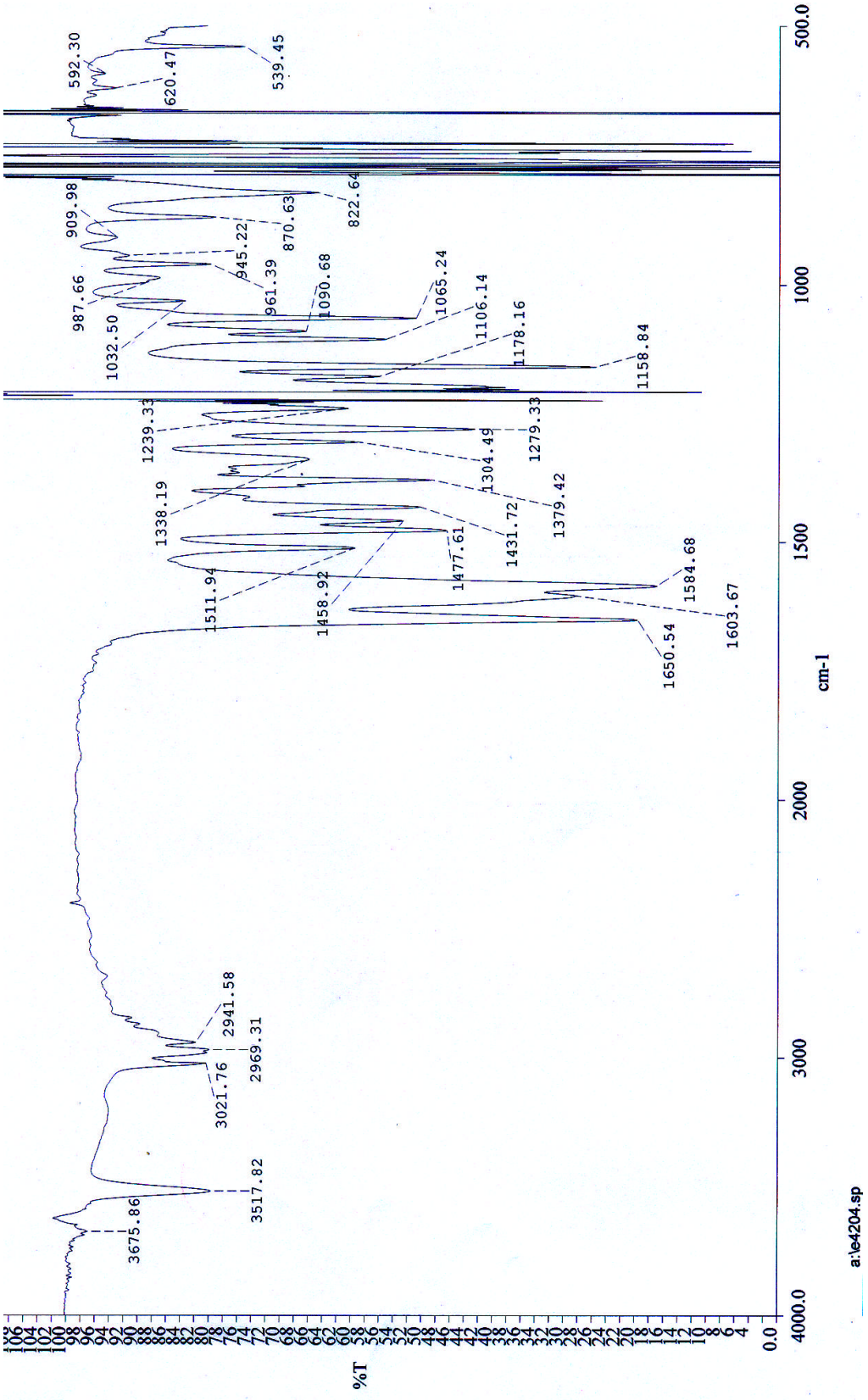

Figure 28 FTIR spectrum of compound **A** in $CHCl_3$

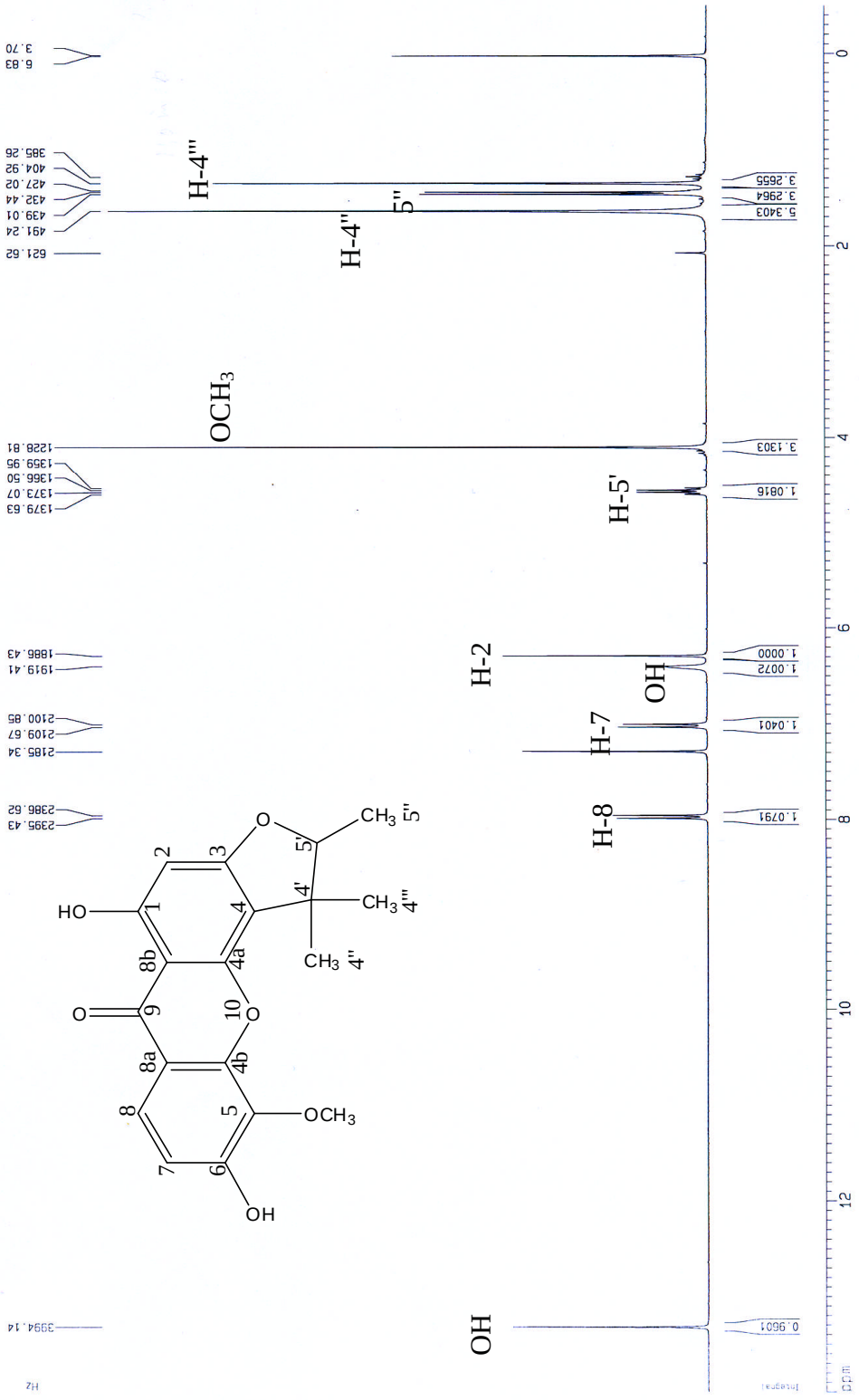

Figure 29 300MHz ^{1}H-NMR spectrum of compound **A** in $CDCl_3$

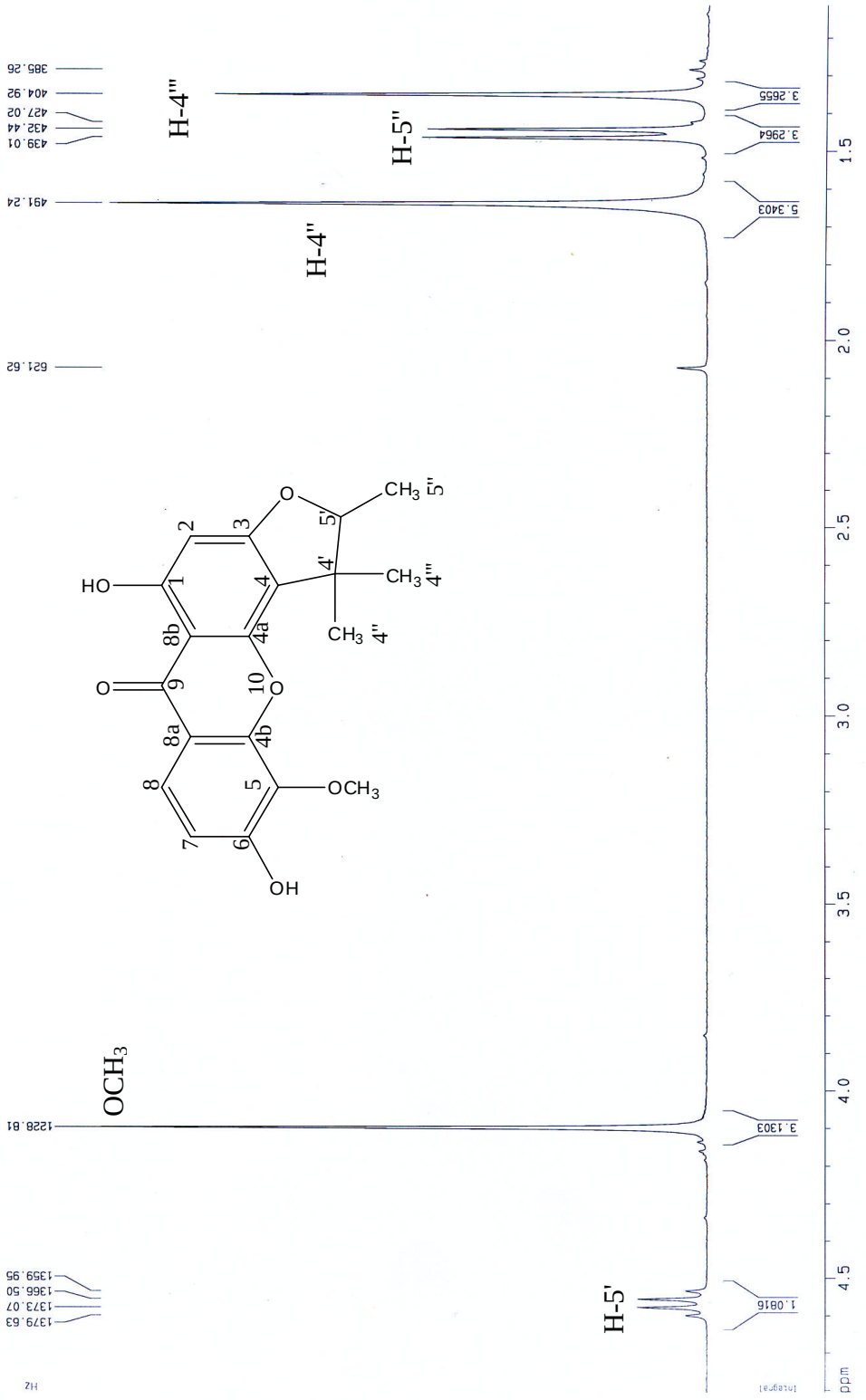

Figure 30 300 MHz ^{1}H-NMR spectrum of compound **A** in $CDCl_3$

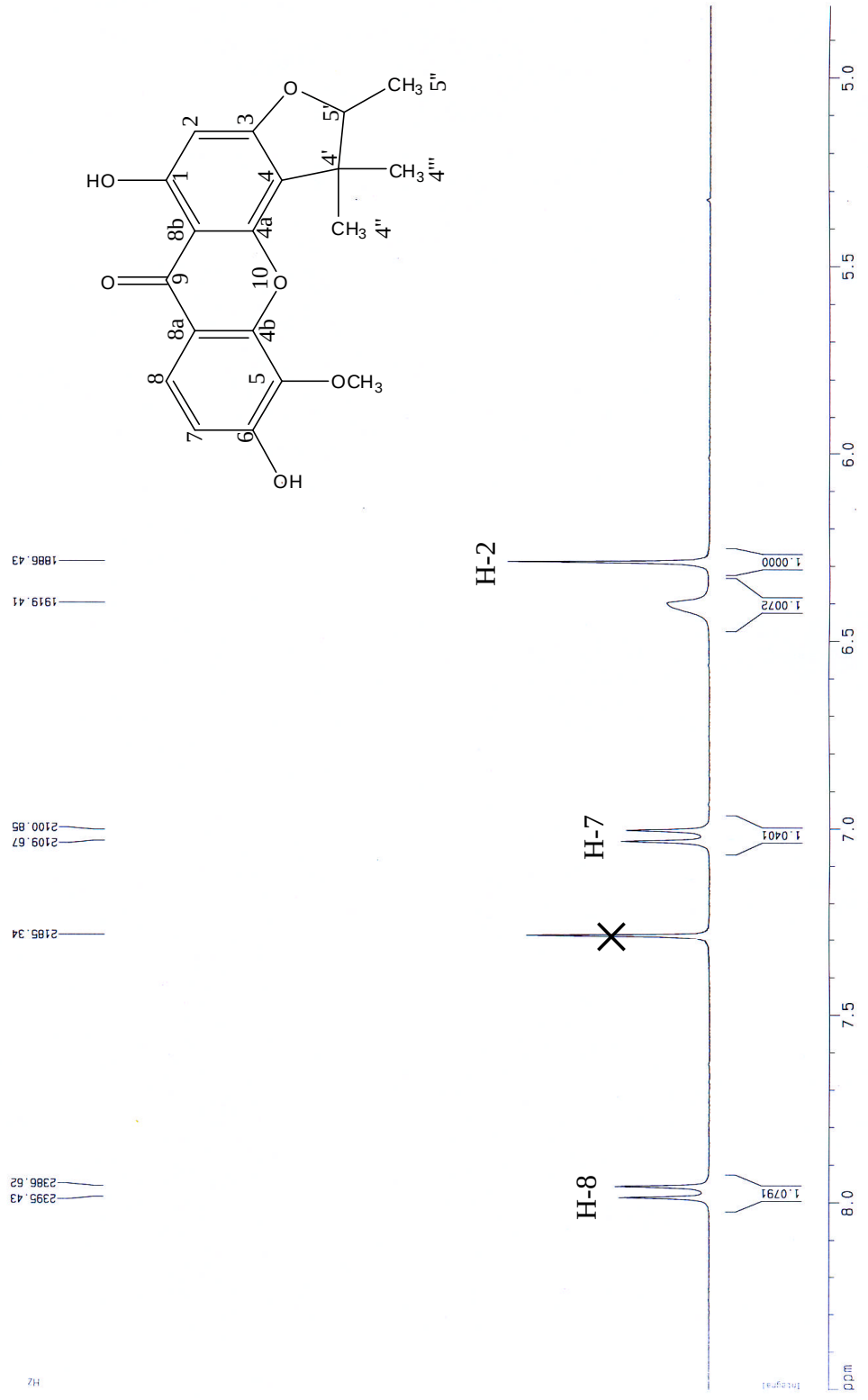

Figure 31 300 MHz ^{1}H-NMR spectrum of compound A in $CDCl_3$

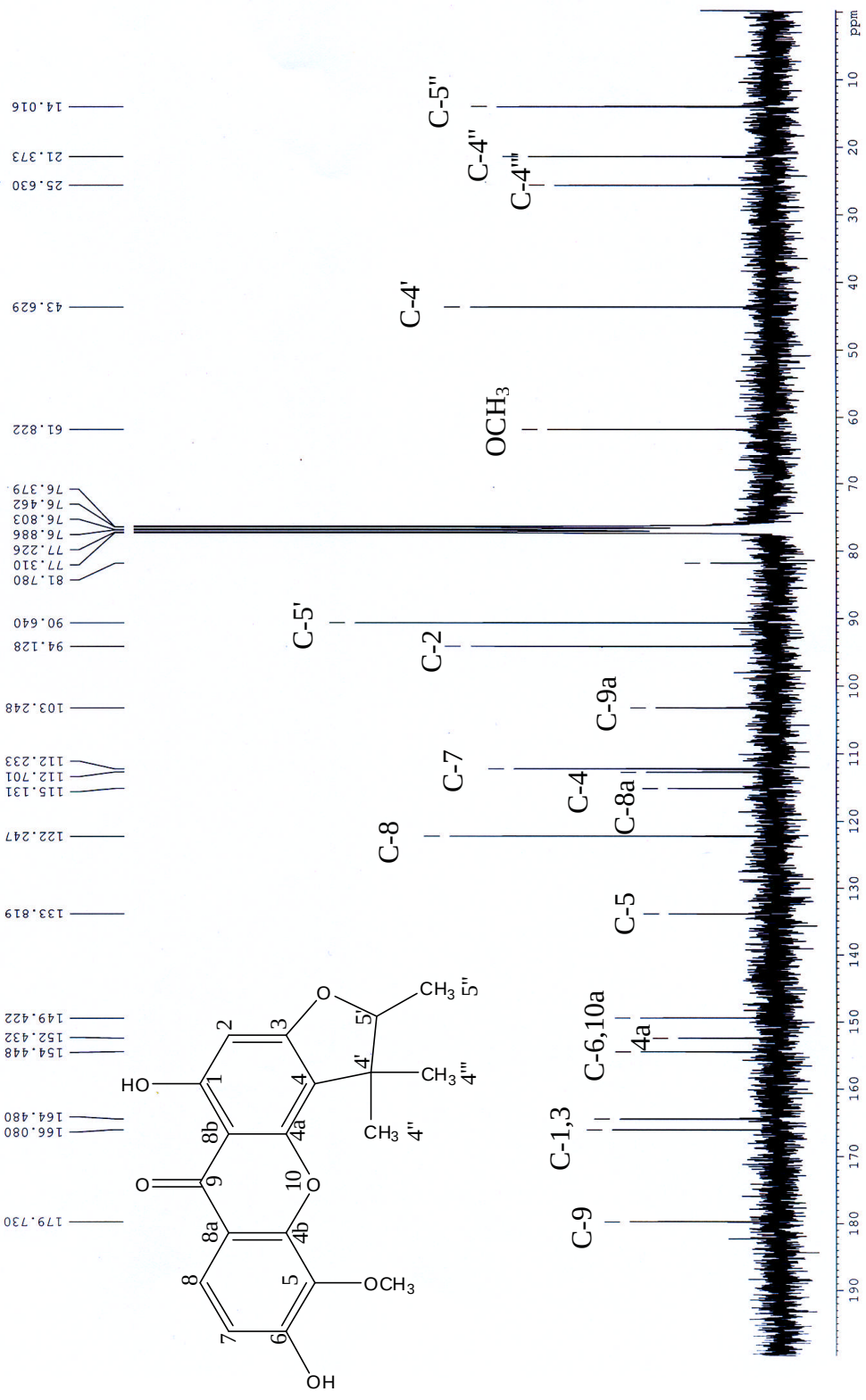

Figure 32 75 MHz ^{13}C-NMR spectrum of compound **A** in $CDCl_3$

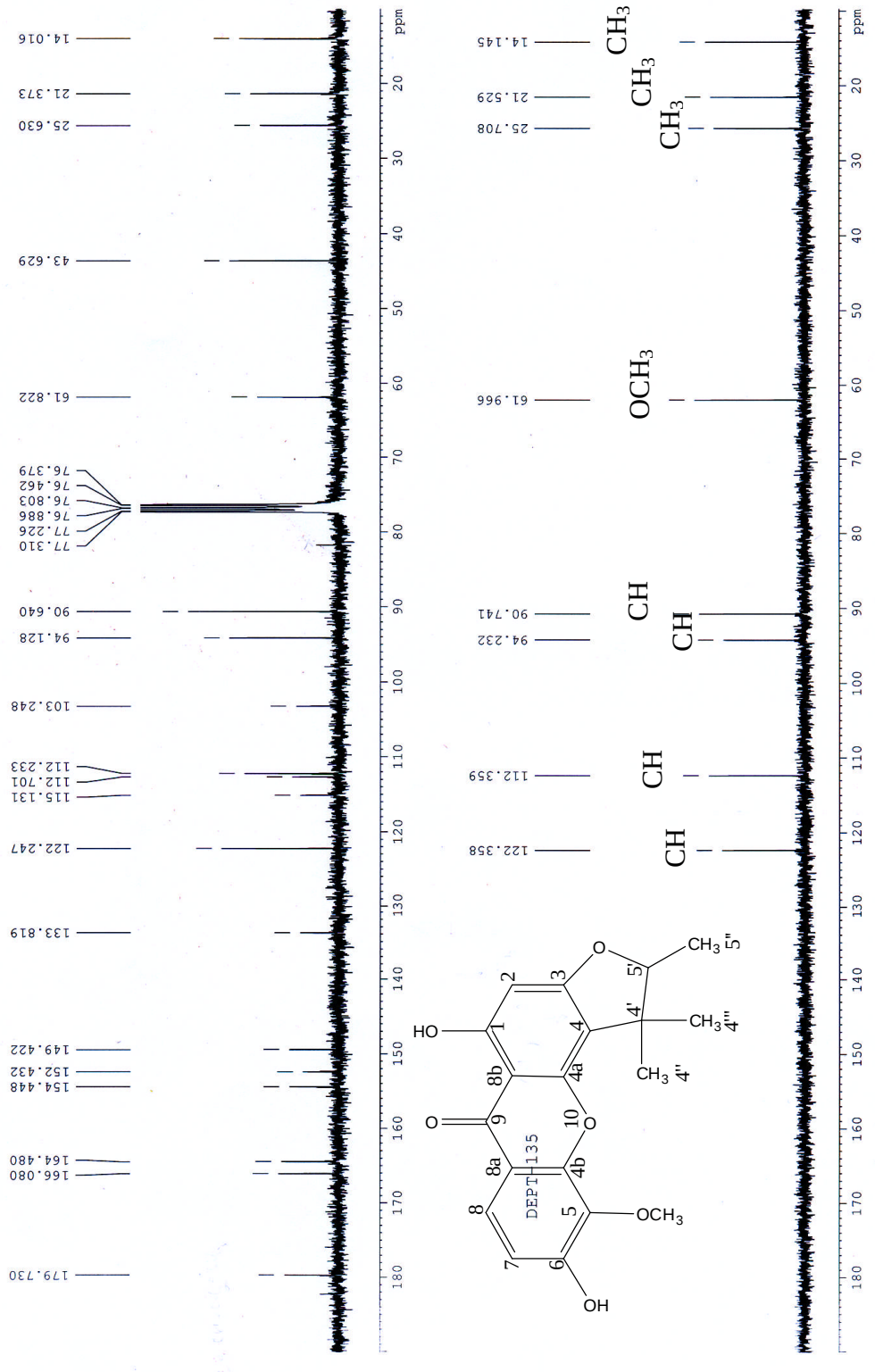

Figure 33 DEPT 135 spectrum of compound **A**

Table 10 ^{13}C-NMR , DEPT 135 and n-HMQC data of compound A

Carbon Position	Compound A (δ ^{13}C)	DEPT 135	n-HMQC
1	166.1	S	
2	94.1	D	6.30 (H-2)
3	164.5	S	
4	112.7	S	
5	133.8	S	
6	154.5	S	
7	112.2	D	7.02 (H-7)
8	122.3	D	9.98 (H-8)
9	179.7	S	
4a	152.4	S	
4b	149.4	S	
8a	115.1	S	
8b	103.3	S	
4′	43.6	S	
5′	90.6	D	4.56 (H-5')
5"-CH_3	14.0	Q	1.45 (5"-H_3)
4"-CH_3	25.6	Q	1.65 (4"-H_3)
4"'-CH_3	21.4	Q	1.35 (4"'-H_3)
5-OCH_3	61.8	Q	4.10 (5-OCH_3)

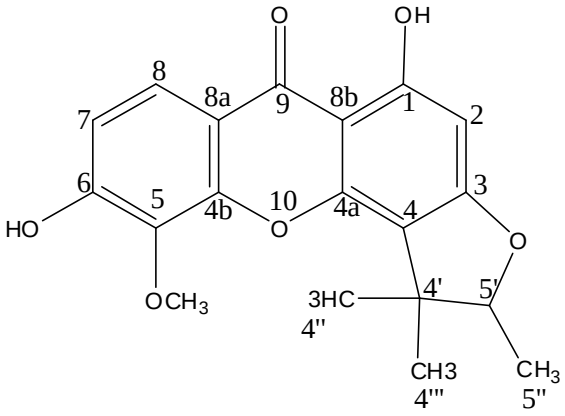

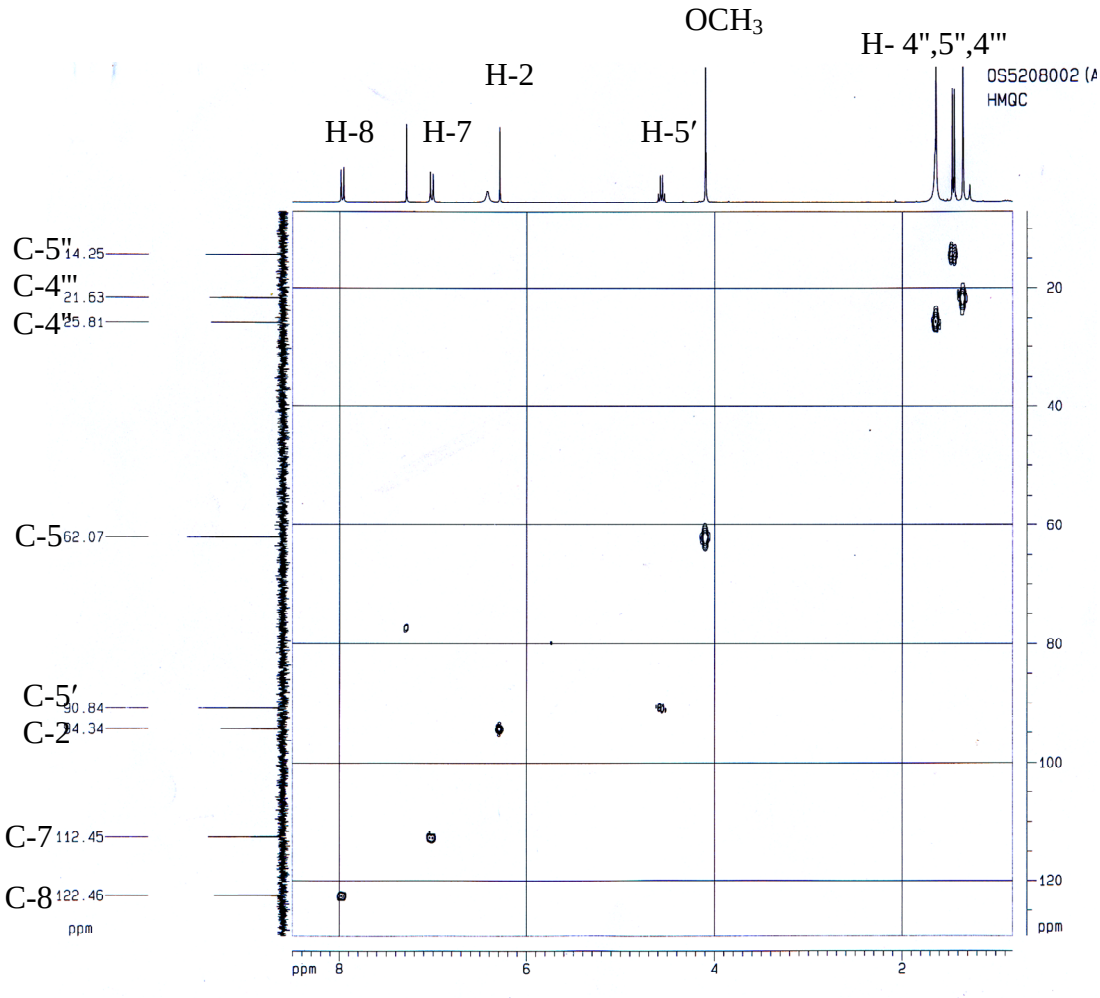

Figure 34 normal- HMQC spectrum of compound **A**

Table 11 ^{13}C-NMR and HMBC data of compound A

Carbon Position	Compound A (δ ^{13}C)	HMBC (δ ^{1}H)
1	166.1	6.30 (H-2), 13.32 (OH)
2	94.1	13.32 (OH)
3	164.5	6.30 (H-2), 13.32 (OH)
4	112.7	6.30 (H-2), 1.65 (H_3-4"), 1.35 (H_3-4"')
5	133.8	7.02 (H-8), 4.10 (OCH_3)
6	154.5	7.02 (H-7), 7.98 (H-8)
7	112.2	
8	122.3	
9	179.7	7.98 (H-8)
4a	152.4	
4b	149.4	7.98 (H-8)
8a	115.1	7.02 (H-7)
8b	103.3	6.30 (H-2), 13.32 (OH)
4´	43.6	1.65 (H_3-4"), 1.43 (H_3-5"), 1.35 (H_3-4"')
5´	90.6	1.65 (H_3-4"), 1.43 (H_3-5"), 1.35 (H_3-4"')
5"	14.0	
4"	25.6	1.35 (H_3-4"')
4"'	21.4	1.65 (H_3-4")
OCH_3	61.8	

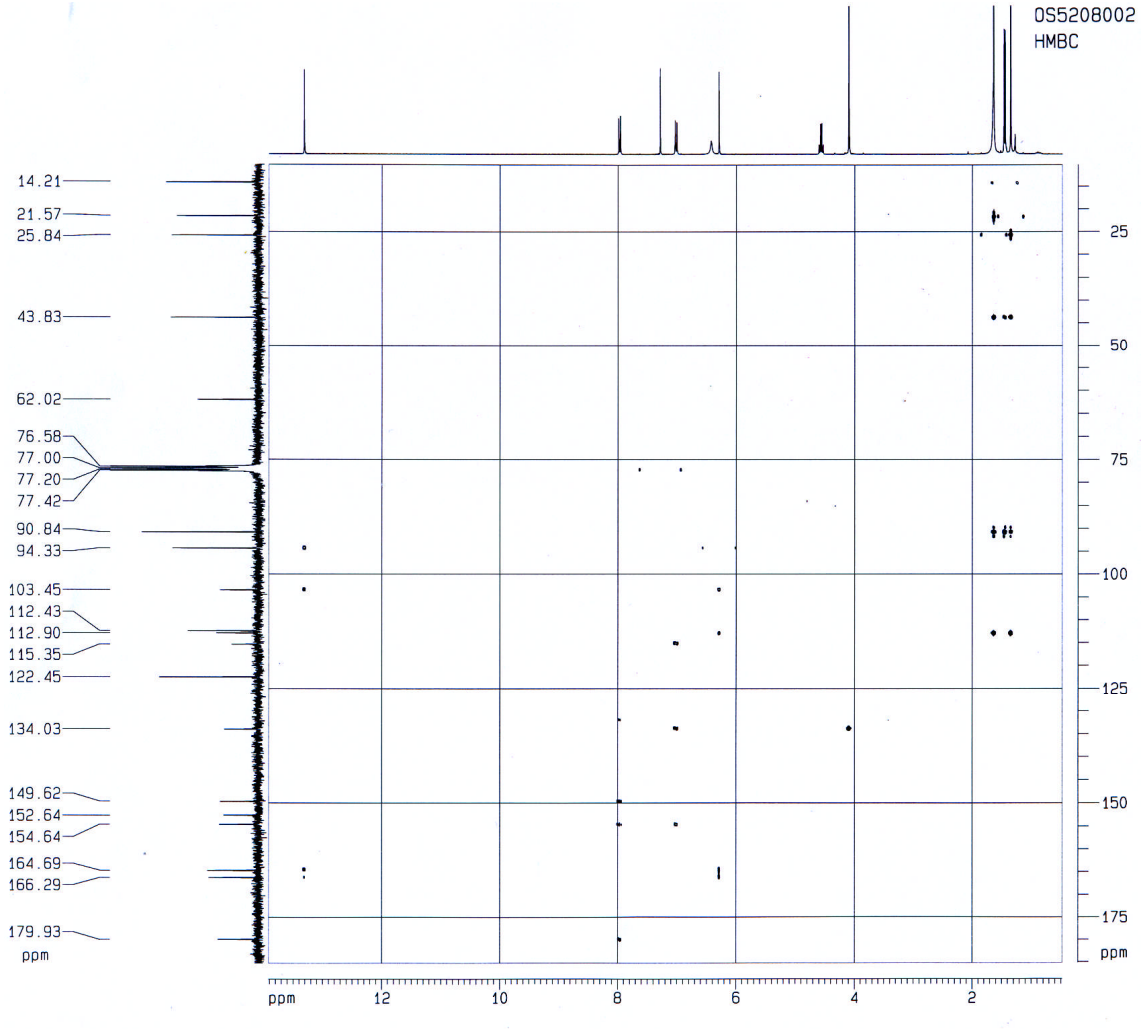

Figure 35 HMBC correlation of compound **A**

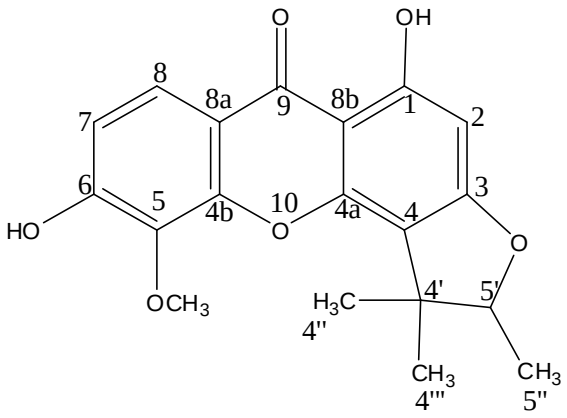

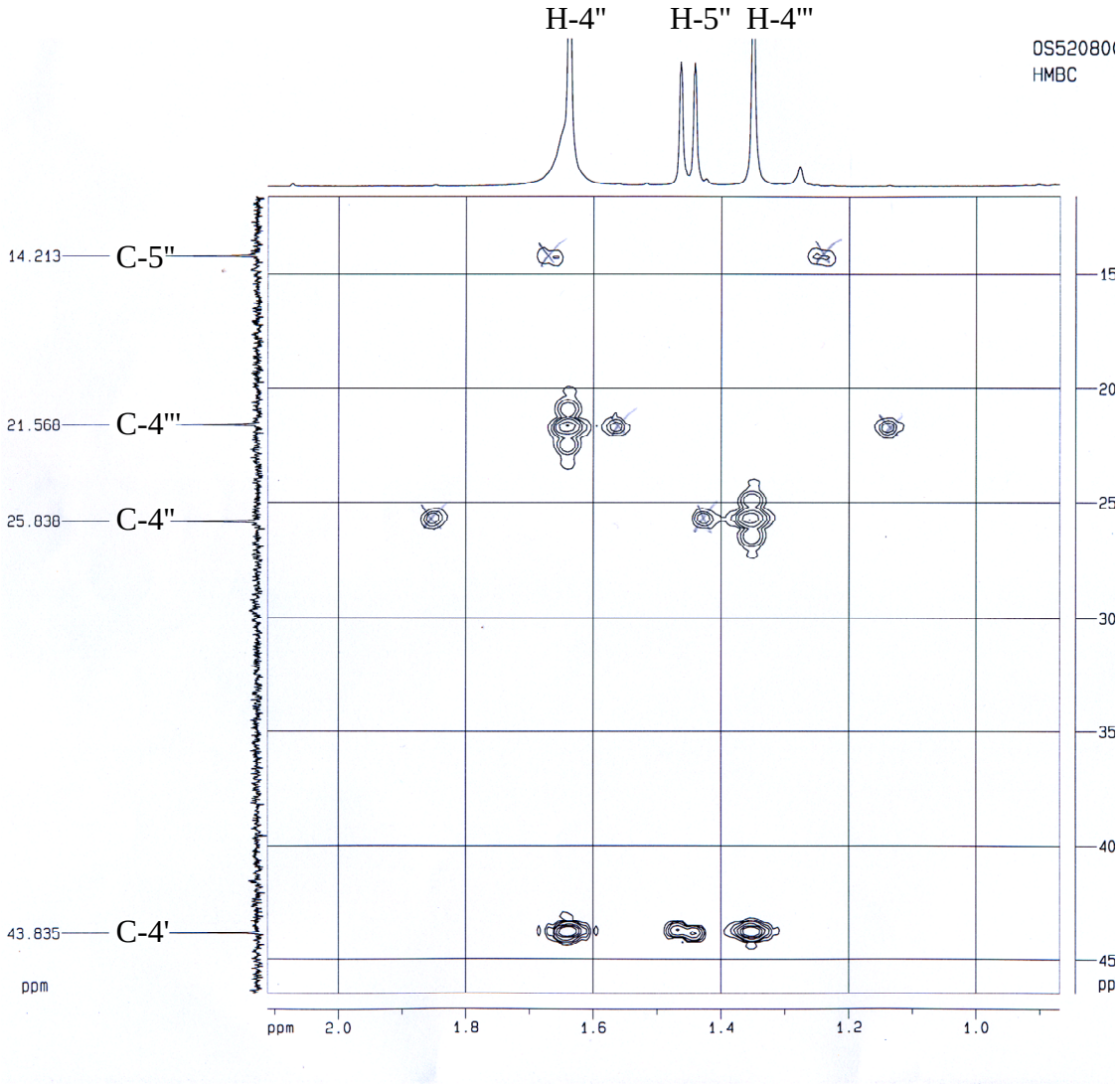

Figure 36 HMBC correlation of compound **A**

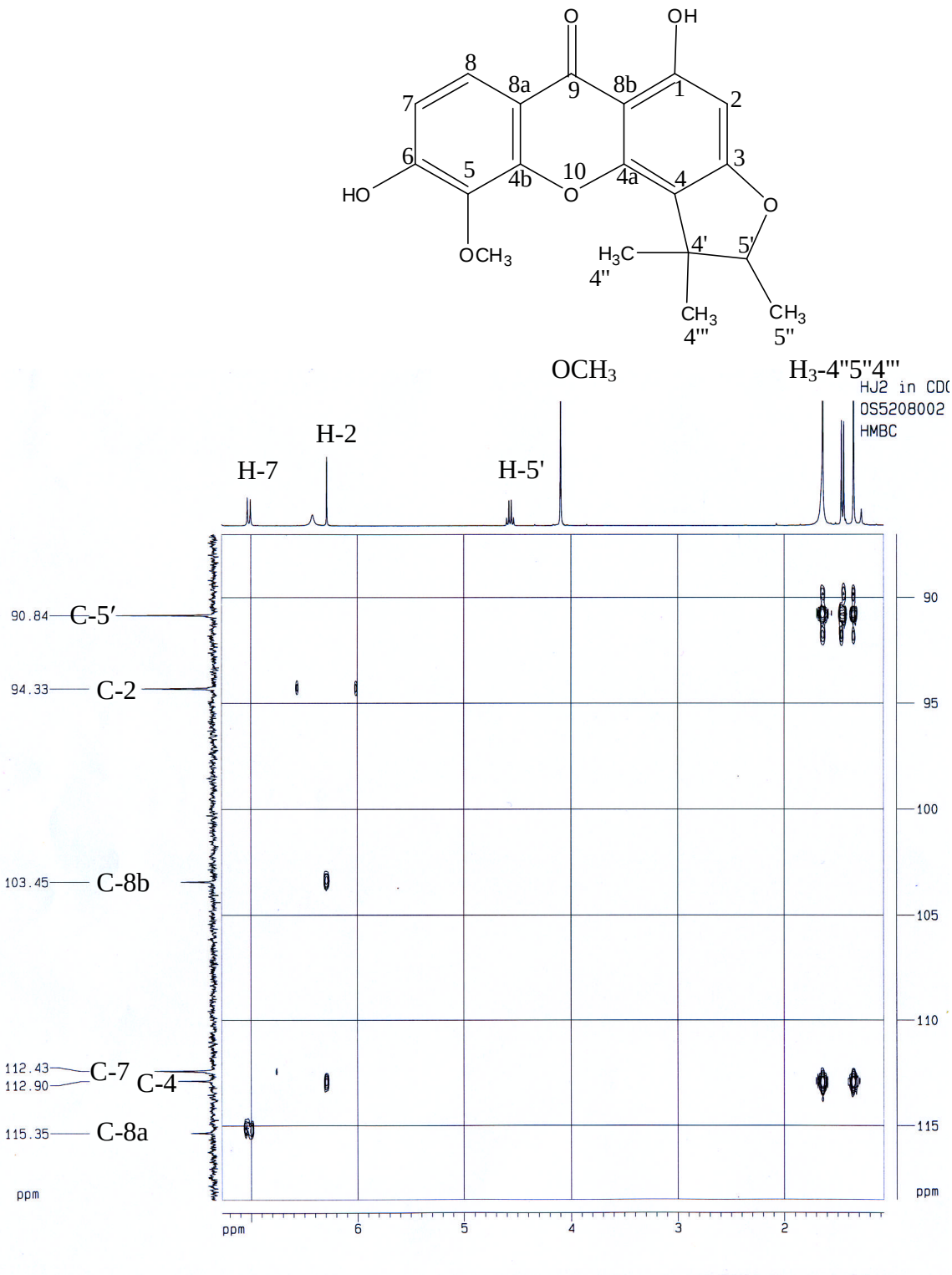

Figure 37 HMBC correlation of compound **A**

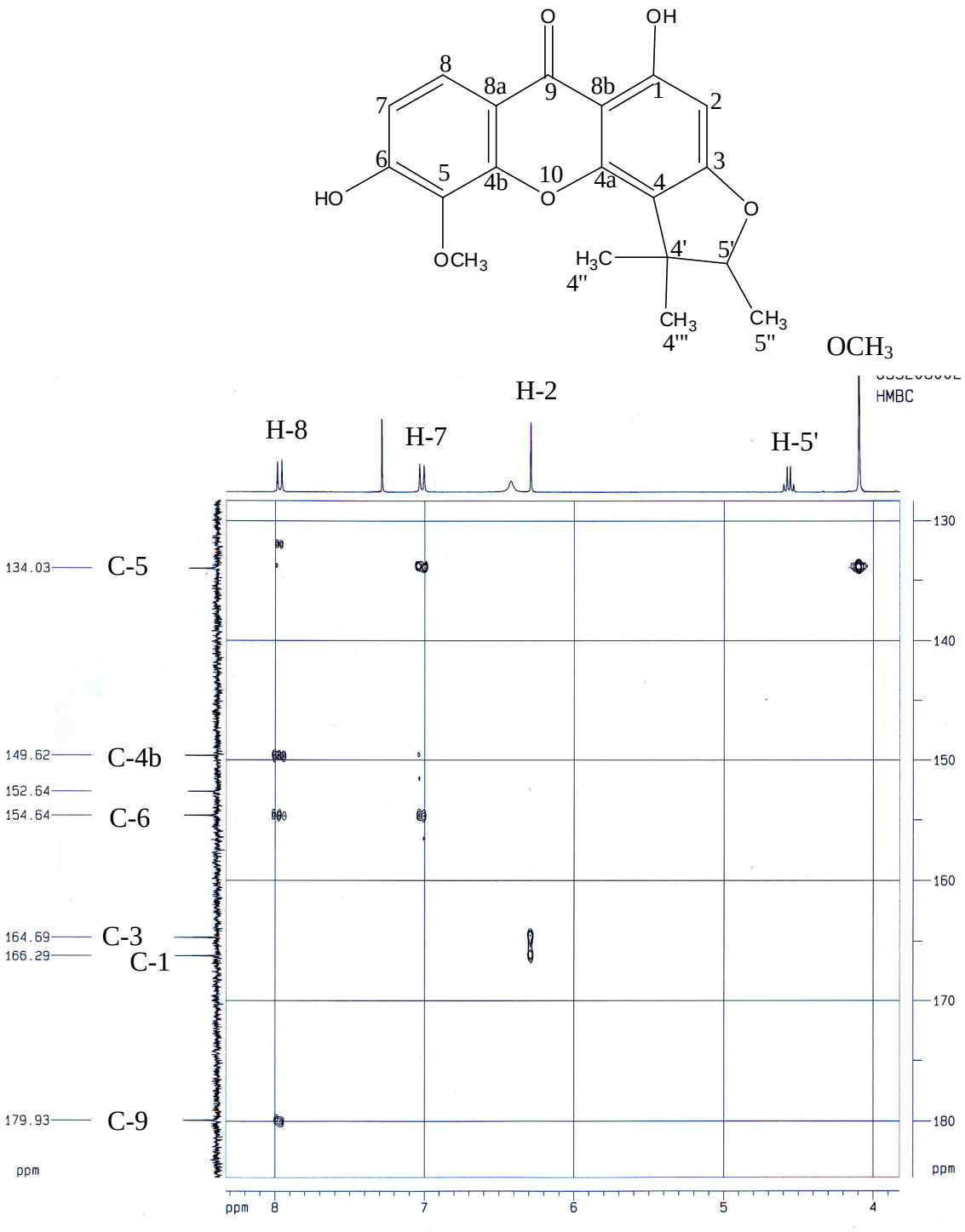

Figure 38 HMBC correlation of compound **A**

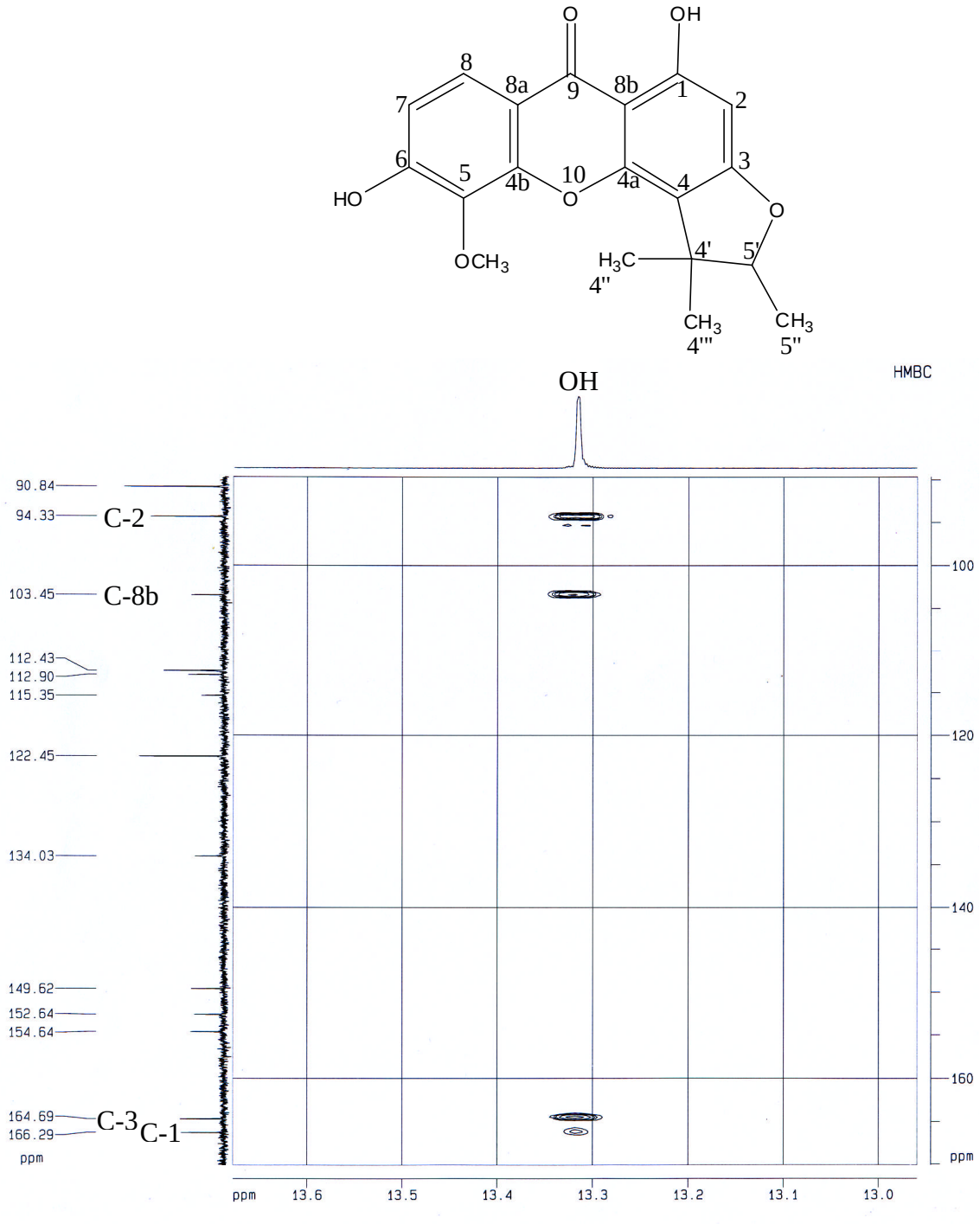

Figure 39 HMBC correlation of compound **A**

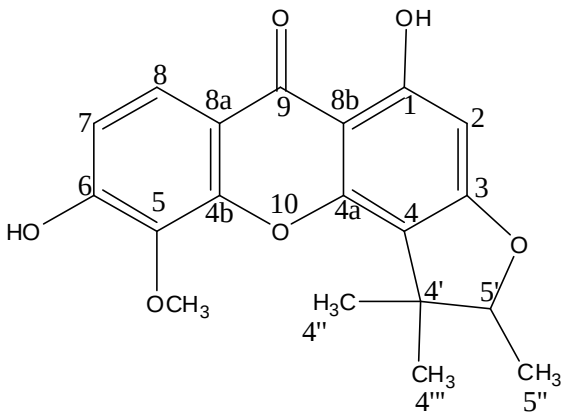

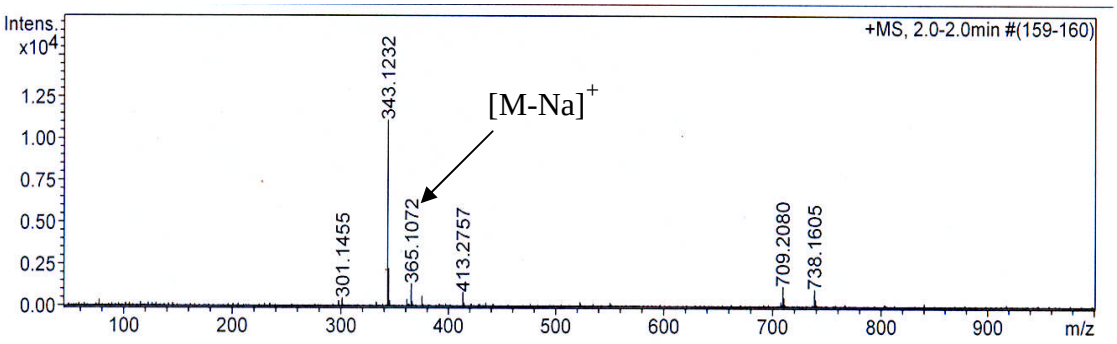

Figure 40 TOF-MS spectrum of compound **A**

4.4.2 Compound B.

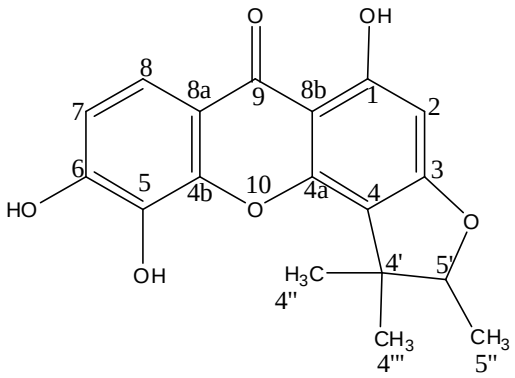

2-deprenlyrheediaxanthone B

Compound B. Yellow crystals with a melting point of 211-213 ^{o}C. The UV spectrum (Figure 41) in methanol of compound B exhibited absorptions at 252, 287 and 328 nm. The FTIR spectrum in chloroform (Figure 42) indicated the vibrations of the hydroxyl stretching (ν_{OH}) at 3434.68 cm^{-1}, carbonyl stretching ($\nu_{C=O}$) from 1654.70 to1609.39 cm^{-1}, double bond of aromatic rings ($\nu_{C=C}$) 1559.65 cm^{-1}. The molecular formula of compound B was deduced to be $C_{18}H_{16}0_6$ from the ^{13}C NMR data. The ^{1}H NMR spectra (Figure 43-44) revealed the presences of a chelated hydroxyl (δ 13.43), two aromatic protons (δ 6.95 and 7.58 ,each, *d*, *J* 8.73 *Hz*, H-7, H-8), methine protons (δ 6.13, *s*, H-2;δ 4.55, *dd*, *J*, 6.57, 13.14 Hz, H-5'); methyl protons (δ 1.40, *d*, *J* 6.56 Hz, H_3-5"); δ 1.60, 1.35, H_3-4", H_3-4'").

The ^{13}C-NMR spectrum data of compound B afforded 18 lines as shown in Figure 45, indicating the number of carbon atoms in the molecule. The resonance at δ 180.18 (C-9) indicated a carbonyl group (C=O), while the resonances at δ 165.84 (C-1), 152.87 (C-6) were assigned to the quaternary carbons near hydroxyl groups. The resonances at δ 112.88 and δ 116.58 were assigned to methine carbons at C-7, C-8 positions, respectively, the other carbons were assigned as presented in **Table 12**.

The carbon type was assisted by DEPT spectrum (Figure 46). The normal HMQC (Figure 47) assisted the proton assignment (**Table 13**).

The ^{1}H and ^{13}C chemical shifts of the compound B were assigned by comparing with the literature (109) as shown in **Table 12** .From the above data, ^{1}H-

NMR and ^{13}C-NMR spectral data of compound B were in good agreement with data given for **2-deprenlyrheediaxanthone B** (109).

Table 12 Comparison of ^{1}H, ^{13}C-NMR data of compound B with literature values (109)

Proton Position	Chemical shift(δ) ^{13}C-NMR		Chemical shift(δ) ^{1}H-NMR	
	Lit. (acetone-d_6)	Compound B (acetone-d_6)	Lit. (acetone-d_6)	Compound B (acetone-d_6)
1	166.8	165.84		
2	93.8	92.90	6.10,*s*, 1H	6.13,*s*, 1H
3	165.2	164.26		
4	113.4	112.29		
5	133.7	132.63		
6	152.6	152.87		
7	113.4	112.88	6.95, *d*, *J* 8.8 Hz	6.98, *d*, *J* 8.73 Hz
8	117.5	116.58	7.58 ,*d J* 8.8 Hz	7.60, *d*, *J* 8.73 Hz
9	181.1	180.18		
4a	152.6	151.38		
4b	147.1	146.16		
8a	114.9	114.00		
8b	103.5	102.66		
4'	44.5	43.54		
5'	91.6	90.72	4.35, *q*, *J* 6.6 Hz, 1H	4.55, *dd*, *J* 6.57, 13.14 Hz, 1H
5"	14.5	13.53	1.36, *d*, *J* 6.6 Hz, H_3-5"	1.40, *d*, *J* 6.57 Hz, H_3-5"
4"	25.8	24.83	1.59, *s*, H_3-4"	1.60, *s*, H_3-4"
4'"	21.4	20.38	1.29, H_3-4'"	1.31, *s*, H_3-4'"

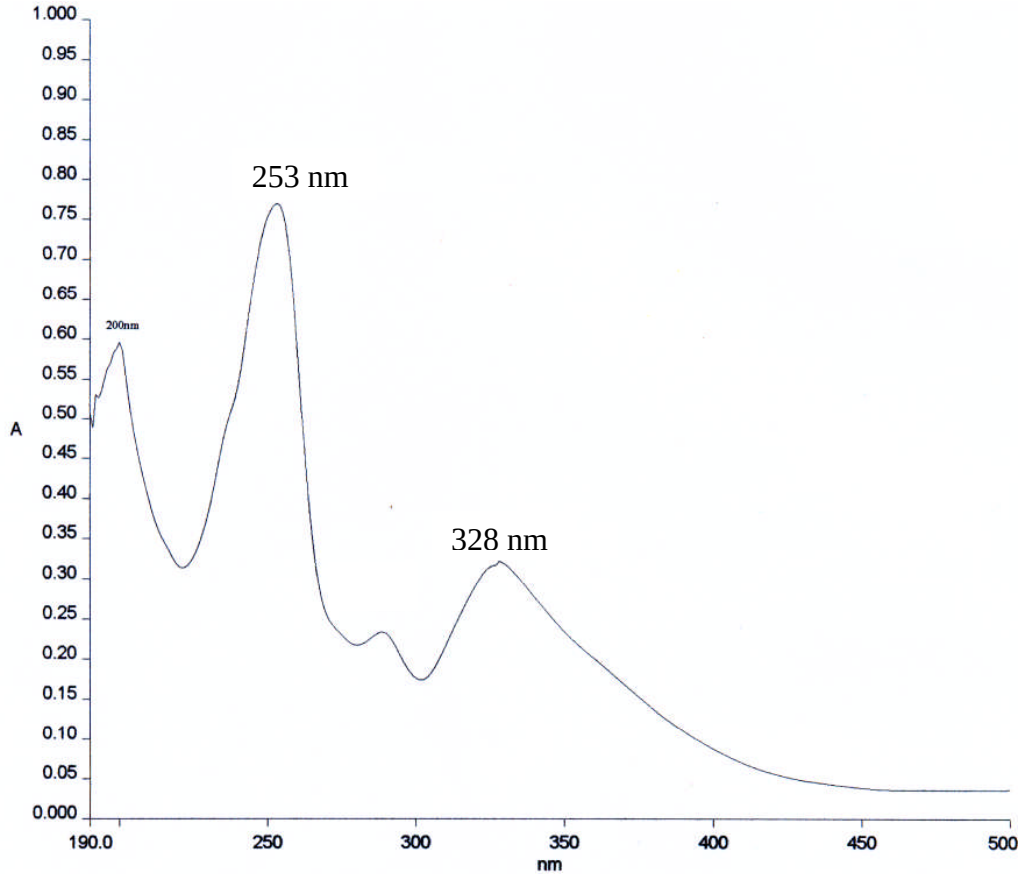

Figure 41 UV spectrum of compound B in methanol

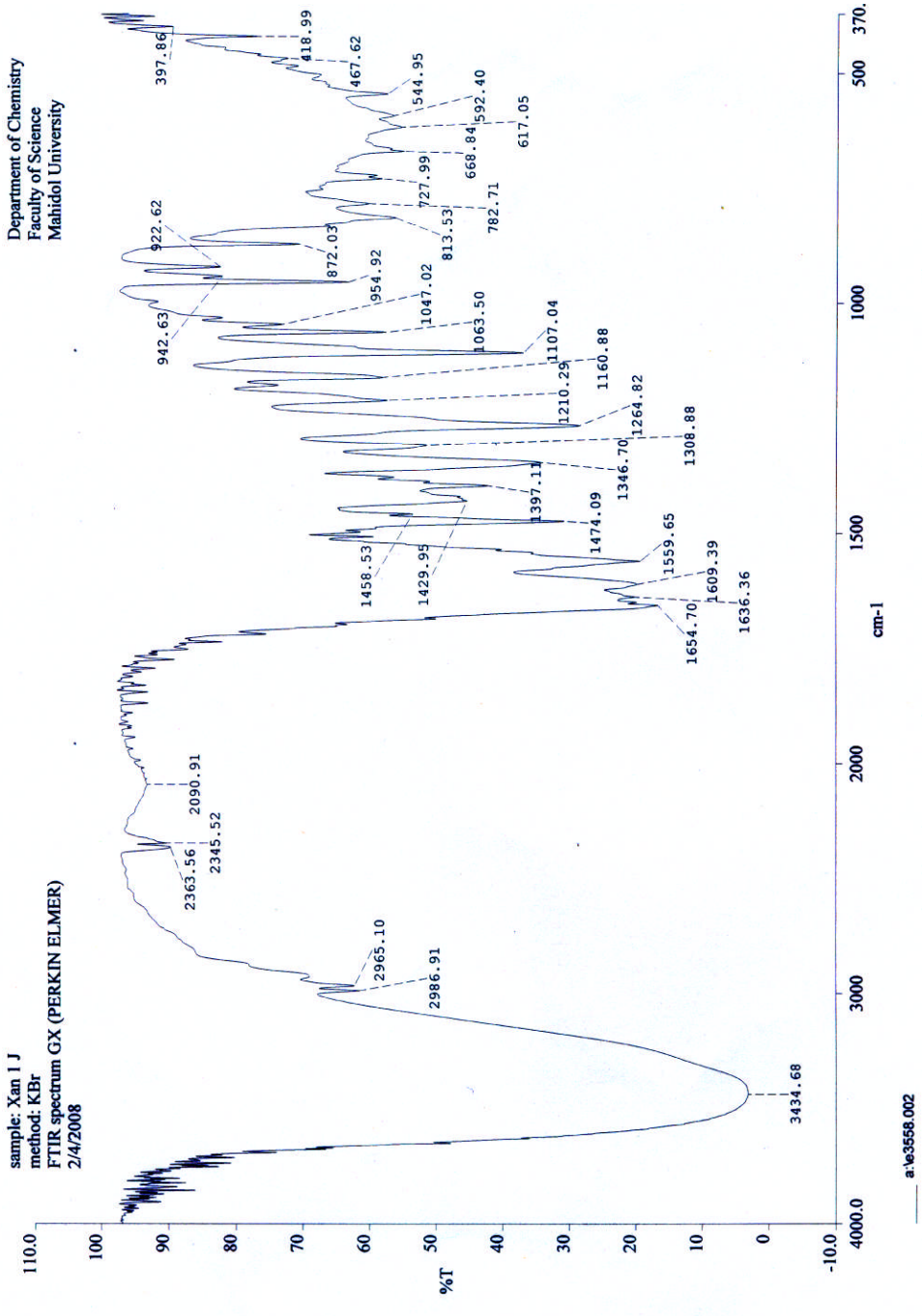

Figure 42 FTIR spectrum of compound B (KBr disc)

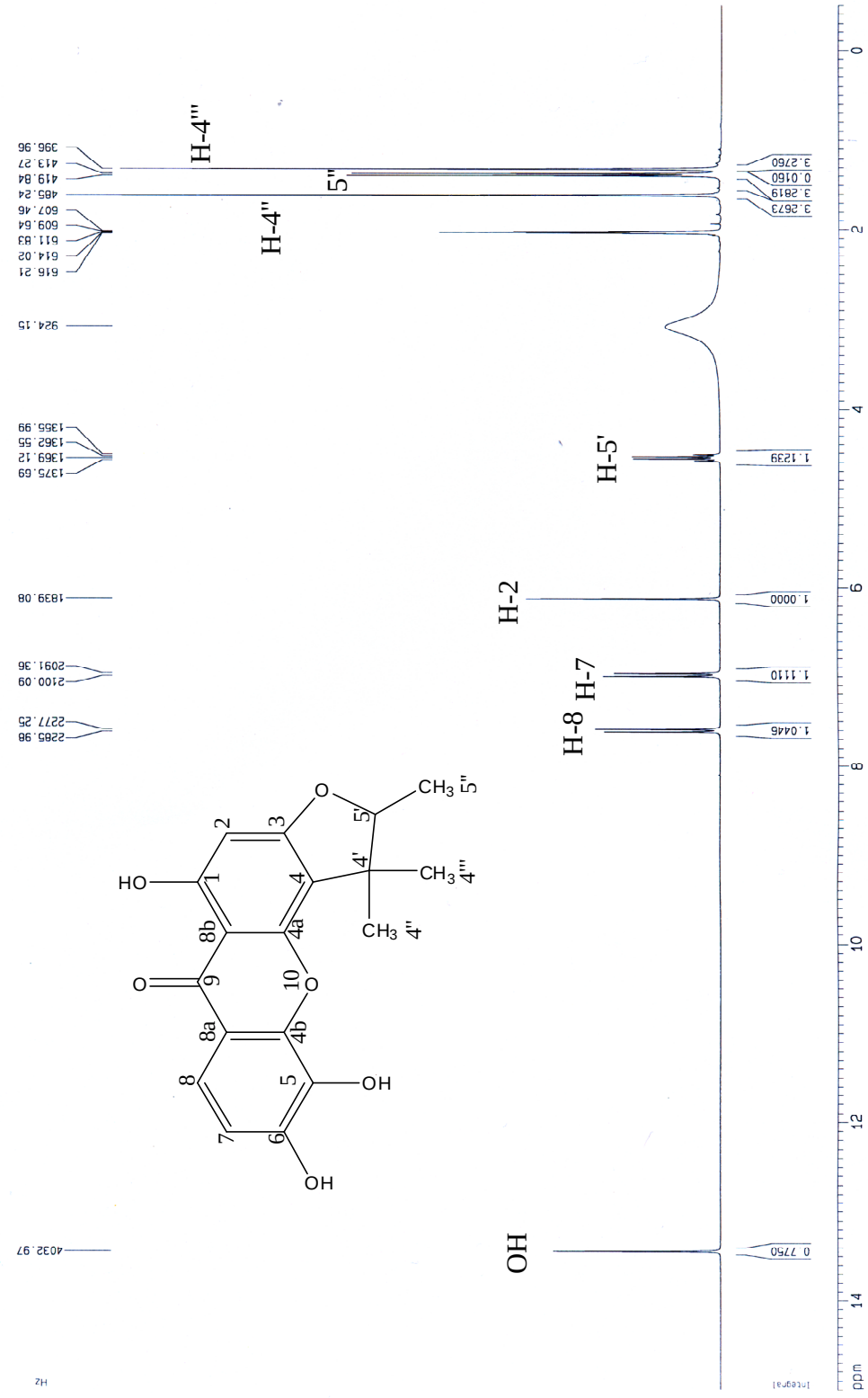

Figure 43 300 MHz ^{1}H-NMR spectrum of compound **B** in acetone-d_6

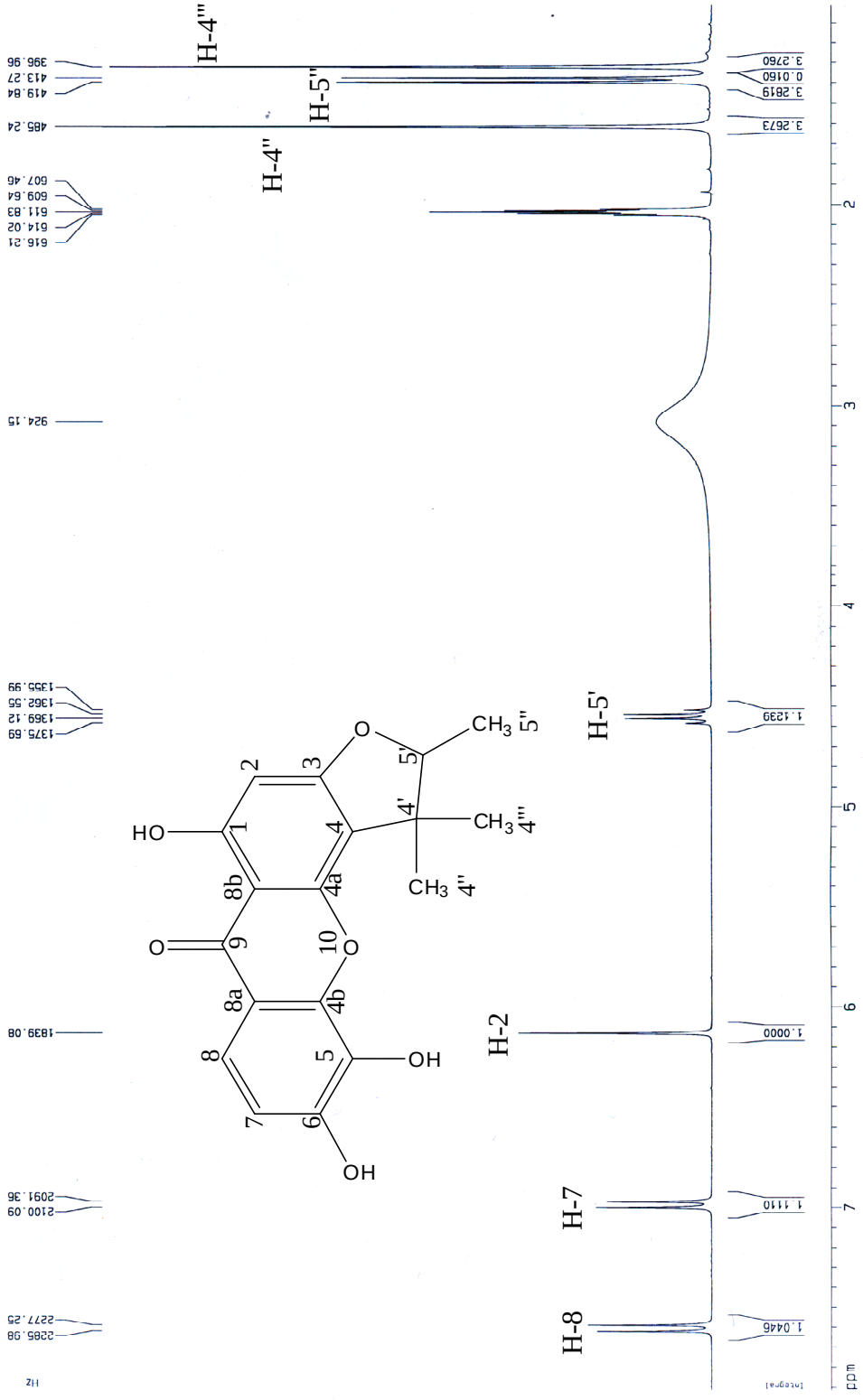

Figure 44 300 MHz ^{1}H-NMR spectrum of compound **B** in acetone-d_6

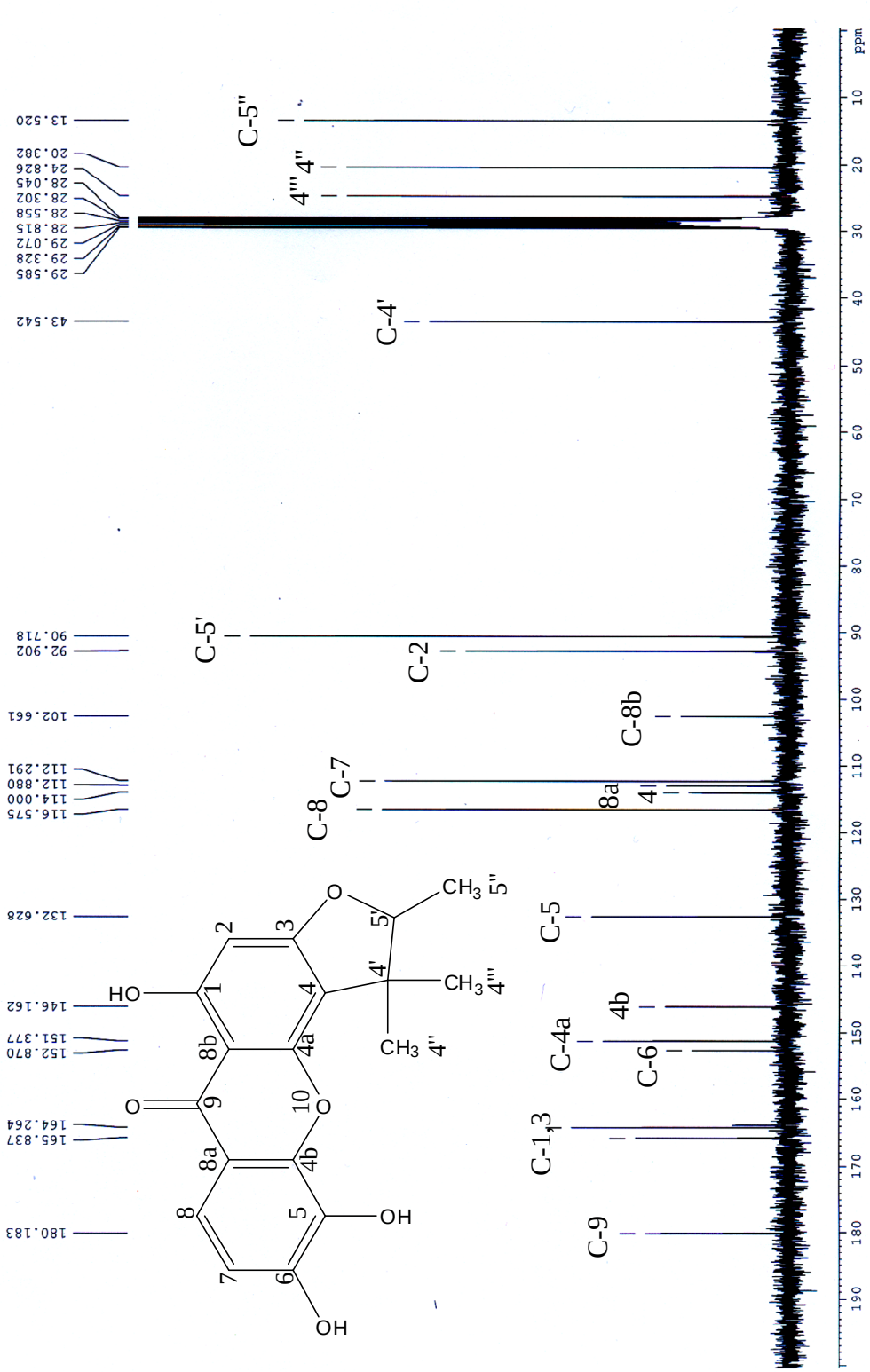

Figure 45 75 MHz ^{13}C-NMR spectrum of compound **B** in acetone-d_6

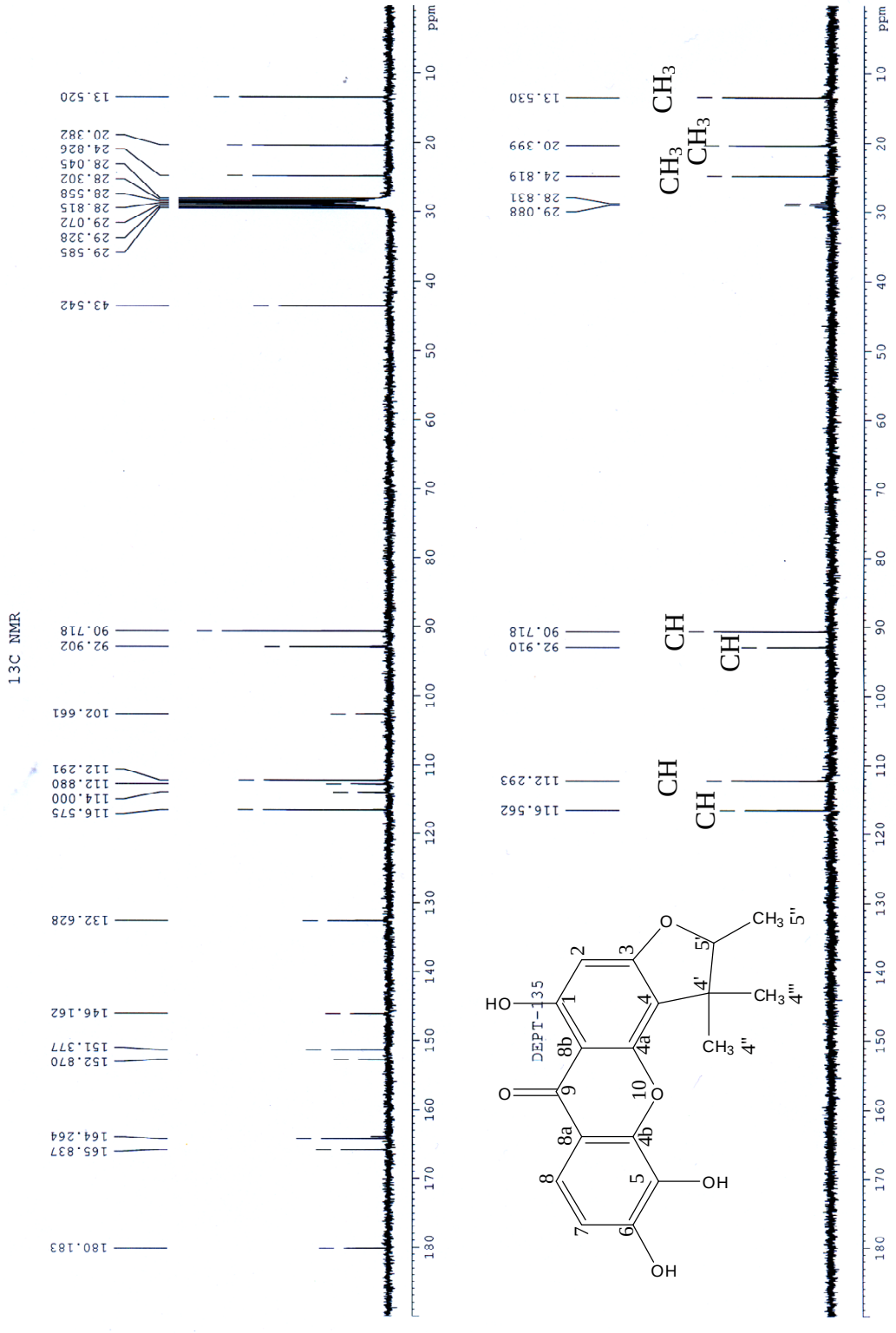

Figure 46 DEPT 135 spectrum of compound **B**

Table 13 ^{13}C-NMR , DEPT 135 and n-HMQC data of compound B

Carbon Position	Compound B (δ ^{13}C)	DEPT 135	n-HMQC
1	165.84	S	
2	92.90	D	6.13 (H-2)
3	164.26	S	
4	112.29	S	
5	132.63	S	
6	152.87	S	
7	112.88	D	6.98 (H-7)
8	116.58	D	7.60 (H-8)
9	180.18	S	
4a	151.38	S	
4b	146.16	S	
8a	114.00	S	
8b	102.66	S	
4'	43.54	S	
5'	90.72	D	4.55 (H-5')
5"	13.53	Q	1.40 (H_3-5")
4"	24.83	Q	1.60 (H_3-4")
4"'	20.38	Q	1.31 (H_3-4"')

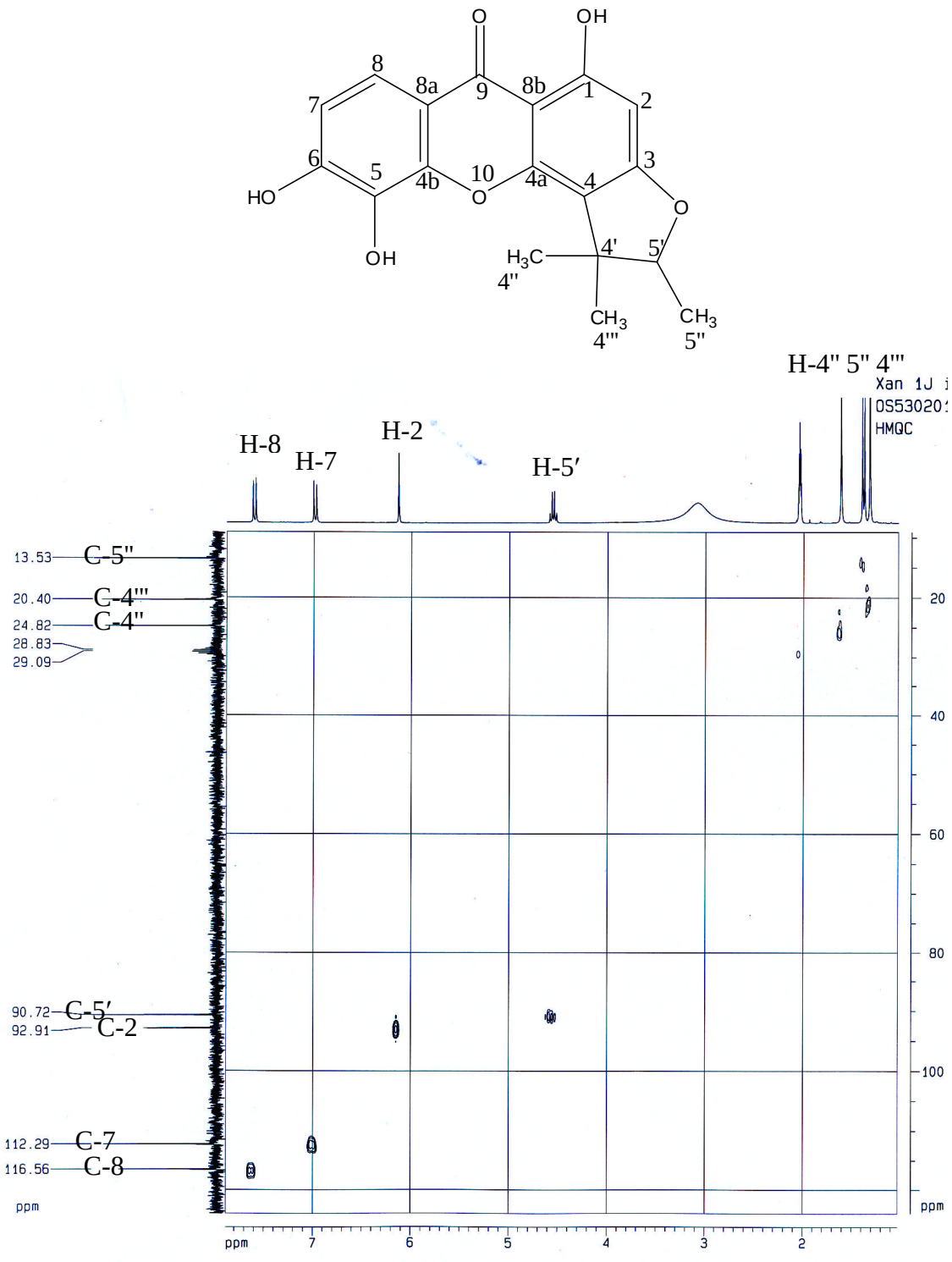

Figure 47 normal-HMQC ^{13}C- spectrum of compound **B**

4.4.3 Compound C

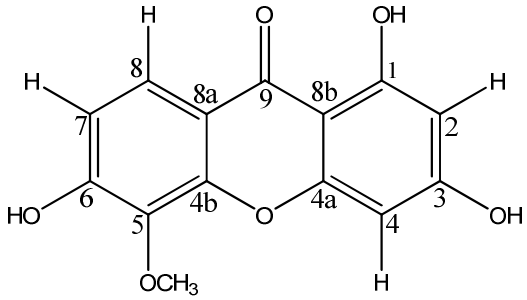

1,3,6-trihydroxy-5-methoxyxanthone

Compound C appeared as yellowish white needles with a melting point of 247-249 ºC (with decomposition). Thin-layer chromatogram of this compound gave a pale green spot with NP/PEG (under UV 366) reagent (Figures 25-26). The UV spectrum in methanol of compound C exhibited absorptions at 243 and 317 nm (Figure 48) corresponding to benzene with hydroxyl substitution (129). The FTIR spectrum (Figure 49) revealed the stretching vibrations of the hydroxyl (ν_{OH}) at 3411 cm^{-1} (broad), the methyl group (ν_{CH3}) at 2955 cm^{-1}, the carbonyl stretching ($\nu_{C=O}$) from 1651 to 1608 cm^{-1}, aromatic double bonds ($\nu_{C=C}$) at 1449 cm^{-1}, ν_{C-O} at 1213 to 1163 cm^{-1}, 1099 and 1068 cm^{-1}.

The EIMS of compound C was determined as $C_{14}H_{10}O_6$, m/z 274 (Figure 50). The ^{13}C-NMR spectrum of compound C showed 13 carbon signals. Analysis of ^{13}C-NMR spectrum (Figure 53) of this compound C (**Table 11**) suggested the presence of one methyl carbon (δ 60.8) including carbonyl carbon (δ 179.8). The ^{1}H-NMR spectra (Figures 51-52) of compound C exhibited the presence of aromatic protons at δ 6.98 and 7.75 ppm (each, 1H, *d*, *J* 8.8 Hz, H-7, H-8), two pairs of doublets at δ 6.21 and 6.45 ppm (each, 1H, *d*, *J* 2.1 Hz, H-2, H-4) and a methoxyl protons at δ 3.90 ppm.

The ^{1}H and ^{13}C chemical shifts of the compound C were assigned by comparing the δ with literature (110) as shown in **Table 14**. From the above data, it could be concluded that the structure of compound C was 1,3,6-trihydroxy-5-methoxyxanthone.

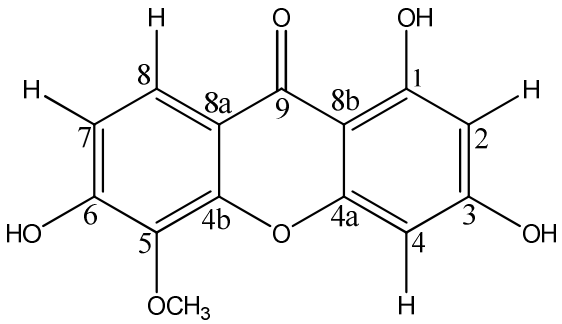

1,3,6-trihydroxy-5-methoxyxanthone

Table 14 500 MHz ^{1}H-NMR and 125^{13}C-NMR data of compound C (in acetone–d_6 +D_2O) compared with literature values (110)

Carbons/ Proton	Chemical shift(δ) ^{13}C-NMR		Chemical shift(δ) ^{1}H-NMR	
	Lit. (DMSO-d_6)	Compound C (acetone-d_6)	Lit. (DMSO-d_6)	Compound B (acetone-d_6)
1	162.9	163.15		
2	98.2	98.14	6.28	6.21, 1H, *d*, *J* 2.12 Hz
3	165.5	165.51		
4	94.2	94.24	6.53	6.45, 1H, *d* ,*J* 2.10 Hz
4a	157.1	156.60		
5	134.5	134.70		
6	157.3	157.77		
7	114.2	113.75	6.98	6.98, 1H, *d J* 8.83 Hz
8	120.9	121.05	7.63	7.75, *d*, *J* 8.84 Hz
8a	112.9	113.75		
9	179.2	179.88		
9a	101.4	101.86		
10a	150.5	150.76		
5-OCH_3	60.8	60.82	3.85	3.90, (H_3, *s*,)

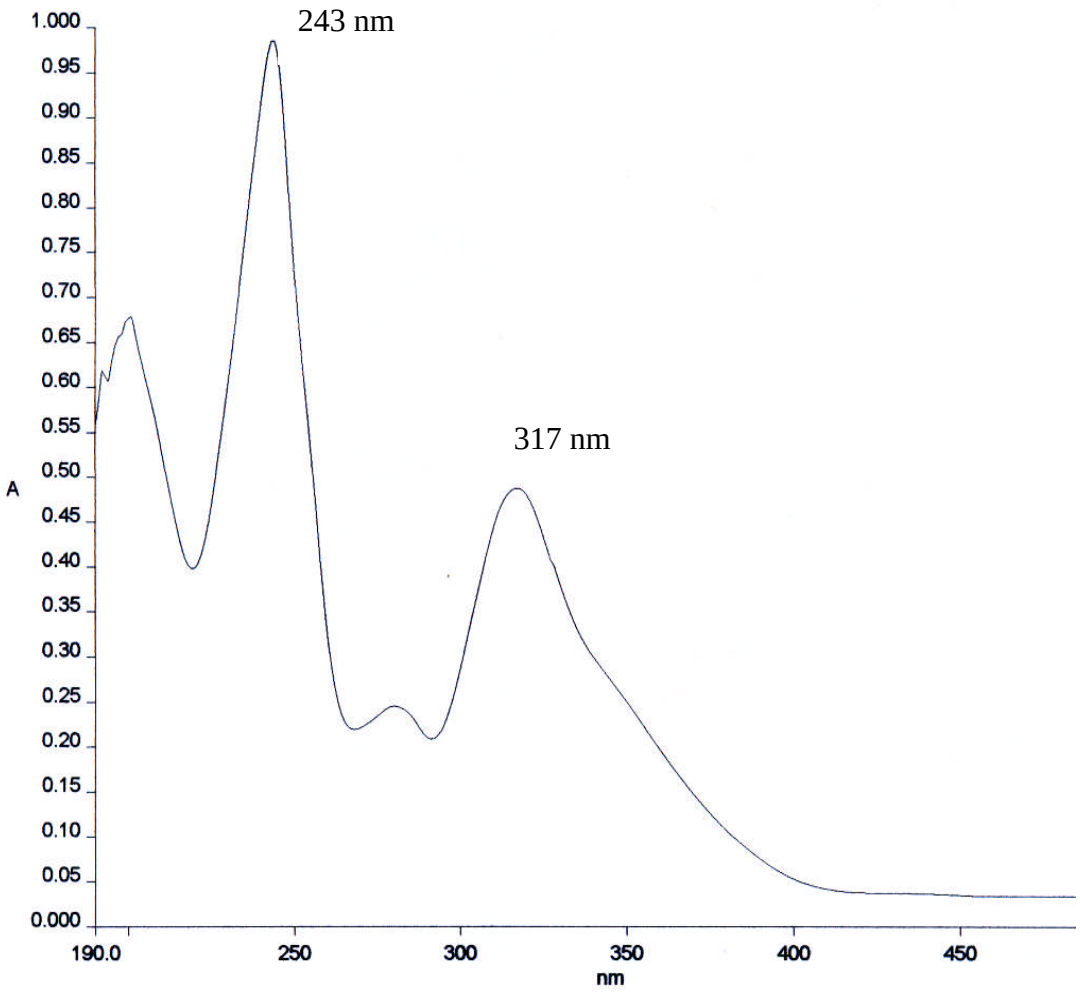

Figure 48 UV spectrum of compound C in methanol

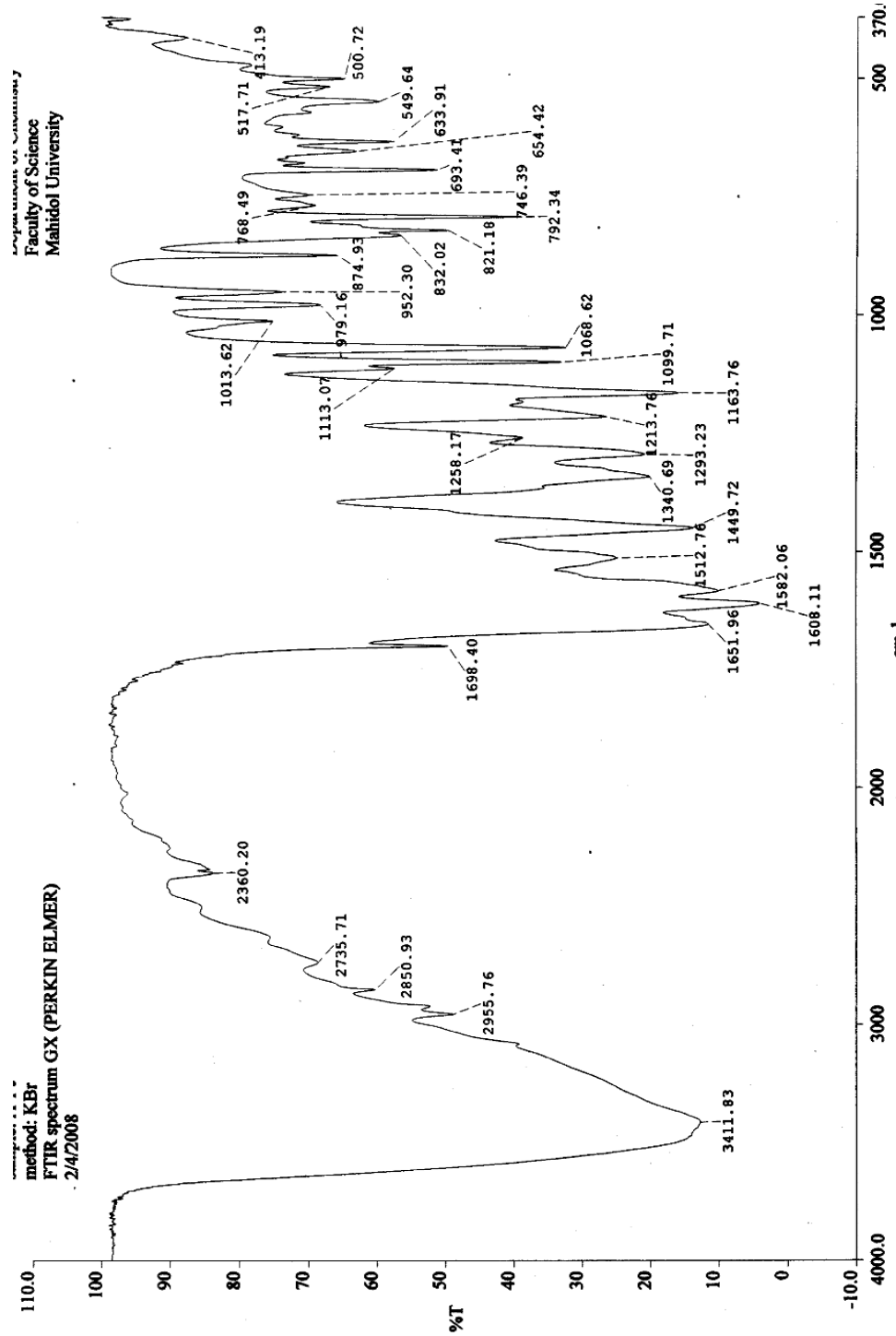

Figure 49 FTIR spectrum of compound C (KBr disc)

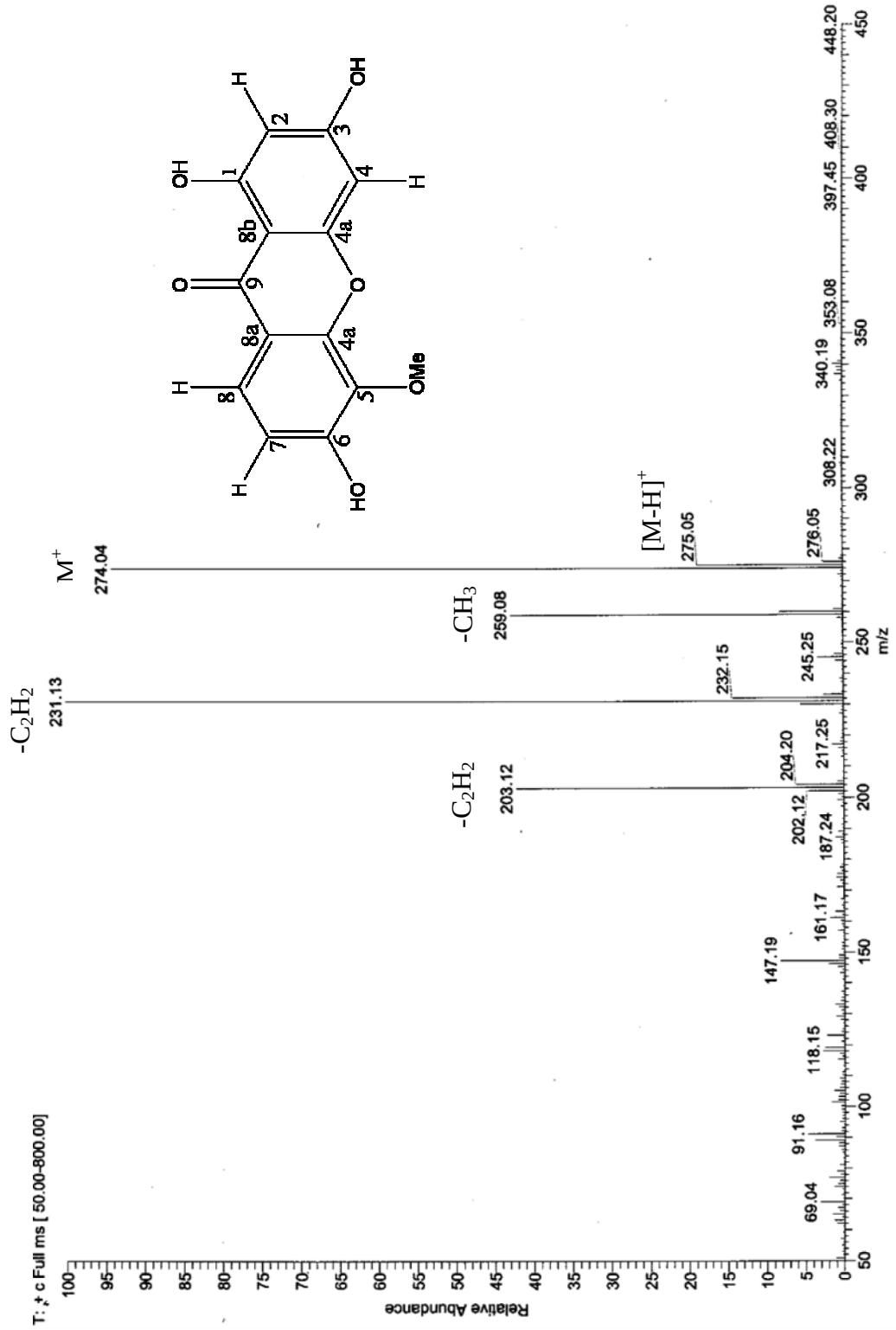

Figure 50 EIMS spectrum of compound C

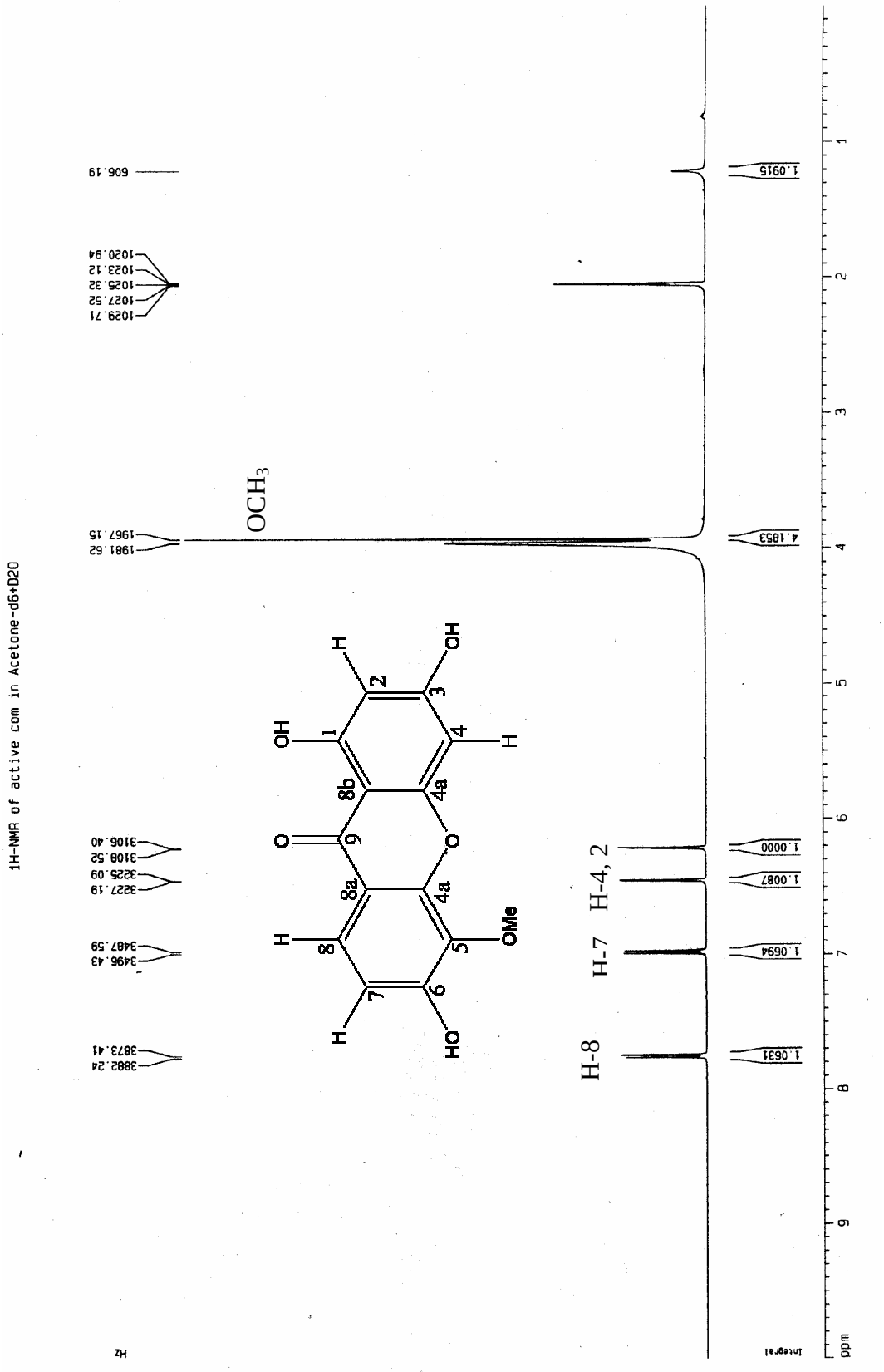

Figure 51 500 MHz ^{1}H-NMR spectrum of compound C in acetone-d_6+D_2O

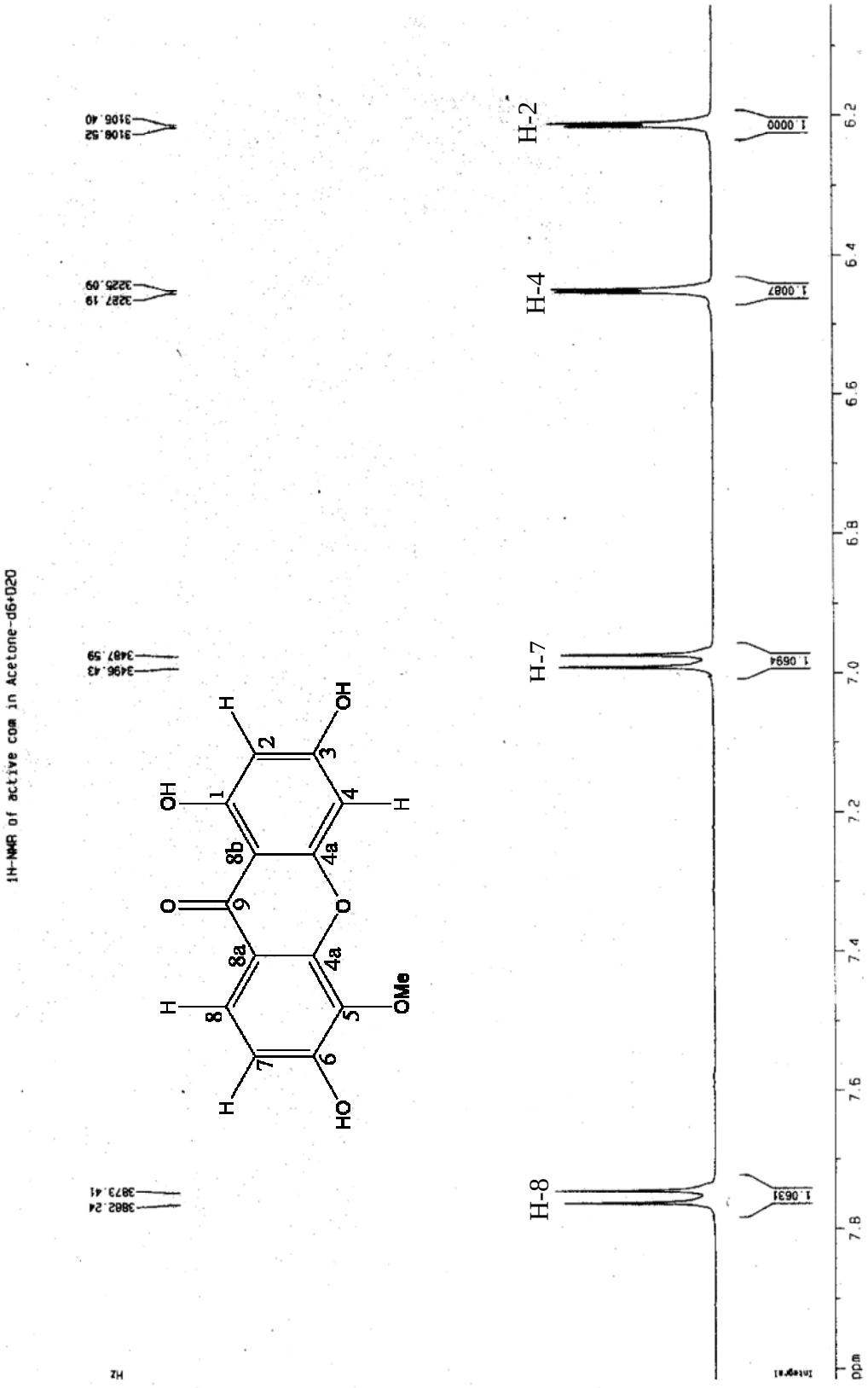

Figure 52 500 MHz ^{1}H-NMR spectrum of compound C in acetone-d_6+D_2O

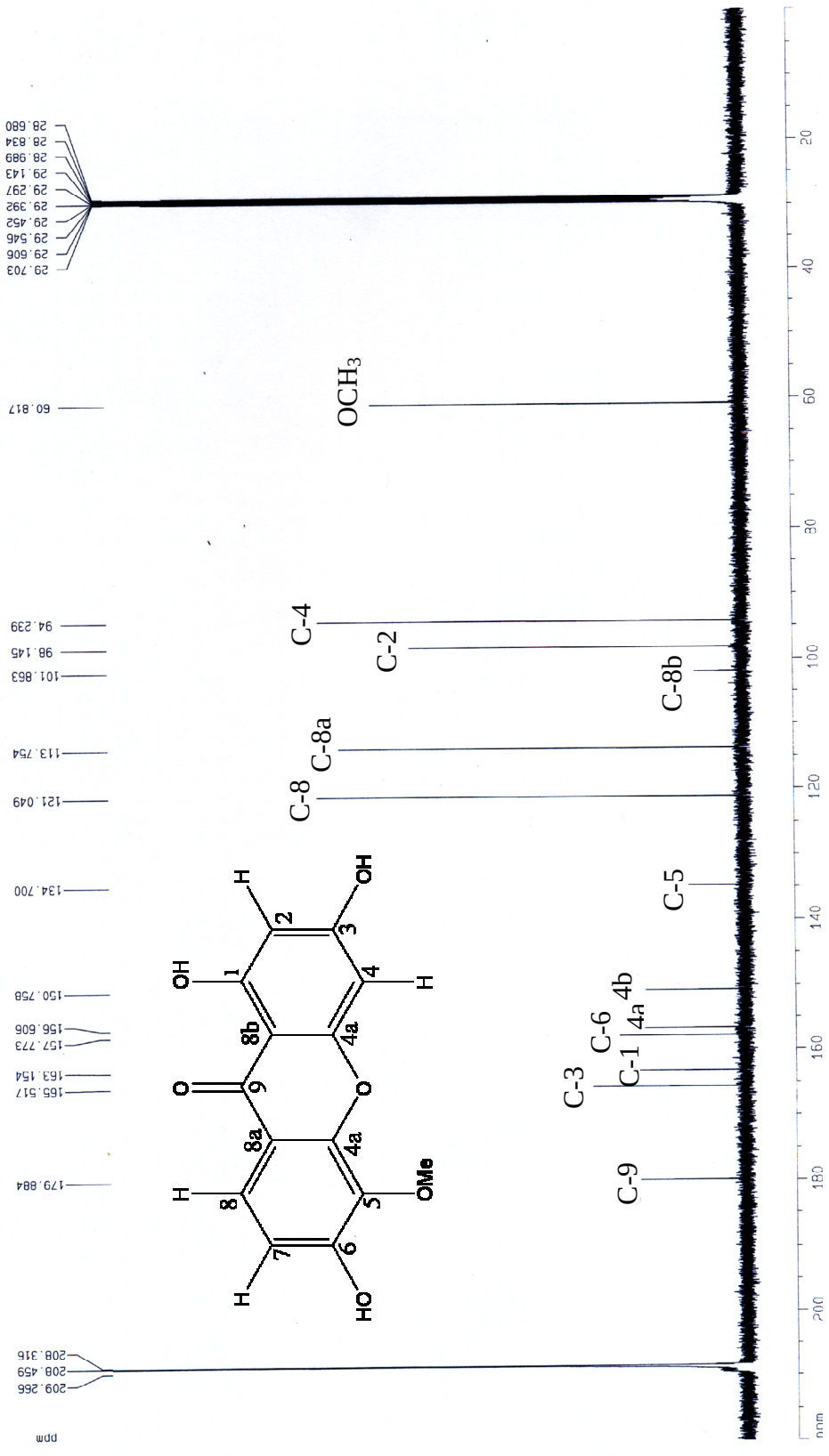

Figure 53 125 MHz ^{13}C-NMR spectrum of compound C in acetone-d_6+D_2O

4.4.4 Compound D

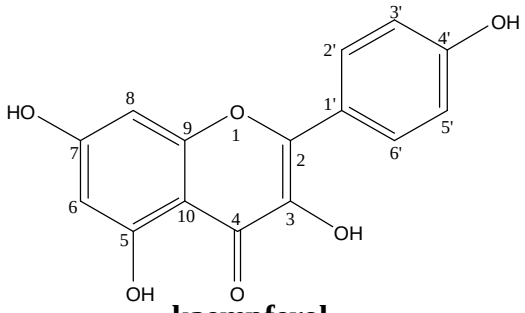

kaempferol

Compound D appeared as pale yellow-amorphous with a melting point of 276-278 ºC. The TLC chromatogram of compound C was shown in Figure 26. After spraying with NP/PEG and under UV 366 nm the band appeared from bluish to greenish. Its UV spectrum in methanol (Figure 54) exhibited characteristic aromatic absorption bands at 266 nm (Band I), 366 nm (Band II) indicating the free 3–OH of flavonol. The FTIR spectrum in KBr (Figure 55) showed the vibrations of the hydroxyl group (ν_{OH}) at 3385.30 cm^{-1} and 2924.25 cm^{-1}, carbonyl stretching ($\nu_{C=O}$) at 1660.47-1615.84 cm^{-1}, $\nu_{C=C}$ 1522.98 cm^{-1}. The ^{13}C –NMR spectral data of the compound D afforded 14 lines as shown in Figure 56, corresponding to a number of carbon atoms in the molecule. The resonance at δ 175.83 indicated a carbonyl group (C=O), while the resonances at δ 163.82 ,160.7 were assigned to the quaternary carbons near to the hydroxyl groups, the downfield shifts at δ 137.26 and 135.54 indicating a 2,3 unsaturated flavonoid nucleus and the resonances at δ129.40 belonging to the equivalent methine carbons at C-2′, C-6′ positions. The assignment of other carbons could be seen in **Table 15**. According to ^{1}H and ^{13}C-NMR spectral data the molecular formula of compound D was deduced as $C_{15}H_{12}O_6$.

The ^{1}H-NMR spectra (Figures 57-58) of compound **D** displayed the characteristic signals of the kaempferol nucleus (111), i.e., two doublets at δ_H 6.20 and 6.43 ppm (*J* 2.0 Hz), assigned to the H-6 and H-8 protons, respectively, A pair of AB system of aromatic protons, assigned to H-3′, H-5′ and H-2′, H-6′, appeared at δ_H 6.92 and 8.03 ppm respectively, each as *d* with *J* 8.8 Hz. The ^{1}H and ^{13}C-NMR assignments (**Table 15**) were accomplished by comparing the chemical shifts with the literature (111).

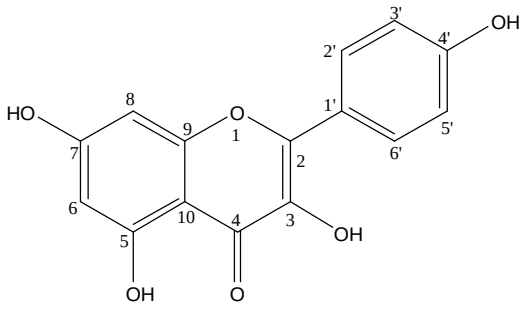

Table 15 300 MHz ^{1}H-NMR, 75 MHz ^{13}C-NMR spectral data of compound D (in DMSO-d_6) compared with the literature (111)

Carbons/ Protons	Lit-Kaempferol ^{13}C	Compound D ^{13}C	Lit.-Kaempferol ^{1}H	Compound D ^{1}H
C-2	146.80	137.26		
C-3	135.65	135.54		
C-4	175.90	175.83		
C-5,	160.70	160.65	12.47 (1H, *brs*-OH, 5-OH)	12.46(1H, *brs*-OH, 5-OH)
C-6	98.19	98.16	6.19 (1H, *J* 1.7 Hz, H-6)	6.20(1H,*d*, *J* 2.0 Hz, H-6)
C-7	163.88	163.82		10.16 (1H, 7-OH)
C-8	93.47	93.43	6.40 (1H, *d*, *J* 1.7 Hz, H-8)	6.43(1H, *d*, *J* 2.0 Hz, H-8)
C-9	156.16	156.16		
C-10	103.04	103.00		
C-1'	121.66	121.63		
C-2',6'	129.50	129.40	8.07 (2H, *d*, *J* 8.5 Hz, H-2',6')	8.03(2H, *d*, *J* 8.84 Hz, H -2',6')
C-3',5'	115.43	115.38	6.91 (2H, *d*, *J* 8.5 Hz, H-3',5')	6.92 (2H, *d*, *J* 8.87 Hz, H-3',5')
C-4'	159.18	159.11		9.42 (1H, 4'-OH)

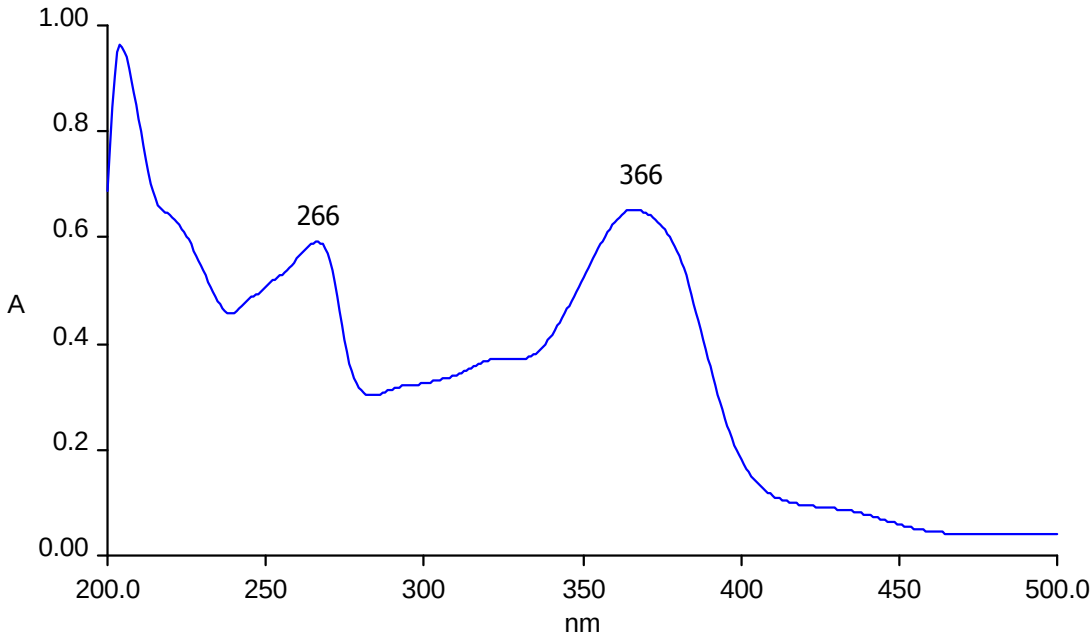

Figure 54 UV spectrum of compound **D** in methanol

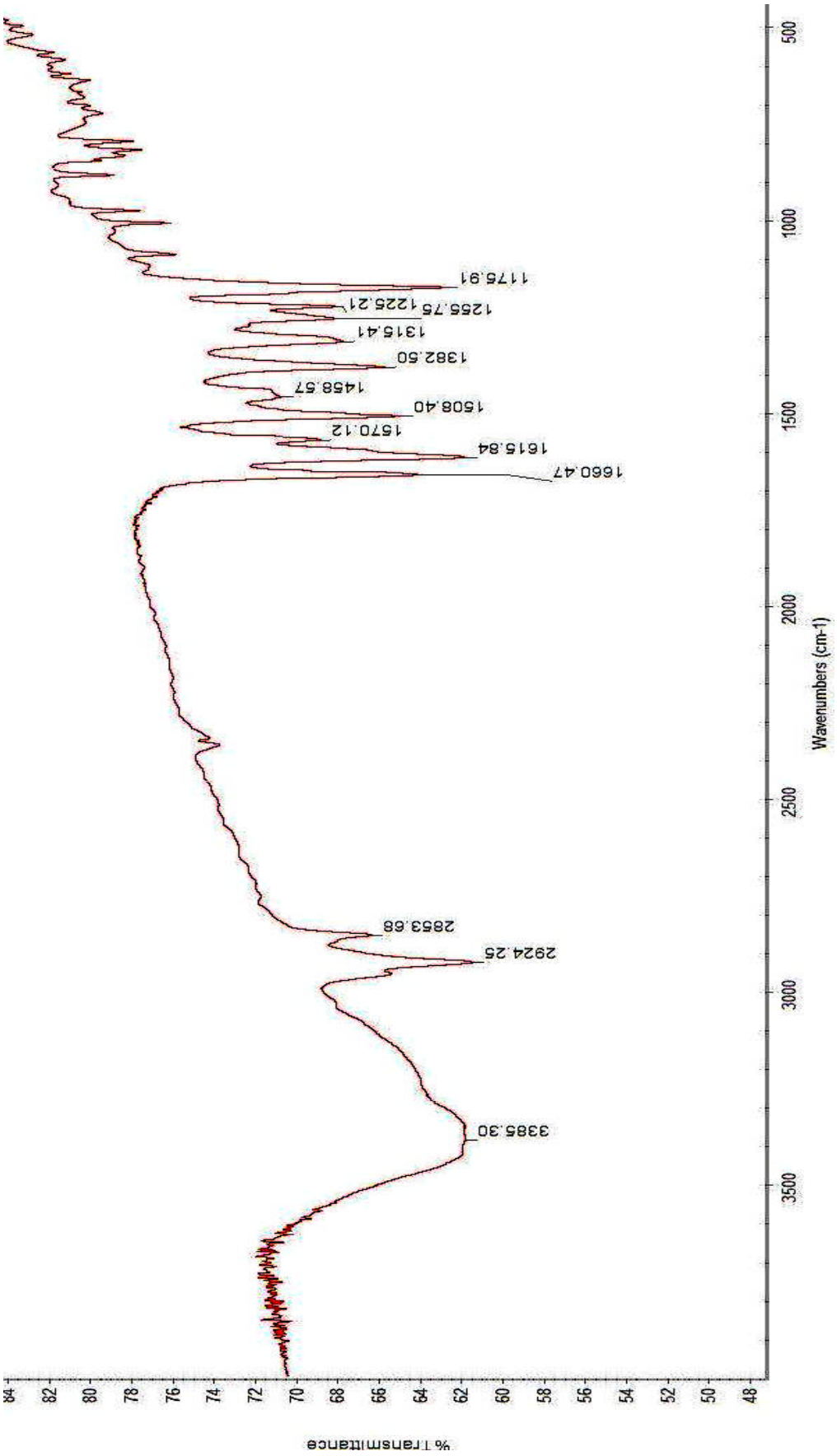

Figure 55 FTIR spectrum of compound **D** (KBr disc)

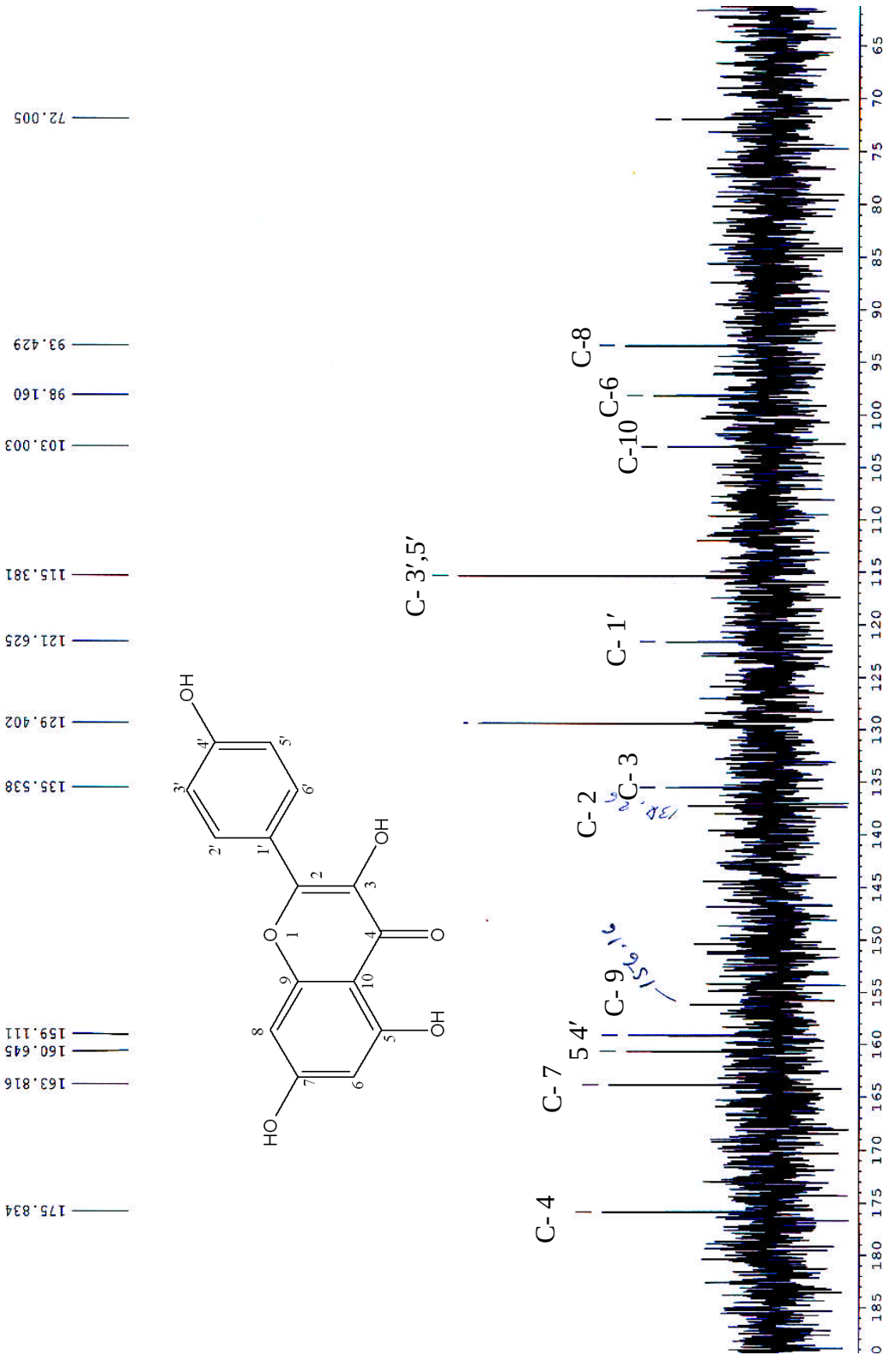

Figure 56 75 MH_Z ^{13}C NMR spectrum of compound **D** in DMSO-d_6

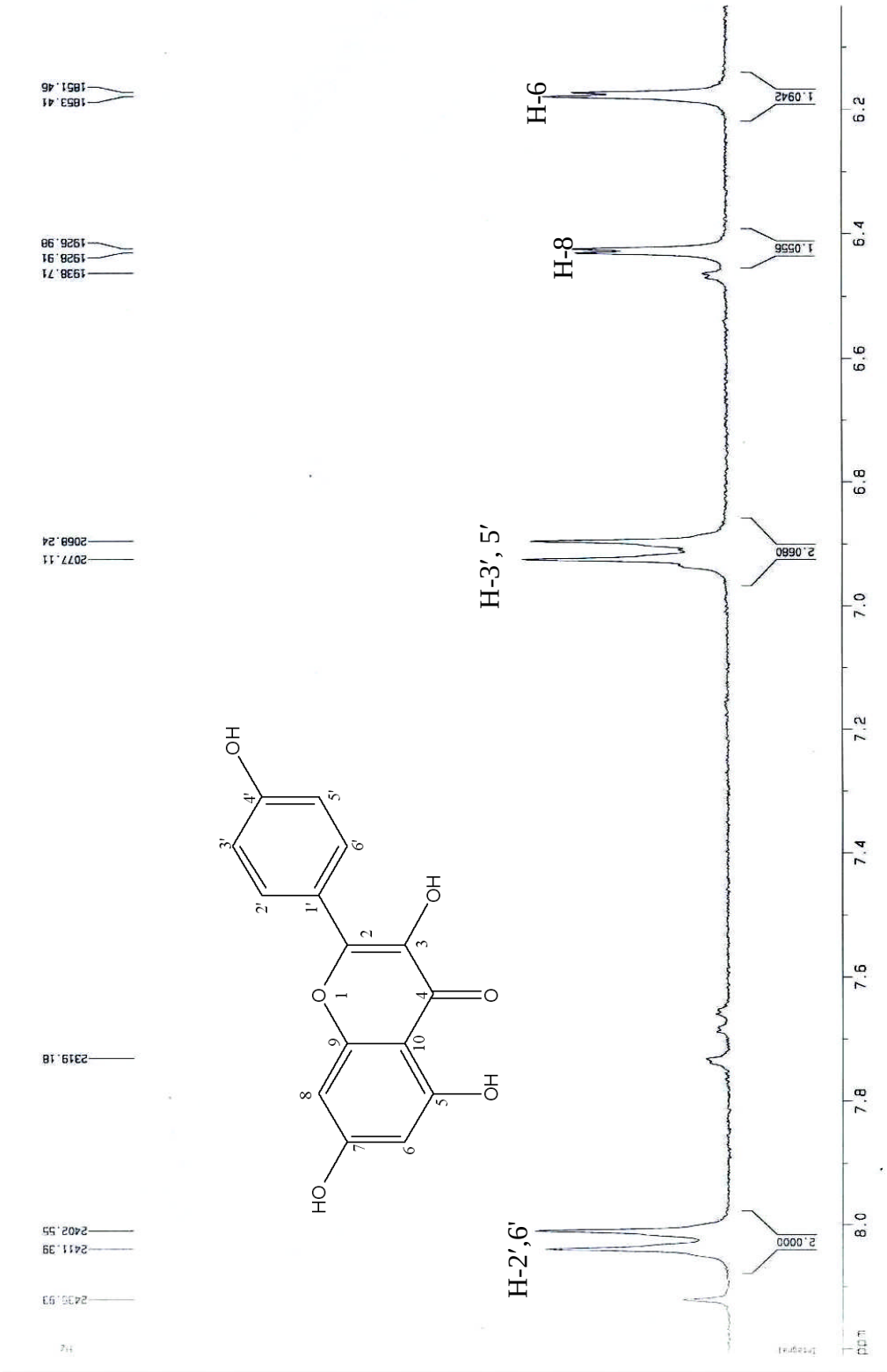

Figure 57 300 MH_Z ^1H NMR spectrum of compound **D** in DMSO-d_6

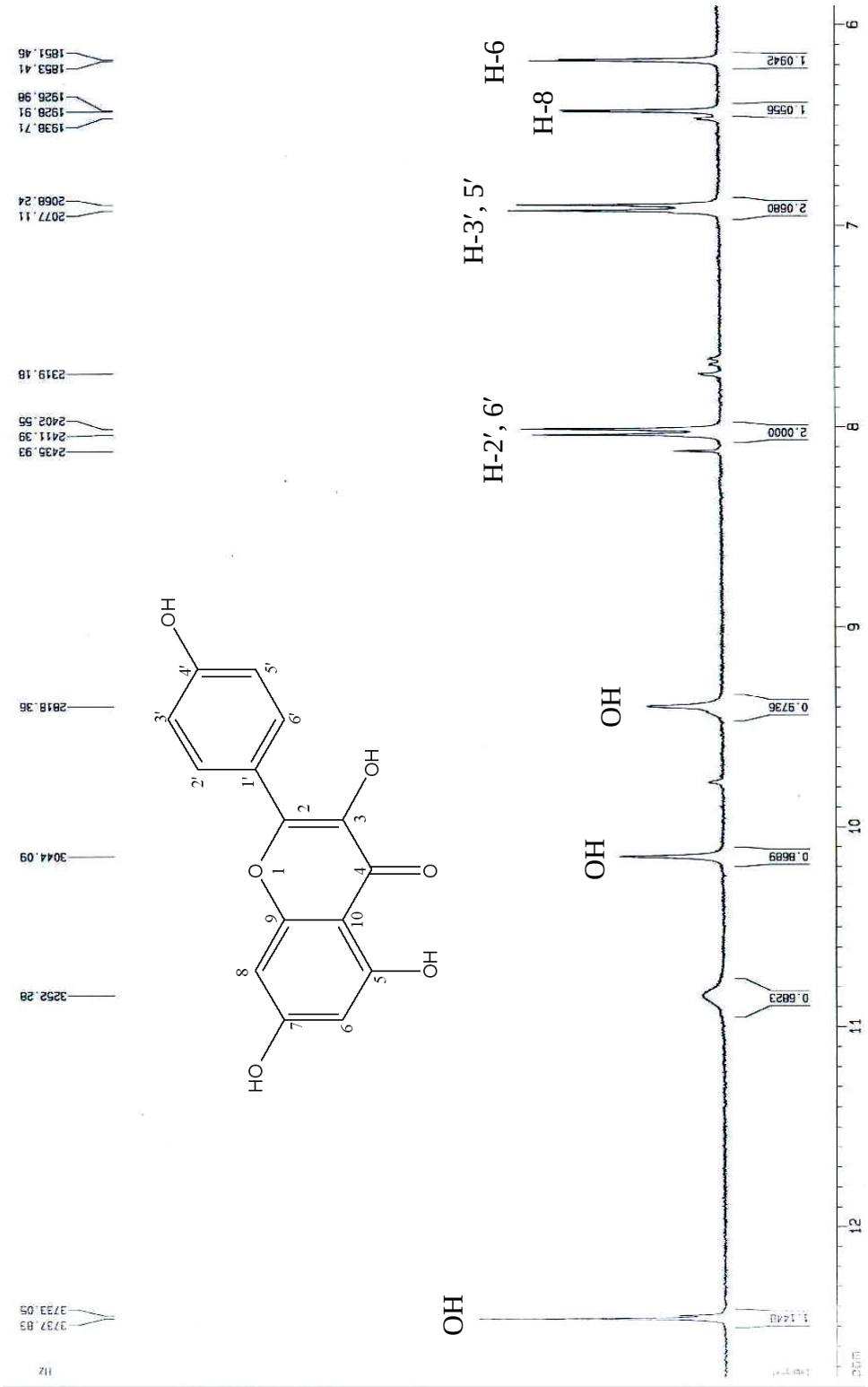

Figure 58 300 MH_Z ^1H NMR spectrum of compound **D** in DMSO-d_6

4.4.5 Compound E

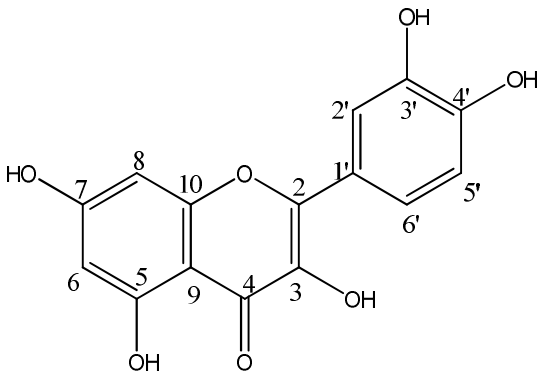

Quercetin

(3,5,6,3',4'-pentahydroxyflavonol)

Compound E appeared as yellow needles with a melting point of 295-305 ºC. The TLC chromatogram of compound D was shown in Figure 27. Its UV spectrum in methanol (Figure 59.) exhibited characteristic aromatic absorption bands at 256 nm (Band I), 375 nm (Band II) indicating the free 3-OH flavonol. The FTIR spectrum in KBr disc (Figure 60.) revealed the vibrations of the hydroxyl group (ν_{OH}) at 3410.83 cm^{-1} and 3295.77 cm^{-1}, carbonyl stretching ($\nu_{C=O}$) at 1671.08, 1613.59 and 1522.98 cm^{-1}.

The ^{13}C-NMR spectral data of the compound D afforded 15 lines as shown in Figures 65-66, indicating a number of carbon atoms in the molecule. The resonance at δ 175.93 indicated a carbonyl group (C=O), while the resonances at δ 161.09, 164.17 ppm were assigned to the quaternary carbons near hydroxyl groups. The downfield shifts at δ 156.83 and 135.82 indicating a 2, 3 unsaturated flavonoid nucleus. The resonances at δ 114.61, 114.84 and 122.75 were assigned to the methine carbons at C-2', C-5' and C-6' positions, respectively. And the other carbons were presented in **Table 16**. According to ^{1}H and ^{13}C-NMR spectral data the molecular formula of compound E was deduced as $C_{15}H_{10}O_7$.

The ^{1}H-NMR spectrum (Figures 61-64) revealed that the proton resonances in the region of 6.17-12.47 ppm. The resonance at δ 6.17 and 6.40 ppm (each, 1H, *d, J* 2.0 *Hz*, H-6, H-8), a pair of doublet signal were attributed to protons positions on the

ring A. The resonance at δ 6.87 ppm belonged to the signal proton at H-5' (1H, *d, J* 8.5 *Hz*), while the resonances at δ 7.53 ppm (1H, *dd, J* 8.5, 2.2 Hz, H-6'), δ7.66 ppm (1H, *d, J* 2.2 Hz, H-2').

The ^{1}H-NMR and ^{13}C-NMR assignment (**Table 16**) was accomplished by comparing the chemical shifts with the literature (118). From the above data, it could be concluded that the structure of compound E was 3,5,6,3',4'-pentahydroxyflavonol (quercetin).

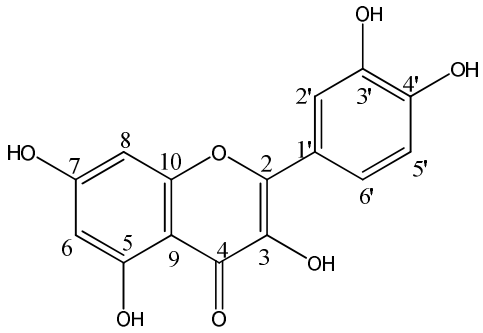

Table 16 500 MHz ^{1}H-NMR and 125^{13}C-NMR spectrum assignment of compound E (in DMSO-d_6) compared with the literature (118)

Carbons / Protons	Lit. ^{13}C	Compound E ^{13}C (in DMSO-d_6)	Lit. ^{1}H (in DMSO-d_6)	Compound D ^{1}H (in DMSO-d_6)
2	155.0	156.83		
3	134.6	135.82		
4	174.7	175.93		
5	159.6	161.09		
6	97.1	97.85	6.22 (1H, *d*, *J* 2.0 Hz)	6.17 (1H, *d*, *J* 2.0 Hz, H-6)
7	162.8	164.17		
8	92.2	93.03	6.44 (1H, *d*, *J* 2.0 Hz)	6.40 (1H, *d*, *J* 2.0 Hz)
9	146.6	147.36		
10	101.9	103.12		
1´	118.9	120.29		
2´	114.0	114.61	7.71 (1H, *d*, *J* 2.2 Hz)	7.66 (1H, *d*, *J* 2.2 Hz)
3´	143.6	144.81		
4´	145.7	146.62		
5´	114.5	114.84	6.92 (1H, *d*, *J* 8.5 Hz)	6.87 (1H, *d*, *J* 8.5 Hz)
6'	120.9	122.75	7.57 (1H, *dd*, *J* 8.5, 2.2 Hz)	7.53 (1H, *dd*, *J* 8.5, 2.2 Hz)

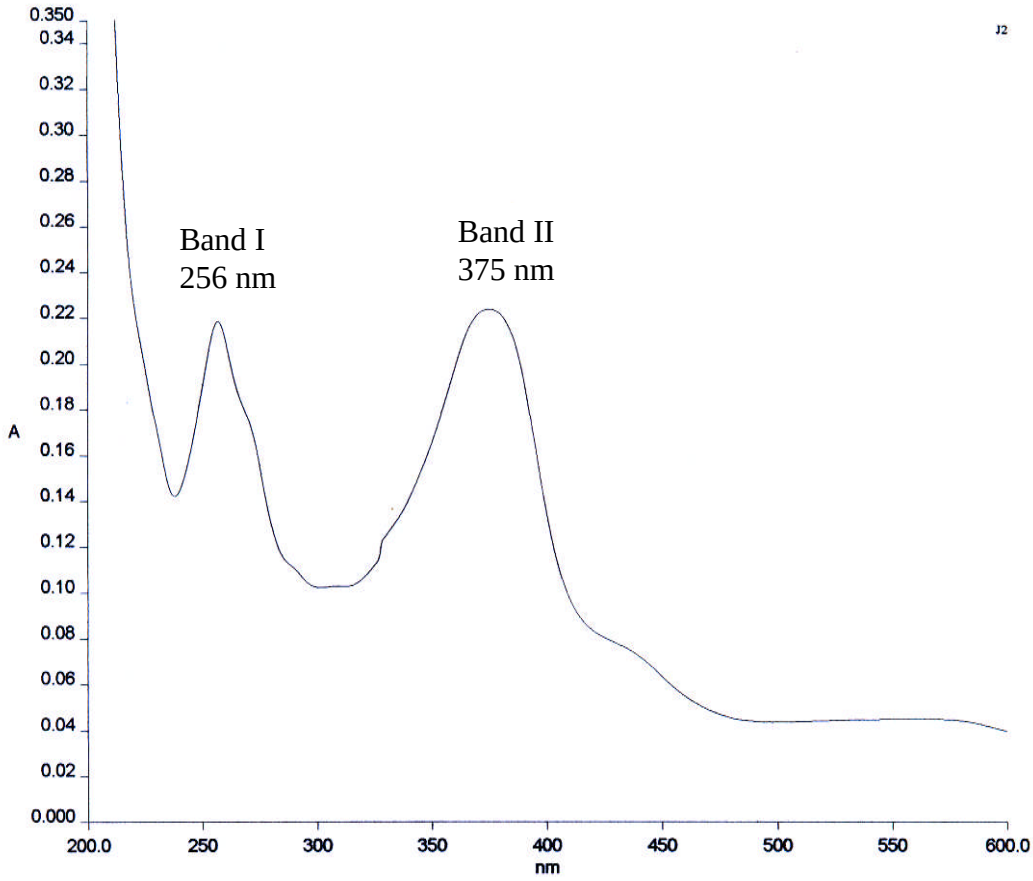

Figure 59 UV spectrum of compound **E** in methanol

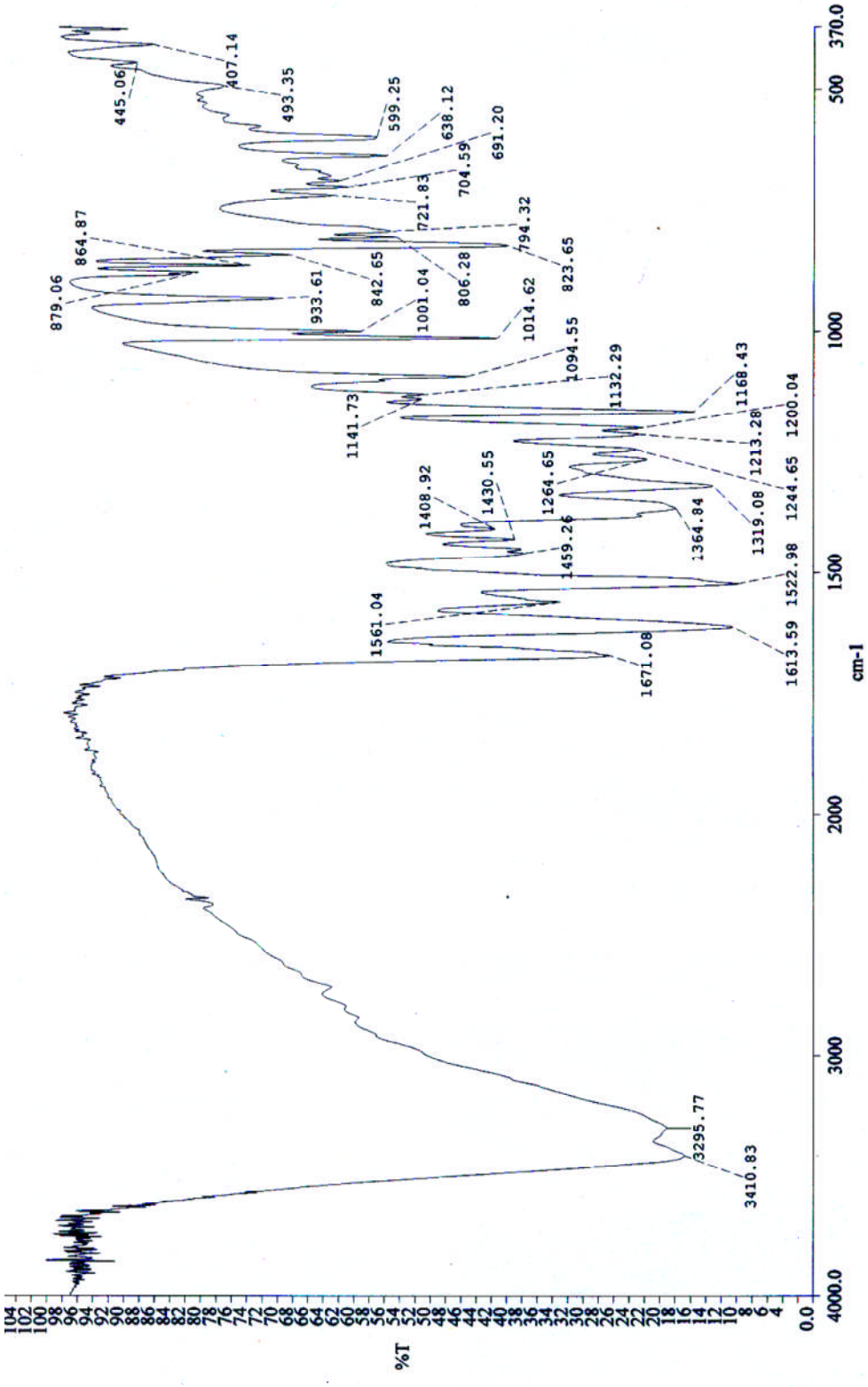

Figure 60 FTIR spectrum of compound **E** (KBr dish)

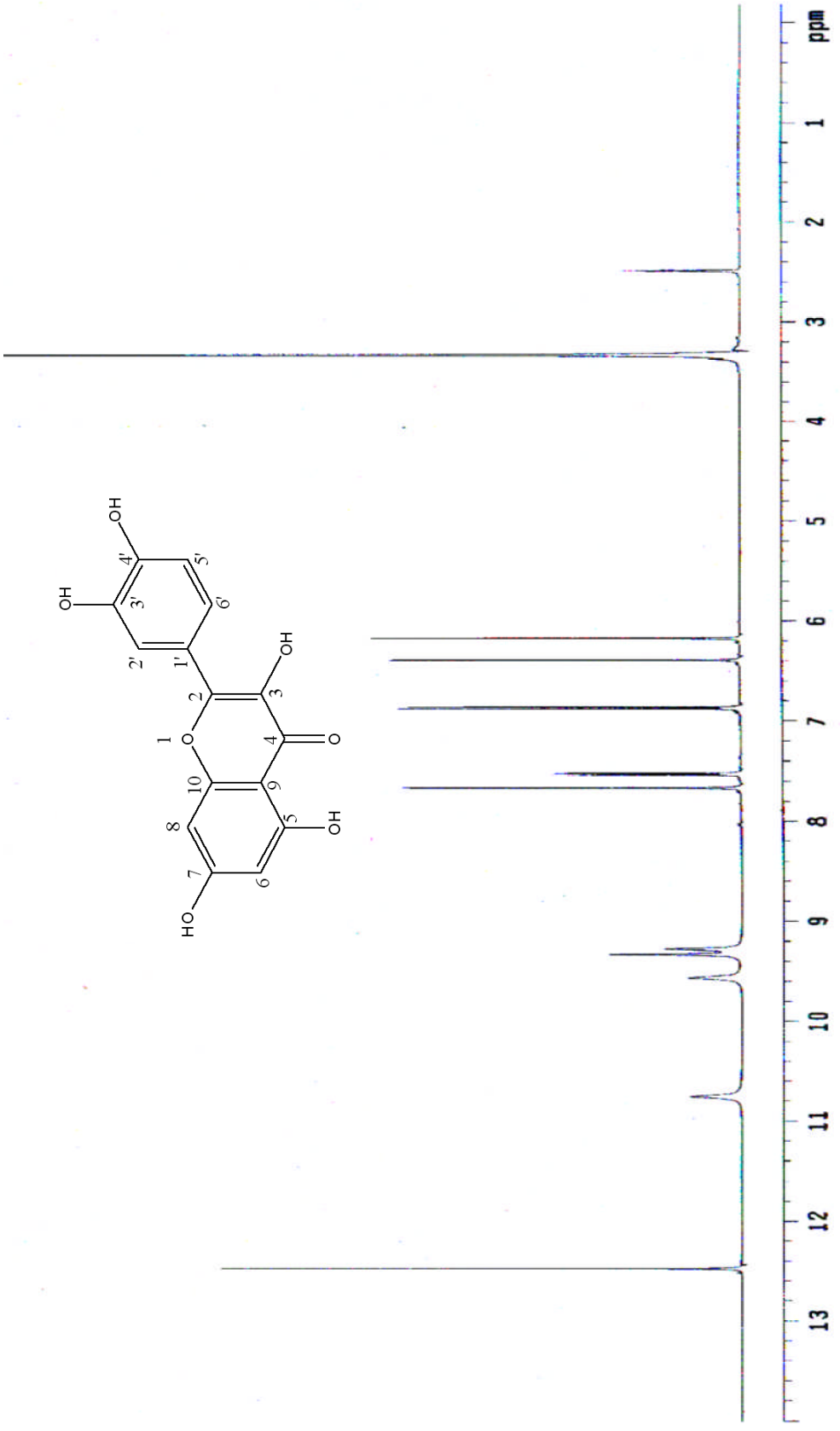

Figure 61 500 ^{1}H-NMR spectrum of compound **E** in DMSO-d_6

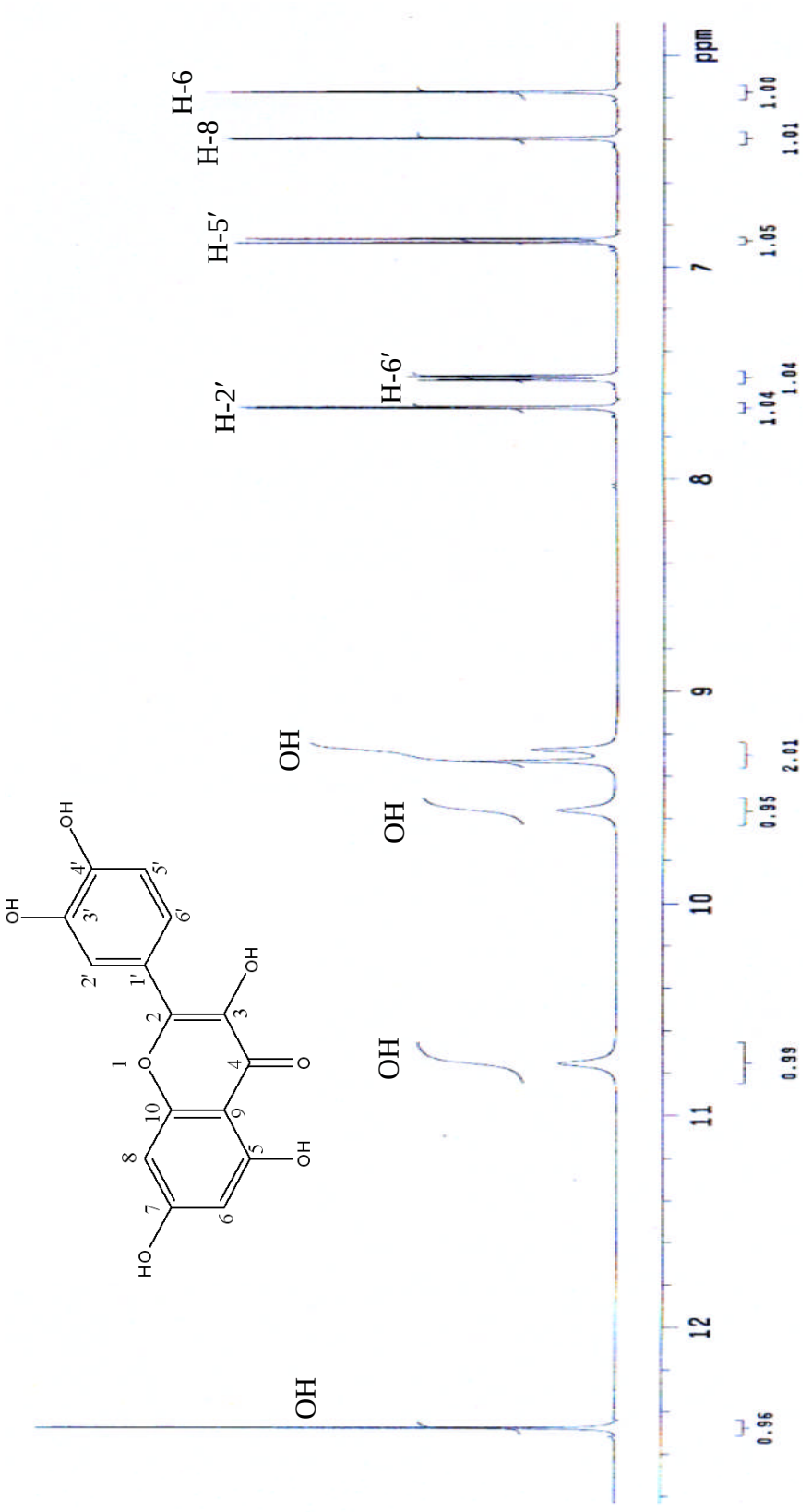

Figure 62 500 ^{1}H-NMR spectrum of compound **E** in DMSO-d_6

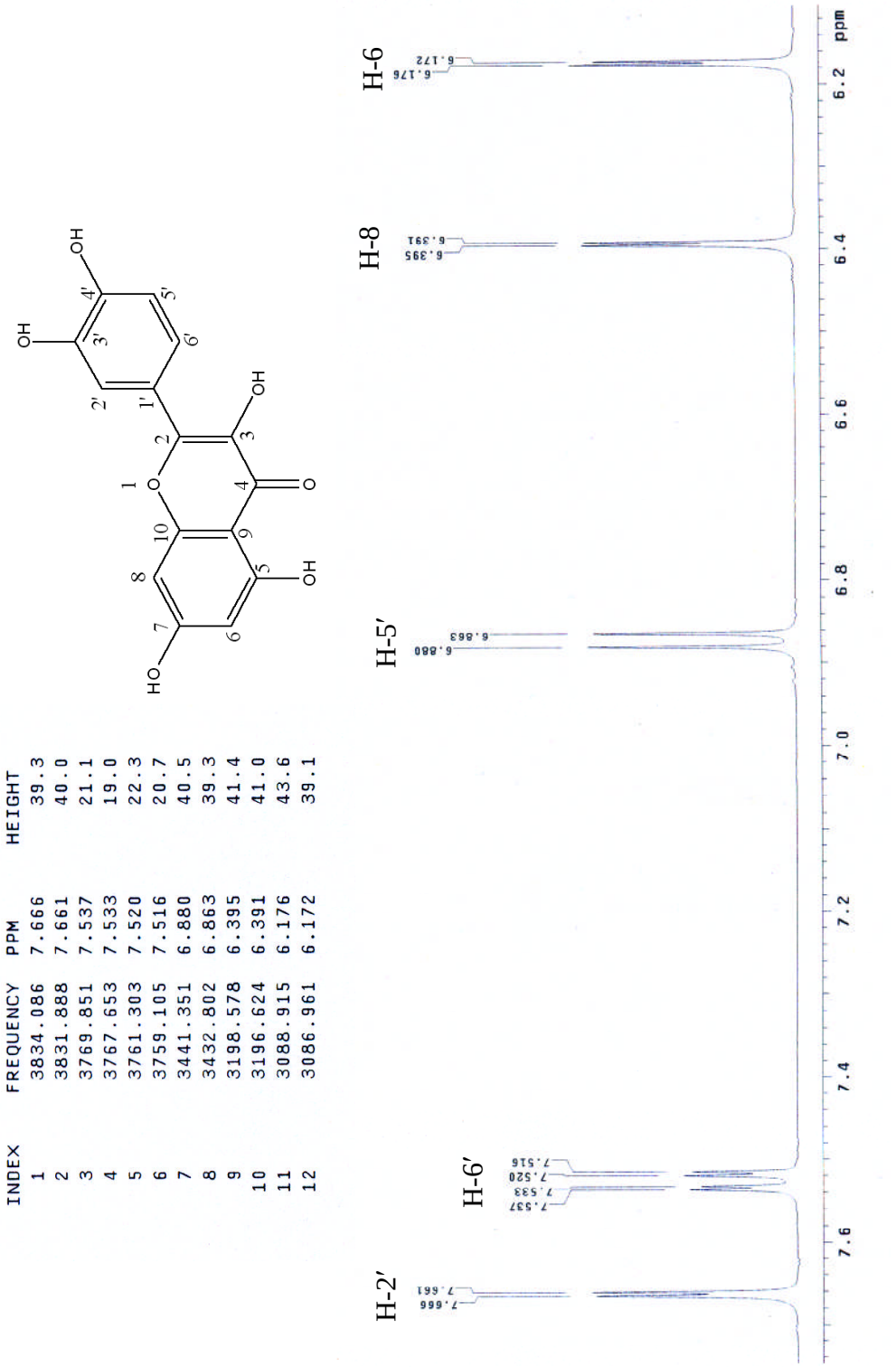

Figure 63 500 MHz ^{1}H-NMR spectrum of compound **E** in DMSO-d_6

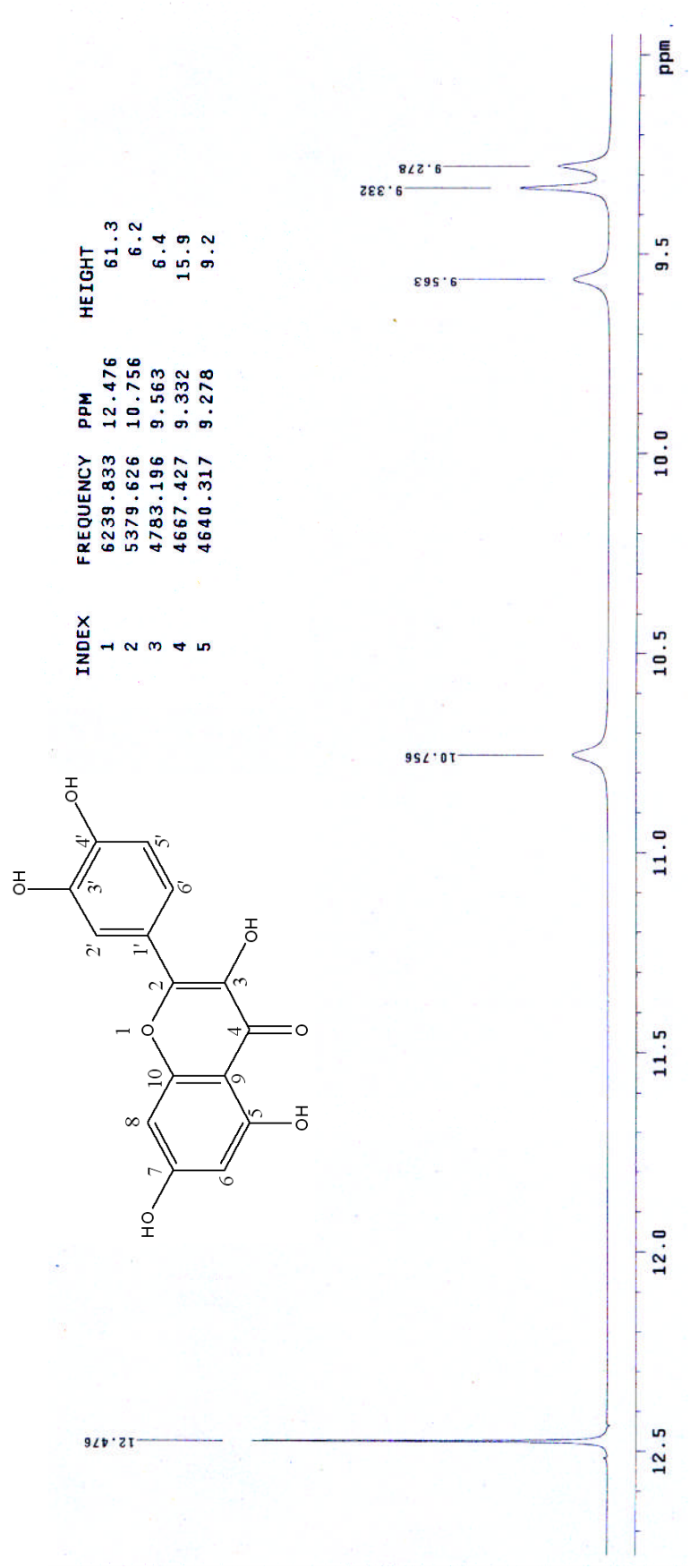

Figure 64 500 ^{1}H-NMR spectrum of compound E in DMSO-d_6

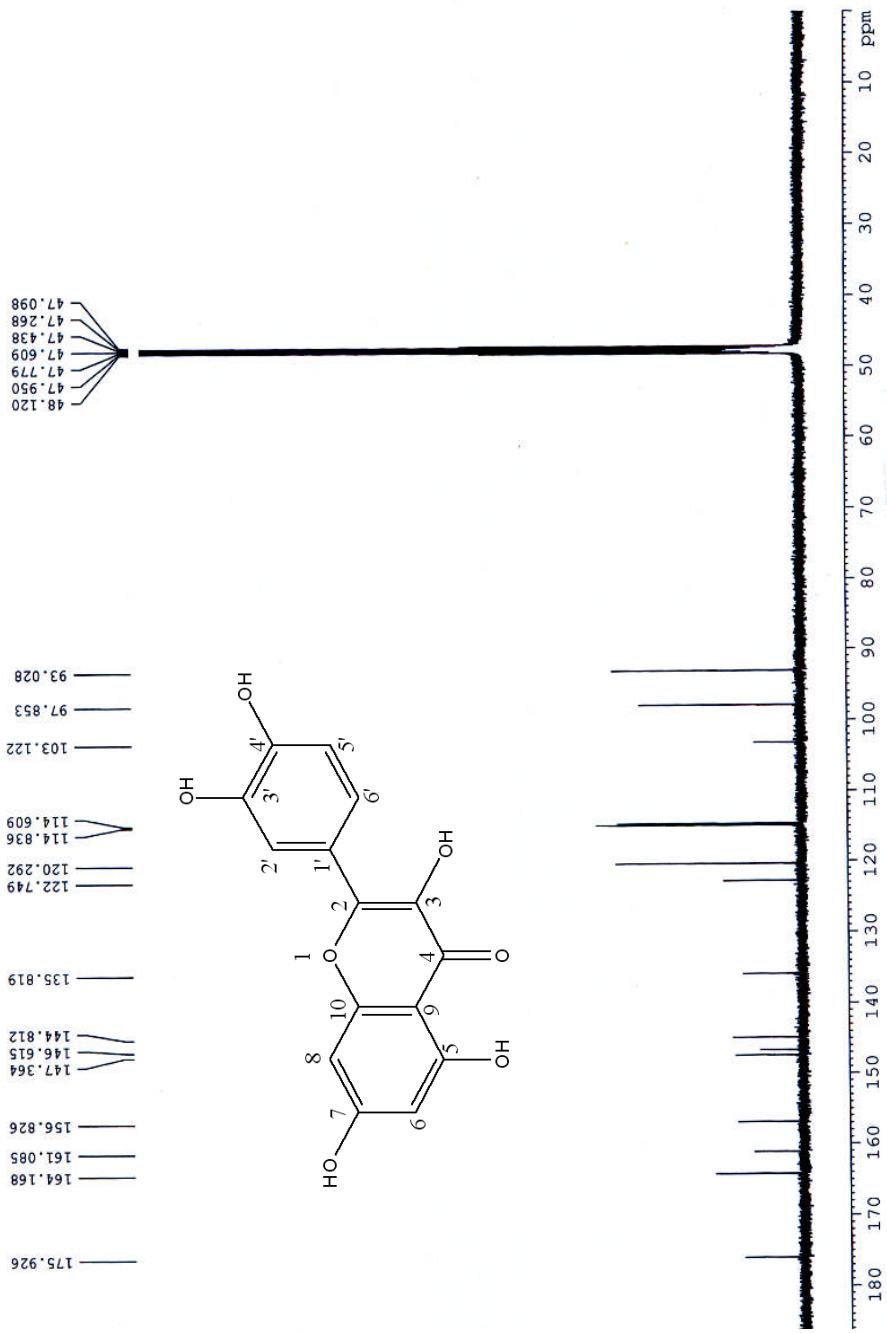

Figure 65 125 MHz ^{13}C-NMR spectrum of compound **E** in DMSO-d_6

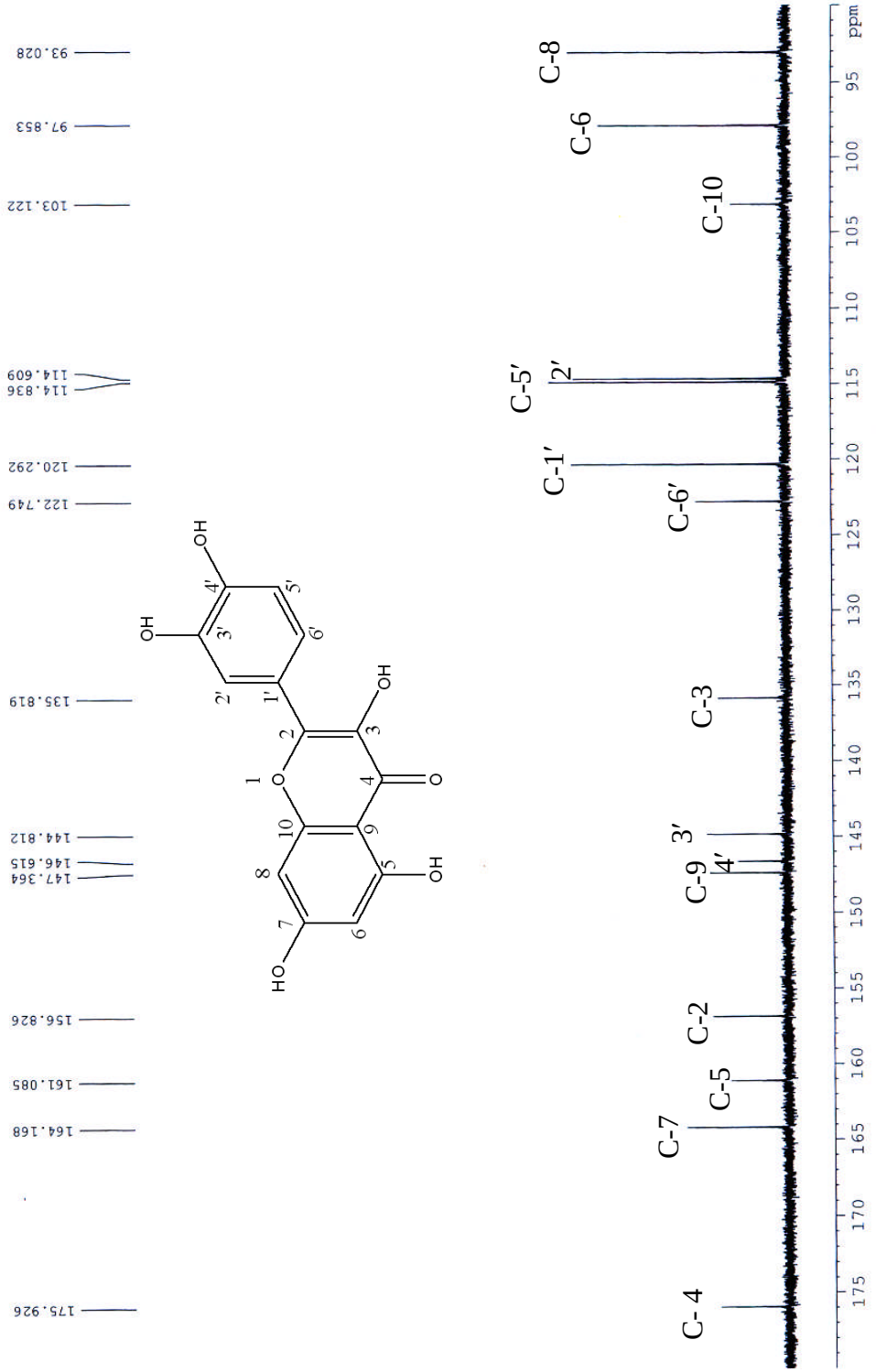

Figure 66 125 MHz ^{13}C-NMR spectrum of compound **E** in DMSO-d_6

4.5 The anti-tyrosinase and free radical scavenging activities of compounds isolated from *Anaxagorea luzonensis*

Phytochemical investigation of *Anaxagorea luzonensis* resulted in the isolation of five compounds. Compound A from the hexane extract and compounds B and C from the dichloromethane extract were identified as xanthone derivatives, while compounds D and E from the ethyl acetate extract were identified as the flavonoid kaempferol and quercetin, respectively. The results of bioactivity test revealed that compounds (**A**), (**B**), (**D**) and (**E**) had strong anti-tyrosinase activity compared to that of kojic acid (IC_{50} 0.197 mM), a well known anti-tyrosinase agent. The results showed that compounds A, B, D and E had IC_{50} values of 1.18, 1.35, 2.49 and 1.56 mM, respectively (**Table 17**). Compounds A and E exhibited the strong scavenging activity toward DPPH radical (ascorbic acid was used as positive control (IC_{50} 3.2 µg/ml)) with IC_{50} values of 5.56 (A), 7.62 (B), 6.94 (D) and 5.30 µM (E). Compound C was shown to be inactive against mushroom tyrosinase and showed little antioxidative activity (**Table 18**).

Table 17 Tyrosinase inhibition activity of compounds isolated from *A .luzonensis*

Compounds of *A.luzonensis* A.Gray	Anti-tyrosinase activity	
	IC_{50}(mg/ml)	IC_{50}(mM)
A	0.405 ± 0.04	1.18 ± 0.12
B	0.444 ± 0.09	1.35 ± 0.27
C	Inactive at conc. 0.91 mg/ml	inactive
D (kaempferol)	0.717 ± 0.03	2.49 ± 0.11
E (quercetin)	0.471 ± 0.24	1.56 ± 0.79
Kojic acid	0.028 ± 0.002	0.197 ± 0.014

Results were means of three measurements ± SD (n =3×3). Kojic acid was used as a positive control.

Table 18 Free radical scavenging activity of compounds isolated from *A. luzonensis*

Compounds of *A.luzonensis* A.Gray	**Free radical scavenging activity**	
	IC_{50}(mg/ml)	IC_{50}(µM)
A	0.0019±0.0005	5.56 ± 1.46
B	0.0025±0.0009	7.62 ± 2.74
C	0.1041±0.0006	379.93 ± 2.19
D (kaempferol)	0.0020±0.0005	6.94 ± 1.74
E (quercetin)	0.0016±0.0005	5.30 ± 1.66
Ascorbic acid	0.0032±0.0002	18.18 ± 1.14

Results were means of three measurements ± SD (*n* =3×3). Ascorbic acid was used as positive control

The structure elucidation of the isolated compounds from *A luzonensis* was accomplished by spectroscopic methods, i.e. UV, IR, MS and NMR spectroscopy. The isolated compounds were identified as follow:

Compound A = 1,6-dihydroxy-5-methoxy-4′,5′-dihydro-4′,4′,5′-trimethyl-furano(2′,3′:3,4)-xanthone which was the 5-methyl ether derivative of compound B. It was first discovered in *Hypericum roeperanum* (109) and was shown to have antifungal activity.

Compound B = 2-deprenyl-rheediaxanthone B (1,5,6-trihydroxy-4′,5′-dihydro-4′,4′,5′-trimethylfurano-(2′,3′:3,4)-xanthone). This compound was found in *Hypericum roeperanum* (109) and *H.japonicum* (112) and also showed antifungal activity.

Compound C = 1,3,6-trihydroxy-5-methoxyxanthone. This compound was isolated from the heartwood of *A. luzonensis* (103), as well as *Canscora decussate* (110) in the family Gentianaceae.

Compound D = kaempferol (3,5,7-trihydroxy-2-(4-hydroxyphenyl)-4H-1-benzopyran-4-one).

Kaempferol was found in the leaves of *Brassica juncea* L (111), *Crocus sativus* L. (115), *Foeniculum vulgare* and *F. dulce* (116), in *Heterotheca inuloides* (117) and other plants. This compound was shown to have antioxidant and anti-tyrosinase activities.

Compound E = quercetin (3,3',4',5,7-pentahydroxyflavone)

Quercetin has been reported to be found in the leaves of *Zanthoxylum piperitum*(118), red onion (*Allium cepa* (119)), *Foeniculum vulgare* and *F. dulce* (116), in *Heterotheca inuloides*(117), *Myrica rubra* (120) as well as in other plant sources. This compound was shown to possess anti-inflammatory, antioxidant and anti-tyrosinase activities.

The results of the in *vitro* anti-tyrosinase activity from the present study suggested that the ethyl acetate and ethanolic extracts of *A.luzonensis* possessed relatively high activity against musroom tyrosinase (> 80% inhibition, Table 6), while the dichloromethane and hexane extracts showed lower activity (58% and 28 % respectively). The hexane extract exhibited the lowest in *vitro* anti-tyrosinase activity (28.56%), but TLC technique showed one active spot against mushroom tyrosinase. Chromatographic separation of this extract, yielded one active compound, compound A, which was a xanthone. The dichloromethane extract afforded two more xanthones derivatives namely compound B and C. Compound B was found to be active against mushroom tyrosinase while compound C was inactive. The ethyl acetate extract, was fractionated using both silica gel and sephadex LH 20 columns to yield large amount of the active compound which was later identified as quercetin. As flavonoids are known to potentiate the activity of anti-tyrosinase agents, it is feasible that they may act synergistically. Summary of the anti-tyrosianse activity of the different extracts and isolated compounds from *A.luzonensis* was shown in **Table 19**.

Table 19 Summary of the anti-tyrosianse activity of the different extracts and isolation compounds from *A.luzonensis*

A. luzonensis Extracts	% Inhibition (at 0.909 mg/ml)	Isolated compounds (yield/mg)	R_f A)	m.p. (°C)	IC_{50} (mM)
Hexane	28.56 ± 0.45	A (10.8)	0.79	221-223	1.18 ± 0.12
Dichloromethane	58.27 ± 0.38	B (39.7)	0.58	211-213	1.35 ± 0.27
		C (1 4.1)	0.49	247-249	inactive
Ethy-acetate	86.76 ± 0.55	C (25.6)	0.49	247-249	Inactive
		D (2.5)	0.45	276-278	2.49 ± 0.11
		E (71.9)	0.28	298-307	1.56 ± 0.79
Ethanol	80.83 ± 0.74	-	-	-	-

A) TLC system = $CHCl_3$: EtOAc : MeOH : formic acid (9: 0.5 :0.5 :0.5)

In all, three xanthones (compounds A, B and C) and two flavonols (compounds D and E) were obtained from the stems of *A.luzonensis*. This is the first time that the study on the anti-tyrosinase activity from *A. luzonensis*, had been carried out. It is also the first report of the anti-tyrosinase activity of the two trimethly-furanoxanthones (compounds A and B) isolated for the first time from *A. luzonensis*. Compound D (kaempferol) and E (quercetin) have already been reported to have anti-tyrosinase activity. Of the five compounds isolated during the course of this study, compound A was the most active, with an IC_{50} of 1.18 mM, followed by compound B (1.35 mM), compound E (quercetin, 1.56 mM) and compound D (kaempferol, 2.49 mM), while compound C was found to be inactive.

From the results of free radical scavenging study, compound A was shown to be the most active with IC_{50} of 5.56 µM, followed by compound E (quercetin), D (kaempferol) and B at 5.30, 6.94 and 7.62 µM, respectively, while compound C was found to be virtually inactive (IC_{50} value of 379.93 µM). However, these compounds were found to have only about one tenth the activity of kojic acid, a compound presently used in the cosmetic industry.

Table 20 Summary of the physical properties and anti-tyrosinase activity of compounds isolated from *A.luzonensis*

Compound	Sttructure	M.W.	m.p. (ºC)	Antityrosianse activity IC_{50} (mM)
A	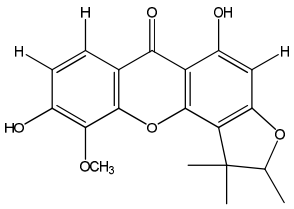	342	221-223	1.18 ± 0.12
B	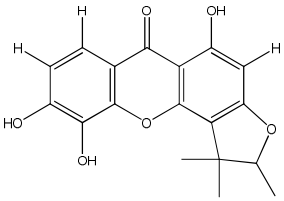	328	211-213	1.35 ± 0.27
C	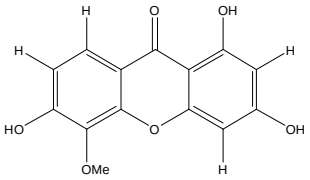	274	247-249	Inactive
D Kaempferol	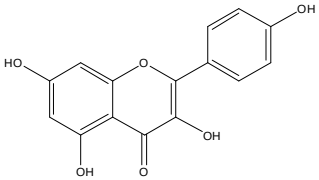	286	276-278	2.49 ± 0.11
E Quercetin	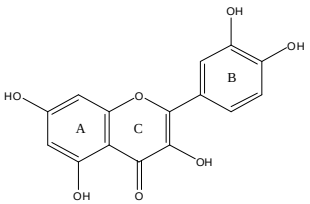	302	298-307	1.56 ± 0.79
Kojic acid	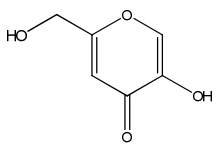	142		0.197 ± 0.014

From previous reports, a number of flavonoids was found to exhibit the anti-tyrosinase activity, with some flavonols acting as copper chelators (117). Quercetin and kaempferol were found to inhibit the oxidation of L-DOPA catalyzed by mushroom tyrosinase. A portion of the structure (3-hydroxy-4-keto moiety) in kaempferol and quercetin, as shown in the bold line, is clearly analogous to kojic acid (IC_{50} = 0.197 mM), a potent tyrosinase inhibitor. The inhibition exerted by kojic acid is well established to come from its ability to chelate the copper atoms in the active sites of the enzyme (117). Kaempferol (IC_{50} = 2.49 mM) and quercetin (IC_{50} = 1.56 mM) have been suggested to inhibit tyrosianse activity by the chelation of copper active sites of the enzyme (115, 117). Extensive studies of the chemical structures of kojic acid kaempferol and quercetin revealed the structure similarity, especially the 3-hydroxy-4-keto moiety which is the important substructure to react with the copper ions of the tyrosinase. In contrast to quercetin, its 3-o-glycosides, isoquercitrin and rutin, were found to behaves as neither inhibitors nor substrate and hence the hydroxyl group at 3-position is likely to relate to the activity. Compound A (IC_{50} = 1.18 mM) and B (IC_{50} = 1.35 mM) had stronger anti-tyrosinase activity against mushroom tyrosinase than quercetin and kaempferol. The inhibition mechanism of the two compounds was also unclear, however the active groups of these compounds are thought to be hydroxyl group as well as the substituted furan ring (2, 3-dihydro-2,3,3-trimethylfuran moiety) which help to increase their inhibition capacity on mushroom tyrosinase. Cudraxanthone M, another furanoxanthone previously isolated from root bark of *Cudrania tricuspidata* (Bounetiaceae and Clusiaceae) was also reported to possess antityrosinase activity with IC_{50} value of 16.5 µM, and appeared to inhibit the polyphenol oxidase activity of tyrosinase in an noncompetitive mode (K_i = 1.6 µM) when L-tyrosine was used as a substrate and kojic acid (IC_{50} value 14.6 µM) as a positive control (91).

Moreover, this study revealed good biological activities of *A.luzonensis* which was shown to contain several constituents of the xanthone and flavonoid groups. Various biological activities, i.e. tyrosinase inhibitory and antioxidant activities are worthy of further study. For example, the browning process in most foods has two components: enzymatic and non-enzymatic oxidation. Hence, potent

antioxidant and tyrosinase inhibitory activity of xanthones and flavonols may render them excellent antibrowning agents. Flavonols are a rare example of tyrosinase inhibitors with antioxidant activity. As safety is of prime concern for an inhibitor to be used in the food industry, there is a constant search for better inhibitors from natural sources as they are largely free of any harmful side effects. Furthermore, the extracts from *A.luzonensis* with tyrosinase inhibitory and antioxidant effects may be of interest to the cosmetic and medicinal industries due to their preventive effects on pigmentation and free-radical disorders.

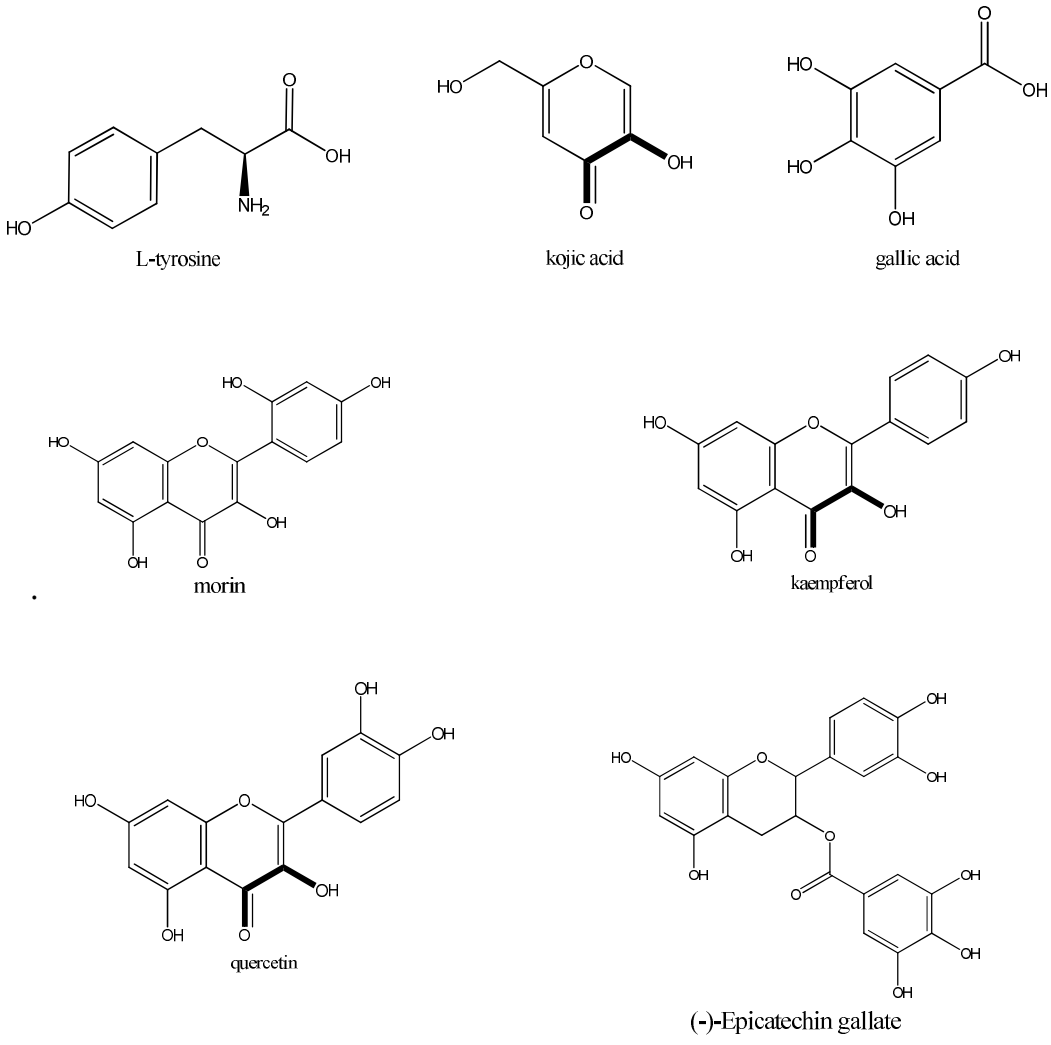

Figure 67 Flavonoids compounds as substrates for tyrosinase and some of the anti-tyrosinase compounds.

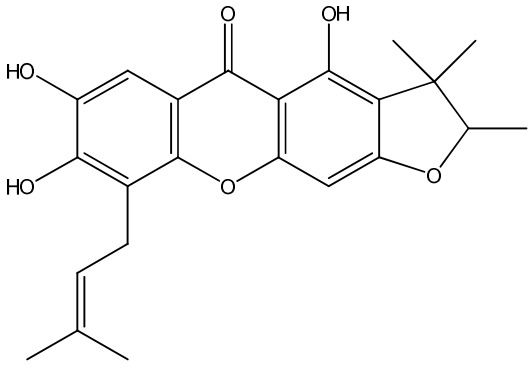

Cudraxanthone M

Figure 67 Flavonoids compounds as substrates for tyrosinase and some of the anti-tyrosinase compounds (cont.)

CHAPTER V
CONCLUSION

A random screening of various plant extracts for the anti-tyrosinase activity revealed that the ethanol extract of the *Anaxagorea luzonensis* A. Gray (Annonaceae) inhibited more than 80% of the mushroom tyrosinase activity. A literature survey of the phytochemistry of this plant indicated the presence of several flavonoids and xanthones with antioxidant activity. Flavonoids are reported to possess a wide range of biological activities.

So far, there has been no report on the anti-tyrosinase activity of *A.luzonensis* (SciFinder, Accessed since November, 2007). Therefore, it was of interest to study *A.luzonensis* as a model for anti tyrosinase and antioxidant agents. The present study was designed to determine the anti tyrosinase and free radical scavenging activities of this plant and to search for active compounds. Crude extracts were fractionated by bioassay-guided chromatographic separation techniques. The anti-tyrosinase and free radical scavenging activities were calculated in terms of % inhibition and comparison was made between different fractions. The structure identification of isolated chemical constituents was performed using spectroscopic techniques. Results from this study are summarized as follows:

5.1. The hexane, dichloromethane and ethyl-acetate extracts of *A.luzonensis* exhibited an anti tyrosinase activity with the percent inhibition of 28.56, 58.27, and 86.76 %, respectively and IC_{50} of 162.70, 10.60, 3.33 µg/ml for free radical scavenging activity, respectively.

5.2. Using bioassay-guided chromatographic separation techniques and spectroscopic techniques, five compounds could be purified, and four bioactive constituents were identified as quercetin, kaempferol, 2-deprenyl-rheediaxanthone B, 1,6-dihydroxy-5-methoxy-4′,5′-dihydro-4′,4′,5′-trimethyl-furano-(2′,3′:3,4)-xanthone while one, 1,3,6-trihydroxy-5-methoxyxanthone was inactive.

5.3. The four bioactive compounds, quercetin, kaempferol, 2-deprenyl-rheediaxanthone B and 1,6-dihydroxy-5-methoxy-4′,5′-dihydro-4′,4′,5′-trimethyl-furano-(2′,3′:3,4)-xanthone isolated from *A.luzonensis*. were investigated for their anti-tyrosinase in comparison with kojic acid and free radical scavenging activities in comparison with ascorbic acid and all four compounds exhibited anti-tyrosinase and free radical scavenging activities with the following affinity: kojic acid (IC_{50} 0.197 mM), 1,6-dihydroxy-5-methoxy-4′,5′-dihydro-4′,4′,5′-trimethyl-furano-(2′,3′:3,4) xanthone (IC_{50} 1.18 mM), > 2-deprenyl-rheediaxanthone B (IC_{50} 1.35 mM), > quercetin (IC_{50} 1.56 mM), > kaempferol (IC_{50} 2.49 mM), an IC_{50} of free radical scavenging activity: 5.56, 7.62, 5.30 and 6.94 µM, respectively.

5.4. Results from this present study revealed that the extracts from *A.luzonensis*, has a high potential for further development as a tyrosianse inhibitor with free radical scavenging activity for the application in the pharmaceutical and cosmeceutical fields.

REFFERENCES

1. Prota G. Progress in the chemistry of melanins and related metabolites. Med. Res. Rev. 1988, 8**:** 525–556.
2. Spritz R. A. and Hearing V. J. Jr. Genetic disorders of pigmentation. Adv. Hum. Genet, 1994, 22**,** 1–45.
3. Frenk, E. Treatment of melasma with depigmenting agents. In: Melasma: New Approaches to treatment. Martin Dunitz Ltd., London, 1995, pp. 9–15.
4. Aroca P. Garcia-Borrh J. Solano F. & Lozano J. Regulation of mammalian melanogenesis 1: partial purification and characterization of a dopachrome converting factor: dopachrome tautomerase, Biochim. Biophys. Actu, 1990, 1035**,** 266-275.
5. Battyani, Z**.,** Xerri, L., Hassoun, J., Bonerandi, J. & Grob, J. Tyrosinase gene expression in human tissues, Pigment Cell Res, 1993, 6, 400-405.
6. ปิยะ เฉลิมกลิ่น, พรรณไม้วงศ์กระดังงา, สำนักพิมพ์บ้านและสวน กรุงเทพฯ (2545) หน้า 44.
7. T.B. Fitzpatrictk, M. Seiji, D. Mcgugan. Medical progress: Melanin pigmentation. The New AEngland Journal of Medicine 1961; 265, 17 : 328-332.
8. Friedman M. Food browning and its prevention: an overview. J. Agric. Food Chem. 1996, 44, 631–653.
9. Shoukat Parvez1, Moonkyu Kang, Hwan-Suck Chung. Survey and mechanism of skin depigmenting and lightening agents. Phytother res, 2006, 20, 921–934.
10. Pawelek J.M. and Körner A.M. The biosynthesis of mammalian melanin. AMSCA, 1982, 70: 136–145.
11. Mayer A. M. Polyphenol oxidases in plants: recent progress. Phytochemistry, 1987, 26: 11–20.
12. Whittaker J. R. In: Food Enzymes, Structure and Mechanism, Wong D. (ed.), Champman and Hall, New York1995, pp 271–307.

13. García-Cánovas F., García-Carmona F., Vera-Sánchez J.,Iborra-Pastor J. L. and Lozano-Teruel J. A. The role of pH in the melanin biosynthesis pathway. J, Biol. Chem, 1982, 257: 8738–8744.
14. Rodríguez-López J. N., Tudela J., Varón R. and García-Cánovas F. Kinetic study on the effect of pH on the melanin biosynthesis pathway. Biochim. Biophys. Acta, 1991, 1076: 379–386.
15. Cooksey C. J., Garratt P. J., Land E. J., Pavel S., Ramsden C.A., Riley P. A. et al. Evidence of the indirect formation of the catecholic intermediate substrate responsible for the autoactivation kinetics of tyrosinase. J. Biol. Chem, 1997, 272, pp 26226–26235.
16. I Kubo, I kuyo, Kinst-Hori. Tyrosinase inhibitors from *anacardium occidentale* fruits. Journal of Natural Products, 1994, Val. 57, NO. 4, pp. 545-551.
17. Narisa Kamkaen, Narong Mulsri and Charoen Treesak. Screening of some tropical vegetables for anti-tyrosinase activity. Thai Pharm Health Sci J, 2007, 2(1):15-19.
18. Barrett F. M. Wound-healing phenoloxidase in larval cuticle of *Calpodes ethulius* (Lepidoptera: Hesperiidae). Can. J. Zool, 1984, 62: 834–838.
19. Sánchez-Ferrer Á, Villalba J and García-Carmona F. Triton X-114 as a tool for purifying spinach polyohenol oxidase. Phytochemistry, 1989, 28, 1321–1325.
20. Sánchez-Ferrer Á., Bru R. and García-Carmona F. Partial purification of a thylakoid-bound enzyme using temperature-induced phase partitioning. Anal. Biochem, 1990, 184: 279–282.
21. Himmelwright R. S., Eickman N. C., Lubein C. D., Solomon E. I. and Lerch K. Chemical and spectroscopic studies of the binuclear copper active site of Neurospora tyrosinase: comparison to hemocyanins. J. Am. Chem. Soc. 1980, 102, 7339– 7344.
22. Solomon E. I., Sundarm U.M. and Machonkin T.E., Mulyicopper oxidases and oxygenase. Chem. Soc. 1996, 96: 2563-2605.
23. Matoba Y, Kumagi, T. *et al*. "Crystallographic evidence that the dinuclear copper center of tyrosinase is flexible during catalysis". J. Biol. Chem, 2006, 281 (13), pp 8981–8990.

24. Sánchez-Ferrer Á, Villalba J and García-Carmona F. Triton X-114 as a tool for purifying spinach polyohenol oxidase. Phytochemistry, 1989, 28, 1321–1325.

25. Solomon E. I., Sundaram U. M. and Machonkin T. E. Multicopper oxidases and oxygenases. Chem. Rev, 1996, 96, 2563– 2605.

26. Mason H. S., Fowlks W. L. and Peterson E. Oxygen transfer and electron transport by the phenolase complex. J. Am. Chem. Soc, 1955, 77, 2914–2915.

27. Nishioka K. Particulate tyrosinase of human malignant melanoma, solubilization purification following trypsin treatment and characterization. Eur. J. Biochem, 1978, 85, 137–146.

28. Lerch K. Primary structure of tyrosinase from *Neurospora crassa*. II. Complete amino acid sequence and chemical structure of a tripeptide containing an unusual thioether. J. Biol. Chem, 1982, 257: 6414–6419.

29. Kwon B. S., Haq A. K., Pomerantz S. H. and Halaban R. Isolation and sequence of a cDNA clone for human tyrosinase that maps at the mouse c-albino locus. Proc. Natl. Acad. Sci. USA 1987, 84: 7473–7477.

30. Kupper U., Niedermann D. M., Travaglini G. and Lerch K, Isolation and characterization of the tyrosinase gene from *Neurospora crassa*. J. Biol. Chem. 1989, 264: 17250–17258.

31. Oetting W. S. and King R. A. Molecular basis of oculocutaneous albinism. J. Invest. Dermatol, 1994, 103: 131S–136S.

32. Robb D. A. Lontie R.(ed). In: Copper Proteins and Copper Enzymes. CRC Press, Boca Raton, FL, 1984, vol. 2, pp. 207.

33. Barrett F. M. Binnigton K. and Retnakaram A. (eds). In: Physiology of the Insect Epidermis, CISRO, East Melbourne, Australia, 1991, pp. 195.

34. Schoot Uiterkamp A. J. M. Monomer and magnetic dipole-coupled Cu^{2+} EPR signals in nitrosylhemocyanin. FEBS Lett, 1972, 20: 93–96.

35. Hepp AF, Himmelwright RS, Eickman NC and Solomon EI. Ligand displacement reactions of oxyhemocyanin: comparison of reactivities of arthropods and mollusks. Biochem. Biophys. Res. Commun. 1979, 89, 1050–1057.

36. Himmelwright RS, Eickman NC, Lubein CD and Solomon E.I. Chemical and spectroscopic comparison of the binuclear copper active site of mollusc and arthropod hemocyanins. J. Am. Chem. Soc. 1980, 102: 5378–5388.

37. Volbeda A. and Hol W. G. Crystal structure of hexameric haemocyanin from *Panulirus interruptus* refined at 3.2 A resolution. J. Mol. Biol. 1989, 209: 249–279.

38. Magnus K. A., Hazes B., Ton-That H., Bonaventura C., Bonaventura J. and Hol W. G. Crystallographic analysis of oxygenated and deoxygenated states of arthropod hemocyanin shows unusual differences. Proteins 19, 1994, 302–309.

39. Lerch K. In: Metal Ions in Biological Systems, Sigel H. (ed.), Marcel Dekker, New York.1981, pp. 143–186.

40. Wilcox DE., Porras AG., Hwang YT, Lerch K., Winkler M. E. and Solomon EI. Substrate analogue binding to the coupled binuclear copper active site in tyrosinase. J. Am. Chem. Soc, 1985, 107: 4015–4027.

41. Sánchez-Ferrer Á, Rodríguez-López JN, García-Cánovas F and García-Carmona F. Tyrosinase: a comprehensive review of its mechanism. Biochim. Biophys. Acta, 1995, 1247: 1–11.

42. Himmelwright RS, Eickman NC and Solomon EI. Reactions and interconversion of met and dimer hemocyanin. Biochem. Biophys. Res. Commun, 1979, 86: 628–634.

43. Solomon E. I. In: Copper Proteins. Spiro T. G. (ed.), Wiley-Interscience, New York. vol. III, 1981, pp. 41–108.

44. Kim Y. J., Chung J. E., Kurisawa M., Uyama H. and KobayashiS. New tyrosinase inhibitors, (+)-catechin–aldehydepolycondensates, Biomacro-molecules, 2004, 5: 474–479.

45. Jackman M. P., Hajnal A. and Lerch K. Albino mutants of *Streptomyces glaucescens* tyrosinase. Biochem, 1991, J**.** 274**:** 707–713.

46. Van Gelder C. W. G., Flurkey W. H. and Wichers H. J. Sequence and structural features of plant and fungal tyrosinase. Phytochemistry, 1997, 45: 1309–1323

47. Sarin Tadtong1, Amornrat Viriyaroj1, Suwanna etc. Antityrosinase and antibacterial activities of *mangosteen pericarp* extract. J Healtb Res 2009, 23(2): 99-102.

48. Burton S. G. Biocatalysis with polyphenol oxidase: a review. Catal. Today 1994, 22, 459–487.

49. Sanjust E, Cecchini G, Sollai F, Curreli N and Rescigno. A. 3-Hydroxykynurenine as a substrate/activator for mushroom tyrosinase. Arch. Biochem. Biophys, 2003, 412, 272– 278.

50. Laskin J. D and Piccinini L. A. Tyrosinase isozyme heterogeneity in differentiating B16/C3 melanoma. J. Biol. Chem. 1986, 261, pp 16626–16635.

51. Cabanes J., García-Cánovas F., Lozano J. A. and García-Carmona F. A kinetic study of the melanization pathway between L-tyrosine and dopachrome. Biochem, Biophys, Acta, 1987, 923: 187–195.

52. Ros J. R., Rodríguez-López J. N. and García-Cánovas F. Effect of ferrous ions on the monophenolase activity of tyrosinase. Biochim. Biophys. Acta, 1993, 1163: 303–308.

53. Fenoll L. G., Rodríguez-López J. N., García-Sevilla F., García- Ruiz P. A., Varón R., García-Cánovas F. et al. Analysis and interpretation of the action mechanism of mushroom tyrosinase on monophenols and diphenols generating highly unstable *o*-quinones. Biochim. Biophys. Acta, 2001, 15, 48, 1–22.

54. Prota G. In: Melanins and Melanigenesis. Academic Press, New York, 1992, 90, pp. 1–2.

55. Ito S. Biochemistry and physiological of melanin in pigmentation and pigmentary disorders, Levine N. (ed.), CRC Press, Boca Raton, FL, 1993, pp. 33–59.

56. Hirobe T. Control of melanocyte proliferation and differentiation in the mouse epidermis. J. Invest. Dermatol, 1991, 5:1–11.

57. Hearing V. J. and King R. A. Determinants of skin color melanocytes and melanization in: pigmentation and pigmentary abnormalities, levine N. (ed.), CRC Press, New York, 1993, pp. 3–32.

58. Kobayashi T., Vieira W. D., Protterf B., Sakai C. and Imokawa G. Modulation of melanogenic protein expression during the switch from eu- to pheomelanogenesis. J. Cell Sci, 1995, 108: 2301–2309.
59. Brun A. and Rosset R. Etude. Electrochemical deoxidation dihydroxy-3,4 phenylalanine (Dopa). Chem, 1974, 49, 287–300.
60. Pawelek JM. After dopachrome pigment cell. Res, 1991, 4: 53–62.
61. Aroca P, García-Borrón JC, Solano F and Lozano JA. Regulation of mammalian melanogenesis I partial purification and characterization of a dopachrome converting factor dopachrome tautomerase. Biochim. Biophys. Acta, 1990, 1035, 266–275.
62. Lambert C., Chacon J. N., Chedekel M. R., Land E. J., Riley P. A., Thompson A. et al. A pulse radiolysis investigation of the oxidation of indolic melanin precursors: evidence for indolequinones and subsequent intermediates. Biochim. Biophys. Acta, 1989, 993: 12–20.
63. Sugumaran M. and Semesi V. Quinone methide as a new intermediate in eumelanin biosynthesis. J. Biol. Chem. 1991, 266, 6073–6078.
64. J.B. Wilkinson, R.J. Moore. Harry's casmeticology. 7th ed. George Godwin, 1982.
65. United States Food and Drug, Administration skin bleaching drug products for over-the-counter product use; Proposed Rule Docket 2006, 1978N-0065 (Report).
66. Urabe K, Hori Y. Dyschromatosis. Semin Cutan Med Surg, 1997, 16, 81–85.
67. Lyon CC, Beck MH. Contact hypersensitivity to monobenzyl ether of hydro-quinone used to treat vitiligo. Contact Dermatitis, 1998, 39, 132–133.
68. Oakley AM. Rapid repigmentation after depigmentation therapy vitiligo treated with monobenzyl ether of hydroquinone. Austr J Dermatol, 1996, 37: 96–98.
69. Kasraee B, Handjani F, Aslani FS.. Enhancement of the depigmenting effect of hydroquinone and 4-hydroxyanisole by all-trans-retinoic acid (tretinoin): the impairment of glutathione-dependent cytoprotection. Dermatology, 2003, 206: 289–291.
70. Ikuyo Hori, Ken-ichi Nihei and Isao Kubo. Structural Criteria for depigmenting Mechanism of arbutin. *Phytother. Res*, 2004, 18, 475–479.

71. Maeda K., Naganuma M., Fukuda M., Matsunaga J., Tomita Y.: Effect of pituitary and ovarian hormones on human melanocytes in vitro. Pigment Cell Res, 1996, 9, 204-212.

72. Hurrell R. F. and Finot P. A. Nutritional consequences of the reactions between proteins and oxidized polyphenolic acids. Adv. Exp. Med. Biol. 1984, 177: 423–435.

73. Deshpande S. S., Sathe S. K. and Salunkhe D. K. Chemistry and safety of plant polyphenols. In: Nutritional and Toxicological Aspects of Food Safety, Friedman M. (ed.), Plenum, New York, 1984, pp 457–495.

74. Martinez M. V. and Whitaker J. R. The biochemistry and control of enzymatic browning. Trends Food Sci. Technol, 1995, 6, 195–200.

75. Wong D. W. S. Mechanism and Theory in Food Chemistry, AVI-Van Nostrand Reinhold, New York, 1989.

76. Route-Mayer M. A., Ralambosa J. and Philippon J. Roles of *o*-quinones and their polymers in the enzymic browning of apples. Phytochemistry, 1990, 29, 435–440.

77. Fulcrand H., Cheminat A., Brouillard R. and Cheynier V. Characterization of compounds obtained by chemical oxidation of caffeic acid in acidic conditions. Phytochemistry, 1994, 35: 499–505.

78. Friedman M. and Bautista F. Inactivation of polyphenol oxidase by thiols in the absence and presence of potato tissue suspensions. J. Agric. Food Chem, 1995, 43: 69–76.

79. Dao L. and Friedman M. Chrologenic acid content of fresh and processed potatoes determined by ultraviolet spectrophotometry. J. Agric. Food Chem, 1992, 40: 2152–2156.

80. Sapers G. M. Browning of foods: control by sulfites, antioxidants and other means. Food Technol. 1993, 10: 75–84.

81. Y.-J. Kima and H. Uyama. Tyrosinase inhibitors from natural and synthetic sources: structure, inhibition mechanism and perspective for the future, CMLS, Cell. Mol. Life Sci, 2005, 62 1707–1723.

82. Parejo J, Viladomat F, Bastida J, Rosas-Romero A, Flerlage N, Burllo J, and Codina C. Comparison between the radical scavenging activity and

antioxidant activity of six distilled and non-distilled Mediterraneen herbs and aromatic plants. J. Agric. Food Chem. 2002, 50, p 6882-6890.

83. Badria F. A. and El Gayyar M. A. A new type of tyrosinase inhibitors from natural products as potential treatments for hyperpigmentation. Boll, Chim. Farma, 2001, 140, 267–271.
84. Parrish F. W., Wiley B. J., Simmons E. G. and Long L. Jr Production of afla-toxins and kojic acid by species of *Aspergillus* and *Penicillium*. Appl. Microbiol, 1966, 14, 139.
85. Wiley J. W., Tyson G. N. and Steller J. S.The configuration of complex kojates formed with some transition elements as determined by magnetic susceptibility measurements. J. Am. Chem. Soc, 1942, 64**:** 963–964.
86. Niwa Y. and Akamatsu H. Kojic acid scavenges free radicals while potentiating leukocyte functions including free radical generation. Inflammation, 1991, 15: 303–315.
87. Hider R. C. and Lerch K.The inhibition of tyrosinase by pyridinones. Biochem. J. 1989, 257: 289–290.
88. Tanaka T., Takeuch M. and Ichishima E. Inhibition study tyrosinase from *Aspergillus oryzae*. Agric. Biol, Chem. 1989, 53**:** 557–558.
89. Chen J. S., Wei C. I. and Marshall M. R. Inhibition mechanism of kojic acid on polyphenol oxidase. J. Agric. Food Chem, 1991, 39**:** 1897–1901.
90. Chen J. S., Wei C. I., Rolle R. S., Otwell W. S., Balaban M. O. and Marshall M. R. Inhibitory effect of kojic acid onsome plant and crustacean polyphenol oxidases. J. Agric. Food Chem. 1991, 39**:** 1396–1401.
91. Sang Seok, Eun Jin Seo, Hoi Yong Kim,ect. Tyrosinase inhibitiry xanthones from *cudrania tricuspidata*. Journal of lift science, 2007, vol 17, No.4, 476-481.
92. Kurtzman, C.P., Fell, J.W. "Yeast Systematics and Phylogeny-Implications of Molecular Identification Methods for Studies in Ecology", Biodiversity and Ecophysiology of Yeasts, The Yeast Handbook, 2006.
93. Kahn V. Effect of kojic acid on the oxidation of DL-DOPA, norepinephrine and dopamine by mushroom tyrosinase. Pigment Cell Res. 1995, 8: 234–240.
94. Kahn V. and Zakin V. Effect of kojic acid on the oxidation of trihydroxyphenols by mushroom tyrosinase. J. Food Biochem. 1995, 18**,** 427–443.

95. Goetghebeur M and Kermasha S. Inhibition of polyphenol oxidase by copper-metallothionein from *aspergillus niger*. Phytochemistry, 1996, 42**,** 935–94.

96. Madhosingh C. and Sundberg L. Purification and properties of tyrosinase inhibitor from mushroom. FEBS Lett, 1974, 49: 156–158.

97. Espín J. C., Jolivet S. and Wichers H. J. Inhibition of mushroom polyphenol oxidase by agaritine. J. Agric. Food Chem, 1998, 46**,** 2976–2980.

98. Zhivko A Velkov, Mikhail K Kolev and Alia V Tadjer. Modelling and statistical analysis of DPPH scavenging activity of phenolics. Czech Chem, 2007, Vol. 72, No. 11, pp. 1461–1471.

99. E.D Merrill, A flora of Manila, vol.I p 205-206.

100. Wongsatit Chuakul, Ampol Boonpleng, Ubonwan Boonpleng. *Anaxagorea javanica* Blume var. *tripetala* Corner (ANNONACEAE), newly discovery from Thailand.Thai Journal of Phytopharmacy, 2005, Vol.12 (1) June.

101. H.N. Didley, J. Hutchinsion. The flora of the Maley Peninsula, vol I, p-62.

102. Byong Won Lee, Jin Hwan Lee, Sung-Tae Lee. Antioxidant and cytotoxic activities of xanthones from Cudrania tricuspidata. Bioorganic & Medicinal Chemistry Letters, 2005, 15 5548–5552.

103. Ryoko Gonda, Tadahiro Takeda and Toshiyuki Akiyama. Studies on the Constituents of *Anaxagorea luzonensis* A. Gray. Chem. Pharm. Bull. 2000, 48(8) 1219-1222.

104. Kiattisak Saeio1, Songwut Yotsawimonwat1 and Siriporn Okonogi1. Tyrosinase Inhibitory and Antioxidant Activities of Essential Oil from Thai Spices 1*Department of Pharmaceutical Sciences, Faculty of Pharmacy, Chiang Mai University, Chiang Mai*.

105. Sakulna Wangthong, IIhum Tonsiripakdee, Thitinun Monhaphol. Post TLC developing technique for tyrosinase inhibitor detection, Biomedical chromatography, 2007, 21: p 94-100.

106. Likhitwitayawuid K. and Sritularak B. A new dimeric stilbene with tyrosinase inhibittory activity from *Artocarpus gomerzianus*. J.Nat. Prod. 2001; 64, 1457-1459.

107. Ravishankara MN, Shrivastava N, Padh H, and Rajani M. Evaluation of antioxidant properties of root bark of *Hemidesmus indicus* R. Br. (*Anantmul*) Phytomedicine; 2002, 9: p153-160.

108. Bao-Qiong Chen a, Xiang-Yu Cui, Antioxidative and acute anti-inflammatory effects of Torreya grandis Fitoterapia 2006, 77, p 262–267.

109. Guido Rath, Olivier Potterat,Stephen Mavi and Kurt Hostettmann, Xanthone from *Hypericum Roperranum*, Phytochemistry, 1996, Vol. 43, No. 2, p. 513-520.

110. S. Ghosal, R.K. Chaudhuri, and A. Nath ; Chemical Constituent of Gentianaceae IV : New Xanthones of *Canscora decussate*. Journal of Pharmaceutical Sciences Vol.62, No1, January 1973 pp 137-139.

111. Jung Eun Kim 1, Mee Jung Jung 1, Hyun Ah Jung ; A New Kaempferol 7-O-Triglucoside from the Leaves of *Brassica juncea* L; Arch Pharm Res 2002, Vol 25, No 5, 621-624.

112. Qing-Li Wu, Sheng-Ping Wang, Li-Jun Du, Jun-Shan Yang and Pei-Gen Xiao. Xanthones from *Hypericum Japonicum* and *H.Hendyi*. Phytochemistry, 1998, Vol 49, No 5, pp 1395-1402.

113. I. Kubo. Y. Yokokawa, I. Kinst-Hori. Tyrosinase inhibiting flavonol glycosides from *Buddleia coriacea*. Phytochemistry 1992; 31(3): 1075-1077.

114. K. Likhitwitayawuid, B.Sritularak, W. De-Eknamkul. Tyrosinase inhibitors from *Artocapus gomezianus*. Planta Medica, 2000; 66: 275-277.

115. I. Kubo, I Kinst-Hori. Flavonols from saffron flower: tyrosinase inhibitory activity and inhibition mechanism. J Agric Food Chem, 1999, 47, 4121-4125.

116. Fathy M, Soliman, Afaf H, Shehata, Amal E, Khaleel and Shahera M Ezzat. An acylated kaempferol glycoside from flowers of *foeniculum vulgare* and *f. Dulce*. Molecules, 2002, 7, p 245-251.

117. Isao Kubo, I Kinst-Hori, Swapan K. Chaudhuri, Yumi Kubo. Flavonols from *Heterotheca inuloides*: Tyrosinase Inhibitory Activity and Structural Criteria. Bioorganic and Medicinal Chemistry, 2000, 8, 1749- 1755.

118. Chang Ho Jeong and Ki Hwan Shim. Tyrosinase Inhibitor Isolated from the leaves of *zanthoxylum piperitum*. Biosci, Biotecnol, Biochem, 68, 9, 1984-1987, 2004.

119. Torgils Fossen, Atle T TLE T. Pedersen and Oyvind M. Andersen. Flavonoids from red onion (*Allium cepa*). Phytochemistry, 1998, Vol. 47, No. 2, pp. 281-285.

120. I. Kubo. In: P.A. Hedin, R.M. Hollingworth, E.P. Masler, J. Miyamoto, D.G. Thompson Tyrosinase inhibitors from plants. Phytochemicals for pest control. ed. ACS publishing; 1997. p. 311-326.

121. Chia-Ying Li, E-Jian Lee, and Tian-Shung Wu. Antityrosinase Principles and Constituents of the Petals of *Crocus sativus*, J. Nat. Prod, 2004, 67 (3), 437-440.

122. I. Kubo. Y. Yokokawa, I. Kinst-Hori. Tyrosinase inhibiting flavonol glycosides from *Buddleia coriacea*. Phytochemistry 1992; 31(3): 1075-1077.

123. K. Shimizu, R. Kondo, K. Sakai, S.H. Lee, H. Sato. The inhibitory components from *Artocapus incisus* on melanin biosynthesis. Planta medica, 1998; 64: 408-412.

124. N.H Shin, S.Y Ryu, E.J. Choi, S.H.Kang, I.M. Chang, K.R. Min, et al. Oxyresveratrol as the potent inhibitor on Dopa oxidase activity of mushroom tyrosinase. Biochem Biophys Res Comm, 1998; 243 : 801-803.

125. K.Inda, K.Shimomura, S. Sudo,S. Kadota, T. Namba. Potent inhibitors of tyrosinase activity and melanin biosynthesis from *Rheum officinale*. Planta Medica 1995; 61: 425-428.

126. I. Kubo, I Kinst-Hori, Y. Yokokawa. Tyrosinase inhibitors from *Anacardium occidentale fruits*. J Nat Prod 1994; 57 (4) :545-551.

127. N. Okamura, N. Hine, S. Harada, T. Fujioka, K. Mihashi, A Yagi. Three chromone components from *Aloe vara* leaves. Phytochemistry 1996; 43(2): 495-498.

128. Isao Kubo, Ikuyo Kinst-Hori,Swapan K. Chaudhuri, Yumi Kubo,Yolanda Sanchez and Tetsuya Ogura. Flavonols from Heterotheca inuloides: Tyrosinase Inhibitory Activity and Structural Criteria. Bioorganic & Medicinal Chemistry 8 (2000) 1749-1755.

129. Jongsung Lee, Eunsun Jung, Junho Park, Kwangseon Jung, Eunkyung Park. Glycyrrhizin Induces Melanogenesis by Elevating a cAMP Level in B16 Melanoma Cells. J Invest Dermatol, 2005, 124:405 –411.

130. Sang Hee Lee , Sang Yoon Chol, Hocheol KIM, Jae Sung HWANG, Byeong Gon Lee,Jian Jun GAO, and Sun Yeou KIM. Mulberroside F Isolated from the Leaves of *Morus alba* Inhibits Melanin Biosynthesis. *Biol. Pharm. Bull.*, 2002, 1045, 25(8) 1045-1048.

131. No JK., Soung DY, Kim YJ, Shim KH, Jun YS, Rhee SH, Yokozawa T, ChungHY. Inhibition of tyrosinase by green tea components. Life Sci. 1999, 65, 241-246.

132. Tomonori M. Development of new skin whitening agents. Inhibition of alpha-MSH-induced melanogenesis by *sophorae* radix extract. Fragr J, 2000, 28 **(**9); 38-44.

133. H. Morita, T. Kayashita, H Kobata, A. Gonda, K. Takeya, H. Itokawa. Pseudostellarins A-C, new tyrosinase inhibitory cyclic peptides from *Pseudstellarin heterophylla*. Tetrahedron 1994, 50 (23), pp 6797-6804.

134. I. Kubo, I. Kinst-Hori. Tyrosinase inhibitors from anise oil. J Agric Food, Chem, 1998; 46: 1268-1271.

135. H. Oh, Y. J. Mun, S. J. Im, S.Y. Lee, H.J. Song, H.S. Lee, et al. Cucurbitacins from *Trihosanthes kirilowii* as the inhibitory components on tyrosinase activity and melanin synthesis of B16/F10 melanoma cells. Planta Medica 2002; 68: 832-833.

136. Y. Masamoto, H. Ando, Y. Murata, Y. Shimoshi, M Tada, K. Takahata. Mushroom tyrosinase inhibitory activityof esculetin isolated from seeds of *Euphorbia lathyris* L. Biosci Biotechem 2003; 67(3): 631-634.

APPENDIX

APPENDIX

1. Determination of Tyrosinase activity

SIGMA QUALITY CONTROL TEST PROCEDURE

(Revised : 10/21/98)

Enzymatic Assay of Tyrosinase

Polyphenol Oxidase Activity

(EC 1.14.18.1)

Principle

L-DOPA + O_2 + Ascorbic acid $\xrightarrow{\text{TYR}}$ *O*-Benzoquinone + H_2O + Dehydro-Ascorbic acid

Abbreviations used :

TYR = Tyrosinase

L-DOPA = L-3,4-Dihydroxyphenylalanine

Condition: T = 25 ºC, pH 6.8, A_{265nm} Light path = 1 cm

Method: Continuous Spectrophotometric Rate Determination

Reagent:

A 50 mM Potassium Phosphate Buffer, pH 6.8 at 25 ºC
(Prepare 100 ml in deionized water using potassium phosphate, Monobasic, Anhydrous, Prod. No. P-5379. Adjust to pH 6.8 at 25 ºC with 1M NaOH)

B 5.0 mM L-3,4-Dihydroxyphenylalanine (L-DOPA)
(Prepare 10 ml in reagent A using L- L-3,4-Dihydroxyphenyl-alanine, Prod. No. D-9628.)

C 2.1 mM Ascorbic acid solution
(Prepare 10 ml in reagent A using L-ascorbic Acid, sodium salt, Prod. No. A-7631.)

D 0.065 mM Ethylenediaminetetra acetic acid (EDTA)
(Prepare 10 ml in reagent A using Ethylenediaminetetra acetic acid, disodium, dehydrate salt, stock No. ED2SS.)

E Tyrosinase enzyme solution (PPO)
(Immediately before use, prepare a solution containing 500-1000 u/ml Tyrosinase in reagent A.)

Procedure:

Pipette (in milliliters) the following reagents into suitable quartz cuvettes:

	Test	Blank
Reagent A (Buffer)	2.60	2.80
Reagent B (L-DOPA)	0.10	0.10
Reagent C (Ascorbic acid)	0.10	-
Reagent D (EDTA)	0.10	0.10

Mix by inversion and equilibrate to 25 ºC. Monitor the $A_{265\ nm}$ until constant, using a suitably thermostatted spectrophotometer. Then add:

Reagent E (TYR)	0.10	-

Immediately mix by inversion and record the decrease in $A_{265\ nm}$ for approximately 5 minutes.

Obtain the ΔA_{265nm} / minute using the maximum linear rate for both the Test and Blank.

Calculation:

$$\text{Units/mg Enzyme} = \frac{\Delta A_{265nm} / \text{min Test} - \Delta A_{265nm} / \text{min Blank}) (df)}{(0.001)(0.1)}$$

0.001 = The change in ΔA_{265nm} / min per unit of polyphenol oxidase in a 3.0 ml reaction mixture at pH 6.5 at 25 ºC

0.1 = Volume (in milliliter) of enzyme used

$$\text{Units/mg solid} = \frac{\text{units/ml enzyme}}{\text{mg solid /ml enzyme}}$$

$$\text{Units/mg protein} = \frac{\text{units/ml enzyme}}{\text{mg solid /ml enzyme}}$$

Unit definition:

One unit is equal to a $A_{265\ nm}$ of 0.001 per min at pH 6.5 at 25 ºC in 3 ml reaction mix containing L-DOPA and L-ascorbic acid.

Final assay concentration:

In a 2.92 ml reaction mix, the final concentrations are 50 mM potassium phosphate, 0.17 mM L-3,4-dihydroxyphenylalanine, 0.072 mM ascorbic acid, 0.002 mM ethylenediaminetetra acetic acid, and 50-100 units of tyrosinase.

Notes:

1. All products and stock numbers, unless otherwise indicated are Sigma product and stock number.

Sigma warrants that the above procedure information is currently utilized at Sigma and that Sigma products conform to the information in Sigma publications. Purchaser must determine the suitability of the information and products for its particular use. Upon purchase of Sigma products, see reverse side of invoice or packing slip for additional terms and conditions of sale.

2. Spectral of compound A, B, C, D and E.

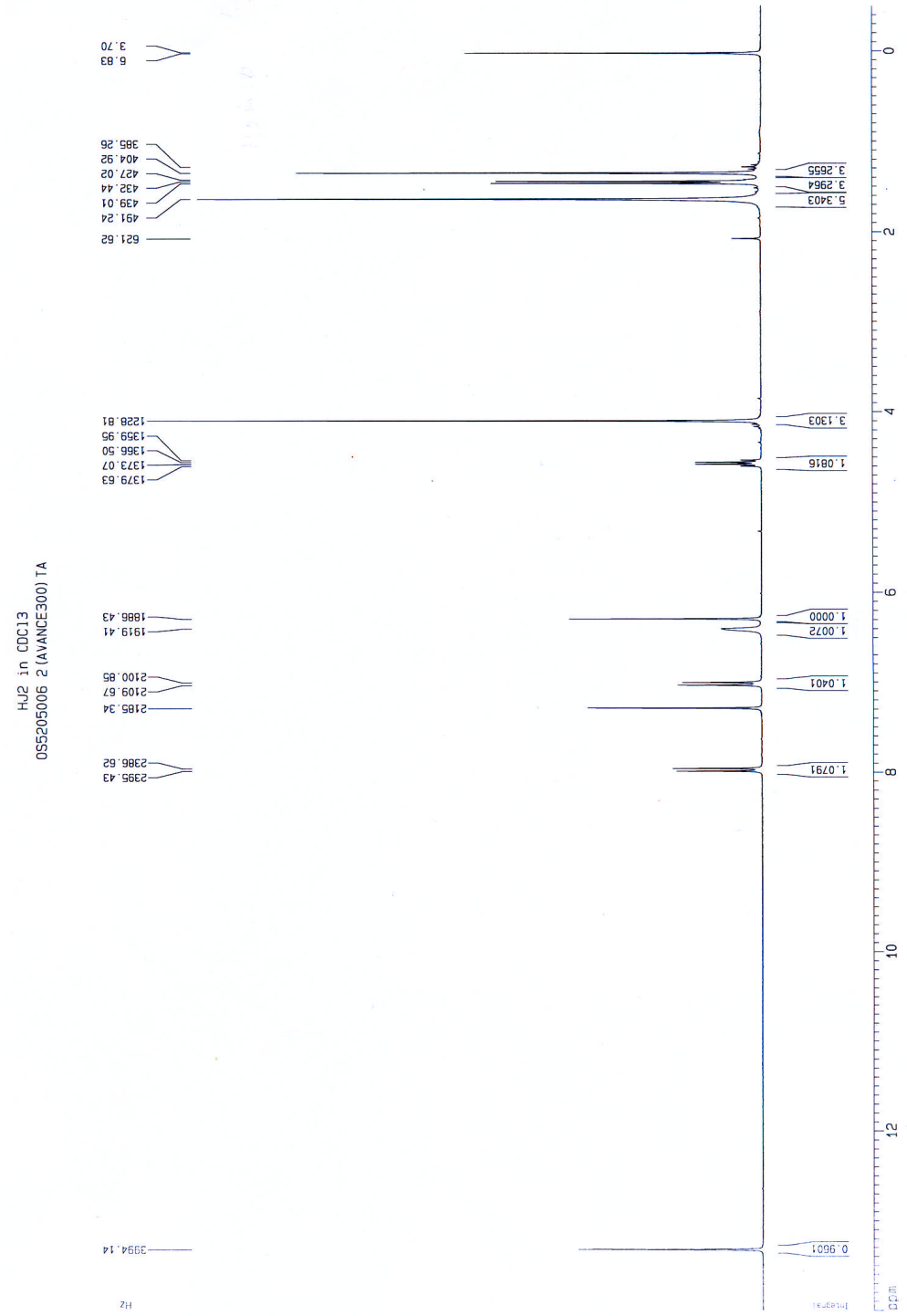

Fig. 300MHz ^{1}H-NMR spectrum of compound **A** in $CDCl_3$

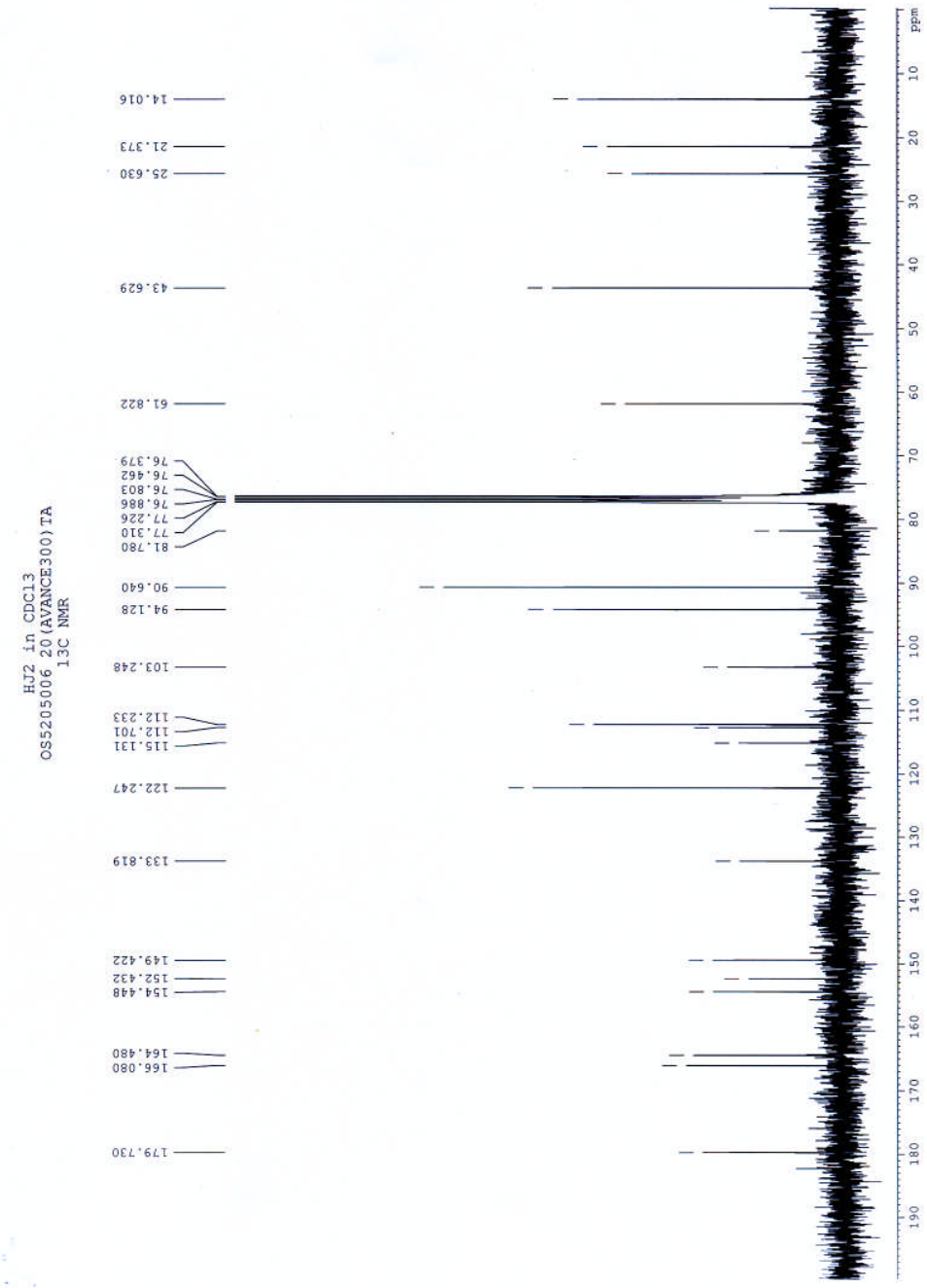

Fig. 75 MHz ^{13}C-NMR spectrum of compound **A** in $CDCl_3$

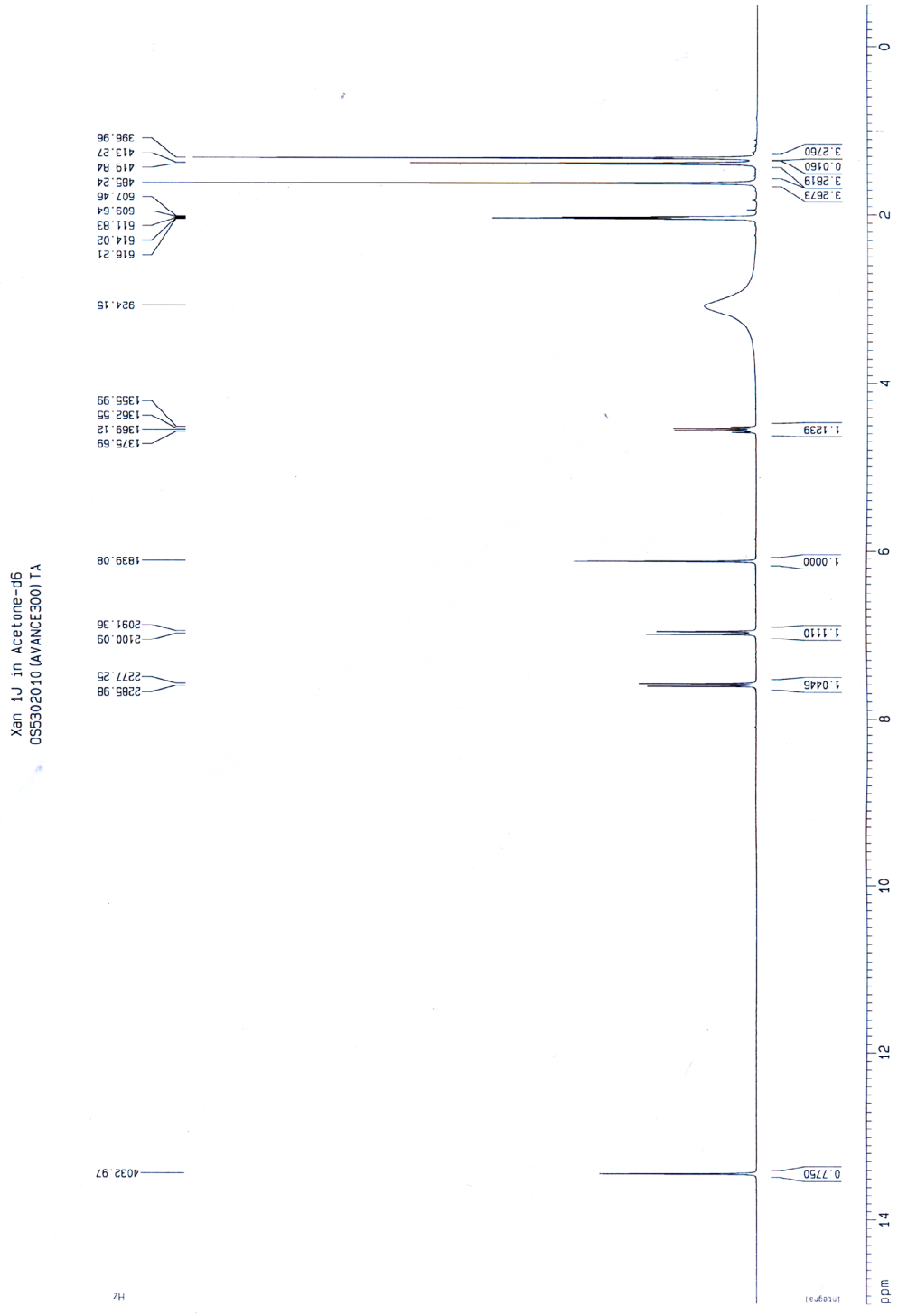

Fig. 300 MHz ^{1}H-NMR spectrum of compound **B** in acetone-d_6

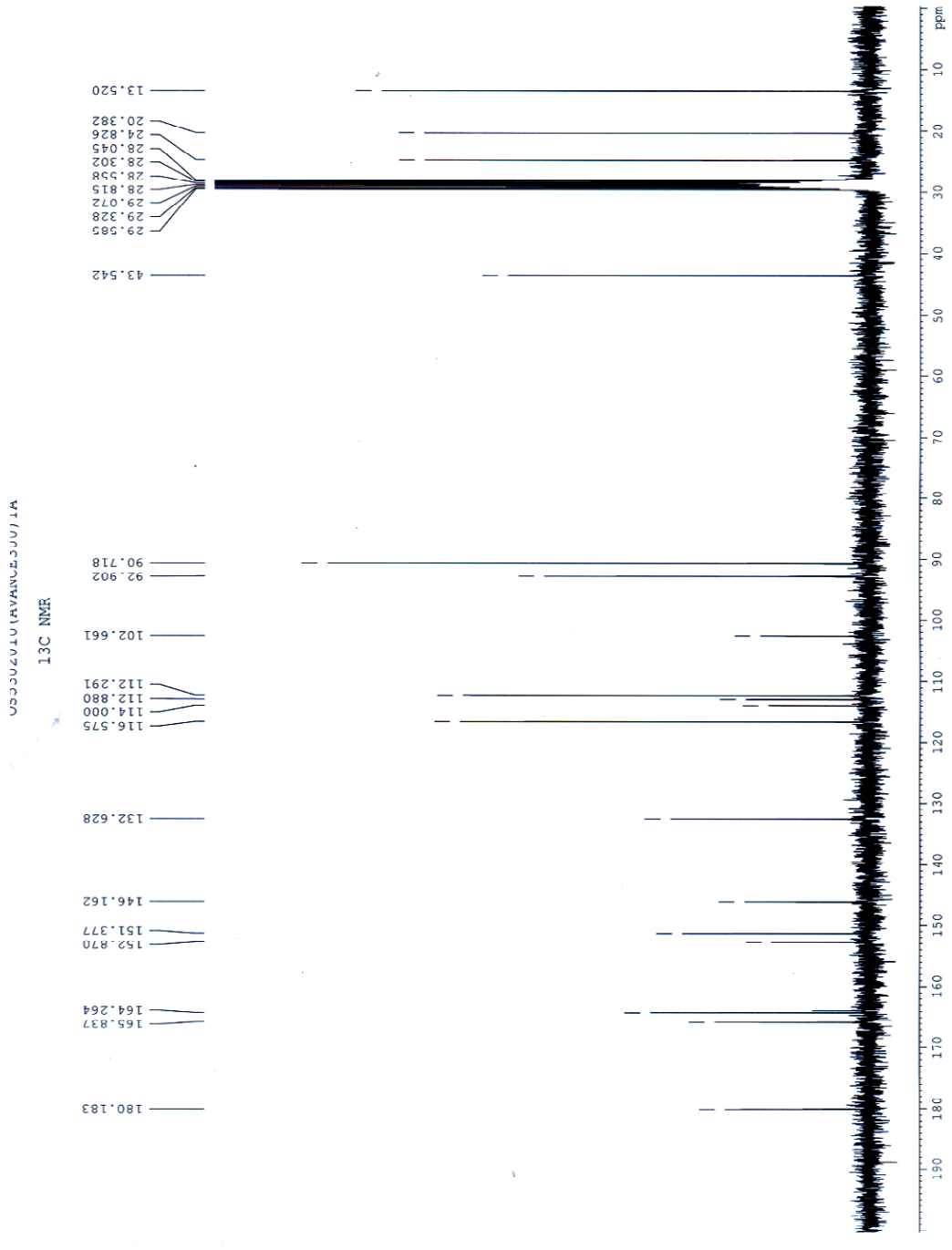

Fig. 75 MHz ^{13}C-NMR spectrum of compound **B** in acetone-d_6

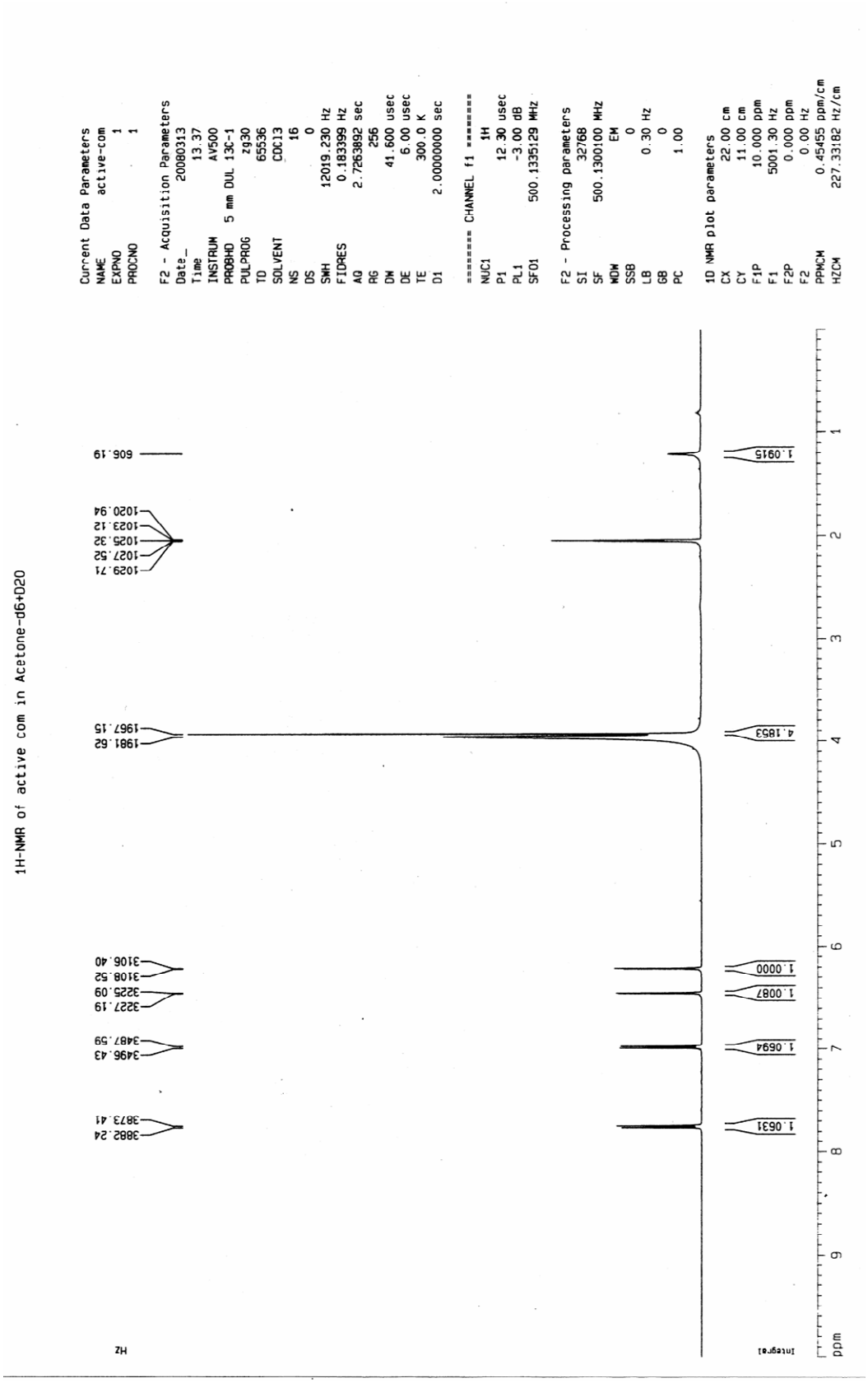

Fig. 500 MHz ^{1}H-NMR spectrum of compound C in acetone-d_6+D_2O

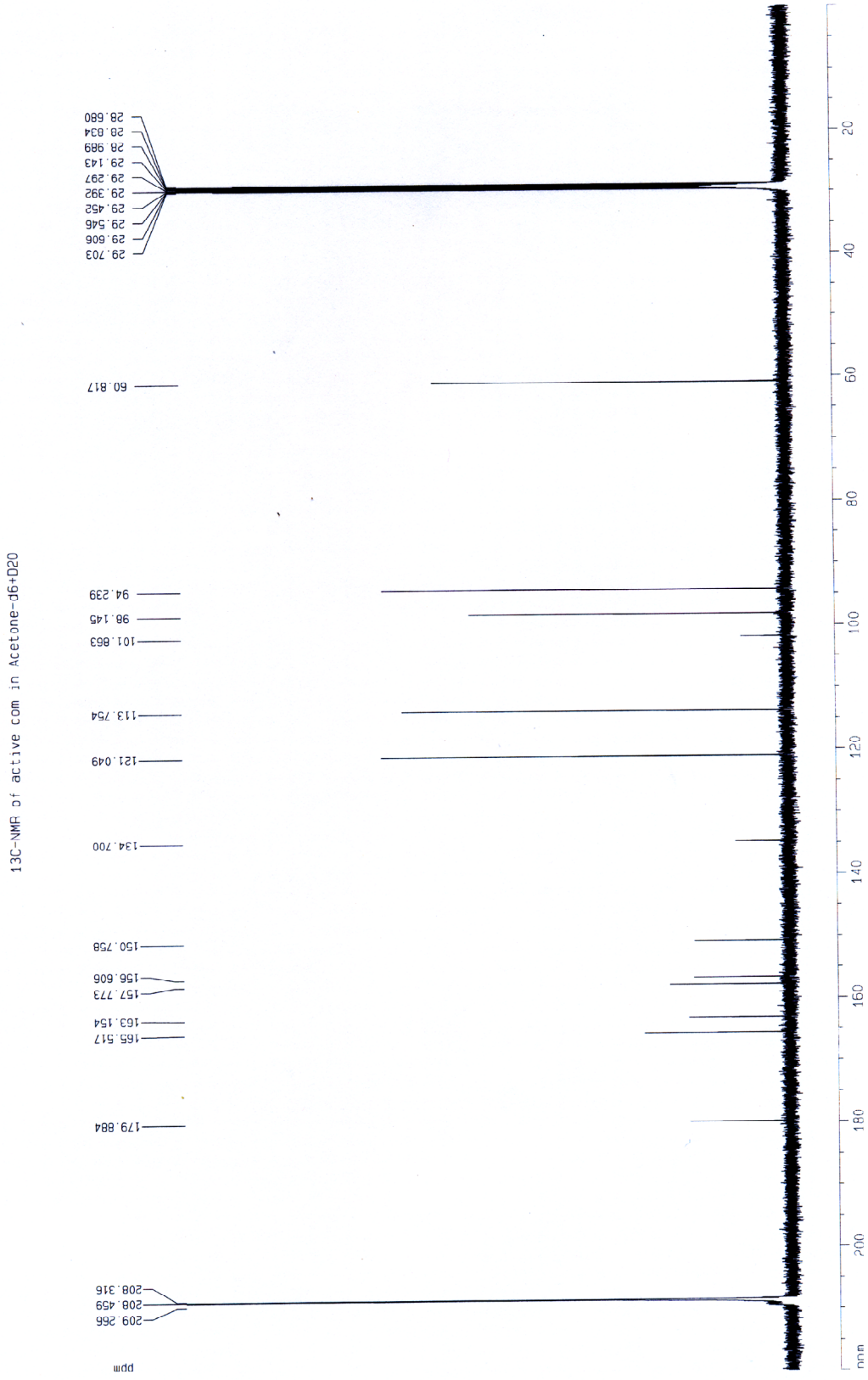

Fig. 125 MHz ^{13}C-NMR spectrum of compound C in acetone-d_6+D_2O

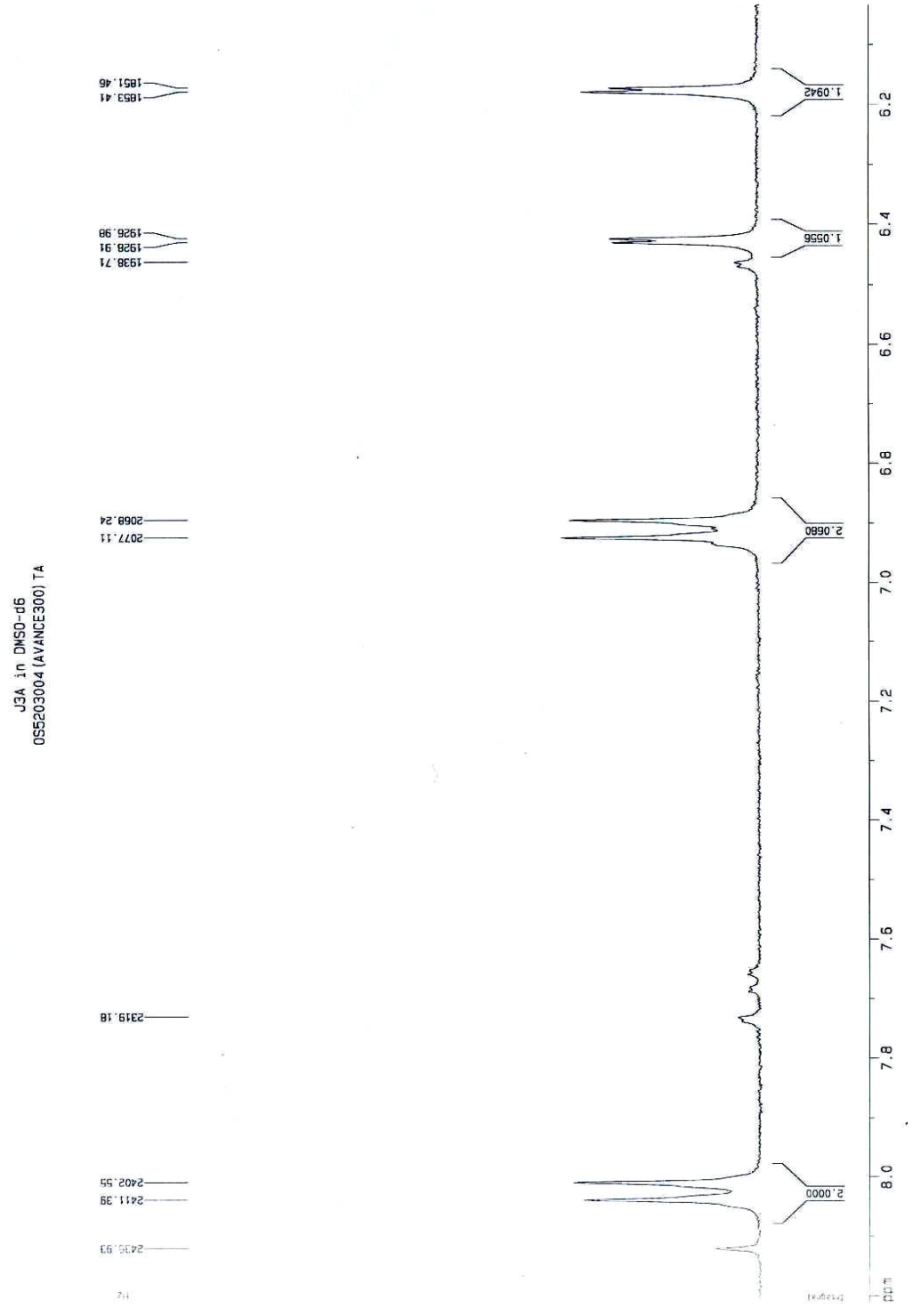

Figure 57 300 MH_Z ^1H NMR spectrum of compound **D** in DMSO-d_6

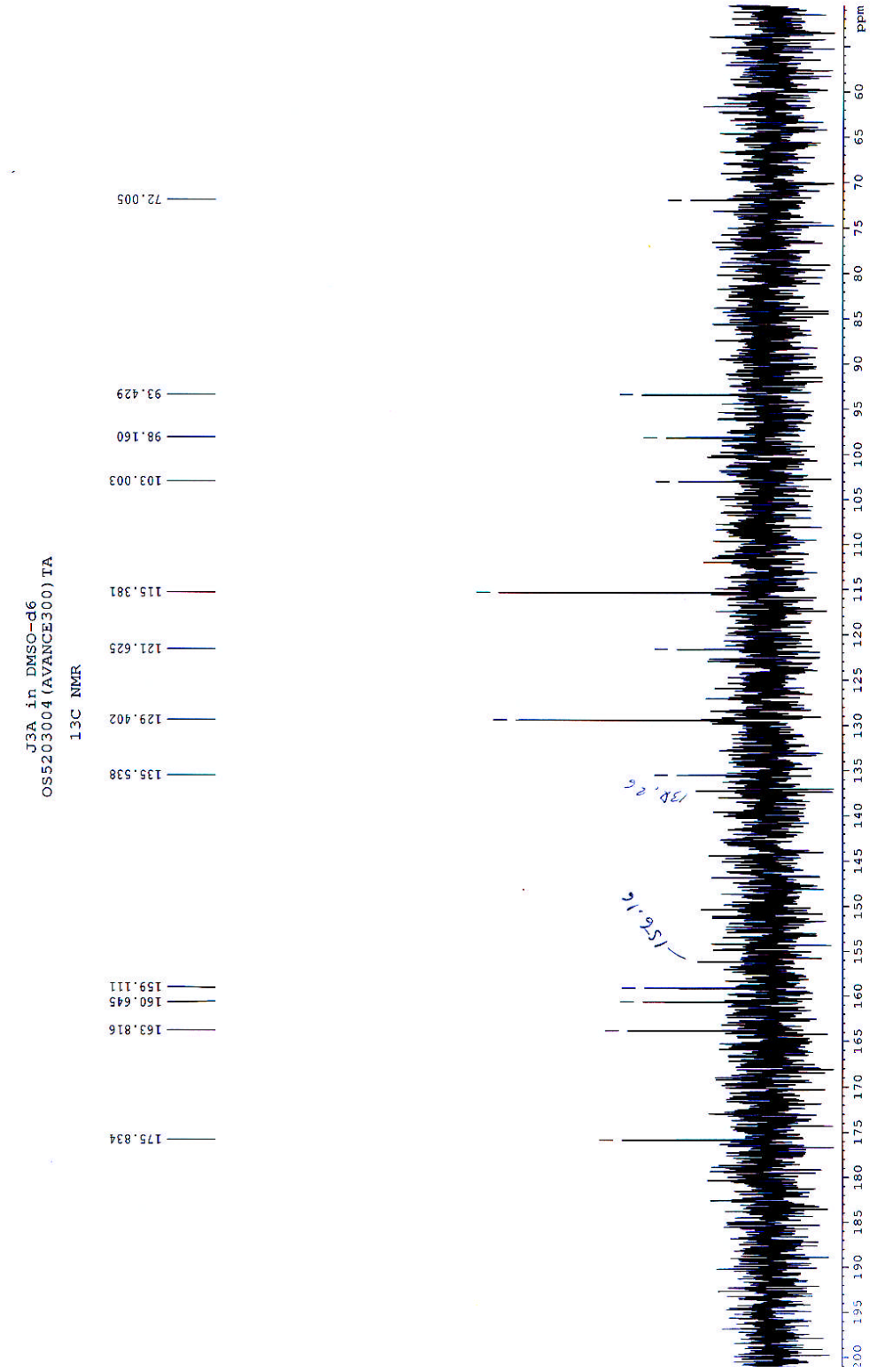

75 MH_Z ^{13}C NMR spectrum of compound **D** in DMSO-d_6

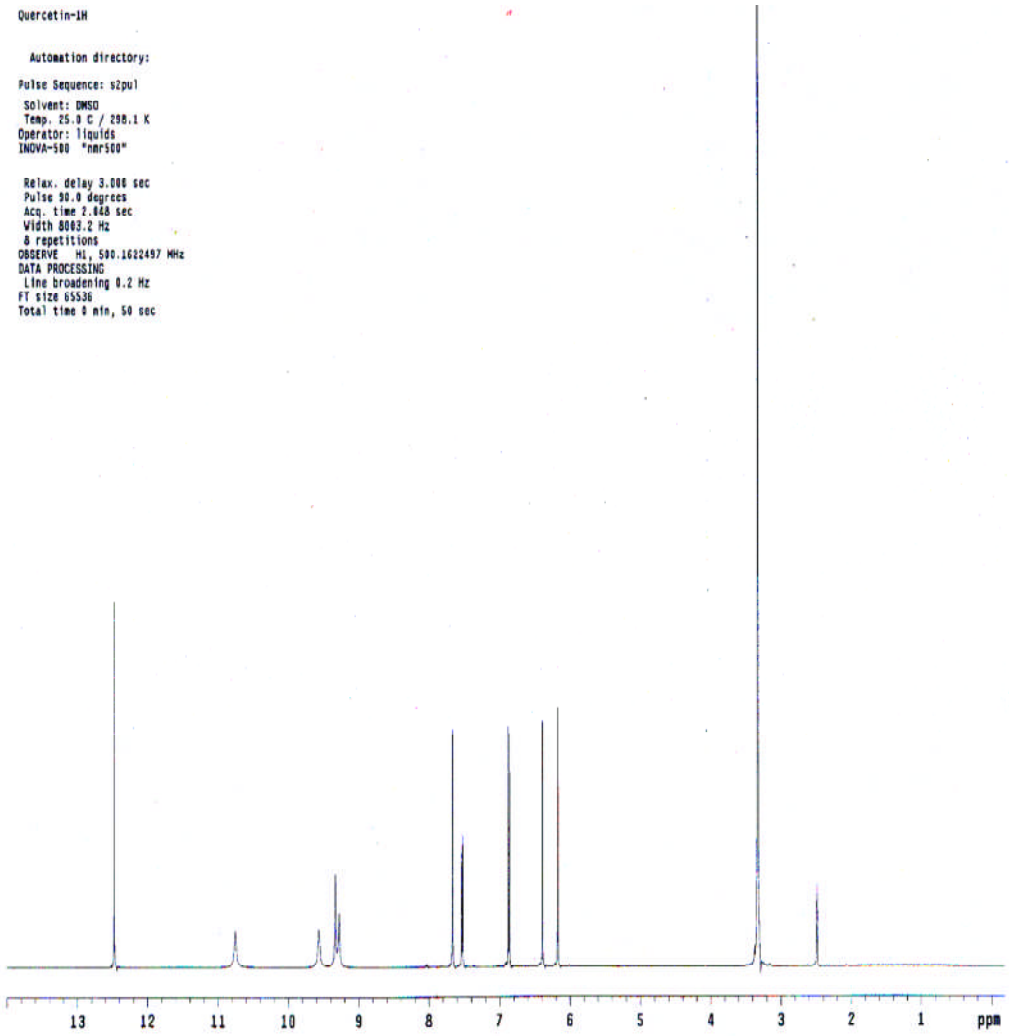

Fig. 500 ^{1}H-NMR spectrum of compound **E** in DMSO-d_6

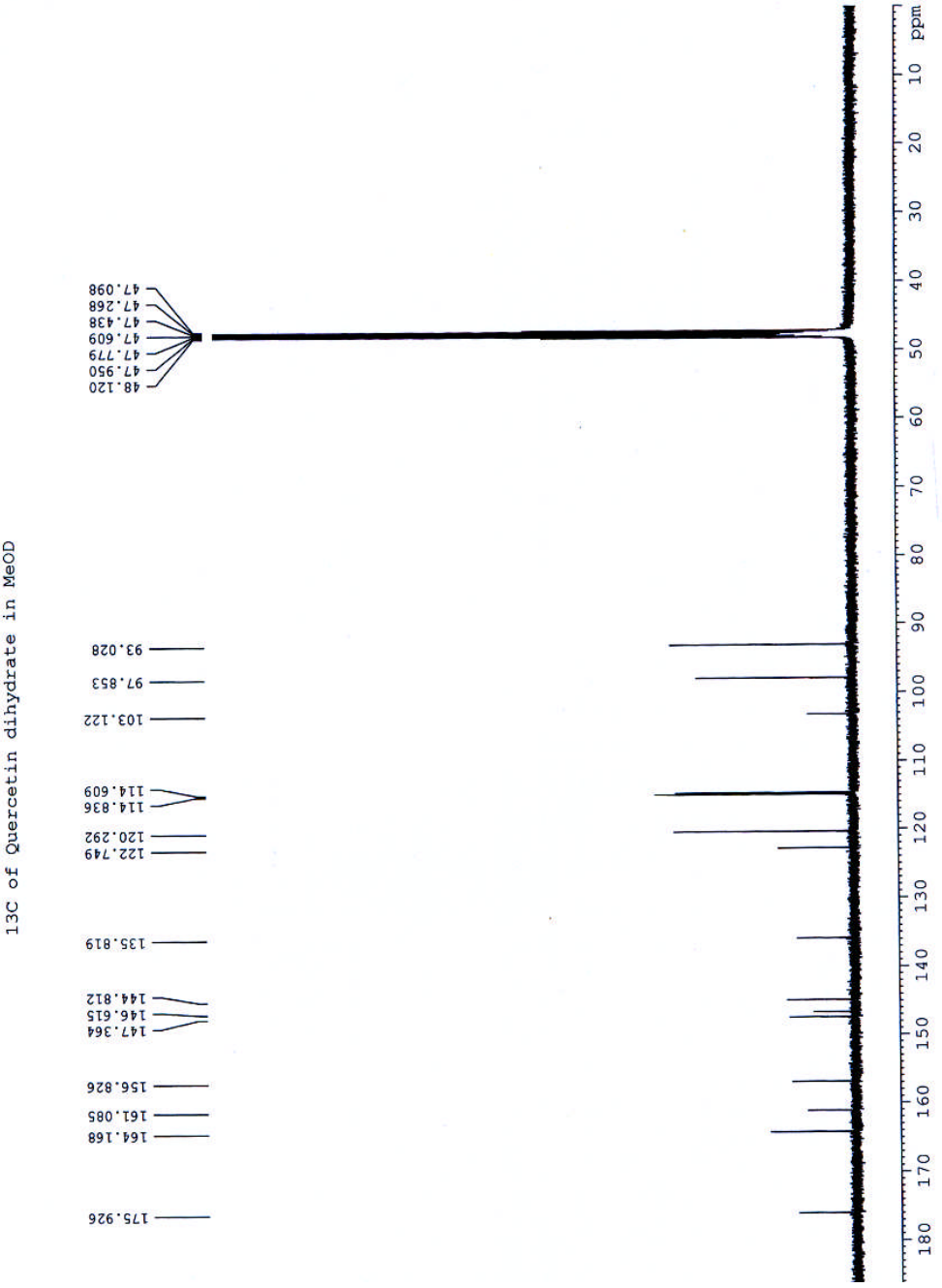

Fig. 125 MHz ^{13}C-NMR spectrum of compound **E** in DMSO-d_6

BIOGRAPHY

NAME	Miss. Wiyada Nooring
DATE OF BIRTH	4 January 1977
PLACE OF BIRTH	Krabi, Thailand
INSTIUTIONS ATTENDED	Ramkhamhaeng University, 1998-2004 : Bachelor of Science in Science (Chemistry) Mahidol University, 2005-2010: Master of Science (Pharmaceutical Chemistry and Phytochemistry)
HOME ADDRESS	40/3 Moo 4 Ban Klonghien Aoulouk Petkasem road Krabi 81110 Thailand
E-MAIL ADDERS	**bkjoy185 @ hotmail.com**